

DEVELOPMENT OF A 6D ELECTRON BEAM DIAGNOSTICS SUITE FOR NOVEL ACCELERATION EXPERIMENTS AT FEBE ON CLARA

T. H. Pacey^{*1}, D. Angal-Kalinin¹, A. R. Bainbridge¹, J. R. Henderson¹, J. K. Jones¹, N. Joshi¹, S. Mathisen¹, A.E. Pollard¹, Y. M. Saveliev¹, E.W. Snedden¹, C. Tollervey¹, D. A. Walsh¹

STFC, Daresbury Laboratory, Warrington, UK

T. J. Overton¹, University of Manchester, Manchester, UK

J. Wolfenden¹, C. Swain, University of Liverpool, Liverpool, UK

¹also at Cockcroft Institute, Sci-Tech Daresbury, Warrington, UK

Abstract

The FEBE beamline at the CLARA facility will combine a 250 MeV FEL quality electron beam with a 100 TW class laser. One area of research FEBE will support is novel acceleration schemes; both structure and plasma based. There are stringent diagnostic requirements for measuring the input electron beam and challenges in characterisation of the accelerated beams produced by these novel schemes. Several of these challenges include measurement of: micrometer scale transverse profiles, 10 fs scale bunch lengths, single shot emittance, broadband energy spectra at high resolution, and laser-electron time of arrival jitter. Furthermore, novel shot-by-shot non-invasive diagnostics are required for machine learning driven optimisation and feedback systems. This paper presents an overview of R&D activities in support of developing a 6D diagnostics suite to meet these challenges.

INTRODUCTION

The Compact Linear Accelerator for Research and Applications (CLARA) is an ultra-bright electron beam test facility being developed at STFC Daresbury Laboratory. CLARA has been designed to test advanced Free Electron Laser (FEL) schemes that could be later implemented on existing and future short wavelength FELs. CLARA is being constructed in phases. Phase 1 was commissioned in 2018, completing the CLARA Front-End, which consists of a S-band photo-injector gun and linac. Phase 1 produced electron bunches at 10 Hz, up to 250 pC in charge and with energy of 50 MeV. A comprehensive review of results from commissioning CLARA Phase 1 can be found in [1]. Phase 1 was used for two periods of competitively allocated beam exploitation, taking place in 2018/19 and 2021/22. A broad range of experiments were performed in these periods, including multiple experiments on novel acceleration techniques: dielectric wakefield acceleration, THz driven acceleration, and plasma wakefield acceleration. These novel acceleration experiments were performed in the CLARA Beam Area 1 (BA1) user hutch where a 100 mJ class laser system was available for exploitation with the electron beam [2].

Phase 2 of CLARA is currently under construction, comprising of an upgrade to the photo-injector gun and installation of 3 further linacs. This will produce bunches at 100 Hz, 250 pC with final energy of 250 MeV. Included

in Phase 2 is the installation of the Full Energy Beam Exploitation (FEBE) hutch. The FEBE hutch represents a step change in experimental capability over BA1, benefiting from both the uplift in electron beam parameters and inclusion of a 100 TW class laser system. The FEBE beamline and hutch will be used for a broad range of experiments, and not exclusively novel acceleration applications. However, it is these novel experiments that pose the greatest challenge for machine performance in terms of beam parameters and subsequent instrumentation.

Phase 3 of CLARA is tied to the R&D requirements for a future UK-XFEL and is not yet funded.

FEBE BEAMLINE

The FEBE beamline is shown in Fig. 1 and comprises of a 4 cell FODO arc, transporting the beam to a shielded hutch with approximately $10 \times 5 \text{ m}^2$ floor space. The room which houses the 100 TW laser system is on the roof directly above the hutch. A detailed discussion of the design of the FEBE beamline can be found in [3]. There are 4 chambers in the FEBE hutch: FMBOX1 for coupling and focusing the laser beam co-linearly with the electron beam, FEC1 ($\approx 2 \text{ m}$ length) for the primary interaction point (IP) with the focus of both electron and laser beams, FMBOX2 for the dumping and diagnostics of the laser beam, and FEC2 as a secondary electron beam interaction point and for housing a suite of diagnostics. The FEBE beamline has an array of well developed or commercially available diagnostic systems including: Ce:YAG screens, stripline beam position monitors (BPMs), integrating current transformers (ICTs), and Faraday cups (F-cups).

The input electron beam parameters for FEBE are shown in Table 1. Beam parameters which are expected to be achieved following initial commissioning are shown, along with potential future parameters which could be achieved following dedicated machine development. Two charge modes are shown, a maximum charge of 250 pC and a low charge of 5 pC; which is the lowest the current BPM electronics will resolve. These parameters are not exhaustive or prescriptive and FEBE will offer very flexible beam setups to users, significantly improved over that provided to users of BA1. Table 1 also indicates those future parameters which will require diagnostics R&D to experimentally validate.

* thomas.pacey@stfc.ac.uk

BEAM TUNING STUDIES IN THE ESS MEBT

N. Milas*, M. Akhyani, R. A. Baron, C. S. Derrez, M. Eshraqi, Y. Levinsen,
 R. Miyamoto, D. Noll, R. Tarkeshian, I. Vojskovic, R. Zeng
 European Spallation Source ERIC, Lund, Sweden

Abstract

The European Spallation Source (ESS), currently under construction and initial commissioning in Lund, Sweden, will be the brightest spallation neutron source in the world once its driving proton linac achieves the design power of 5 MW at 2 GeV. Such a high power requires production, efficient acceleration, and almost loss-free transport of a high current beam, thus making the design and beam commissioning of this machine challenging. During the commissioning period in 2022 a campaign for a full characterization of the ESS Medium Energy Beam Transport session (MEBT) was carried out. Both transverse optics and longitudinal parameters were measured and compared to simulations, among them: buncher cavity tuning, transverse emittance, and initial Twiss parameters. In this paper, we present the results and future plans.

INTRODUCTION

The European Spallation Source (ESS), currently shifting from construction to testing and initial beam commissioning in Lund, Sweden, will be a spallation neutron source driven by a long pulse proton linac [1]. The linac consists of normal-conducting (NC) accelerating structures and three sections of superconducting cavities, as well as three transfer-lines. The NC accelerating structures include an ion source (ISrc), a radio frequency quadrupole (RFQ), and a drift tube linac (DTL). The beam commissioning of the ESS linac is being conducted in stages [2–4]. Commissioning of the first stage, for the ISrc and LEPT, started in September 2018 and continued until early July 2019. The beam was transported through the RFQ and part of the MEBT in 2021. In the first half of 2022 beam was transported to the end of the first DTL tank (DTL1), reaching an energy of 21 MeV. Schedules of the completed commissioning steps are listed in Table 1.

This paper will highlight the studies in the Medium Energy Beam Transport section (MEBT), which follows the RFQ, performed in 2021 and 2022. The main results is an attempt of estimating the input Twiss parameters to the MEBT in all 3 planes, using the Wire Scanners and the sum signals of BPMs. A measurement of the RFQ output energy and beam based calibration of the buncher cavity amplitude will also be presented.

COMMISSIONING HIGHLIGHTS

The first part of the MEBT commissioning started in 2021 (Step 2A in Table 1), and, during this first period, the main focus was on beam transmission through the RFQ and less

* natalia.milas@ess.eu

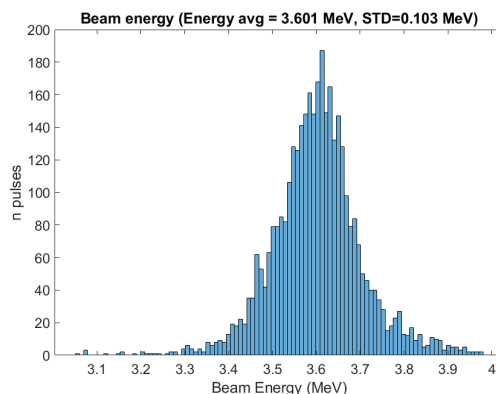


Figure 1: Histogram of the measured RFQ energy with time-of-flight.

on the MEBT characterization. During this period, a cautious approach was taken before sending the beam to the RFQ and ramping up beam parameters. Time was spent verifying the systems critical for machine protection, such as the Beam Current Monitors (BCMs), the LEPT chopper, timing configuration [5], and machine protection systems [6]. Nevertheless, within the allocated period of five weeks, the beam was successfully accelerated with the RFQ and a stable beam with 6 mA, 50 μ s, and 1 Hz was established up to the MEBT Faraday cup (FC), without any accident. The output energy of the RFQ was verified to be 3.6 ± 0.1 MeV with time-of-flight measurements (Fig. 1). In the very end of this first commissioning round some of the Wire Scanners became available for testing and preliminary measurements [7].

In 2022, two additional commissioning periods with approximately nine weeks in total took place (Steps 2B and 2C in Table 1). A stable beam with the nominal 62.5 mA current was established up to the MEBT FC, with an excellent RFQ transmission of $\sim 95\%$. Testing of the closed-loop operation of the low-level RF (LLRF) of the RFQ also made good progress during these periods, and the RFQ ran with both

Table 1: NC Linac Commissioning Schedule (Two additional periods were allocated for the second step.)

Step	Destination	Start	End
1	Tank after LEPT	2018-09-19	2019-07-03
2A	MEBT	2021-11-10	2021-12-17
2B	MEBT	2022-02-23	2022-03-12
2C	MEBT	2022-04-06	2022-05-23
3	DTL1	2022-05-30	2022-07-13

STATISTICAL PROPERTIES OF UNDULATOR RADIATION*

I. Lobach[†], Argonne National Laboratory, Lemont, IL, USA
S. Nagaitsev¹, A. Romanov, A. Shemyakin, G. Stancari, Fermilab, Batavia, IL, USA
¹also at The University of Chicago, Chicago, IL, USA

Abstract

Two experiments were carried out to study the statistical properties of undulator radiation in the Integrable Optics Test Accelerator (IOTA) storage ring at Fermilab. The first experiment studied the turn-to-turn fluctuations in the power of the radiation generated by an electron bunch. The magnitude of these fluctuations depends on the 6D phase-space distribution of the electron bunch. In IOTA, we demonstrated that this effect can be used to measure some electron bunch parameters, small transverse emittances in particular. In the second experiment, a single electron was stored in the ring, emitting a photon only once per several hundred turns. In this regime, any classical interference-related collective effects were eliminated, and the quantum fluctuations could be studied in detail to search for possible deviations from the expected Poissonian photon statistics. In addition, the photocount arrival times were used to track the longitudinal motion of a single electron and to compare it with simulations. This allowed us to determine several dynamical parameters of the storage ring such as the rf cavity phase jitter and the dependence of the synchrotron motion period on amplitude.

INTRODUCTION

In our previous experiments [1–4] with an electron bunch we showed that turn-to-turn fluctuations $\text{var}(\mathcal{N})$ of the number of detected undulator radiation photons per turn \mathcal{N} have two contributions: (1) a Poissonian contribution equal to $\langle \mathcal{N} \rangle$, due to the discrete quantum nature of light, and (2) a collective contribution $\propto \langle \mathcal{N} \rangle^2$, related to the interference between the fields generated by the electrons in the bunch. In this paper, we get rid of the collective contribution by considering a single electron circulating in the Integrable Optics Test Accelerator (IOTA) storage ring at Fermilab in order to thoroughly study the quantum fluctuations and verify that they follow the Poissonian photostatistics $\text{var}(\mathcal{N}) = \langle \mathcal{N} \rangle$, predicted by [5–8]. This research is motivated by the surprising observation of sub-Poissonian photostatistics ($\text{var}(\mathcal{N}) < \langle \mathcal{N} \rangle$) in synchrotron radiation reported in Ref. [9] in a similar experiment setting. In addition, we will use the recorded detection times to study the synchrotron motion of a single electron in IOTA [10], similar to previous experiments in Novosibirsk [11, 12].

* The work is supported by the U.S. Department of Energy, Office of Science, Office of Basic Energy Sciences, under Contract No. DE-AC02-06CH11357.

[†] ilobach@anl.gov

APPARATUS

In our experiment, a single electron circulated in IOTA with a revolution period of 133 ns and an energy of 96.4 MeV. The undulator parameter is $K_u = 1.0$ with the number of periods $N_u = 10.5$ and the period length $\lambda_u = 5.5$ cm. The wavelength of the fundamental was $\lambda_1 = \lambda_u(1 + K_u^2/2)/(2\gamma^2) = 1.16 \mu\text{m}$, where $\gamma = 188.6$ is the Lorentz factor. The second harmonic was in the visible wavelength range. We used a Single Photon Avalanche Diode (SPAD) [13] as a detector, which was mostly sensitive to the visible light with detection efficiency of up to 65%. Two edge-pass filters were used to only collect the radiation between 550 nm and 800 nm. The radiation was focused on the sensitive area of the detector ($\varnothing 180 \mu\text{m}$) by a single focusing lens with a focal distance of 180 mm, see Figs. 1(a),(b). The radiation was collected in a large angle $> 1/\gamma$. The SPAD detector produced a 10-ns-long TTL pulse at each detection event. Its dead time (20 ns) was shorter than the IOTA revolution period (133 ns). Our data acquisition system [Fig. 1(c)] allowed us to record the revolution number and the arrival time relative to the IOTA revolution marker for each detection event for as long as 1 minute at a time.

PHOTOSTATISTICS MEASUREMENTS

In the optimal focusing, the measured photocount rate was 24.7 kHz, or one photocount per 304 revolutions in IOTA (on average). The dark count rate of the SPAD detector was 108 Hz. In addition, we used a 5-ns-long gate around the expected detection arrival time, which allowed us to reduce the effective dark count rate to 4.0 Hz.

Before any analysis of the photostatistics, it was important to realize that the SPAD detector is binary. It produces the same type of pulses (TTL, 10-ns-long) no matter how many photons are detected per one pass. The collected turn-by-turn data can be represented as a sequence of zeros and ones only. Therefore, we had to alter our original expectation of Poissonian photostatistics to a sequence of Bernoulli trials, i.e., there is a probability p of a detection at every revolution, and a probability $(1 - p)$ of no detection. In our case, $p = (3.29 \pm 0.02) \times 10^{-3}$. Figure 2 illustrates the comparison between the expectation (for a sequence of Bernoulli trials) and the measurement for (a) the distribution of interarrival times and for (b) the distribution of the number of photocounts in a certain time window. In both cases, the χ^2 goodness-of-fit test [14, p. 637] results in a P-value [14, p. 140] above the conventional 0.05 threshold. This means that the null hypothesis (exponential or binomial distribution, respectively) cannot be rejected.

SLS 2.0 – STATUS OF THE DIAGNOSTICS

C. Ozkan Loch[†], A. Bonnin, J. Vila-Comamala, N. Samadi, A. M. M. Stampfli, R. Ischebeck
 Paul Scherrer Institut (PSI), Villigen PSI, Switzerland

Abstract

In this contribution we give an overview of the diagnostics development for SLS 2.0, focusing on the beam size monitors in the storage ring, the screen monitors for the booster-to-ring transfer line, and beam loss monitors for the storage ring. Test results carried out at the SLS will also be presented. Diagnostics that will only receive a DAQ system upgrade will not be discussed here.

INTRODUCTION

The Swiss Light Source (SLS) synchrotron storage ring will be upgraded to a new diffraction-limited lattice [1], and its booster-to-ring transfer line (BRTL) will also be improved accordingly [2]. The current monitor for the storage ring and charge monitor in the BRTL will be re-used with new DAQ systems but same functionalities [2]. Hence, these systems will not be discussed here.

Up until recently, in the SLS there were beam loss monitors only at the exit of insertion devices. The distributed loss monitor system based on a CMOS camera readout [3] was developed for locating losses around the storage ring. The first prototype monitor was used to locate losses due to a beam dump, to survey possible losses in the first three arcs, and look for changes with respect to undulator gap changes. As a result, the loss detection scintillators were improved. An update on the status of these loss monitors will be discussed later in this proceeding.

Beam size monitoring at the SLS depends on the π -polarization [4] technique, using the visible light at 364 nm from a bend magnet. However, this technique only provides the vertical source size. In order to measure both dimensions of the small source size at SLS 2.0 ($< 8 \mu\text{m}$), X ray imaging optics based on zone plates will be used. This monitor is based on [5, 6]. The source size will also be monitored in two locations in order to determine the energy spread of the storage ring.

The present screen monitors in the BRTL use a 200 μm Ce:YAG scintillator at 45° angle to visualize the beam. The optical resolution is 30 μm . One of the screen monitors was modified to house a 100 μm Ce:YAG scintillator normal to the beam with a mirror at 45° angle to couple out the scintillation light. The imaging camera and objective were changed and a spatial resolution of 19 μm was achieved. This will be further improved for the new BRTL. The requirements and details are discussed in the next section.

SCREEN MONITORS

The booster-to-ring transfer line (BRTL) will provide nominal injection into the SLS 2.0 storage ring. It also allows performing beam parameter measurements during set up and commissioning. The purpose of the BRTL screen

monitors is to determine the beam profiles, transverse emittance and energy spread. The BRTL optics design and layout with the location of all diagnostics components can be found in the SLS 2.0 technical design report [2].

Apart from beam profile measurements in the nominal BTR injection mode, the first BRTL screen will be used for emittance measurements by scanning the upstream quadrupoles, and the second screen will be used for determination of the energy spread. The last screen will be used for the adjustment of the transverse beam size (matching) at the “thick” storage ring injection septum.

Table 1: Screen Monitor Requirements Based on Expected Smallest Beam Size, Required Resolution and Field of View

	Emittance	Energy spread	Thick septum
Beam size	$< 20 \mu\text{m}$	700 μm	$< 20 \mu\text{m}$
Screen resolution	$< 10 \mu\text{m}$	10 μm for precision of 3%	10 μm
FOV dia.	20 mm	20 mm	20 mm

A scintillator crystal (Ce:YAG) will be inserted in the electron beam path by means of linear UHV-feedthroughs and pneumatic controls. To view the entire range of beam motion, the scintillator screen will be normal to the beam with a mirror at 45° angle behind it to couple out the scintillation light (Fig. 1a).

An OTR screen will also be installed at 45° angle with respect to the beam and the camera will be mounted in the Scheimpflug [7, 8] geometry to correct the focal plane. To measure the emittance an iris and focus control of the camera objective is necessary. In order to facilitate simple switching between Ce:YAG and OTR measurements, an optical setup per screen will be installed at the emittance measuring screen monitor (Fig. 1b).

DISTRIBUTED BEAM LOSS MONITOR

It was initially planned to use beam loss detectors based on organic fiber scintillators in the storage ring and BRTL to locate losses and monitor the loss pattern during injection (storage ring filling and top-up operation). Similar to the SwissFEL [9], 2-meter long fiber scintillators were coupled to plastic optical fibers (POF) that guide the scintillator light to the detection system. A CMOS camera was used to image the light from 28 fibers simultaneously.

A system was built and tested at SLS. Injection losses were detected during top-up. The location of the fiber scintillator that gives the highest signals during beam dump supports the radiation measurement results concerning the

[†] cigdem.ozkan@psi.ch

AN OPTICAL DIAGNOSTIC BEAMLINE FOR THE BESSY II BOOSTER

T. Atkinson*, Ji-Gwang Hwang, G. Rehm, M. Ries, G. Schiwietz, S. Wiese
Helmholtz-Zentrum Berlin für Materialien und Energie, Berlin, Germany

Abstract

As part of the global refurbishment of the injector at BESSY II, a new optical beamline has been installed in the booster. This paper covers the conceptual design: incorporating the beamline into an operational facility without downtime, the simulation and expectations of the optical transport line, mechanical installation and commissioning with beam. These first results with the present beam delivery system have already achieved source-point imaging and bunch length measurements using a fast diode. With the additional PETRA cavity installed for this booster upgrade and connection to acquire RF power in the 2022 summer shutdown planned, the bunch length diagnostics are critical. The beamline will also undergo a final mechanical upgrade and then see the installation of a streak camera.

MOTIVATION

In a familiar fashion that characterized 3rd generation light sources across the world, injection into the BESSY II storage ring is from a low energy linac followed by a full energy booster synchrotron.

The present injection scheme is highly reliable [1], but a global upgrade was necessary for the BESSY VSR project [2]. The most prominent aspect with respect to the injector is the evidence that the bunch length on injection into the VSR-storage ring needs to be reduced from its present value, by at least a factor of two in order to keep the high injection efficiencies.

The preferred method to produce shorter bunches from the booster is an upgrade of the existing 500 MHz RF system. An additional 5-cell PETRA cavity driven by a 40 kW transmitter has been installed. In terms of beam commissioning, slowly increasing the total RF gradient is a subtle way to actively control and diagnose the beam in all dimensions.

DESIGN CRITERIA

The design criteria was to keep the optical beamline as short and as simple as possible: use established in-house components and install everything over four shutdowns without any dark-time of the high level source-point diagnostics. In order to minimize the beamline transport length, the output port in the booster was moved in 2020 to a more convenient straight section. This modification to the booster hardware was part of a global reshuffle to accommodate the additional cavities, bunch-by-bunch feedback [3] and redundancy for TopUp current measurement. For beam transport, a total of 7 mirrors each 2 inch in diameter are mounted in the standard HZB holders used throughout the facility, see Fig. 1. Motorized 2-point tilt adjustment is possible.

* terry.atkinson@helmholtz-berlin.de

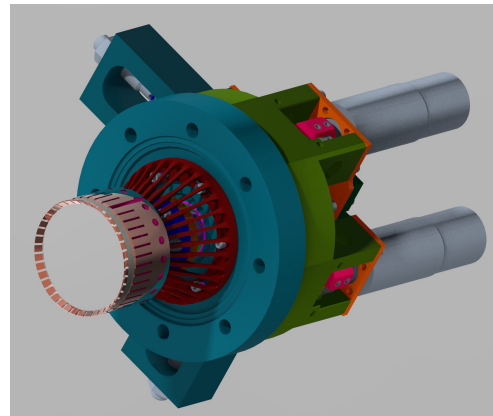


Figure 1: Standard HZB [4] motorized holder for a 2 inch diameter mirror.

The mirrors in the transport line have a surface flatness of $\lambda/20$ to achieve high precision in terms of phase [5]. This allows the source imaging system to measure a spot size close to its diffraction limit.

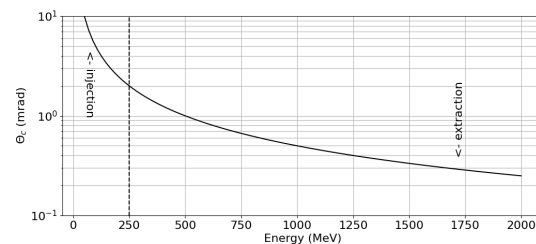


Figure 2: Critical angle of emitted light over the energy ramp of the booster. Without refractive optic, visible light will be outside the angular acceptance for energies < 250 MeV.

From the source, the divergence of the emitted light is corrected using refractive optics, then collimated beam is transported through beamline using the remaining mirrors. There is a 2 degree angle at the output port from the bending magnet.

Noticeably installed is a Intermediate Viewing Point (IVP) consisting of a motorized linear stage and CCD camera at the halfway stage to help align the components. Here both the photon beam and alignment laser were simultaneously observed. Next the beam is transported through the labyrinth out to the optical table. Due to building constraints, a further 20 degree angle is introduced in the labyrinth.

The entire beamline is under vacuum, contains presently one UHV wedged window at the booster output port. This window protects the vacuum in the accelerator and the wedged angle helps to separate spatially unwanted reflection. A second wedged window will be installed next year to com-

STATUS OVERVIEW OF THE HESR BEAM INSTRUMENTATION

C. Böhme, V. Kamerzhiev¹, Forschungszentrum Jülich, Germany

A. Halama, G.Rupsch, GSI Helmholtzzentrum für Schwerionenforschung, Darmstadt, Germany

¹also at GSI Helmholtzzentrum für Schwerionenforschung, Darmstadt, Germany

Abstract

The High Energy Storage Ring (HESR), within the FAIR project, will according to current planning provide anti-proton beams for PANDA and heavy ion beams for a.o. SPARC. With the beam instrumentation devices envisaged in larger quantities, e.g. BPM and BLM, testing is well underway. Other beam instrumentation instruments like Viewer are in late production stage, Scraper is being tested and for the IPM the 1st of series production has started. An overview of the status of the work package beam instrumentation will be presented as well as test bench results of already produced instruments.

INTRODUCTION

The HESR, part of the FAIR project in Darmstadt, Germany, is dedicated to the field of antiproton and heavy ion physics. The envisaged energy range is 0.8 GeV to 14 GeV for antiprotons and 0.17 GeV/a to 5 GeV/a for heavy ions [1]. The ring will be 574 m long in a racetrack shape. The foreseen beam instrumentation within the modularized start version is:

- 64 Diagonally Cut Beam Position Monitors (BPM)
- 118 Beam Loss Monitors (BLM)
- 2 Beam Current Transformers (BCT)
- 2 Ionization Beam Profile Monitor (IPM)
- 1 In-gap particle measurement
- 1 Schottky Pick-up
- 1 Phase Pick-up
- 1 Dynamical Tune-meter
- 5 Viewer
- 2 Scraper

BPM SYSTEM

The pick-up design is based upon the COSY BPMs [2], which is a diagonally cut pick-up design. The design was shown in detail in [3]. While 63 BPMs will have the inner diameter of 89 mm, one is designated to be located closely after the injection septum, where the beam pipe has a diameter of 150 mm. Therefore, to not limit the aperture at this place, one BPM has to have a larger diameter. This one is still to be designed.

BPM Testing

Of the 64 envisaged BPMs, 44 have been tested, with an additional 11 recently received from production to be tested in the near future. Every BPM is tested using a wire test bench to check general electrical functionality and determine the linear coefficients and electrical offsets per plane. The

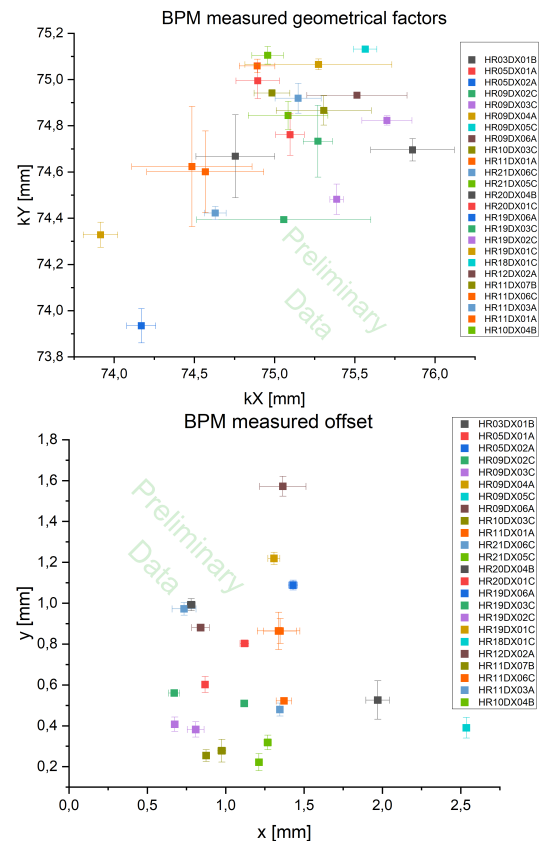


Figure 1: Measured properties of the first 25 BPMs. On the top picture the geometrical factors and the lower picture the electrical offsets compared to the mechanical middle position.

test bench is fitted with μ -meter precision linear drives and optical micrometers for moving the wire and determining the precise position. In every BPM two highly precise measured reference markers are added during manufacturing, which are functioning as reference for the wire positioning. The signals are amplified by head amplifiers and the AMPLIFIER 110, before being digitized by a Spectrum 16-bit 250 MHz ADC card. The whole measurement process, including the positioning of the wire, control of the gain of the AMPLIFIER 110, the ADC signal readout, and writing the measured values to a file is done with LabView.

Figure 1 shows the preliminary results of the first 25 tested BPMs for the measurements of the geometrical factors (upper figure) and the electrical center in regards to the mechanical center (lower figure). While the mechanical tolerances for the parts of the BPM directly involved in the measurement process, like the pick-up electrodes, have been specified

FIBER BRAGG GRATING SENSORS AS BEAM-INDUCED HEATING MONITOR FOR THE CENTRAL BEAM PIPE OF CMS

F. Fienga^{1,*}, L. Sito¹, V. R. Marrazzo¹, A. Irace, and G. Breglio¹

Univeristy of Naples Federico II, Naples, Italy

F. Carra, F. Giordano, and B. Salvant,

European Organization for Nuclear Research (CERN), Geneva, Switzerland

N. Beni¹, and Z. Szillasi¹,

Institute for Nuclear Research of Eötvös Loránd Research Network, Debrecen, Hungary

S. Buontempo¹, National Institute for Nuclear Physics (INFN), Naples, Italy

¹also at European Organization for Nuclear Research (CERN), Geneva, Switzerland

Abstract

The passage of a high-intensity particle beam inside accelerator components generates heating, potentially leading to degradation of the accelerator performance or damage to the component itself. It is therefore essential to monitor such beam-induced heating in accelerators. This paper showcases the capabilities of iPipe, which is a set of Fiber Bragg Grating sensors stuck on the inner beam pipe of the Compact Muon Solenoid (CMS) experiment installed in the CERN Large Hadron Collider (LHC). In this study, the wavelength shift, linked directly to the temperature shift, is measured and is compared with the computed dissipated power for a set of LHC fills. Electromagnetic and thermal simulations were also coupled to predict the beam-induced temperature increase along the beam pipe. These results further validate the sensing system and the methods used to design accelerator components to mitigate beam-induced heating.

INTRODUCTION

An increase in energy and intensity of the beams is expected as part of the CERN's Large Hadron Collider (LHC) High Luminosity (HL) upgrade [1]. One of the major potential limitations for this upgrade [2] is the heating of accelerator components produced by the presence of the beam itself. This is called beam-induced heating (BIH).

The beam-induced heat load is deposited on the device primarily in three ways: (i) synchrotron radiation [3], (ii) electron cloud [4], and (iii) heating due to impedance [5].

These phenomena can lead to several issues (delays, beam dumps, and even component damage) like, for instance, what occurred in June 2011 during the first Run of LHC [6]. Therefore, it is essential that the components' design phase is able to appropriately account for heating. Additionally, it is necessary to have suitable monitoring systems to regularly monitor temperature-related parameters.

One sensing solution that has spread in the last decade in the High Energy Physics domain is Fiber Optic Sensing (FOS). This work focuses on iPipe, an innovative measuring system based on Fiber Bragg Gratings (FBGs), mounted

in the CMS experiment and in acquisition since 2015 [7]. The iPipe system is monitoring CMS's vacuum chamber, the Central Beam Pipe (CBP). Since the CBP is located at one of the interaction points, it is hosting both beams simultaneously to allow them to collide. This two counter-rotating beams situation causes interference phenomena that can lead to an anomalous dissipated power distribution [5].

The possibility to infer various beam parameters using data logged by the iPipe system has already been demonstrated [8]. This work aims to go further, comparing the temperature excursion acquired by the iPipe system during machine operation with a temperature map produced using coupled electromagnetic and thermal simulations. The main goal is to demonstrate the capability of the iPipe system to measure directly the BIH. Moreover, this benchmark enables to further validate the analytical model (with regards to the two counter-rotating beams case in particular) and simulation methodologies that are typically used at CERN.

MEASUREMENTS

FBGs are periodic changes in the refractive index of the optical fiber's core. Such a structure behaves as a stop band filter: it reflects light centered at a specific wavelength, that is called Bragg wavelength (λ_B), and that depends on the effective refractive index of the core (n_{eff}) and the spatial periodicity of the grating (Λ). These dependencies are described in Eq. (1).

$$\lambda_B = 2n_{eff}\Lambda. \quad (1)$$

This structure is intrinsically a sensor since any change either in the refractive index of the core or in the grating period results in a change of the Bragg wavelength. A temperature difference (ΔT) and/or an applied strain (ε) may cause these changes and, as described by Eq. (2), it is possible to correlate the superposition of the two physical effects with the Bragg wavelength variation that they induce [9].

$$\Delta\lambda_B(T, \varepsilon) = \lambda_B \cdot [(1 - \rho_e) \cdot \varepsilon + (\alpha_\Lambda + \alpha_n) \cdot \Delta T], \quad (2)$$

where ρ_e is the photo-elastic effect coefficient, α_Λ is the thermal expansion coefficient, and α_n is the thermo-optic effect coefficient.

* francesco.fienga@unina.it

BEAM INSTRUMENTATION PERFORMANCE DURING COMMISSIONING OF THE ESS RFQ, MEBT, AND DTL

T. J. Shea, R. A. Baron, C. S. Derrez, E. M. Donegani, V. Grishin, H. Hassanzadegan, I. Dolenc Kittelmann, H. Kocevar, N. Milas, D. Noll, H. A. Silva, R. Tarkeshian, C. Thomas, European Spallation Source ERIC, Lund, Sweden
 T. Papaevangelou, L. Segui, CEA-IRFU, Gif-sur-Yvette, France
 I. Bustinduy, ESS Bilbao, Zamudio, Spain
 M. Ferianis, Elettra-Sincrotrone Trieste S.C.p.A., Basovizza, Italy

Abstract

In late 2021 through mid 2022, the first protons were accelerated and transported through the European Spallation Source (ESS) Radio Frequency Quadrupole and Medium Energy Transport line at 3.6 MeV, and finally through the first Drift Tube Linac tank at 21 MeV. To enable these achievements, the following beam instrumentation systems were deployed: Ion Source power supply monitors, beam chopping systems, Faraday Cups, Beam Current Monitors (BCM) and Beam Position Monitors (BPM) that also measured phase. Additional systems were deployed for dedicated studies, including Wire Scanners, a slit and grid Emittance Measurement Unit, neutron Beam Loss Monitors and fast BCM and BPM systems. The instrumentation deployment is the culmination of efforts by a partnership of the ESS beam diagnostics section, multiple ESS groups and institutes across the globe. This paper summarizes the beam tests that characterized the performance of the instrumentation systems and verified the achievement of commissioning goals.

INTRODUCTION

Five weeks at the end of 2021 and several more weeks in early 2022 were dedicated to commissioning of the ESS Radio Frequency Quadrupole (RFQ) and Medium Energy Beam Transport line (MEBT) up to a Faraday Cup (FC) located in MEBT. After chopping in the Low Energy Beam Transport line (LEBT) and successful acceleration in the RFQ, the proton beam energy was 3.6 MeV. During June and July of 2022, several more weeks were dedicated to commissioning through the first Drift Tube Linac (DTL) tank with 21 MeV protons transported to a shielded FC. To support commissioning, the instrumentation systems were deployed in each linac section as depicted in Fig. 1. Most were designed to measure beam pulses 5 to 50 μ s long with peak current ranging from 6 to 80 mA. This paper focuses on the instrumentation performance that underlies the commissioning results reported in overview papers [1–3].

The ESS beam instrumentation suite includes a wide variety of systems [4] deployed in a staged approach. Systems that are critical for meeting commissioning goals are verified in the laboratory prior to deployment, tested again with other systems in the accelerator environment and then formally verified with beam to achieve operational status. The Faraday

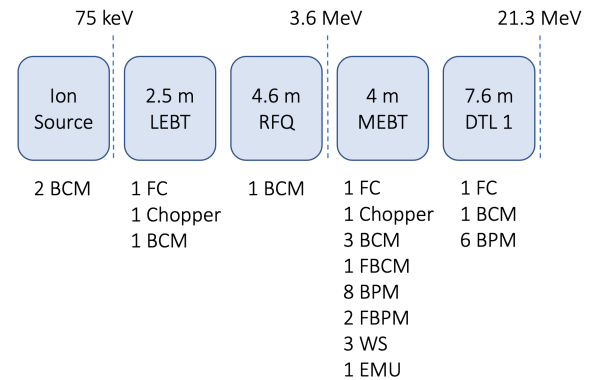


Figure 1: Layout of the linac sections and the beam instrumentation used during the 2021 and 2022 commissioning runs.

Cup (FC), Beam Current Monitor (BCM), Beam Position Monitor (BPM) and Chopper systems have all gone through this workflow. In addition, several other systems were verified for diagnostic beam studies with intent of gaining early experience with beam, sometimes at an intermediate stage of system development. For the recent commissioning runs, the neutron Beam Loss Monitors (nBLM), Wire Scanners (WS) and Emittance Measurement Unit (EMU) were deployed at this level and provided valuable data for the dual purposes of system development and beam characterization.

BEAM ACCOUNTING

Current Measurements

Six BCMs and three FCs measured the peak beam current that ranged from below 1 mA to beyond the nominal current of 62.5 mA. Figure 2 shows the proton current measured by the BCMs in each of the linac sections, as well as by the FC which was the beam destination at the end of the DTL1. An additional BCM channel also measured the 6 ms pulse extracted from the ion source and this is shown in the inner plot of Fig. 2. The few mA difference between the DTL1 BCM and the DTL1 FC flat top current are due to at least three reasons. Firstly, the DTL1 FC has an entrance foil that filters protons below the nominal energy; secondly, the electron repeller of the DTL1 FC was off; thirdly, the beam is expanded while travelling through the one meter long pipe connecting the DTL1 tank to the shielded beam

DEVELOPMENT OF A WAVEGUIDE BPM SYSTEM*

A. Lyapin[†], W. Shields

John Adams Institute at Royal Holloway, University of London, Egham, UK

Abstract

A mode-selective waveguide beam position monitor (BPM) is under development. It is aimed primarily at electron linacs, although with its low impedance and wide bandwidth it could find alternative applications. In this paper we go over the design of the waveguide BPM system including the sensor and analog electronics, consider requirements to the digital processing and present some simulated results.

INTRODUCTION

Back in 2011, we reported on an idea of a mode-selective waveguide BPM, please, refer to [1] for full details and references to previous work. In a nutshell, we realised that waveguides can be made to selectively couple to the difference mode of the field travelling together with the beam by a special arrangement of coupling slots within the beampipe. At the same time, they suppress the common mode in a way similar to how selective coupling works in cavity BPMs and wakefield suppressing couplers in some accelerating structures. In this proceeding we report on a short project we ran recently that concentrated on advancing this idea towards a design of a complete BPM system. We also discuss the next steps towards a proof-of-principle test.

BENCH MEASUREMENTS

Previously a prototype waveguide BPM had been built for bench testing, Fig. 1. One of the tests carried out with this prototype since the last report was a linearity test. It was done by inserting an antenna into the beampipe to radiate a signal imitating the beam and measuring the transmission from the antenna to the outputs of the waveguide couplers. The aim was to demonstrate the linearity of the device by scanning the antenna position and looking at the corresponding change in the transmission from the antenna to the output port.

The result of this test is shown in Fig. 2. The plot presents the measured transmission coefficient on the complex plane. One can see that all the points lie on a straight line, so the position signal always comes in a certain phase, just like it is the case with cavity BPMs. This allows to separate the position signal from angle and reduce the out-of-phase noise and interference using a phase reference. The measured points corresponding to equal position steps are equidistant, which confirms the device's position linearity.

SENSOR DESIGN

With the encouraging results from bench testing we were able to start designing a prototype for beam measurements. As a starting point, we chose a beam aperture of 8 mm as

* Work supported by STFC Follow On Fund grant number ST/T003413/1
[†] alexey.lyapin@rhul.ac.uk

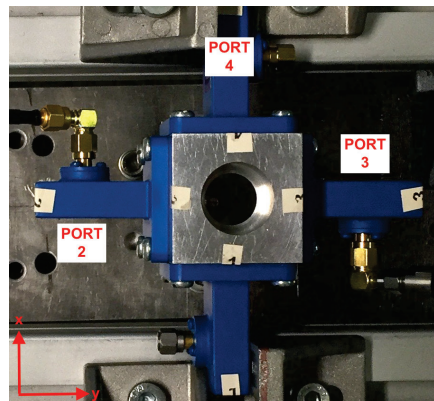


Figure 1: Prototype sensor on a test bench.

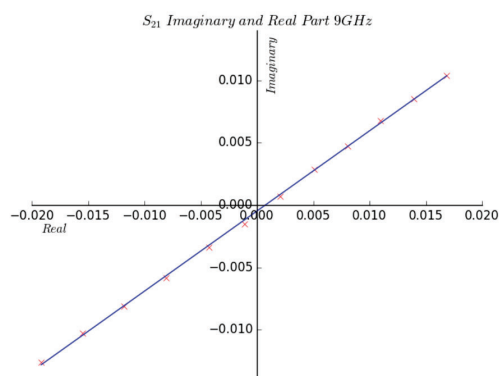


Figure 2: Port transmission measured with a moving antenna.

with little or no modification this would be a fitting design for most undulator beamlines of Free Electron Lasers (FEL). It is also compatible with such a major accelerator project as the Compact Linear Collider (CLIC) and its former test facility now CERN Linear Electron Accelerator for Research (CLEAR), which makes CLEAR a perfect location for future beam tests. We decided to choose 15 GHz as the nominal processing frequency as it was compatible with the selected beampipe diameter. Also, at 15 GHz the waveguide BPM processing can share some parts with the complementary cavity BPM programme running at CLEAR.

The design had thus been optimised for 15 GHz, which is roughly the middle of the chosen WR62 waveguide's passband. Using a Finite Difference Time Domain code GdfidL [2] we tuned the transmission of the difference mode of the beampipe into the output waveguide of the sensor. The resulting transmission curve is shown in Fig. 3. Depending on the chosen processing scheme, a wider or narrower part of the available bandwidth can be used, but up to 10 GHz bandwidth is available.

TOWARDS HIGHER STABILITY IN LARGE SCALE CAVITY BPM SYSTEMS*

A. Lyapin[†], M. S. McCallum

John Adams Institute at Royal Holloway, University of London, Egham, UK

A. Aryshev, K. Kruchinin, High Energy Accelerator Research Organisation (KEK), Ibaraki, Japan

Abstract

In this contribution we consider a possible solution to long-term stability issues common in cavity BPM systems. The method will see a wider use active in-situ calibration systems injecting a tone into the measurement channel. We plan to compensate the bulk of the beam generated signal and so potentially extend the dynamic range of the electronics, reduce the amount of wakefield seen by the beam. The signal matching the real beam can then be used for mimicking the beam and calibrating out any drifts of the whole sensing and processing chain. We present the concept, give some simulated results and consider possible hardware solutions.

INTRODUCTION

In a large accelerator such as a Free Electron Laser (FEL) or a Collider, it is critical to ensure a stable and reproducible beam orbit. Therefore, beam position monitors (BPM) need to provide reliable readings during start-up and operation.

Most FELs employ cavity BPMs to achieve sub- μm resolution at low beam charge. Due to overall high stability requirements their machine tunnel is often kept at a very stable temperature, which reduces any drifts in cavity BPMs and allows them to achieve high stability [1]. This is not likely a plausible scenario for a Collider: it may be unreasonable to expect the same level of stability from a 30 km long facility. Therefore, a different solution may be required.

At KEK (Japan), ATF2 is a model of a collider beam delivery system which relies on cavity BPMs [2]. The facility typically operates over the workdays restarting on a Monday. Cavity BPMs are re-calibrated once a stable beam is available. For operational reasons, calibrations may take about 6-8 hours. While within a week cavity BPMs do not experience substantial drifts, calibrations are rarely transferable to the next week due to changing conditions. The cavity BPM system there is equipped with a subsystem generating a test tone, currently injected directly into the processing electronics. While this system demonstrated that the electronics are responsible for a small fraction of the observed drifts, with modifications it can inject a signal directly into the cavities. In this paper we discuss how the injected pulse can be utilised and how such a system could reduce operational and construction costs in a linear collider.

* Work supported by Royal Society International Exchanges IEC313050 and JAI institutional grant STFC ST/V001620/1

[†] alexey.lyapin@rhul.ac.uk

SYSTEM CONSIDERATIONS

Cavity BPM

Most cavity BPMs deployed at ATF2 use selective waveguide coupling and operate at 6424 MHz (C-band), Fig. 1. Two types of cavities are in use: position sensitive cavities operating the first dipole mode and smaller reference cavities with the first monopole mode tuned to the same frequency $f_{ref} = f_{pos}$ for phase and charge normalisation (Fig. 2). Using the pillbox approximation, the radii of the two types of cavities are then locked by the equality of their frequencies:

$$\frac{j_{01}}{R_{ref}} = \frac{j_{11}}{R_{pos}}, \quad (1)$$

where j_{nm} are Bessel function zeros. This would also mean that in the same environment for both cavities for a change of temperature ΔT the change in diameter is $\Delta R = \alpha \Delta T R$ and the two cavities experience the same frequency offset for a given change in temperature:

$$\frac{\Delta f_{ref}}{\Delta f_{pos}} = \frac{j_{01}}{R_{ref}(1 - \alpha \Delta T)} \frac{R_{pos}(1 - \alpha \Delta T)}{j_{11}} = 1. \quad (2)$$

However, this closed-cavity model does not take into account the effect of the beampipe, which usually has the same or a very similar diameter in both cavities. Moreover, the cavities always have a small frequency mismatch in the order of 2-3 MHz, varying from cavity to cavity. Together with changes in beam trigger timing these can result in significant phase drifts.

Let us estimate the frequency drifts numerically, again, using a simple model consisting of a cylindrical cavity with only a beampipe attached using the dimensions of ATF2 C-band cavities. The thermal expansion coefficient $\alpha = 17 \cdot 10^{-6}$ for copper. A one degree temperature change would result in the radii of the cavity and beam pipe to expand by 0.91 and 0.34 μm in the position cavity and by 0.65 and 0.27 μm in the reference cavity respectively. In terms of frequency, these changes would result in $39 + 17 = 56$ kHz for the position and $251 - 36 = 215$ kHz for the reference. Note that for the reference cavity the change in beampipe diameter even has the opposite sign as the perturbation introduced by the beampipe depends on the mode structure. While this actually helps reducing the reference's higher temperature sensitivity, it is still four times that of the position cavity. The temperature sensitivity does not appear so dramatic until it is expressed in terms of the phase advance it produces. These numbers result in about 19 and 72 degree

REMOVING NOISE IN BPM MEASUREMENTS WITH VARIATIONAL AUTOENCODERS

J. P. Edelen, M. J. Henderson, J. Einstein-Curtis, C. C. Hall, RadiaSoft LLC, CO, USA
A. L. Romanov, Fermilab, IL, USA

Abstract

Noise in beam measurements is an ever-present challenge in accelerator operations. In addition to the challenges presented by hardware and signal processing, new operational regimes, such as ultra-short bunches, create additional difficulties in routine beam measurements. Techniques in machine learning have been successfully applied in other domains to overcome challenges inherent in noisy data. Variational autoencoders (VAEs) are shown to be capable of removing significant levels of noise. A VAE can be used as a pre-processing tool for noise removal before the de-noised data is analyzed via other methods, or the VAE can be directly used to make beam dynamics measurements. Here we present the use of VAEs as a tool for addressing noise in BPM measurements.

INTRODUCTION

In recent years machine learning (ML) has been identified as having the potential for significant impact on the modeling, operation, and control of particle accelerators (e.g. see [1, 2]). Specifically, in the diagnostics space, there have been many efforts focused on improving measurement capabilities and detecting faulty instruments. Relatively recently, ML methods have been utilized to improve optics measurements from beam position monitor data [3]. Additionally, machine learning has been used to identify and remove malfunctioning beam position monitors in the Large Hadron Collider (LHC), prior to application of standard optics correction algorithms [4]. However, noise in BPM measurements remains an issue for processing in even functioning BPMs. The ability to remove noise from these measurements would greatly improve our ability to extract meaningful information from these instruments.

Variational autoencoders (VAEs) are a well established tool for noise reduction due to the enforcement of a smoothness condition in the latent-space representation. This feature of VAEs has been applied to gravitational wave research [5, 6] and geophysical data [7], for example. Recurrent autoencoders have the added advantage of being well suited to work with data sequences. In this paper we explore the use of Variational Recurrent Autoencoders (VRAEs) to remove different power law spectra (colors) of noise from simulated BPM data in a ring. We begin with a review of our data generation model, we then analyze the noise reduction capabilities for Gaussian noise. Finally we test our method using additive noise with different power law spectra.

DATA GENERATION

To simplify exploration of this noise removal technique in this work, we only consider data generated from a simplified model of a circular (periodic) accelerator with analytic solutions [8]. Rather than composing the accelerator of discrete focusing magnets we consider a uniform focusing channel with coupled optics. This reduces the problem to that of a coupled oscillator. We are only considering motion in the transverse plane, such that the equations of motion will be:

$$\begin{aligned} \frac{d^2x}{d\theta} + \nu_x x + C y &= 0 \\ \frac{d^2y}{d\theta} + \nu_y y + C x &= 0. \end{aligned} \quad (1)$$

Where C is the coupling strength and $\theta = 2\pi f t$ is the fractional revolution period in radians. The solutions to the coupled equations of motion will then be:

$$\begin{aligned} x(\theta) &= A_x \cos(\nu_+ \theta) + B_x \cos(\nu_- \theta) \\ y(\theta) &= A_y \cos(\nu_+ \theta) + B_y \cos(\nu_- \theta), \end{aligned} \quad (2)$$

with the coupled oscillation frequency given by:

$$\nu_{\pm}^2 = \frac{1}{2} \left(\nu_x^2 + \nu_y^2 \pm \sqrt{(\nu_x^2 + \nu_y^2)^2 + 4C^2} \right). \quad (3)$$

The principal goal of the analysis tools developed in this paper will be to extract correct, independent frequencies from noisy, periodic measurements of x and y . These are referred to as the tunes, ν_x and ν_y , in Eq. (1). The amplitude coefficients may be uniquely determined from the initial x and y positions, but are not included here as we do not use them in analyzing performance of the methods presented. Our dataset was generated with tune values ranging from 0.05 to 1.6 and a coupling parameter of 0.1. Figure 1 shows an example of this generated data.

To create test and training data x and y , position data is sampled as if from M BPMs placed around a ring so that BPM m will have a phase offset of $\varphi = 2\pi \nu m / M$. Noise in the measurements at each turn N is sampled from a normal distribution $\mathcal{N}(0, \sigma_M)$, where the variance σ_M , representing the noisiness of each BPM, has been set by sampling from a normal distribution $\mathcal{N}(0, \sigma_{noise})$.

The Variational Recurrent Autoencoder Model

For the VAE model, since we are analyzing time series data, we use a recurrent network architecture for the encoder and decoder, which we will refer to as a VRAE. The implementation of the VRAE architecture is based on [9] and uses Long Short-Term Memory (LSTM) units for both the

PRODUCTION OF CAVITY BEAM POSITION MONITORS FOR THE ARES ACCELERATOR AT DESY

D. Lipka*, M. Holz, S. Vilcins
 Deutsches Elektronen-Synchrotron DESY, Hamburg, Germany

Abstract

The SINBAD facility (Short and INnovative Bunches and Accelerators at DESY) hosts various experiments in the field of production of ultra-short electron bunches and novel high gradient acceleration techniques. The SINBAD facility, also called ARES (Accelerator Research Experiment at SINBAD), is a conventional S-band linear RF accelerator allowing the production of low charge ultra-short electron bunches within a range between 0.5 pC and 1000 pC. The positions of the low charge bunches will be detected by cavity beam position monitors. The principal design is based on the experience from the Eu-XFEL cavity beam position monitors. It consists of a 316 LN stainless steel body with a design loaded quality factor of 70, a resonance frequency of 3.3 GHz and a relative wide gap of 15 mm to reach a high peak position sensitivity of 4.25 V/(nC · mm). This poster covered, the manufacture of the individual mechanical parts, as well as presents the special features in the manufacture of customer designed UHV feedthroughs.

and therefore can not be used for tuning. In general the design is optimized to avoid any tuning in frequency and quality factors by defining all mechanical tolerances small enough to be prepared for mass production. The feedthroughs are connected to the body with flanges to be able to exchange them in case of failure, see Fig. 1. The design values are shown in Table 1.

Table 1: CBPM Design Properties [6]

	Dipole	Reference
f_L	3300.0 MHz	
Q_L	69.9	68.9
Q_0	1264	514
Q_{ext}	74.1	79.6
S	4.25 V/(nCmm)	44.5 V/nC

MOTIVATION

SINBAD is a dedicated accelerator R&D facility at DESY, Hamburg, and hosts the ARES linac (Accelerator Research Experiment at SINBAD). It consists of a normal conducting photo-injector and a 100 MeV S-band linear accelerator with beam repetition rates between 10 and 50 Hz for the production of low charge beams (0.5-30 pC) with (sub-) fs duration and excellent arrival time stability [1–4]. For dedicated user experiments bunch charges up to 1000 pC are foreseen. To observe the beam transverse position with highest precision the requirements include a resolution of 5 μm for a beam charge between 5 and 100 pC. To achieve this requirement a cavity beam position monitor (CBPM) is developed.

DESIGN

The CBPM consist of 3 stainless steel discs brazed together which forms the dipole and reference resonators. The dipole mode of the dipole resonator is coupled with 4 symmetric slots to reduce the influence of the monopole mode of the same dipole resonator [5]. The distance of both resonators is chosen to reduce the influence of the reference resonator monopole mode below -100 dB in the dipole resonator mode because both have the same frequency and would add a beam offset, this value corresponds to a maximum of 0.1 μm position offset. The antennas are coupled to the magnetic field of the resonance with multi-contact springs in the body which results in a connection in the body

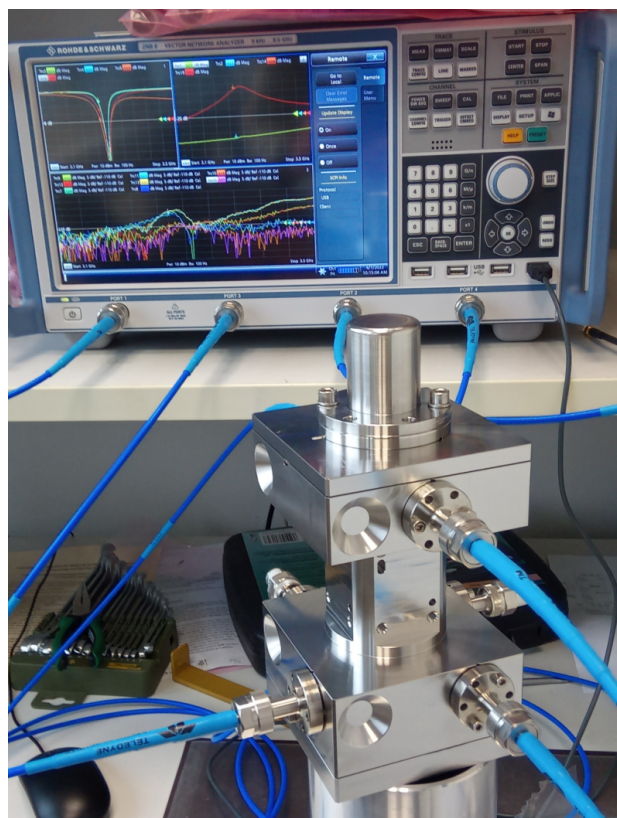


Figure 1: Photo of the CBPM in the laboratory during NWA measurement.

The design is similar to the one for the Eu-XFEL where a low quality factor is required for single bunch measurement with bunch repetition rate of up to 4.5 MHz [7]. The basis

* dirk.lipka@desy.de

TEST AND MEASUREMENTS RESULTS OF THE PILOT TONE FRONT END INDUSTRIALIZATION FOR ELETTRA 2.0

G. Brajnik*, R. De Monte, Elettra Sincrotrone Trieste, Trieste, Italy
M. Cargnelutti, U. Dragonja, P. Leban, P. Paglovec, B. Repič, A. Vigali
Instrumentation Technologies, Solkan, Slovenia

Abstract

Elettra 2.0 will be the low-emittance upgrade of the present machine, a third-generation lightsource based in Trieste, Italy. The new machine, foreseen to be completed in 2025-2026, will be equipped with 168 beam position readout systems divided into 12 cells. The BPM electronics will be based on the prototypes developed by the laboratory, relying on the pilot-tone compensation technique for assuring the required resolution and long-term stability. The industrialization and production of the BPM electronics system are being carried out in partnership with Instrumentation Technologies, a company that has experience with BPM readout systems within the accelerator field. This paper will present the results of the industrialization of one of BPM system's key component: the Pilot Tone Front End, focusing on its improvements introduced on electronic and mechanical sides, giving not only a significant performance gain with respect to the previous prototype but also improving robustness and reliability. An overview of the testing procedures that will assure the performance repeatability of the series will also be provided.

INTRODUCTION

In previous conferences we already presented the overall development of the new electron beam position monitoring system for Elettra 2.0, the low-emittance upgrade of the Italian synchrotron, from the early pilot tone proof of concept [1] to the integration of the complete prototype system in Elettra's global orbit feedback [2]. The partnership signed with Instrumentation Technologies has accelerated the process towards the final industrialized system, foreseen to be installed in 168 locations of the new machine in 2025-2026. In particular, thanks to the modular approach, we firstly focused on the improvement of the pilot tone front end (PTFE) [3] before moving to the digital acquisition unit. In this paper we present the industrialization results of the former, a mature product ready to be produced in series.

MECHANICAL AND ELECTRONIC IMPROVEMENTS

In Ref. [3] we listed the foreseen improvements, such as the possibility of changing the bandpass filter, the extra gain stage, the single board design, the integrated power over ethernet feature. After implementing them, further modifications have been made for increasing reliability and performance.

* gabriele.brajnik@elettra.eu



Figure 1: Pilot Tone Front end.

Shielding and heat management: a large-area aluminium heatsink has been applied over the PCB, with mounting holes for future installation on girders: this allows for an homogeneous heat distribution and adequate dissipation (see Fig. 1). The heatsink serves also as an EMI shield, covering all the RF traces. In addition, another aluminium block completely covers the filters section, reducing external temperature influence.

Amplifiers matching: input and output matching of RF amplifiers that are inside the front end was improved, in order to reduce as much as possible signal reflections and standing waves, with a trade-off between topology of matching circuit, number and value of its components and performance and repeatability of the design. Still, the obtained gain with respect to the original prototype is significant: S_{11} parameter went from -14 dB to -31 dB and S_{22} parameter from -14 dB to -26 dB, measured at 500 MHz.

Ethernet controller: the Ethernet to UART communication chip has been changed from Lantronix to Wiznet, due to PoE compatibility of the latter. The new design is about ten times cheaper, with benefits in term of lower EMI, lower generated heat and power consumption.

Pilot tone generation: accuracy and phase noise of the internal pilot tone generator have been improved: the former has been increased with carefully tuning of crystal's load capacitors, the latter reduced with a new implementation of PLL's loop filter. In addition, the user can choose an external source for supplying the pilot signal.

DESIGN AND IMPLEMENTATION OF AN FPGA-BASED DIGITAL PROCESSOR FOR BPM APPLICATIONS

M. Colja*, S. Carrato, University of Trieste, Trieste, Italy
G. Brajnik, R. De Monte, Elettra-Sincrotrone Trieste, Trieste, Italy

Abstract

Digital processing systems have been proven to often outperform analog elaboration. Indeed, thanks to high-density DSPs and FPGAs, operations in digital domain give results that are impossible to achieve in other ways. On the other side, dealing with this great performance and flexibility is not always straightforward: the processing chain needs to be accurately planned to reach the desired goals, avoiding erratic behaviours in the digital domain. In this paper, we focus on the design and implementation of an FPGA-based digital processor that will be used in the electron beam position monitors of Elettra 2.0. After digitizing the 500 MHz beam signals from the pickups, the system executes a digital down conversion, followed by several filtering and demodulating stages, in order to have a selectable data rate that is suitable for both diagnostics and feedback. The position calculation is also performed in FPGA as well, with the well-known difference-over-sum algorithm. According to results provided by a fixed-point simulation, the overall system has been implemented in an Intel Arria 10 FPGA, demonstrating the correct design functionality that meets the specified requirements.

INTRODUCTION

Digital signal processing has become a standard approach for realizing beam position monitor systems (BPM), thanks to the availability of high-speed, high-performance ADCs and FPGAs [1]. In synchrotrons, it is well known that information about beam position lies in the amplitude of the signal detected by the pickups: due to the typical beam fill patterns used in those machines and after a mandatory analog signal conditioning, it can be seen as a sine with a frequency equal to RF frequency of the accelerator. So, to extract its amplitude after digitization, there is the need for a digital receiver and demodulator that can do it properly for extracting its amplitude after digitization. Then, position calculation algorithm like difference-over-sum can be applied on demodulated amplitudes, converting them into a real beam position, related to vacuum chamber dimensions using a suitable scale factor.

This architecture will be used for the new eBPM system of Elettra 2.0, the low-emittance upgrade of the current machine. The overall modular system and some of its components (e.g. the pilot tone front end) have been already presented [2]; but in this paper we will focus on simulation and FPGA implementation of the complete digital processing chain, from ADC data to calculated position.

* matija.colja@elettra.eu

DIGITAL PLATFORM AND A/D CONVERSION

The digital platform (Fig. 1) has already been presented in previous papers [2, 3]: analog signals from the front end are digitized by an FMC card with four LTC2107, 16-bit ADCs running at 150.38 MS/s, that is 130 times the revolution frequency and phase-locked with it.

Thanks to bandpass sampling technique [4] there is no need for an analog downconversion stage: the 499.654 MHz signal is seen by the ADCs as a 48.514 MHz sine, since it is folded back in the Nyquist zone corresponding to three times the sampling frequency. Obviously, this approach needs a high-performance, low-jitter clocking stage and an analog bandpass filter to reduce out-of-band noise.

Then, ADC data are processed by an Intel Arria 10 GX FPGA: the high amount of logic gates and DSP resources render it possible to realize in digital the complete processing chain. Connections with external devices are assured by internal transceivers attached to SFP+ modules capable to go at a speed up to 10 Gb/s.



Figure 1: Digital platform.

DEVELOPMENT OF NON-INVASIVE CALIBRATION SOFTWARE FOR FRONT END X-RAY BEAM POSITION MONITORS AT DIAMOND LIGHT SOURCE

C. Houghton*, C. Bloomer, L. Bobb, Diamond Light Source Ltd, United Kingdom

Abstract

Tungsten blade based photoemission X-ray Beam Position Monitors (XBPMs) are widely used as white beam diagnostics at synchrotrons. Traditionally, the scale factors are determined by stepper motor movements of the XBPM, or by controlled electron beam displacements, and measuring the response. These measurements must be repeated for each ID gap to produce a complete set of scale factors for all operational conditions. This calibration procedure takes time and cannot be done while users are acquiring data. In addition, the scale factors can vary over time due to changes to the storage ring. It is possible for these scale factors to become inaccurate, reducing the accuracy of the beam position measured by the XBPMs. By using the intrinsic kHz electron beam movements and correlating the signals from electron beam position monitors and XBPMs it is possible to have real-time calculation of the scale factors without the need to disturb user operation. Presented in this paper is a method to non-invasively calculate scale factors during normal user operation. A comparison of the precision of this method versus the traditional stepper motor method is presented.

INTRODUCTION

To monitor and improve the stability of the photon beam Diamond Light Source utilises two X-ray beam position monitor (XBPMs) on most insertion device (ID) front ends. Each XBPM is mounted on stepper motors to enable precise alignment of the XBPM with the incident X-ray beam. Traditionally, the XBPM calibration factors, or ‘scale factors’ are obtained by measuring the position response of the XBPM whilst a known stepper motor offset is applied, to simulate real X-ray beam movements. Alternatively, the beam movements can be generated using an electron beam bump. Corrector magnets are used to induce a known angular offset through the ID. This in turn produces a fixed offset of the X-ray beam at the XBPM. A scale factor, K , can be calculated by comparing the measured response of the four XBPM blades to the known applied beam offset. The response of the XBPM is defined by

$$(\Delta/\Sigma)_x = \frac{(I_A + I_D) - (I_C + I_B)}{I_A + I_B + I_C + I_D} \quad (1a)$$

$$(\Delta/\Sigma)_y = \frac{(I_A + I_B) - (I_C + I_D)}{I_A + I_B + I_C + I_D} \quad (1b)$$

where Δ/Σ is a dimensionless position and $I_{(A,B,C,D)}$ are the currents from the four XBPM blades (A = top-left;

* claire.houghton@diamond.ac.uk

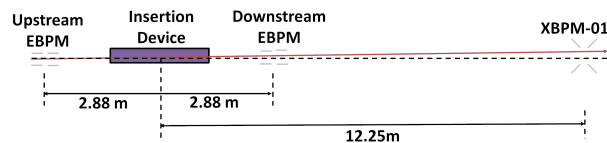


Figure 1: Schematic of the EBPM and XBPM locations for a typical Diamond Light Source Insertion Device straight.

B = top-right; C = bottom-right; D = bottom-left) when viewed from the X-ray source. The calculation of the XBPM scale factors using these methods has several limitations. Firstly, both these methods require specific machine development time and cannot be done during user operation. Secondly, the XBPM scale factor is dependent on the ID settings particularly the ID gap. As the ID gap varies there are changes to the XBPM sensitivities due to the change in the photon beam distribution [1, 2]. Currently, the scale factors, K_x and K_y , are calculated for a selection of ID gaps and can be used to convert the dimensionless position, Δ/Σ , to a horizontal and vertical position in millimeters. Current methods for calibration use interpolation in order to populate lookup tables for all possible ID gaps.

Presented in this paper is a method for utilising the intrinsic electron beam movements and fast electronics in order to calculate XBPM scale factors passively during user operation.

SET-UP

Diamond Light Source has a Fast Acquisition network which can synchronously capture the position data from electron beam position monitors (EBPMs) and XBPMs at a rate of 10 kHz [3]. This data stream allows for the comparison of the electron beam trajectory through the ID with the X-ray beam position at the XBPM. For the duration of one user run at Diamond Light Source, 1 s of the 10 kHz position data was collected from the EBPMs and XBPMs at intervals of 10 seconds from the I14 insertion device beamline. The ‘projected’ position of the X-ray beam at the XBPM is determined from a geometric projection of the EBPM measurements from either side of the insertion device out to the distance of the XBPM. Figure 1 shows a schematic of the system and distance to these components.

The projected and measured X-ray beam positions are analysed by calculating the Singular Value Decomposition (SVD); finding the major axis between the two data sets returns the scale factor between the XBPM response and the EBPM projections [4]. Figure 2 shows the correlation between the measured and the projected XBPM measurement.

TIME RESOLVED DYNAMICS OF TRANSVERSE RESONANCE ISLAND BUCKETS AT SPEAR3*

K. Tian[†], J. Corbett, J. Kim, J. Safranek
 SLAC National Accelerator Laboratory, CA, USA

Abstract

Transverse Resonance Island Buckets have been studied at SPEAR3 as an option for timing experiment mode operation. In this mode, with proper lattice optics settings, the electron beam populates to island orbits with the excitation from a kicker. In this paper, we will report the experimental observation of beam dynamics with turn by turn beam position monitors and a fast gated camera.

INTRODUCTION

The SPEAR3 3-GeV, high-brightness third-generation storage ring, upgraded in 2004, operates at 500 mA in top-off mode, with high reliability and low emittance. Recently, there is growing interest in conducting time-resolved experiments from the user community. To enhance the timing mode experimental capability of SPEAR3 and fulfill the requirements of timing users and high-brightness users simultaneously, efforts have been devoted to develop new operation modes in SPEAR3.

Beam resonances in a storage ring are generally considered as limiting factors for the beam performance. Therefore, operational betatron tunes are chosen to avoid harmful resonance lines such as those of integer tunes and half-integer tunes. However, when a potential-well is formed around certain high-order resonances, a bunch can be trapped inside the potential-well and become stable. This so-called Transverse Resonance Island Bucket (TRIBs) mode has been studied and demonstrated at BESSY II [1] and MAX-IV [2]. Operating in this mode, it is possible to select and populate part of the bunch train on a different closed orbit from the main bunch. At the interested beamline, the unwanted X-ray from the main bunch train can be blocked to improve the signal-to-noise ratio of the timing experiment. The under-development 6 nm lattice of SPEAR3, has a designed ν_x of 15.32, which can be successfully exploited for the TRIBs studies. The TRIBs mode can be activated by either the SPEAR3 transverse multi-bunch feed back (TMFB) kicker [3] or one of the three injection kickers, K1, under slightly different lattice settings.

SPEAR3 TRIBs MODE

Tracking Simulations

Prior to our experimental studies, tracking simulations were first conducted with the 6 nm lattice to confirm the possibility for running TRIBs mode in this lattice. Using

ELEGANT [4], single particles with variable initial offsets were tracked in a lattice obtained from optics fitting with LOCO [5]. The distribution of three resonance islands is visualized in the top plot of Fig. 1 as three potential wells when $\nu_x = 0.3333$. Once the electron beam is trapped in one of these islands, the new orbit (x, x') , passing through the centers of the 3 islands as shown in the bottom plot of Fig. 1, is closed every 3 turns.

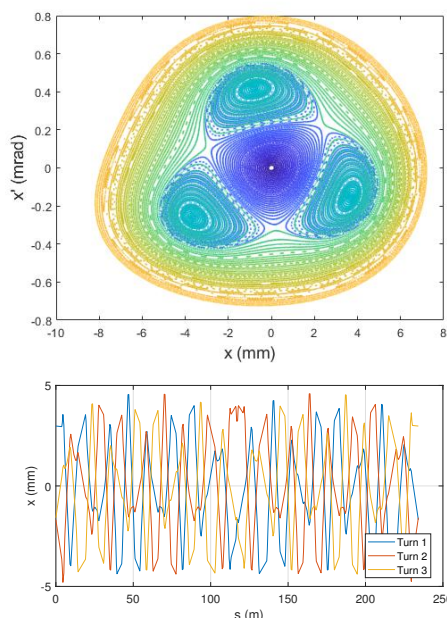


Figure 1: Closed orbit for SPEAR3 TRIBs optics.

TRIBs Excitation

The nominal chromaticity of the 6-nm lattice is +2 for both the horizontal and the vertical planes. During our TRIBs study, the horizontal chromaticity, ξ_x , was reduced to nearly 0 using a chromaticity response matrix. $\xi_x = 0$ helps to avoid tune shifts caused by momentum deviation when driving the beam horizontally. Experimentally, it was found that the TRIBs mode could be better excited when ξ_x was slightly larger than zero. We were able to drive the TRIBs mode either with the TMFB kicker or the injection kicker, K1. With the TMFB kicker, ν_x was increased to 0.3297 from the design value of 0.32 due to the relatively weak strength of the kicker. In addition, the kicker needed to be set up with a frequency sweep within a short period of time. On the other hand, the K1 kicker strength was strong enough to move the beam to the TRIBs islands with a single pulse. Because the excitation from the K1 kicker was relatively

* Work supported by U.S. Department of Energy under Contract No. DE-AC02-76SF00515

[†] ktian@slac.stanford.edu

DEVELOPMENT OF A SCINTILLATION FIBRE TRANSVERSE PROFILE MONITOR FOR LOW-INTENSITY ION BEAMS AT HIT*

R. Hermann^{†, 1,2}, T. Haberer², A. Peters², T. Gehrke^{1,3,4}, B. Leverington⁵ and M. Galonska²

¹Heidelberg University Hospital, Department of Radiation Oncology, Heidelberg, Germany

²Heidelberg Ion-Beam Therapy Center (HIT), Department of Radiation Oncology, Heidelberg University Hospital, Heidelberg, Germany

³German Cancer Research Centre (DKFZ), Department of Medical Physics in Radiation Oncology, Heidelberg, Germany

⁴National Center for Radiation Research in Oncology (NCRO), Heidelberg Institute for Radiation Oncology (HIRO), Heidelberg, Germany

⁵Physikalisches Institut, Ruprecht-Karls-Universität Heidelberg, Heidelberg, Germany

Abstract

The Heidelberg Ion-Beam Therapy Center (HIT) provides proton, helium, and carbon-ion beams with different energies and intensities for cancer treatment and oxygen-ion beams for experimentation. The accelerator is able to provide ion beam intensities below the range used for therapies by manually degrading the beam. The beam monitoring system instrumentation currently installed is unable to measure the beam profile at these intensities. A secondary system that could cover this low intensity range is therefore of interest. The principle of operation is based on scintillating fibres, particularly those with enhanced radiation hardness. The fibres transform the deposited energy of a traversing ion into photons, which are then converted and amplified via silicon photomultipliers (SiPMs) into electric pulses. These pulses are recorded and processed by a novel and dedicated readout electronics: the front-end readout system (FERS) A5200 by CAEN. A prototype set-up consisting of all the above-mentioned parts was tested in beam and has proven to record the transverse beam profile successfully from intensities of $1E7$ ions/s down to $1E2$ ions/s.

INTRODUCTION

The HIT facility provides proton, carbon, and helium ion pencil beams for cancer treatment and research, and oxygen ion beams for experiments, all with various energies, beam spot sizes and intensities. HIT uses the method of intensity-controlled raster scanning of pencil beams as a dose delivery system.

The beam position and width (focus) in the horizontal and vertical plane are constantly monitored by two multi-wire proportional chambers (MWPC) and the intensity by three ionization chambers (IC). Their signals are used for position and intensity control via a feedback system. As this built-in setup is specifically designed for tumour treatments it does not need to be, and is not, sensitive to low-intensity ion beams, i.e. below $1E5$ ions/s. This detector reported in this contribution closes this gap.

Low intensity beams are of interest for experiments, but also for a new imaging modality with potential of treatment verification: helium-beam radiography [1]. The presented work is part of this project. Only low intensities may be used as radiation dose in the patient has to be limited to the lowest amount possible and ion tracking based on single ion imaging is desirable. For an optimized performance, the low-intensity ion beam needs to be provided in a controlled way.

Out of three possible detector technologies (gas, semiconductor, and scintillating fibre based) the scintillating fibre was chosen because of its advantages in terms of permanent use and placement within the beamline of an accelerator: the relatively low cost of the fibres while covering a larger active area, no need of attached subsystems like cooling, gas or vacuum and electronics remain in a safe distance from the beam. This idea follows techniques used in high energy physics, coupling scintillating fibres to silicon photomultipliers for single particle tracking [2]. The Super Proton Synchrotron has developed a similar system, although with different readout electronics and beam conditions [3].

A novel specialized commercial front-end readout electronic board came into use: the FERS A5202 by CAEN, which was for instance successfully implemented in a dual readout calorimeter by the team of R. Santoro [4]. Due to the commercial character, there was no need for an own development in electronics or software. Thus, one can concentrate on specific data evaluation routines. Also scaling up the detector to the desired size of 25×25 cm² with a sub-millimetre resolution is feasible to implement due to the scalability of the readout system.

MATERIALS AND METHODS

Ion Beam Characteristics

Adopted to the dose delivery system, the HIT accelerator provides ion beams for cancer treatment by a slow extraction scheme, i.e. the ions are extracted over several seconds (“Spill length”, here: 5 s). The energy/intensity range is given in Table 1. The beam spot sizes range from about 3 to 30 mm defined as full-width half-maximum (FWHM), depending on the ion type and energy. For reaching low

* Work funded by the German Research Foundation (Deutsche Forschungsgemeinschaft, DFG), project number 426970603.

† richard.hermann@med.uni-heidelberg.de

X-RAY PINHOLE CAMERA SPATIAL RESOLUTION USING HIGH ASPECT RATIO LIGA PINHOLE APERTURES

N. Vitoratou*, L. Bobb, Diamond Light Source, Oxfordshire, UK
G. Rehm, Helmholtz-Zentrum für Materialien und Energie, Berlin, Germany
A. Last, Karlsruhe Institute of Technology, Karlsruhe, Germany

Abstract

X-ray pinhole cameras are employed to provide the transverse profile of the electron beam from which the emittance, coupling and energy spread are calculated in the storage ring of Diamond Light Source. Tungsten blades separated by shims are commonly used to form the pinhole aperture. However, this approach introduces uncertainties regarding the aperture size. X-ray lithography, electroplating and moulding, known as LIGA, has been used to provide thin screens with well-defined and high aspect ratio pinhole apertures. Thus, the optimal aperture size given the beam spectrum can be used to improve the spatial resolution of the pinhole camera. Experimental results using a LIGA screen of different aperture sizes have been compared to SRW-Python simulations over the 15–35 keV photon energy range. Good agreement has been demonstrated between the experimental and the simulation data. Challenges and considerations for this method are also presented.

INTRODUCTION

X-ray pinhole cameras (XPCs) are a well-established diagnostic tool for measurement of the 2D transverse beam profile of the electron beam in the storage ring [1]. From the acquired beam size measurement, combined with knowledge of the lattice parameters, the emittance and coupling are calculated. The expected beam sizes in Diamond-II will be smaller than the nominal operation of Diamond, particularly for emittance measurement of the squeezed beam after correction of the lattice using the linear optics from closed orbits (LOCO) method [2].

The Point Spread Function (PSF) of the imaging system should be minimised to improve the spatial resolution. The overall PSF is represented by the contributions of the scintillator screen, the lens, the camera sensor and the pinhole aperture itself which is a fundamental component in the pinhole camera. Reduction of the PSF can be achieved by using the optimal pinhole aperture size for the given photon beam energy of the synchrotron radiation [1]. For sufficient contrast at photon energies in the 15–60 keV range, the pinhole aperture must be formed using a material with a high atomic number.

High Z-number materials are often difficult to machine, especially to form high aspect ratio structures, e.g. a rectangular square aperture of $10\ \mu\text{m} \times 10\ \mu\text{m}$ with a thickness of $250\ \mu\text{m}$ to $1\ \text{mm}$. Due to this, the pinhole aperture is often formed by stacking two orthogonal sets of tungsten blades

separated by precisely machined shims. The thickness of the shims between the tungsten blades sets the aperture size [3]. Although the blades have surfaces that are easy to polish and the shims can be manufactured to the specified thickness, there are drawbacks to this stacked design. Firstly the pinhole aperture, which from theory should be an infinitesimally thin screen is a 10 mm long tunnel, making simulation challenging. Secondly, the effective aperture size is typically larger than the shim thickness. And thirdly, the absolute measurement of the effective aperture size in this geometry is not trivial.

LIGA (X-ray lithography) technology [4] enables the fabrication of high-aspect ratio structures using high-Z materials such that the pinhole aperture size is known and controllable. Furthermore, the tunnel-like geometry of the aperture is removed to provide better agreement with theoretical models. At the Karlsruhe Institute of Technology, unique LIGA screens are produced. These are made from gold with a thickness up to $250\ \mu\text{m}$. Thus, allowing the comparison between simulations of the pinhole camera with real acquired data on the accelerator. This could enable simulation of the PSF of the pinhole camera instead of PSF measurement using Touschek calibration with beam which is time-consuming [5].

In this paper, simulations and measured pinhole camera images from a bending magnet sourcepoint using a LIGA screen are compared.

EXPERIMENTAL SETUP

Pinhole camera 3 is installed on the Diagnostics X-ray beamline inside the storage ring tunnel for the purpose of R&D. A schematic of the setup is shown in Fig. 1. The pinhole-to-scintillator distance is 9.72 m, the source-to-

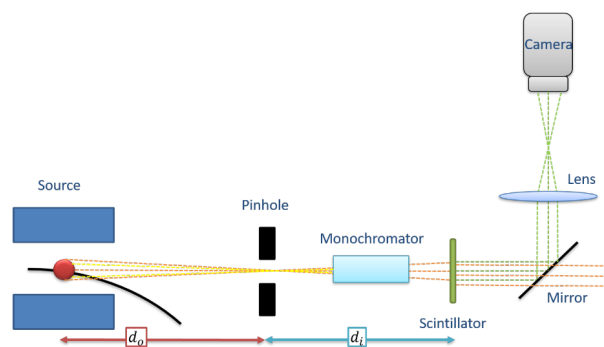


Figure 1: Schematic of an X-ray pinhole camera from a bending magnet sourcepoint.

* niki.vitoratou@diamond.ac.uk

COMMISSIONING OF THE RENEWED LONG RADIAL PROBE IN PSI's RING CYCLOTRON

M. Sapinski*, R. Dölling, M. Rohrer, Paul Scherrer Institut, Villigen, Switzerland

Abstract

PSI's Ring cyclotron is a high intensity proton cyclotron producing a CW proton beam of 2 mA. The beam is accelerated over about 180 turns from 72 MeV to 590 MeV. The Long Radial Probe, called RRL scans the beam along a machine radius over the whole range of turns, i.e. from 2048 mm to 4480 mm. A replacement for the RRL has been developed in the last years. The recently installed new probe drives three carbon fibers with 30 μm diameter through the turns and measures secondary electron emission (SE) currents, providing information on horizontal and vertical beam shape and position. Additional drives are available for a later extension of measurement capabilities. The main challenges are the coupling of the device elements to RF fields leaking from the accelerating cavities, plasma interfering with the measured signal, and the performance of the carbon fibers in a harsh environment with a high-intensity beam and RF heating. We report on the commissioning of the probe with RF and beam and discuss measurement results.

INSTRUMENT DESIGN

The RRL drives three carbon fibers stretched between the upper and bottom trolley, along the radius of PSI's Main Ring cyclotron [1, 2]. The trolleys, powered by the same stepper motor, move synchronously with a speed of 29.7 mm/s. The fibres are oriented vertically and tilted -45° and $+45^\circ$ seen in the beam direction. The setup is visualized in Fig. 2 of [3].

The vertical wire (0°) crosses all orbits in the cyclotron, the -45° wire misses the first orbit and the $+45^\circ$ wire misses the first four orbits. Each scan is performed in two directions: from the parking position at a radius of 4480 mm to the most inner position at 2048 mm (scan *in*) and back (scan *out*).

Between the upper and bottom parts of the main structure of the probe there is a 40 mm clearance for the beam. The structure is milled out of an aluminum alloy (EN AW-5083) and its overall weight is around 100 kg. It contains cables, cable trays, metallic perforated transmission belts used to move the trolleys, and thermocouples to measure the main probe structure temperature. It is grounded at the top and bottom of the vacuum chamber by 20 roller contacts each (Fig. 1). The contacts are installed in pairs, spaced by 25 cm. Four shields are installed on both sides to protect fibres from RF fields and plasma.

Measurement of trolley vibrations performed with PCB-356B18 triaxial accelerometer revealed that the highest vibration amplitude is in the direction of the scan (Fig. 2). The frequency spectrum is broad and drops above 400 Hz, however, it is not yet clear how it affects the signal quality.



Figure 1: Roller contact for grounding probe structure.

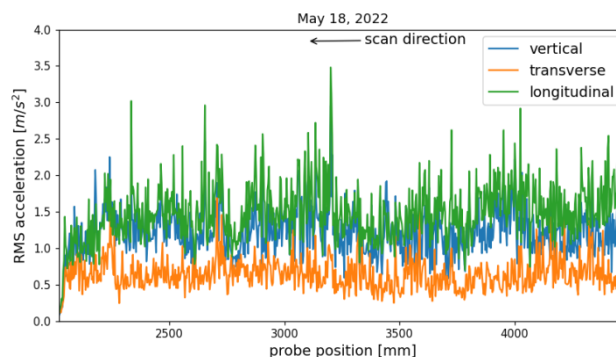


Figure 2: The RMS acceleration measured on the trolley during the scan.

The RRL is installed in the intermediate sector chamber #2, an area of the cyclotron in between two dipole magnets and not equipped with a RF cavity (see Fig. 3 of [2]). This sector contains the electrostatic injection septum EIC and is on the outside equipped with three air-filled ionization chambers called MRI2 at the low radius, MRI9 at the high radius, and MRI9B in the middle.

The signals from the carbon fibers are digitized by MESON logarithmic amplifier modules [4] outside of the bunker, which also control the movement of the trolleys.

COMMISSIONING WITHOUT BEAM

One of the main concerns was the coupling of the RRL structure and the carbon wires to the RF fields leaking out of the cyclotron RF cavities. Therefore, numerous RRL measurements were performed during the RF-conditioning period in March and April 2022.

Observation of RF Heating

Fast detection of eventual strong temperature changes of RRL elements is not possible with the thermocouples due to the large thermal inertia of the main structure. Hence, a FLIR AX8 camera with infrared and visible light sensors has been installed at the height of the machine midplane (Fig. 3). The viewport with a ZnSe IR-transparent window was mounted on a specially-designed flange with an angle allowing for optimal coverage of the probe structure. This flange was equipped with RF shields due to concerns about

* e-mail address: mariusz.sapinski@psi.ch

FIRST RESULTS OF PEPITES A NEW TRANSPARENT PROFILER BASED ON SECONDARY ELECTRON EMISSION FOR CHARGED PARTICLE BEAMS

C. Thiebaut[†], L. Bernardi, F. Gastaldi, Y. Geerebaert, R. Guillaumat, F. Magniette, P. Manigot, M. Verderi, Laboratoire Leprince-Ringuet, CNRS-Ecole polytechnique, Institut Polytechnique de Paris, Palaiseau, France
E. Delagnes, F. Gebreyohannes, O. Gevin, CEA-IRFU, Université Paris-Saclay, Saclay, France
F. Haddad¹, C Koumeir, F. Poirier, GIP ARRONAX, Saint-Herblain, France
¹also at Laboratoire SUBATECH, Nantes, France
N. Servagent, Laboratoire SUBATECH, IMT Atlantique, Nantes, France

Abstract

The PEPITES project* consists of a brand new operational prototype of an ultra-thin and radiation-resistant profiler capable of continuous operation on mid-energy (O(100 MeV)) charged particle accelerators in the vacuum of the beamline. Secondary Electron Emission (SEE) is chosen for the signal because it requires a small amount of material and is very linear. The monitor is made of segmented electrodes (strips), generating the SEE signal when crossed by the beam. Signals from the strips are carried outside the beamline and are read by a dedicated low-noise and high-dynamic electronic. A demonstrator is installed at ARRONAX and has been successfully operated on a wide dynamic. Its permanent installation will allow a long-term feedback.

INTRODUCTION

Protontherapy dose delivery requires a continuous and accurate measurement of beam properties, intensity, position and profile during patient treatment. The beam monitors must be thin enough to limit the effects of scattering to a submillimeter lateral spread of the beam at the patient. For monitors located a few meters upstream of the patient, this translates into a material budget of less than 15 μm water equivalent thickness (WET). Good resistance to radiation is also necessary, as the long exposure time results in integrated doses of some 10^6 to 10^8 Gy per year.

To fulfil these requirements, PEPITES [1,2], a new type of transparent beam profiler ($< 10 \mu\text{m}$ WET) has been developed. It equips the beam line of the ARRONAX cyclotron [3] and will be used daily to monitor the beam during radiobiological and preclinical experiments [4]. The profiler will measure the lateral beam shape in a broad range of energy (15 – 70 MeV) and a wide range of intensity (100 fA – 10 nA), for alpha, proton and deuteron particles.

PRINCIPLES

PEPITES uses secondary electron emission (SEE) for the signal as it requires only a minimal thickness of material (~ 10 nm); very linear, it also offers a great dynamic.

The SEE yield is proportional to the dE/dx of the beam particles [5,6] and is independent of the beam intensity up to current far beyond expected needs both for medical use and radiobiology needs. The lateral beam profile is sampled using segmented electrodes, constructed by thin film methods. Gold strips, as thin as the electrical conductivity allows (50 nm), are deposited on an as thin as possible insulating substrate which, in contrast with conventional systems like ionization chambers, are free from mechanical constraints and can be as thin as achievable. Polyimides (PI), such as Kapton[®] or CP1[™], are chosen as polymer substrates because of their insulating properties and the presence of aromatic cycles in their structure that make them extremely resistant to radiation [7]. When crossing the gold, the beam ejects the electrons by SEE, the current thus formed in each strip allows the sampling.

The thinness of the monitor disturbs very little the incident beam, which can then be delivered to the patient while keeping the profiler in the line, ensuring continuous monitoring. Also, it makes the energy deposit very small allowing the monitor to tolerate higher currents than existing systems without suffering from overheating problems. Besides, the absence of mechanical efforts on the membranes makes radiation damages of less consequence than with classical systems like ionization chambers allowing to extend the operation duration of the system.

Detector Layout

The layout of the prototype is shown in Fig. 1. It consists of four electrodes: two segmented cathodes each facing an anode (with a 15 mm gap) biased at 100 V to ensure the collection of secondary electrons emitted by the strips. The four electrodes are made of 50 nm thick gold deposited by chemical vapor phase on polymer membranes: 32 strips for cathodes and fully metallized anodes. The membranes are made of 1.5 μm thick CP1[™], a colorless polyimide produced by the NeXolve company¹. Initially developed for

* Work supported by Agence Nationale de la Recherche ANR-17-CE31-0015, ANR-11-EQPX-0004

[†] thiebaut@llr.in2p3.fr

¹<https://www.nexolvematerials.com/>

DEVELOPMENT OF NEW BEAM POSITION DETECTORS FOR THE NA61/SHINE EXPERIMENT

M. Urbaniak*, Y. Balkova, S. Kowalski, S. Puławski, K. Wójcik
University of Silesia, Institute of Physics, Chorzów, Poland

Abstract

NA61/SHINE is a fixed-target experiment located at the CERN Super Proton Synchrotron (SPS). The development of new beam position detectors is part of the upgrade of the detector system. Two types of detectors have been manufactured and tested. The first one is a scintillating fibers detector with a photomultiplier as a readout. The scintillating fibers detector consists of two ribbons, which are arranged perpendicularly to each other. Each ribbon is made of two layers of 250 μm diameter fibers. The grouping method was used, which allows using of a single multichannel photomultiplier for one detector. The second type of detector is based on the single-sided silicon strip detector (SSD). In this project, Si strips produced by Hamamatsu (S13804) were used, where the pitch has a width equal to 190 μm . The developed detectors must meet several requirements: they should work efficiently with proton and lead beams with beam intensity on the level of 100 kHz, the detector's material on the beam-line should be minimized, and the detectors should be able to determine the position of X and Y hit of each beam particle with maximum possible accuracy.

INTRODUCTION

NA61/SHINE is a fixed-target experiment located in the North Area of the CERN Super Proton Synchrotron (SPS) [1]. Developing a new Beam Position Detector (BPD) is part of the upgrade of the detection system of the experiment during the Long Shutdown 2 (LS2) upgrade. Two alternative BPD designs are described in the paper.

The NA61/SHINE detector system includes Time Projection Chambers (TPCs), Time of Flight detectors (ToF), and Vertex Detector (VD) downstream of the target. The system's primary goal is to measure the particles produced in the interaction of the beam particles with the target. Additionally, upstream of the target is located a set of beam detectors that provides the identification, timing references, and beam position measurements. The schematic layout of the detector system is shown in Fig. 1.

Beam Position Detectors are used to calculate the trajectory of the incoming beam particle based on its measurement in X and Y planes along the beamline. The new beam position detectors should allow for the measurement of the trajectory of each proton or lead beam particle separately with intensities on the level of 100 kHz with maximum possible accuracy. Additionally, the detector should operate in a vacuum. Two types of detector have been designed and manufactured and are currently being tested: a scintillating fibers detector and a single-sided silicon strip detector.

* marta.urbania@us.edu.pl

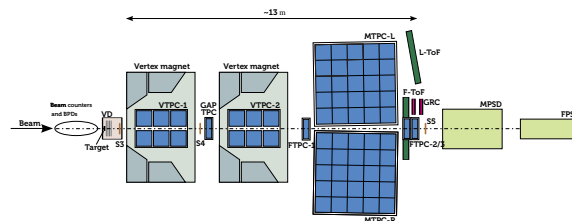


Figure 1: Schematic layout of the NA61/SHINE experiment after the LS2 upgrade.

SCINTILLATING FIBERS DETECTOR

The scintillating fibers detector consists of two ribbons placed perpendicularly to each other. Such construction allows measuring the position of the particle passage in the XY plane. Each ribbon is made of two layers of scintillating fibers. Saint-Gobain, round shape, double cladding scintillating fibers (BCF-60) with 250 μm diameter were chosen [2]. The BCF-60 has an extra 3HF formulation which increases its radiation hardness. Layers are shifted relative to each other by a distance equal to the radius of a single fiber, which minimizes the detector's dead area. The end of each ribbon is connected to the 256-channel multianode Hamamatsu photomultiplier (H9500). The photo of the prototype detector is presented in Fig. 2.

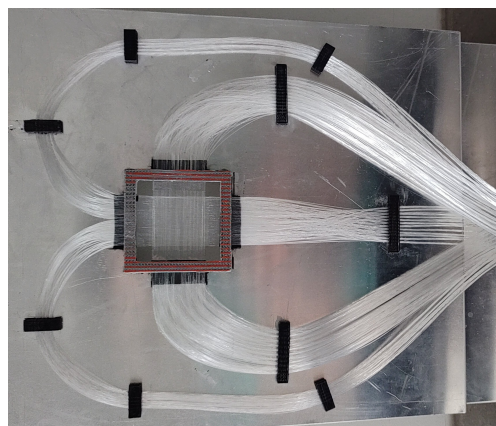


Figure 2: Photo of the scintillating fibers detector.

Finally, grouping of the fibers was implemented to reduce the number of readout channels from 480 to 88. Instead of connecting each fiber to one photomultiplier pixel, ten or twelve fibers are connected into groups and applied to a single pixel. The grouping is as follows: the fiber ends

RECENT LHC SR INTERFEROMETER SIMULATIONS AND EXPERIMENTAL RESULTS

D. Butti^{*,1}, E. Bravin, G. Trad, CERN, Geneva, Switzerland
S. Gibson, Royal Holloway, University of London, Egham, United Kingdom
¹also at Royal Holloway, University of London, Egham, United Kingdom

Abstract

At the CERN Large Hadron Collider (LHC), among the different systems exploiting Synchrotron Radiation (SR) for beam diagnostics, interferometry is under study as a non-invasive technique for measuring absolute transverse beam sizes. Extensive numerical simulations, recently completed for characterising the spatial coherence of the LHC SR source, facilitated the optimisation of the LHC interferometer design and the existing prototype system tested in the past has been refurbished to include the new simulation findings. This contribution will describe the simulation specificity and then focus on the first measurements performed in a very tight schedule during the LHC Run 3 test run in October 2021. Such experiments allowed to obtain a first validation of the expected system performance at the injection energy of 450 GeV. A complete benchmark of the simulations will be carried out in 2022 as soon as the LHC will reach its top energy of 6.8 TeV.

INTRODUCTION

The transverse beam diagnostics at the Large Hadron Collider (LHC) is currently performed with two families of operational instruments [1]. Wire scanners (WS) provide an absolute size measurement but their usage is limited below a certain beam intensity due to damage to the wire caused by beam-wire interactions. A second instrument, the Beam Synchrotron Radiation Telescope (BSRT), exploits synchrotron radiation imaging for the continuous monitoring of the beam size. At present the BSRT cannot provide an absolute measurement and so a cross-calibration with the WS is required.

Synchrotron radiation interferometry is an optical technique, alternative to imaging, that can provide a non-invasive and absolute measurement of the transverse size of a luminous source [2]. This technique has been proposed for beam diagnostics [3] and it is currently exploited at the LHC to complement the operational instrumentation with a redundant and independent system [4].

The Beam Synchrotron Radiation Interferometer (BSRI) installed at the LHC is a classical Young's double slit interferometer. The visible synchrotron radiation (SR) emitted by the beam is sampled by two slits. The wavelets propagate through an optical system that produces the SR interferogram onto an intensified camera. The technique is based on a fundamental result of classical optics, the Van Cittert and Zernike theorem (VCZ). This theorem states that the spatial

coherence $|\gamma_{12}|$ of the points sampled by the slits coincides with the Fourier transform of the source transverse profile [5]. For Gaussian sources, the coherence as a function of the slit separation D is still a Gaussian

$$|\gamma_{12}| = \exp\left[-\frac{D^2}{2\sigma_{coh}^2}\right]. \quad (1)$$

The standard deviation $\sigma_{coh} = (\lambda L_0)/(2\pi\sigma)$ defines the coherence area of the radiation, where λ is the wavelength, L_0 the source distance and σ the source size.

Experimentally, the spatial coherence is measurable through the visibility of the radiation interferogram

$$V = \frac{2\sqrt{I_1 I_2}}{I_1 + I_2} |\gamma_{12}|, \quad (2)$$

being I_1 and I_2 the total light transmitted through each aperture whose effect is to reduce the expected visibility if the slits are unevenly illuminated, i.e. $I_1 \neq I_2$.

The VCZ theorem strictly applies to thermal sources which consist of many point-like independent emitters radiating an isotropic wavefront. In case of non-thermal sources, such as SR radiated by relativistic beams, the theorem has to be validated on a case-by-case basis [6, 7].

In this paper, the unique features of the LHC SR source are presented and the results of the VCZ validation by means of SR simulations are discussed.

THE LHC SYNCHROTRON RADIATION SOURCE

The radiation source used for beam diagnostics at the LHC consists of two types of magnetic devices [8]. At injection energy, visible light is emitted by a superconducting undulator. As the beam energy increases, the undulator spectrum drifts towards the soft X-rays region. Above 2 TeV, the main source of visible light becomes the D3_R, a D3-type dipole located just downstream of the undulator. The undulator and the D3_R are the main devices of the LHC SR source. A second D3-type dipole, the D3_L, contributes to the SR emitted at high beam energy. This dipole is located approximately 100 m upstream of the undulator, on the opposite side of the RF cavity section. After the source, the SR propagates for ~ 25 m inside the beam chamber until it is intercepted and extracted by an in-vacuum mirror that sends the light towards the BSRI slits. Figure 1 shows a layout of the source devices and the extraction system.

The contribution from the D3_L has been recently detected with the SR interferometer [9]. The presence of this dipole is in fact negligible for the BSRT as it is far away from the

* daniele.butti@cern.ch

TEST OF A PROTOTYPE FOR MODULAR PROFILE AND POSITION MONITORS IN THE SHIELDING OF THE 590 MeV BEAM LINE AT HIPA

R. Dölling[†], M. Sapinski, F. Marcellini, Paul Scherrer Institut, Villigen, Switzerland

Abstract

A new generation of monitor plugs is under development as spares for the ageing wire profile monitors and beam position monitors inserted into massive shielding in the target regions of the 590 MeV proton beam line at HIPA. A prototype was installed recently in the beam line to the ultra-cold neutron source UCN, to test the performance of wire monitor, BPM and modular mechanical design in a low-radiation environment. We report on first measurements with beam.

INTRODUCTION

The design of the prototype [1, 2] and its vacuum chamber closely resembles the one foreseen in the target region, just the intermediate section with the shielding is subtracted. Beam to UCN is provided either continuously as a splitted beam of a few μA or as the full deflected 1800 μA beam for 8 s, repeated every 300 s.

WIRE MONITOR

At the location of the prototype, the vertical width of the beam is narrow, resulting in the highest thermal load to a wire monitor in the 590 MeV beam lines. The load is higher at the horizontally moving wires MBPT1 than at the vertically moving wires MBPT2. In addition, the wire speed of the prototype is actually only 0.06 m/s, four times lower than that of most in-shielding monitors. This is due to the maximum rate of full steps of 2 kHz, which can be provided by the actual MESON modules [3] driving the stepper motor and reading the signal currents from the wires. The speed will be increased at a later step, when the new driver electronics, based on an extension of the read-out electronics [2] under development, is available. To compensate for the low speed, we reduced the diameter of the molybdenum wires from 48 μm to 25 μm in a first step. In a second step we reduced the diameter to 13 μm and the number of wires per monitor from two to one. In each scan the wires of horizontal and vertical monitor synchronously pass the beam with a forward and a backward motion, ‘meeting’ at the beam axis twice. Each scan is documented by the control software.

Wire Performance

Secondary emission (SE) as well as thermionic emission (TE) can contribute to the wire signal. Unlike [4], we did not bias the wires to a positive potential for suppressing TE. With the 25 μm wires we observed an evolution of TE over a few passes with higher beam current applied (Figs. 1-4).

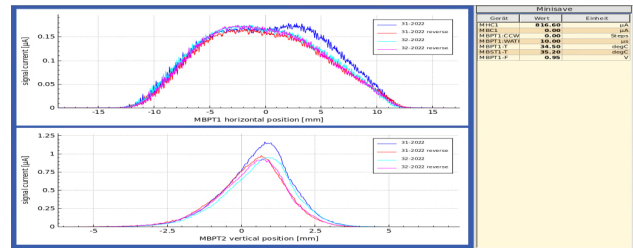


Figure 1: Two scans at a beam current of 820 μA (first time above 100 μA). In the first pass, a TE contribution is visible at MBPT1, but in the following three passes not. (The beam current was stable during this time.) A single pass at 820 μA seems sufficient to ‘condition’ the surface for lower TE.

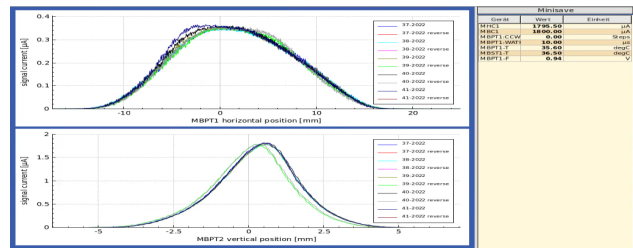


Figure 2: After five further scans with beam current increased to 1800 μA , first signs of TE appeared at MBPT1.

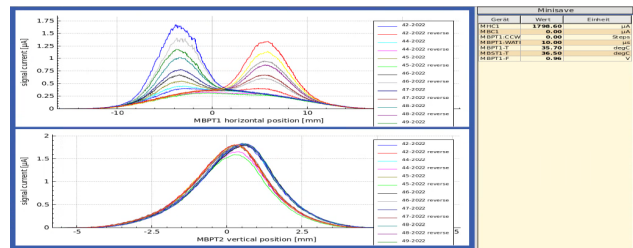


Figure 3: In the following 9 runs at 1800 μA , TE reappeared strongly at MBPT1 in the second half of the passes, where the wire has already heated up. However, the signal without TE, visible in the first half of the passes, does not change much. This indicates that the wire diameter is not reduced due to evaporation.

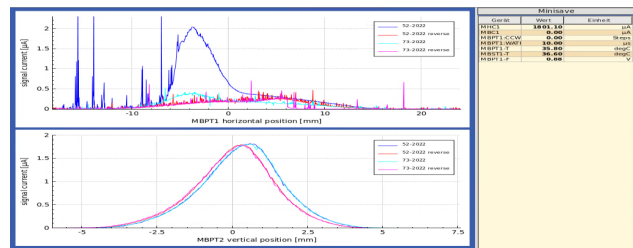


Figure 4: In the next scan, the 21st with beam current above 800 μA , the first of the horizontally moving wires (MBPT1) broke. This resulted in increased noise from the dangling wire ends. In the 39th scan, the second horizontally moving wire also broke.

[†] doelling@protonmail.com

Content from this work may be used under the terms of the CC BY 4.0 licence (© 2021). Any distribution of this work must maintain attribution to the author(s), title of the work, publisher, and DOI

BUNCH LENGTH MEASUREMENT SYSTEMS AT S-DALINAC*

A. Brauch[†], M. Arnold, J. Enders, L. E. Jürgensen, N. Pietralla, S. Weih
 Technische Universität Darmstadt, Institute for Nuclear Physics, Darmstadt, Germany

Abstract

A high-quality beam is necessary for electron scattering experiments at the superconducting Darmstadt electron linear accelerator S-DALINAC. An optimisation of the bunch length to typical values of < 2 ps is performed to reach a high energy resolution of 10^{-4} . Currently, this is accomplished by inducing a linear momentum spread on the bunch in one of the accelerating cavities. The bunch length can then be measured with a target downstream. This method is time consuming and provides only an upper limit of the bunch length. Two new setups for bunch length measurements will improve the optimisation process significantly. On the one hand, a new diagnostic beam line is set up in the low energy beam area. It includes a deflecting copper cavity used for measuring the bunch length by shearing the bunch and projecting its length on a target. On the other hand, a streak camera placed at different positions downstream the injector and the main linac will be used to measure the bunch length. Optical transition radiation from an aluminium coated kapton target is used to perform this measurement. The present layout of both systems and their current status will be presented in this contribution.

INTRODUCTION

Since 1991 the institute operates the S-DALINAC for high-resolution electron scattering experiments [1]. It is a thrice-recirculating linear electron accelerator that produces a continuous-wave electron beam at a frequency of 2.997 GHz. The accelerator is designed to reach its maximum energy resolution of 10^{-4} with bunch lengths < 2 ps [2]. Currently, this property of the electron bunches is checked with a method involving the last cavities of injector and linac as well as a dispersion calibrated target. By operating these cavities 90° off-crest the length of the passing bunches is changed and made visible on the beam target. As a result, an estimate for the bunch length can be extracted. Although the method works and provides a useful result for accelerator diagnostics, it causes some difficulties:

- Because of the intrinsic transversal beam size of the bunch and broadening caused by the used targets, the bunch length measured is only an upper estimate.
- The bunch length is only determined at the position of the last cavities of injector and linac and must be extrapolated for other locations.
- The method does not allow for an evaluation of the bunch length when all cavities are operated as intended.

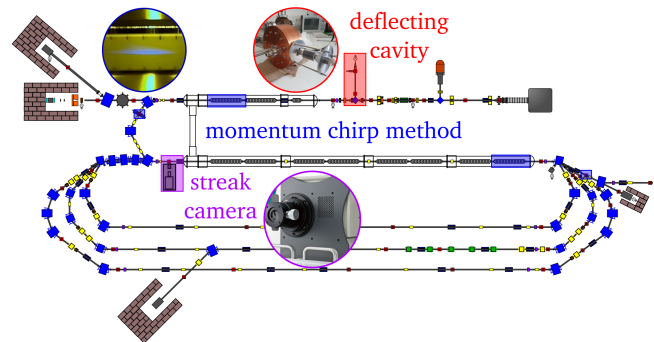


Figure 1: Floorplan of the S-DALINAC. The positions for the current method for bunch length measurements (picture from [3]) are highlighted in blue. The new methods using a deflecting cavity and a streak camera (picture from [4]) are planned to be used at the locations in red and purple.

To tackle these issues, two new devices for bunch length measurements are planned to be used at the S-DALINAC. One of these is a deflecting copper RF cavity that is placed in an upward diagnostic beam line (see Fig. 1). It will enable a bunch length measurement in the normal-conducting beam line area in front of the injector. While it is possible to do a bunch length measurement with the prebuncher this method also only provides an upper estimate of the bunch length [3]. Instead, the deflecting cavity will allow for a direct measurement of the bunch length. The width broadening caused by the target is planned to be eliminated by replacing the target with a wire scanner. The simulated properties of the diagnostic beam line and its current status will be presented in the following section. The other device is a streak camera used for the high energy areas of the accelerator. Therefore, the planned setup and its parameters will be presented here.

SETUP FOR BUNCH LENGTH MEASUREMENTS IN FRONT OF THE INJECTOR

A sketch of the setup for bunch length measurements with the deflecting cavity is shown in Fig. 2. A dipole magnet, which can be used to lead the beam into the upward diagnostic section, is situated downstream a chopper prebuncher system. The magnet is broadening the beam in one transversal dimension. The energy resolution of the bunch can be estimated by measuring the width on the target. A deflecting copper cavity with its TM_{110} mode imposes a shear on the bunch for the bunch length measurement.

* Work supported by DFG (GRK 2128) and the State of Hesse within the Research Cluster ELEMENTS (Project ID 500/10.006).

[†] abrauch@ikp.tu-darmstadt.de

DESIGN CONSIDERATIONS OF THE CORRUGATED STRUCTURES IN A VACUUM CHAMBER FOR IMPEDANCE STUDIES AT KARA

S. Maier*, M. Brosi†, H. J. Cha, A. Mochihashi, M. J. Nasse, P. Schreiber, M. Schwarz, A.-S. Müller
Karlsruhe Institute of Technology, Karlsruhe, Germany

Abstract

Two parallel, corrugated plates will be installed at the KIT storage ring KARA (KARlsruhe Research Accelerator). This impedance manipulation structure can be used to study and eventually control the electron beam dynamics and the emitted coherent synchrotron radiation (CSR) at KARA. In this contribution, we present the design of the impedance manipulation structure with corrugated plates, simulation results showing the influence of different corrugation parameters on its impedance, and the impact of this additional impedance source on the temporal changes in the emitted CSR in the presence of the microbunching instability.

INTRODUCTION

Unlike the incoherent synchrotron radiation, the coherent synchrotron radiation (CSR) does not scale linearly but quadratically with the number of emitting particles, so consequently the emitted photon flux can be enhanced by multiple orders of magnitude, for typical electron synchrotron radiation facilities. This makes it attractive to use the CSR for various kinds of applications. However, the emitted radiation is only coherent when its wavelength is longer than the emitting structure. Therefore, very short bunches and thus a high particle density is required to extend the CSR to a higher frequency range and to increase the total radiation intensities. In such a short-bunch regime, collective phenomena occur due to an interaction of an electron bunch with its own self-emitted CSR, which can lead to bunch deformations and dynamic instabilities like the so-called microbunching instability [1]. Especially, the microbunching instability leads to dynamically changing substructures and thereby intermittent regions of increased longitudinal charge density causing intense bursts of CSR in the THz frequency range.

A versatile impedance manipulation chamber is in development and will be installed into the KIT storage ring, KARA. The purpose of this chamber is to study the effect on the microbunching instability by manipulating the longitudinal impedance and thereby affecting the longitudinal beam dynamics of the electron bunches. The additional impedance is generated by a pair of horizontal, parallel plates with periodic, rectangular corrugations. Figure 1 shows a schematic drawing with the parameters corrugation depth h , corrugation width g , periodic length L , and plate distance $2b$. A cylindrical corrugated pipe has been tested in a linear accelerator by Bane *et al.* [2, 3], where they produced narrow-banded THz pulses of Smith-Purcell radiation [4], which

is not examined in the KARA project. To our knowledge, such a structure has not yet been tested in a storage ring, where the wakefields in the corrugated structure can affect frequently the bunch profile and the resulting CSR due to the passing of the structure with a revolution frequency of 2.7 MHz (for KARA).

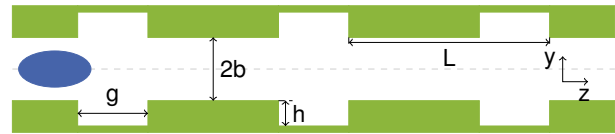


Figure 1: The corrugated pipe in cross section with the relevant geometric parameters corrugation depth h , corrugation width g , periodic length L , and plate distance $2b$ is shown. The electron bunch is indicated in blue.

The longitudinal impedance Z^{\parallel} of a cylindrical, corrugated pipe has been theoretically described in Ng *et al.* [5] with the validity range $L \lesssim h \ll b$, as

$$\frac{Z^{\parallel}}{L} = \frac{Z_{\text{vac}}}{\pi b^2} \left[\pi k_{\text{res}} \delta \left(k^2 - k_{\text{res}}^2 \right) + i \cdot \text{P.V.} \left(\frac{k}{k^2 - k_{\text{res}}^2} \right) \right] \quad (1)$$

with the resonance wave number $k_{\text{res}} = \sqrt{\frac{2L}{bgh}}$, the wave number $k = \frac{\omega}{c}$, the vacuum impedance $Z_{\text{vac}} \approx 377 \Omega$, the δ -distribution, and the principal value P.V.(x) [6].

At KARA, the CSR impedance is the dominant longitudinal impedance source in the short-bunch operation mode at 1.3 GeV. In the frequency range below 200 GHz, the parallel plate impedance gives for the impedance per revolution the highest contribution with up to 10 k Ω and thus an additional impedance of 1 k Ω , which can be generated by the corrugated structure, could significantly contribute to the total impedance. For now, the parameter values of the corrugations in Table 1 were chosen so that the theoretical resonance frequency $f_{\text{res}} = \frac{c}{2\pi} k_{\text{res}}$ lies between 50 GHz and 200 GHz. The simulated impedance can be described by an effective resonator model [7] that is characterized by the resonance frequency f_{res} , the shunt impedance Z_0 , and the quality factor Q .

Table 1: Parameter Values Used for the Simulations

Parameter	Variable	Range
Periodic length	L	50 μm to 200 μm
Corrugation depth	h	50 μm to 300 μm
Corrugation width	g	12.5 μm to 150 μm

* sebastian.maier@kit.edu

† Now at MAX IV Laboratory, Lund, Sweden

IMPROVEMENTS IN LONGITUDINAL PHASE SPACE TOMOGRAPHY AT PITZ

N. Aftab*, Z. Aboulbanine, P. Boonpornprasert, G. Georgiev, J. Good, M. Gross, A. Hoffmann, M. Krasilnikov, X.-K. Li, A. Lueangaramwong, R. Niemczyk, A. Oppelt, H. Qian, C. Richard, F. Stephan, G. Vashchenko, Deutsches Elektronen-Synchrotron DESY, Zeuthen, Germany
 W. Hillert, University of Hamburg, Institute for Experimental Physics, Hamburg, Germany
 A. J. Reader, School of Biomedical Engineering and Imaging Sciences, King's College London, UK

Abstract

Methodical studies to improve the longitudinal phase space (LPS) tomography of space-charge dominated electron beams were carried out at the Photo Injector Test facility at DESY in Zeuthen (PITZ). An analytical model was developed to quantify mean momentum, RMS energy spread, bunch length and phase advance. Phase advance analysis determined the booster phase scan range and step size to be used for obtaining momentum projections. A slit was introduced before the booster to truncate the beam in transverse plane to strongly reduce the space charge effects. The signal resolution of this truncated beam was improved by careful beta function control at the reference screen of the momentum measurements. The reconstruction algorithm was changed from Algebraic Reconstruction Technique (ART) to Image Space Reconstruction Algorithm (ISRA) owing to its assurance of non-negative solutions. In addition, the initial physically justified assumption of LPS, based on low-energy section measurements, was established to clear out noise-like artefacts. This paper will highlight the improvements made in the LPS tomography and compare the simulated and experimental results.

INTRODUCTION

Free-electron Lasers (FELs) require high-brightness electron beams to generate coherent radiation with short wavelength and high intensity. The Photo Injector Test facility at DESY in Zeuthen (PITZ) was established as a test stand of high-brightness electron sources for the European XFEL and FLASH [1]. The PITZ beamline consists of a normal conducting L-band 1.6-cell copper gun cavity with a Cs₂Te photocathode that produces ~6.5 MeV electron bunches with variable bunch lengths and up to several nC charge. The electron beam is further accelerated by a cut-disc type accelerating structure called booster, to an energy of up to ~20 MeV. Downstream the booster, the beamline consists of different diagnostics for detailed measurements of the electron beam properties. The transverse phase space characterization of the beam is done using a slit scan technique [2]. The longitudinal phase space (LPS) characterization is done using a transverse deflecting structure [3]. To determine LPS of the beam before the booster, a tomographic reconstruction technique is applied [4]. Figure 1 shows the PITZ beamline till the high energy spectrometer.

* namra.aftab@desy.de

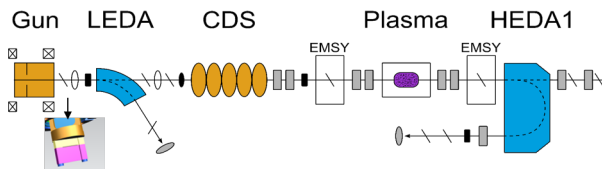


Figure 1: PITZ beamline till the high energy spectrometer with a slit shown at the first screen station after the gun.

The results of tomography obtained by the existing method has many artefacts and hence overestimates the longitudinal emittance. A hard charge cut is applied on the reconstructed LPS to give correct values. Also, the reconstruction results are more accurate for low-charge beams ~10 pC since space-charge forces are not catered for the algorithm. Typically, 250 pC beams are characterized at PITZ since this is the working point of the European XFEL.

In this paper, the procedure adopted in the experiment for obtaining the momentum projections for 250 pC beam will be explained. The optimized projections are fed to an Image Space Reconstruction Algorithm (ISRA) [5]. The algorithm will be described as well as the formulation of the initial estimate for the iterations. This initial estimate is built from the low energy section and plays a vital role for reliable reconstruction. An analytical model to understand the longitudinal phase advance of the beam is also described. The paper discusses the improvements made in the LPS tomography and compares the simulated and experimental results.

LPS MODELLING

The particle motion can be characterized in LPS by the momentum p_z of the particle corresponding to the phase of the booster. This can be used to understand and quantify the quality of an electron beam for accelerator design and phase space manipulations. To derive an analytical model for such a beam, the distribution of the particles can be approximated by an ellipse with some correlation as shown in Fig. 2.

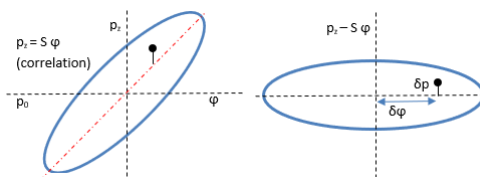


Figure 2: LPS with correlation (left) w/o correlation (right).

LOW GAIN AVALANCHE DETECTOR APPLICATION FOR BEAM MONITORING

V. Kedych*, T. Galatyuk¹, W. Krüger

Institut für Kernphysik, Technische Universität Darmstadt, Darmstadt, Germany

S. Linev, J. Pietraszko, C. J. Schmidt, M. Träger, M. Traxler, F. Ulrich-Pur

GSI Helmholtzzentrum für Schwerionenforschung GmbH, Darmstadt, Germany

J. Michel, Goethe-Universität, Frankfurt, Germany

A. Rost, FAIR GmbH, Darmstadt, Germany

V. Svintozelskyi, Taras Shevchenko National University of Kyiv, Kyiv, Ukraine

¹also at GSI Helmholtzzentrum für Schwerionenforschung GmbH, Darmstadt, Germany

Abstract

The Superconducting Darmstadt LINear ACcelerator (S-DALINAC) was constructed as a twice-recirculating electron accelerator. During the upgrade in 2015/2016 a third recirculation line as well as the option to operate the S-DALINAC in Energy recovery LINAC (ERL) mode were added. In order to optimize the beam during operation in ERL mode, it is important to provide a dedicated non-destructive beam monitoring system. A promising detector technology for this task is the low gain avalanche diode (LGAD), which is a novel silicon detector optimized for 4D-tracking, i.e. the simultaneous measurement of the particle's position and time with high spatial ($< 100 \mu\text{m}$) and timing ($\geq 30 \text{ ps}$) precision. In this contribution we present the results of a first proof-of-principle measurement utilizing LGAD technology for beam time structure monitoring at the S-DALINAC at the Technical University of Darmstadt, Germany, in the normal (non ERL) operation mode.

INTRODUCTION

Energy recovery LINAC (ERL) is a novel technique in electron beam acceleration [1]. In contrast to the normal operation mode, where the major part of the beam energy remains unused, the beam in ERL mode can be sent back to the accelerator with a phase shift of 180° resulting in a negative energy gain. Consequently, energy is put back into a radio frequency (RF) field of the accelerating cavity, which can be used for the acceleration of the next beam. Thus, ERL reduces the required RF power for the acceleration and allows to accelerate high current beams with higher energy in comparison to traditional LINACs.

The S-DALINAC [2] (Fig. 1) is a superconductive linear electron accelerator at TU Darmstadt, Germany. It was constructed as a twice-recirculating accelerator in continuous wave (cw) operation at 3 GHz. Since an upgrade with a third recirculating beam line in 2015/2016, it is possible to operate S-DALINAC as an ERL [1]. A one circulation ERL mode was successfully demonstrated in 2017 with efficiency $92.1^{+3.7}_{-13.9} \%$ [1]. In August 2021 S-DALINAC was successfully operated in twice recirculated ERL mode [3]. In this mode both once decelerated and once accelerated beams

* v.kedych@gsi.de

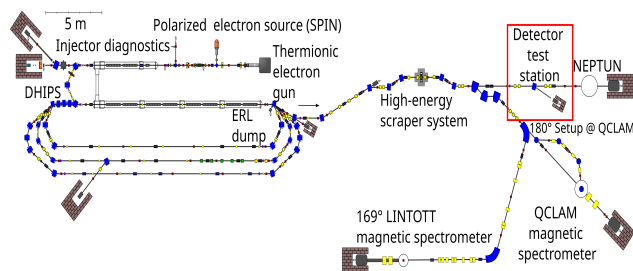


Figure 1: Layout of the S-DALINAC including experimental areas. The red rectangle represent the position of the experimental setup.

share the same beam line but have a different orbit, leading to a repetitive bunch rate of 6 GHz. In order to measure both beams simultaneously and to optimize the acceleration and deceleration process, a non-destructive beam monitoring system able to resolve this 6 GHz time structure, corresponding to 166 ps between the bunches, is required [4]. A promising detector technology that could potentially fulfil this task is the low gain avalanche diode (LGAD), which is a novel silicon detector optimized for 4D-tracking applications [5]. The high spatial granularity ($< 100 \mu\text{m}$) and excellent time resolution ($< 50 \text{ ps}$ [6]) of LGADs make an LGAD-based detector a promising candidate for beam time monitoring tool at the S-DALINAC.

In October 2021, the first proof of principle measurement of an LGAD-based beam monitoring system was performed at the S-DALINAC. The main goal of this experiment was to resolve the beam time structure of an 85 MeV electron beam using an LGAD strip sensor. For this purpose, a simplified setup was prepared and placed in a dedicated test beam area (marked by the red square in Fig. 1) outside the recirculating beam lines. Since placing the detector outside the accelerator made it impossible to simultaneously monitor the accelerated and decelerated beams, the measurement was done in the S-DALINAC normal operation mode, which, in contrast to its ERL mode, features a beam time structure of 3 GHz. Although the overall goal is to eventually use an LGAD-based setup as a monitoring tool during the ERL operation of the S-DALINAC, measuring the S-DALINAC in its normal operation mode still allowed to show the proof-

AUTOMATIC ADJUSTMENT AND MEASUREMENT OF THE ELECTRON BEAM CURRENT AT THE METROLOGY LIGHT SOURCE (MLS)

Y. Petenev, J. Feikes, J. Li

Helmholtz-Zentrum Berlin für Materialien und Energie (HZB), Berlin, Germany

R. Klein, M. Müller, A. Barboutis

Physikalisch-Technische Bundesanstalt (PTB), Berlin, Germany

Abstract

The electron storage ring MLS (Metrology Light Source) is used by the Physikalisch-Technische Bundesanstalt (PTB), the German metrology institute, as a primary source standard of calculable synchrotron radiation in the ultraviolet and vacuum ultraviolet spectral range. For this, all storage ring parameters have to be appropriately set and measured with low uncertainty. E.g., the electron beam current can be varied by more than 11 orders. This adjustment of the electron beam current, and thus the spectral radiant intensity of the synchrotron radiation, for the specific calibration task is conveniently performed fully automatic by a computer program.

INTRODUCTION

The PTB, the German metrology institute, utilizes the electron storage ring Metrology Light Source (MLS) [1] in Berlin - Adlershof for the realization of the radiometric units in the near infrared, visible, ultraviolet and vacuum ultraviolet spectral range. For this purpose, the MLS is operated as a primary source standard, i.e., the spectral radiant intensity of the synchrotron radiation (SR) is calculated by means of the Schwinger equation [2]. Adapting this to electron storage rings, where the electron revolves, the Schwinger equation has to be multiplied with the revolution frequency n , yielding the spectral radiant intensity for one stored electron. If N electrons are stored, which is equivalent to a stored electron beam current I of

$$I = N e n, \quad (1)$$

then the spectral radiant intensity of synchrotron radiation from electron storage rings is directly proportional to the stored electron beam current, i.e., the number of stored electrons [3]. With the necessary equipment installed to measure and control the electron beam current over a wide dynamic range, the radiant intensity of the synchrotron radiation can be adjusted accordingly. It should be mentioned that the stated direct proportionality between N and the spectral radiant power is only valid for wavelengths that are shorter than the length of the stored electron bunches, typically being in the mm range, and therefore no coherence effects are present in the near IR, VIS, VUV and soft X-ray spectral range.

The variation of the electron beam current does not change the spectral characteristics of the synchrotron radiation. The spectral characteristics, on the other hand, can be changed by adjustment of the electron energy. At the MLS, e.g., the electron beam energy can be chosen to be

between 105 MeV and 630 MeV, which changes the characteristic wavelength between 735 nm and 3.4 nm, respectively. This allows creating a tailor-made spectral shape for specific applications and avoiding unwanted high-energy parts of the spectrum, which could lead to instabilities due to thermal load, optics degradation, higher diffraction orders or increased stray light, but this is not the focus of this paper.

In this paper we focus on the variation of the electron beam current over more than 11 decades. The adjustment of the electron beam current is widely used for the calibration of wavelength-dispersive spectrographs or for the calibration of counting detectors, with very low electron beam currents, even single photon detectors can be calibrated. To facilitate these calibrations, a fully automated program was developed for the adjustment of the electron beam current to the desired value and its accurate measurement.

INSTRUMENTATION

At the MLS, the stored electron beam current can be varied by more than 11 decades, that means from a maximum current of approx. 200 mA down to a single stored electron (1 pA). As a matter of course, the equipment for a controlled adjustment of the electron beam current must be installed at the storage ring in order to utilize this potential. This is implemented only at a few other facilities worldwide, since most electron storage rings are operated as large-scale synchrotron radiation user facilities, which do not have the flexibility of changing the operational parameters such as electron beam current or electron beam energy. At the MLS, equipment is also installed to monitor the beam size over the whole possible range of electron beam current.

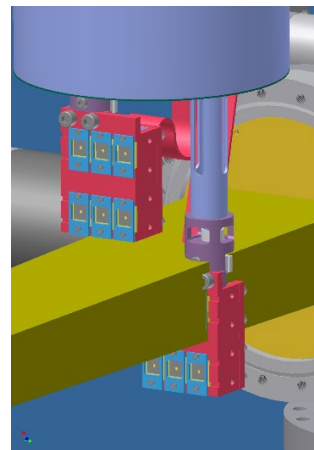


Figure 1: Schematics of the photo diodes assembly (red) as illuminated by the synchrotron radiation (green).

ANALOG FRONT END FOR MEASURING 1 TO 250 pC BUNCH CHARGE AT CLARA

S. L. Mathisen^{1, *}, T. H. Pacey¹, R. J. Smith¹, UKRI STFC, Sci-Tech Daresbury, Warrington, UK
¹also at Cockcroft Institute, Sci-Tech Daresbury, Warrington, UK

Abstract

As part of the development of the CLARA electron accelerator at Daresbury Laboratory, a new analog front end for bunch charge measurement has been developed to provide accurate measurements across a wide range of operating charges with repetition rates of up to 400 Hz. The qualification tests of the front end are presented. These include tests of the online calibration system, compared to a bench Faraday cup test setup; online beam test data with a Faraday cup from 1 to 200 pC; online beam test data with a wall current monitor from 1 to 200 pC, and tests using signal processing such as singular value decomposition. This is demonstrated to enable the measurement of bunch charges in the order of 100 fC using both Faraday Cups and Wall Current Monitors.

INTRODUCTION

The CLARA front-end is the first phase of the CLARA 250 MeV Free Electron Laser (FEL) test facility, based at Daresbury Laboratory. The front-end has been used to provide high energy electrons for experiments during two experimental runs in 2018/19 [1] and 2021/22 [2]. The combined CLARA/VELA facility currently incorporates two Wall Current Monitors (WCMs), four Faraday Cups (FCs) and one Integrated Current Transformer (ICT) for bunch charge diagnostics, and plans for the full CLARA facility, due to be commissioned in 2024, will include further charge devices.

The existing charge diagnostics system installed on the CLARA/VELA FCs and WCMs is based on an *LC* integrator circuit with a resonance frequency of 30 MHz [3]. This system has many problems: It relies on out-of-production components, it requires interpolation after being digitized to accurately measure charge, each front-end requires two multi-core cables run through the radiation shielding and it lacks important features, such as automatic calibration or multiple sensitivity settings to better support low charge operations.

This paper presents results from the final production version of an upgraded front end for charge detection, based on an earlier presented prototype [4]. This final system is substantially improved over both the older *LC* integrator circuit and the previously presented prototype in many ways. First an overview of the front end will be presented briefly, followed by bench tests to verify the system's operation and quantify measurement uncertainty. Finally tests conducted as part of the CLARA 2021/22 experimental run are presented, including online measurement of ultra low charges.

* storm.mathisen@stfc.ac.uk

SYSTEM DESIGN

The system design is presented in three sections: The analog signal chain that converts signals from charge devices into an output pulse with an amplitude proportional to charge, the charge injection circuit for onboard calibration of the analog signal chain; and the digital control circuitry to enable operators to adjust the settings of the front end. Figure 1 shows a functional diagram of the circuit.

Analog Signal Chain

The analog signal chain is divided into three sections: Input filter and buffer, charge integration circuitry and output buffer. The input filter consists of a 100 MHz cut-off low-pass filter which enables the front end to be agnostic about the bandwidth of the charge device it is connected to. The bandwidth of an FC is controlled through the impedance it is discharged through, but a WCM can have a bandwidth up to several GHz. The filter is a simple *RC* filter. Following the input filter is an analog switch that select any of three inputs: Charge device input with the input filter, an unfiltered input for front end testing, and the onboard charge injection circuitry. The input is buffered by a unity gain FET op-amp, and is enclosed within an RF shield to limit the effect of external noise sources.

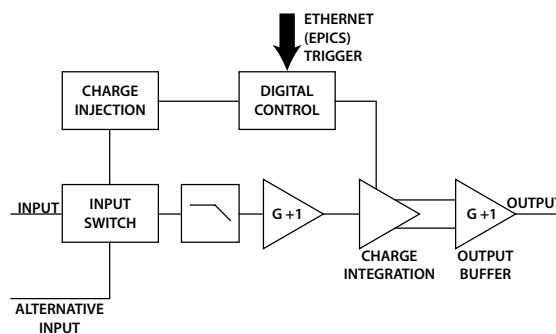


Figure 1: Block diagram of the presented front-end.

The charge integration circuit relies on an ADA4350 Analog Front End integrated circuit [5]. This circuit features a FET input amplifier with six switchable feedback paths, a differential output buffer and control via a serial interface. Five of the feedback paths are used for different integrator sensitivity settings, and the last one to amplify the signal without integration. The values of the components used in the feedback network were selected to ensure that each feedback path has the same frequency response. One goal of the new front end was to enable shot-by-shot measurement of both bunch charge and dark current simultaneously, a

BEAM CURRENT MEASUREMENTS AT THE NANO-AMPERE LEVEL USING A CURRENT TRANSFORMER

M. Xiao[†], M. J. van Goethem, S. Brandenburg

PARTREC UMCG, University of Groningen, Groningen, Netherlands

T. Delaviere, L. Dupuy, F. Stulle, Bergoz Instrumentation, Saint-Genis-Pouilly, France

Abstract

In conventional proton therapy (PT) typical beam currents are of the order of 0.1 nA. At these currents dose monitoring is reliably achieved with an ionization chamber. However, at the very high dose rates used in FLASH irradiations (employing beam currents >100 nA) ionization chambers will exhibit large intensity dependent recombination effects and cannot be used. A possible solution is a current transformer. Here we report on the performance of the LC-CWCT (Bergoz Instrumentation, France) which has been developed to push noise floor of such non-destructive current measurement systems into the nano-ampere range. We present first beam current measurements at the PARTREC cyclotron (Netherlands). Beam currents measured by the LC-CWCT and a Faraday Cup were shown to linearly correlate up to the maximum intensity of 400 nA used in the measurements. For pulsed beams, charge measured by the LC-CWCT linearly correlated with pulse length over the measurement range from 50 to 1000 μ s. Measurement noise as low as 2.8 nA was achieved. The results confirm that the LC-CWCT has the potential to be applied in FLASH PT for accurate determination of beam current and macro pulse charge.

INTRODUCTION

FLASH PT aims to use ultra-high dose rate (>40 Gy/s) beams for cancer treatment, which has been proven in pre-clinical studies to spare doses for healthy tissues while maintaining the treatment effects on some specific tumour models [1-3] compared to conventional PT. The beam current extracted for FLASH PT is around 1000 times higher than for clinical PT (~0.1 nA), which leads to a challenge for beam extraction in clinical cyclotrons.

Some studies also show that the beam time structure causes a variation of the FLASH effect [4]. Further studies need to be done to examine conditions and beam parameters, i.e. current, pulse width, energy, frequency, triggering the FLASH effect in clinical practices. Thus, it is of great significance to have a flexible test bench capable of providing varying beam parameters for FLASH PT studies.

The PARTREC cyclotron is expected to provide ultra-high dose rates for FLASH pre-clinical studies over the next few years. Because the PARTREC facility is not in clinical use it is more flexible and modifications to beam intensity and time structure can be implemented more easily than at a clinical facility.

However, the beam monitor and control system designed for use at clinical dose rates, which is based on ionization chambers (ICs), faces a challenge in delivering precise

[†] m.xiao@umcg.nl

doses at beam currents used to achieve FLASH beam dose rates. Specifically, the response of plane-parallel ICs [5-7] shows a dependence on dose rate which can become unacceptably large at ultra-high beam currents due to volume recombination effects; an effect which can be neglected in clinical settings. For FLASH PT studies, it is essential to improve the beam monitoring system for high currents (i.e. a few 100 nA to μ A). Tests have shown that the ion collection efficiency of a plane-parallel IC designed at PARTREC is around 83% with a peak current of 543 nA (at 150 MeV beam energy).

A Faraday cup was applied in previous experiments to control the delivered proton fluence and to deduce IC efficiency, assuming the Faraday cup is dose rate independent. For FLASH dose rates, a current transformer, which is non-destructive to the beam, can provide the necessary redundancy in dose delivery by measuring beam currents for both CW and pulsed beams.

For the present study we tested a specially developed current transformer, the LC-CWCT, with a 150 MeV proton beam at the PARTREC cyclotron. Macro-pulse length and average current were varied during the measurements. A Faraday cup was installed at the end of the beamline to give a reference value for the input beam current. The aim of this work was to verify the noise levels of the LC-CWCT output signals of different bandwidths (100 Hz, 10 kHz and 350 kHz) in a real beam environment, and the potential of using an LC-CWCT in FLASH PT for real-time beam monitoring and control under complicate beam conditions.

LC-CWCT AND BCM-CW-E

The CWCT and the corresponding BCM-CW-E electronics [8] have been successfully used to measure micro-ampere beam currents with sub-microampere resolution [9]. By applying a fast sample-and-hold measurement the BCM-CW-E deduces level of the CWCT output signal between any two consecutive beam pulses. From these signal levels average input currents can be deduced. The only necessary condition is that input beam bunches are well separated. For convenience the output signal is provided with three different bandwidths: 350 kHz, 10 kHz and 100 Hz.

The CWCT can be considered a noise free current source. All noise is either coming from the signal processing on the BCM-CW-E electronics, or from environmental noise, for example, captured by the coaxial cables connecting CWCT and BCM-CW-E.

In such a situation a very effective way of boosting the signal-to-noise ratio is to amplify the signal directly at the source. That means, by adding a low noise amplifier directly at the CWCT output the measurement range can be

NEW X-RAYS DIAGNOSTICS AT ESRF: THE X-BPMs AND THE HALO-MONITOR

E. Buratin*, K. Scheidt, European Synchrotron Radiation Facility, Grenoble, France

Abstract

Two new X-ray diagnostics have been installed in the Front-Ends of the Storage Ring of the ESRF's Extremely Brilliant Source (EBS) recently.

Two independent optical X-BPMs at 23 m distance from their bending magnet source-point are giving extremely useful additional information on the vertical beam stability in comparison to the e-BPMs data.

A vertical beam Halo-monitor allows to measure permanently and quantitatively the level the electron density at large distance (1 – 3 mm) from the beam core, in a non-destructive manner.

INTRODUCTION

The Extreme Brilliant Source (EBS) ring at the European Synchrotron Radiation Facility (ESRF) is operational since mid-2020, generating coherent and bright x-rays for the scientific users [1]. The X-rays are generated by an electron beam of 6 GeV and 200 mA, with horizontal and vertical emittances of 120 pm and 10 pm, respectively. EBS can run with different filling schemes, such as 7/8 multibunch with a single bunch up to 8 mA, uniform, 16 bunches and 4 bunches.

A large range of diagnostics are in operation since the commissioning to measure the parameters, characteristics and behaviour of the beam [2].

Since last autumn we have added two new X-rays diagnostics: 1) the X-rays Beam Position Monitor (X-BPM) to check the vertical beam stability and 2) the Halo-monitor to measure the vertical halo at large distance from the beam core. In this paper we present the systems and the first results.

THE X-BPMs

Two optical X-BPMs have been implemented in the Front End (FE) of the beamlines BM8 and BM16 that have 0.85 T bending magnets as their X-ray source. These X-BPMs are of a first version that aimed at satisfying the proof-of-principle of getting a reliable image of the passing X-rays and to use that for verifying the mid- and long-term positional stability of these X-rays. This first version allows, through use of UHV-bellows etc., the sensor to be inserted, and so to measure, but not to serve the beamline, or to be extracted, thereby letting the full X-rays to the beamline. After the here below reported success with this first version we are now installing a 2nd version (in October) that will measure permanently while leaving the X-rays for the beam line users unperturbed.

* elena.buratin@esrf.fr

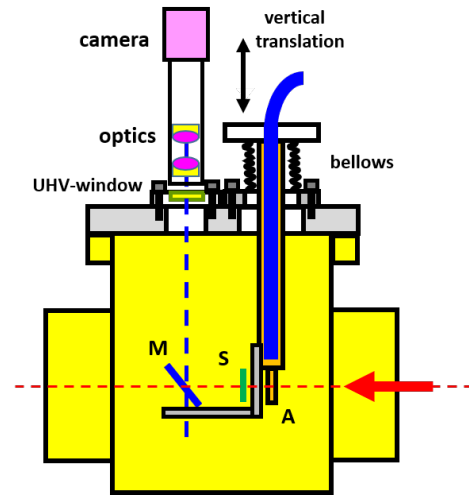


Figure 1: The X-BPM shown in inserted position.

The X-BPM (see Fig. 1) consists of a scintillator (S) behind a cooled copper absorber (A), a 45-degree mirror (M), an UHV viewport and a camera with a set of achromats. The latter focusses on to the camera array the image that the X-rays emits by passing through the scintillator screen. (see Fig. 2).

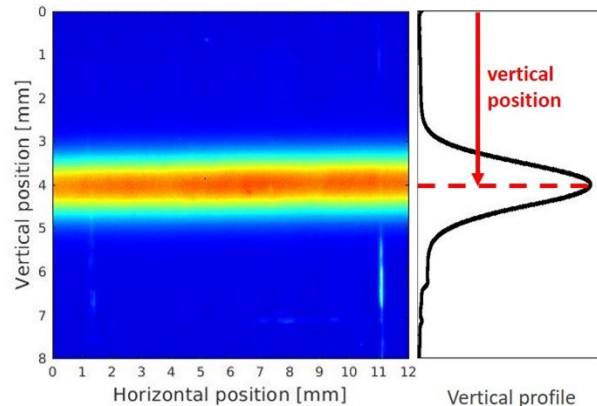


Figure 2: The BM8 X-ray image with 200 mA beam current, 1 ms exposure time, 0 dB gain, 2*2 binning.

The centre of the vertical profile is essentially the vertical X-ray beam position, and the only value of interest to us. It is calculated and stored at 1 Hz and these vertical X-rays positions can then be compared with fully independent readings obtained from a duo of standard electron e-BPMs in the region of the source-points of these BMs. From these 2 e-BPMs both the angle and the position of the electron beam at the BM source-point is obtained, thereby allowing a calculation of the position of the X-ray beam at 23 m distance.

In Fig. 3 is shown the vertical position of the BM8 X-rays as measured by our new X-BPM (purple) and that obtained

NEW MEASUREMENTS USING LIBERA-SPARK ELECTRONICS AT ESRF: THE HIGH-QUALITY PHASE-MONITOR AND THE SINGLE-ELECTRON

E. Buratin*, P. Borowiec, G. Denat, N. Benoist, J. Jacob, K. Scheidt, F. Taoutaou
 European Synchrotron Radiation Facility, Grenoble, France

Abstract

Several new diagnostics have been installed and exploited at the ESRF's new Extremely Brilliant Source (EBS) at the end 2021. A Libera-Spark BPM device has been implemented to measure the phase of Booster and EBS rings, with high resolution and up to turn-by-turn rate. In the Storage Ring we achieved irrefutably the control, injection and measurement of single electron(s) with the use of transfer-line screens, the visible-light extraction system and a low-cost photo-multiplier tube, combined with the commercial Spark Beam Loss Monitor. Further planned developments, like the TCPC technique, on this are on-going and will be essential to verify that our Booster cleaning process reaches a level of zero-electron bunch pollution in EBS.

INTRODUCTION

The Extremely Brilliant Source (EBS) ring is a fourth-generation machine that generates X-rays with a 6-GeV and 200-mA electron beam. The complex chain includes a Linac, a Booster and the EBS ring and it is operational since 2020 at the European Synchrotron Radiation Facility (ESRF) in Grenoble [1].

A large number of diagnostics were used to commission the ring and these devices continue their operation and use for both the User-mode operation (USM) and for studies during the Machine Dedicated Time (MDT) [2, 3].

New diagnostics were implemented recently that exploit to the full the Libera electronics: a beam-phase-monitoring for both the Booster and EBS rings with a Spark-BPM and a single-electron measurement with a Libera Beam Loss Monitor (BLM) [4].

THE PHASE-MONITOR

The measurement of the beam phases of both the Booster and EBS is done by a single Libera Spark, the same model used for the BPMs. With beam phase is defined here the phase relation w.r.t. the ESRF's RF-master source, which is the reference for all cases and results reported here below. This master source is at the heart of both the RF-accelerator system and the distribution of timing signals used for numerous purposes in the ESRF facility.

The principle of using a Spark BPM is similar to a former version that used a Libera-Brilliance-BPM [4]. It uses the so-called I and Q digital signals that are generated on each of the 4 RF input signals. It important to stress that neither the Spark's under-sampling of the rf-frequency (352.2 MHz), nor the internal PLL being a simple software

version (quasi-PLL) and therefore wobbly w.r.t. to any external signal to such Spark, does not affect its potential for measuring with high resolution and precision the phase relation between the 4 RF-inputs.

Figure 1 shows the connections of the timing signals and the 4 RF inputs: a) the Booster signal coming from a stripline, b) the EBS-SR signal coming from BPM buttons, and the c) and d) fed by the RF-master-source. For the latter, having 2 identical signals at 2 different inputs allows to assess the resolution of the device.

With an upgraded firmware the Spark now generates directly the phase relations between the 4 RF signal in the SA-stream of 20 Hz.

The I and Q data also being available from triggered buffers, with the turn-by-turn as the fastest rate (355 kHz), also means that the phase information is fully available for studying very fast events.

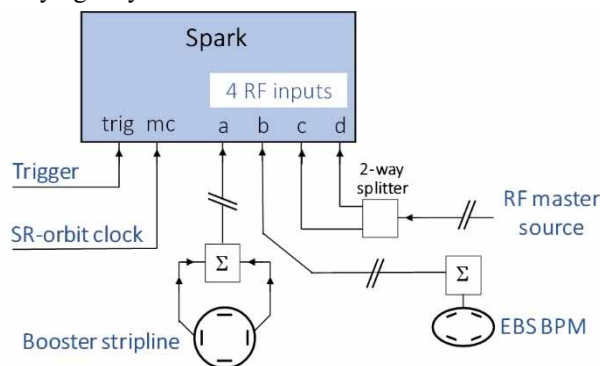


Figure 1: The connections of the phase-monitor.

The Phase Measurement Results, Slow and Fast

The slow (20 Hz) output of the phase monitor is shown in Fig. 2 which shows the phase of the beam under two distinct conditions: the (digital) phase-control-loop in the RF-transmitter system being ON and OFF. This control loop has a (slight) digitization problem that explains the noisy behaviour in the left part of the graph.

The typical resolution with this 20 Hz stream is a few millidegrees.

The device also provides the phase data at the faster rates of 355 kHz and 5.5 kHz (i.e. 2.8 μs and 180 μs sampling time) through triggered buffers. This allows to measure precisely at the injection time and results of this are shown in Figs. 3 and 4.

The green curves in these graphs show the real phase resolution of this measurement monitor, since measured by the device at 2 dedicated channels and in exactly the same manner and at the same time.

* elena.buratin@esrf.fr

NOVEL BEAM EXCITATION SYSTEM BASED ON SOFTWARE-DEFINED RADIO

P. J. Niedermayer*, R. Singh,
 GSI Helmholtzzentrum für Schwerionenforschung, Darmstadt, Germany

Abstract

A signal generator for transverse excitation of stored particle beams is developed and commissioned at GSI SIS18. Thereby a novel approach using a software-defined radio system and the open-source GNU Radio ecosystem is taken. This allows for a low cost yet highly flexible setup for creating customizable and tuneable excitation spectra. Due to its open-source nature, it has the potential for long term maintainability and integrability into the accelerator environment. Furthermore, this opens up the possibility to easily share algorithms for the generation of waveforms across accelerator facilities.

As a first application, the device is used to control the coherence and amplitude of transverse oscillations by excitation in the vicinity of betatron sidebands. It enables measurement of beam parameters like tune and chromaticity. On a longer term, it will be used for more complex tasks such as beam shaping, extraction and automated parameter scans towards these complex processes.

SOFTWARE-DEFINED RADIOS

Software-defined radio (SDR) describes an RF transceiver technology in which signal processing is implemented in software. It is widely used in radio communication systems, but has potential applications in many fields. An SDR typically consists of a frontend with ADCs and DACs, and a backend performing the digital signal processing (DSP). Here, a universal software radio peripheral (USRP) was used as off-the-shelf frontend to generate the RF signals. For implementation of the DSP the open source GNU Radio framework [1] was chosen, which allows to graphically design signal processing flow graphs. The large flexibility and low cost of modification make the device a natural choice not only for prototyping [2], but also for experiments and regular use in the accelerator environment. A general challenge with DSP is the unavoidable processing delay. However, as will be shown in this contribution, modern computer technology and active data flow control enable overcoming this obstacle.

NEW SIGNAL GENERATOR FOR BEAM EXCITATION

For transverse excitation one typically needs two independent signals for the horizontal and vertical plane which are linked to the changing revolution frequency of the accelerated beam. It must also be possible to start the signal by means of a trigger. Figure 1 depicts the working principle of the signal generator meeting these requirements. The USRP

digitizes the revolution frequency reference signal (sine with frequency f_{rev}) and receives the trigger (TTL pulse) via the general purpose input/outputs (GPIOs). It streams the data via Gigabit Ethernet to an industrial PC, where GNU Radio performs the DSP. The generated signals are streamed back to the USRP and delivered at the two RF ports.

We use the model N210 and low-frequency daughterboards with parameters listed in Table 1. The DACs provide sampling rates of up to 400 MS/s. In practice, however, this is limited by the data processing rate to about 10 MS/s, allowing to handle and generate frequencies up to 5 MHz.

Table 1: Specification of the USRP N210

Frequency range	0 to 30 MHz
DAC/ADC resolution	16/14 bit (± 1 V)
RF ports	2 in- and 2 outputs (50 Ω)
GPIO ports	2 \times 16 (TTL)

Minimisation of Signal Delay

The challenge in using an SDR for applications requiring feedback and trigger is to achieve a low signal processing delay. A GNU Radio flow graph consists of blocks performing discrete operations on the signal data stream. The data is processed in chunks and buffered in between these blocks, which improves efficiency but introduces an artificial delay. While GNU Radio is able to optimize buffer usage and data processing to find a trade-off [3], it requires a settling time and is not optimal if a minimal processing delay is crucial. In our application, the data flows from ADC to DAC, which both have a fixed sampling rate. Until the first data sample has been processed by GNU Radio and transmitted back to the USRP, the DAC buffer lacks samples and can not

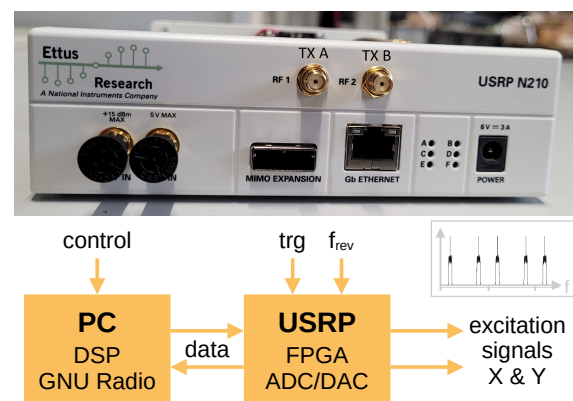


Figure 1: USRP hardware and signal generation scheme.

* p.niedermayer@gsi.de

BEAM POLARIZATION MEASUREMENTS WITH THE REVISED COMPTON POLARIMETER AT ELSA

M. Switka*, K. Desch, D. Elsner, Physikalisches Institut, University of Bonn, Germany
W. Hillert, Institut für Experimentalphysik, University of Hamburg, Germany

Abstract

The Compton Polarimeter at the ELSA 3.2 GeV storage ring has been designed to measure the polarization degree of the stored electron beam by analyzing the profile of the back-scattered gamma-beam with a silicon microstrip detector. Utilizing a scattering asymmetry from interaction with circularly polarized laser light, the electron beam polarization is determined from the vertical shift of the gamma-beam's center of gravity in respect to the handedness of the laser light. The installation of a new laser source and silicon strip detector has improved the polarimeter's performance significantly. Additionally, the profile analysis could be enhanced by using a Pearson type peak function fit. The analyzing power was determined through the observation of the Sokolov-Ternov effect and a statistical measurement accuracy of 2% could be obtained within 5 minutes of measurement time. The polarimeter resolves the expected spin dynamical effects occurring in the storage ring and has shown to be a robust and reliable measurement system for operation with the GaAs source for polarized electrons.

INTRODUCTION

Electron beam polarimetry based on the Compton effect has been successfully performed at multiple laboratories operating with spin-polarized beams. However, the approach to determine the beam polarization from a profile analysis of the backscattered photons is to our knowledge unique at ELSA [1]. The backscattered beam profile has a polarization-dependent vertical asymmetry which results in a shift of the profile's center of gravity \bar{z} under photon beam helicity change (left to right-handed or vice-versa):

$$\Delta z = \bar{z}_L - \bar{z}_R = \mathcal{D} \cdot \mathcal{P}_e \cdot S_3, \quad (1)$$

where \mathcal{D} is the analyzing power of the polarimeter, S_3 the degree of circular photon polarization and \mathcal{P}_e the electron polarization degree parallel or anti-parallel to the magnetic bending field. Simulations for ELSA [2] show that $\mathcal{D} \geq 70 \mu\text{m}$ for a detector 15 m away from the photon-electron interaction point. Hence, we use a silicon microstrip detector with sufficient vertical resolution to measure the backscattered beam profile to obtain the polarization degree of the electron beam.

THE COMPTON POLARIMETER

Optical System and γ -Beam Detector

Circularly polarized laser photons of 532 nm wavelength are focused onto the center of a defocusing quadrupole mag-

* switka@physik.uni-bonn.de

net (compare with Fig. 1), where the transverse electron beam profile has minimum ellipticity $\sigma_z/\sigma_x = 0.69$ to 0.44 between 1.2 GeV to 3.2 GeV.

With an **optical system** [3] the beam waist can be varied from $\omega_0 = 0.66$ mm to 1.6 mm to match the transverse size of the electron beam. As photon source a cw laser with 18 W beam power is used, of which approx. 14 W were measured to be available at the interaction point. The helicity of the photon polarization can be changed through pneumatically driven rotatable $\lambda/4$ waveplates. The degree of circular polarization is measured before the beam dump.

The **detector** [4] for the backscattered photons with up to 328 MeV energy consists of a lead converter target in front of an in-house developed silicon microstrip detector. With 768 vertically distributed 13-bit channels at 50 μm pitch it yields a resolution of $\Delta z_b = 14 \mu\text{m}$.

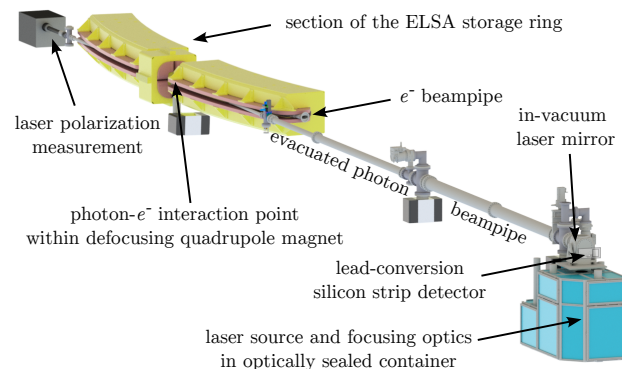


Figure 1: Compton polarimeter at ELSA: A cw laser beam of circularly polarized photons is focused onto the center of a quadrupole magnet. The backscattered γ -photons from head-on collisions with stored electrons are detected by a microstrip detector with vertical resolution.

Backscattered Beam Profile and Function Fit

An exemplary measured vertical photon profile which backscattered off a 1.3 GeV electron beam is shown in Fig. 2. While the measurands \bar{z}_L and \bar{z}_R can be obtained by determining the distribution's mean ("center of gravity"), this approach was found to be prone to the influence of stray radiation and statistical count fluctuation [3]. A more robust method includes a data fit to a conformable function, such as the Pearson type IV distribution:

$$P_{IV}(x) = h \cdot \left[1 + \left(\frac{x - x_0}{s} \right)^2 \right]^{-l} \cdot \exp \left[-\nu \cdot \arctan \left(\frac{x - x_0}{s} \right) \right] \quad (2)$$

BEAM PROFILE MONITORING AND DISTRIBUTED ANALYSIS USING THE RabbitMQ MESSAGE BROKER

D. Proft*, K. Desch, D. Elsner, F. Frommberger, S. Kronenberg, A. Spreitzer, M. Switka
Physikalisches Institut, University of Bonn, Germany

Abstract

The ELSA facility utilizes several digital cameras for beam profile measurements on luminous screens and synchrotron radiation monitors. Currently a multitude of devices with analog signal output are being replaced in favor of digital outputs, preferably with data transfer via Ethernet. The increased network traffic for streaming, analyzing, and distribution of processed data to control system and machine operators is managed through a supplementary camera network in which distributed computing is performed by the RabbitMQ message broker. This allows performant and platform-independent image acquisition from multiple cameras, real time profile analysis, and supports programming interfaces for C++ and Python. The setup and performance of the implementation are presented.

INTRODUCTION

As in most facilities the beam images at ELSA [1] are obtained through several different observation techniques via synchrotron radiation or luminous screens based on fluorescence, intensified phosphorescence or transition radiation. Thereby numerous camera systems from various manufacturers are in use, whose data acquisition and transfer techniques are based on different interfaces. In practice, this makes it difficult to grant reliable and permanent access to all imaging systems for operators or control system algorithms, especially when hardware from different decades with individual digitizers, software, and software platforms are required. In the following we present an approach of unifying the various image streams to provide more reliable and uniformly accessible beam image data for beam observation, profile analysis, beam parameter measurements, and hence, machine optimization.

IMAGING HARDWARE

Cameras With Analog Output

The prevalent form of imaging has been based on cameras with analog output signals (e.g. *composite video*), which served its purpose for basic adjustment procedures, such as beam alignment. However, the analog signals are usually transmitted over long coaxial lines to distant video multiplexers and digitizers and are prone to interference with a multitude of disturbing signals from the accelerator environment. In those setups the requirements for quantitative beam profile measurements with adequate precision are rarely met due to visual defects from transmission or imperfect exposure settings, as shown in Fig. 1 a). In addition, multiple

digitizer cards installed at different work stations suffer from aging and incompatibility with modern operating systems. Some images are not digitized at all and broadcasted to a screen in the control room, lacking the advanced capability for processing by computer vision algorithms.

Cameras with Digital Output

The usage of cameras with digital signal output overcomes the above mentioned issues and the *GigE Vision* communication interface allows for cameras to be conveniently connected through a network of Ethernet switches allowing bi-directional communication between camera and accelerator control system (e.g. to set shutter time or frame rate). In this configuration power can be provided over the Ethernet cable itself (PoE), implying convenient hardware connectivity up to 100 m away from a network switch (compare with Fig. 1 b)). This is especially useful for temporarily installed monitoring cameras, which only require an Ethernet cable (e.g. on a reel) to function. As explicated below, cameras with *GenICam* interface allow good software connectivity.

Some camera systems often operate through enclosed, proprietary software environments running on dedicated computers, such as a streak camera (see Fig. 1 c). Usually, data transfer and device control interfaces via TCP/IP protocol are available and the computers can be used as image servers, whose data stream is manageable through prevalent programming environments such as *Python* or *C++*. This way any computer operating digitizer cards (*framegrabber*) can be integrated into the camera network.

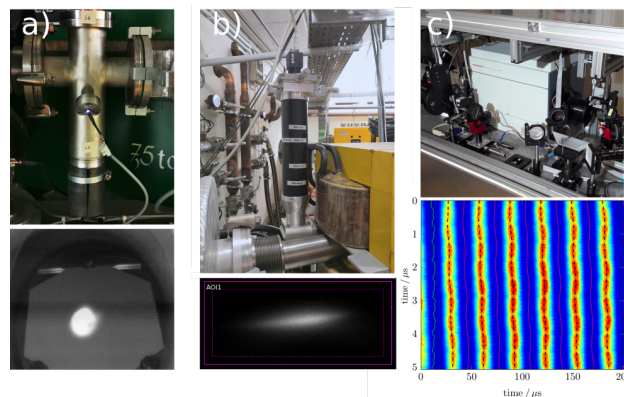


Figure 1: Exemplary hardware and corresponding beam images: a) chromox screen monitor with saturated image and visual defects from analog signal, b) synchrotron radiation monitor equipped with Ethernet camera, c) streak camera as bunch train monitor with analyzed image (tune measurement).

* proft@physik.uni-bonn.de

DEVELOPMENT OF COMPACT RADIO FREQUENCY SOURCES

M. S. McCallum*, A. Lyapin

John Adams Institute at Royal Holloway, University of London, Egham, United Kingdom

Abstract

Our group is developing a family of compact radio frequency sources aiming to cover 50 MHz to 20 GHz with several models. The primary goal is to provide an alternative to using expensive laboratory generators in permanent installations. In addition, we work towards providing a higher specification than similar telecommunications devices as this is a typical requirement in accelerator instrumentation. We take a minimalistic approach with only a network interface planned, assuming that such a device operates remotely in a large facility. An interface is in the works for monitoring and control using EPICS (Experimental Physics and Industrial Control System). In this paper, we present the results of rapid prototyping with XMicrowave components. The first measurements show encouraging phase noise performance and spectral purity.

INTRODUCTION

The aim of our project is to achieve the phase noise and spectral purity performance of a mid-range benchtop radio frequency (RF) generator, albeit at the loss of versatility. This loss is deemed acceptable if the only purpose of the source is to generate a stable signal at a fixed frequency, for example in a local oscillator (LO) application. In these proceedings we are looking at the performance of a signal source based on a low cost frequency synthesizer in comparison with commercially available examples of sources in both compact and benchtop formats.

We will thus be looking at 3 sources: a high quality Rohde and Schwarz SMA 100A [1] benchtop generator, an AtlanTecRF ASG-3000 compact signal source [2] aimed at Communications market, and our source developed around the Analog Devices' ADF4355 [3]. For brevity, these will be called SMA 100A, ASG, and ADF4355 respectively.

ADF4355 FREQUENCY SYNTHESIZER

The ADF4355 chip combines a Phase Locked-Loop (PLL) and a Voltage Controlled Oscillator in one package and allows for the implementation of integer-N and fractional-N PLL frequencies. Apart from a reference frequency, it requires only a handful of external components to operate. A series of internal frequency dividers allows for an operating frequency range of 54 MHz to 4.4 GHz. The ADF4355 chip has programmable output power, RF output mute, and can be controlled by a 3 wire Serial Peripheral Interface (SPI). We are currently using the device at the default loop bandwidth of 20 kHz.

Our implementation employs a budget Raspberry Pi 2040 microcontroller, housed on a W5100S-EVB-Pico by WIZ-

net [4]. Beside the low cost, this device has the advantage of running MicroPython, which shortens the development cycle compared to a classic microcontroller. We chose a board incorporating the Ethernet interface, as this is our preferred way of communicating with the device. ADF4355 along with other variable components following it are controlled using the GPIO pins of the microcontroller via SPI. A custom software stored in the FLASH memory of the board is initialised at the powerup and waits for an external command. Commands are sent via the Ethernet port, which are at the moment limited to changes in output frequency and power. The controller then calculates the required settings for the synthesizer chip and programs its registers accordingly.

Behind the scenes the changes of frequency and power settings trigger additional adjustments to filter banks and variable attenuators aimed at optimising the harmonics content and equalising the signal at different frequencies.

For the first prototype, we used rapid microwave prototyping blocks provided by XMicrowave [5]. A convenience PCB hosts the W5100S-EVB-Pico along with a few ancillary components, and simplifies connections to the RF blocks. A 3D printed enclosure houses all the elements of the prototype, including a high quality reference source.

PERFORMANCE COMPARISON

We compare the performance of the three sources by analysing their Phase Noise Measurements (PNM) at three different "inconvenient" fractional frequencies: 1033.33 MHz, 1879.68 MHz, and 2998.75 MHz. We also look at the spectral purity of each of the three sources. The data for these measurements was taken on a Rohde and Schwarz FSW 50 with a resolution bandwidth (RBW) of 20 kHz and a video bandwidth (VBW) of 30 Hz.

Phase Noise Performance

In Figure 1 we can see the PNM for each of the three sources at an output frequency of 1033.33 MHz. Looking at the phase noise for the ASG, blue line, we can see that the phase noise is relatively high at low frequency offsets. As the frequency offset becomes larger, the PNM decreases and plateaus. Next we can see the appearance of spurs, which increase the phase noise. Finally, the phase noise rolls off to about -105 dBc/Hz.

The black line shows the phase noise performance of the ADF4355 frequency synthesizer. There the phase noise starts low at about -80 dBc/Hz, and decreases to about -105 dBc/Hz. Then it increases to about -90 dBc/Hz at the edges of the PLL bandwidth before steeply decreasing to -140 dBc/Hz at a higher frequency offsets.

Lastly, we have the phase noise performance of the SMA 100A in red. This source starts with a low phase noise of

* Contact Email: mark.mccallum@rhul.ac.uk

SYNCHRONOUS DATA SERVICE AT THE EUROPEAN SPALLATION SOURCE

R. Titmarsh*, ISIS, STFC, Rutherford Appleton Laboratory, Oxfordshire, UK
J. F. Esteban Müller, J. P. S. Martins, European Spallation Source ERIC, Lund, Sweden

Abstract

The Synchronous Data Service (SDS) is a tool to monitor and capture events in the European Spallation Source, building on top of the EPICS control system. Large amounts of data from different input-output controllers are acquired and synchronised at the level of beam pulses. The acquisition can be triggered by beam events through the timing system or manually by a user. Captured data is stored in standardised NeXus files and indexed in a database for easy searching and retrieval.

INTRODUCTION

At ESS, the operation of the proton linac, target, and neutron experiments are controlled using the EPICS [1] control system. EPICS is a distributed control system, and that means that the data produced in different Input/Output Controllers (IOC) is received by clients in a non-deterministic order.

At our facility, EPICS' data is archived by the Archiver Appliance [2]. This tool stores each signal as a time series, so the effort of correlating data from different sources lies with the client side.

In some applications, it is important to obtain a snapshot of the machine status containing several signals from various sources that belong to the same beam pulse. Typical examples are machine tuning and optimization, or troubleshooting of failures (post-mortem).

In order to ensure that the data is synchronized in all relevant devices, a precise timing system capable to generate triggering signals is required. In this paper we describe both the hardware and software implementation under development at ESS that will allow pulse-synchronous data acquisitions and archival, which we refer to as the Synchronous Data Service (SDS).

SOFTWARE ARCHITECTURE

A diagram of the SDS architecture is shown in Fig. 1. The main design goals are scalability and flexibility, and for that reason we followed a microservices pattern.

The service consists of 3 different types of components or microservices: one or more collector services that collect data from EPICS IOCs and produce NeXus [3] files, an indexer service that aggregates metadata from the collectors, and one or more data retriever services that allow users to query for the data in different ways. These components and their prototype implementation are described in more detail below.

* ross.titmarsh@stfc.ac.uk

These microservices rely on a storage backend consisting of an Elasticsearch [4] database that stores the metadata and a CEPH-based [5] distributed file system that contains the NeXus files.

Collector Services

We developed a prototype version of a generic collector service. It is implemented in Python 3 using the asyncio framework. PV Access is supported through the p4p [6] package. Channel Access support was considered not necessary since our control system is fully EPICS7 compliant.

This service creates a set of "collectors" from definitions in a JSON file, each collector listens for a single type of event on a set of EPICS PVs. Each instance of this service has a "collector manager" that listens to the EPICS PVs of the collectors within it, parses the received messages and forwards them to the relevant collector. Multiple instances of the service can be deployed to distribute the load. The collector collects the events into "datasets" by the pulse ID of the triggering pulse. The information about the triggering event must be included by the IOC and it is discussed later.

Using asyncio allows the many collectors to run concurrently, allowing multiple datasets to be constructed at the same time. This means it can handle events arriving out of order or overlapping each other.

The dataset is a virtual HDF5 file that is expanded as events are received. When the dataset is complete (defined as a configurable timeout, default is 2 seconds), it is written to a remote file system for storage and its metadata is sent to the indexer service. Datasets can be submitted with an "expire by" timestamp after which the data can be removed from storage.

Custom collector services can be developed to support other protocols or for different use cases. For instance, a post-mortem event triggered after the machine trips can generate a huge amount of data. In that case some systems may be configured to act as collector services by storing data locally for later transferring it to the central storage and to the indexer service.

Indexer Service

This service receives the collector definitions and the datasets' metadata and stores them in a database to enable fast search and retrieval.

The prototype was developed in Python 3 using the FastAPI [7] framework. It provides a REST interface that can be consumed by the collector services.

The Elasticsearch database was chosen for its capability of handling large volumes of data and for enabling complex

KINGFISHER: A FRAMEWORK FOR FAST MACHINE LEARNING INFERENCE FOR AUTONOMOUS ACCELERATOR SYSTEMS

L. Scomparin*, E. Blomley, T. Boltz†, E. Bründermann, M. Caselle, T. Dritschler, A. Kopmann, A. Mochihashi, A.-S. Müller, A. Santamaria Garcia, P. Schreiber, J. L. Steinmann, M. Weber
Karlsruhe Institute of Technology, Karlsruhe, Germany

Abstract

Modern particle accelerator facilities allow new and exciting beam properties and operation modes. Traditional real-time control systems, albeit powerful, have bandwidth and latency constraints that limit the range of operating conditions currently made available to users. The capability of Reinforcement Learning to perform self-learning control policies by interacting with the accelerator is intriguing. The extreme dynamic conditions require fast real-time feedback throughout the whole control loop from the diagnostic, with novel and intelligent detector systems, all the way to the interaction with the accelerator components. In this contribution, the novel KINGFISHER framework based on the modern Xilinx Versal devices will be presented. Versal combines several computational engines, specifically combining powerful FPGA logic with programmable AI Engines in a single device. Furthermore, this system can be natively integrated with the fastest beam diagnostic tools already available, e.g. KAPTURE and KALYPSO.

INTRODUCTION

Ensuring stable operation of the future particle accelerator facilities will pose a challenging problem, where traditional control systems are expected to not reach the desired performance. An interesting possibility is the use of Machine Learning (ML) techniques. Reinforcement Learning (RL) [1] is a prominent approach, which recently has shown several relevant results [2–5]. The basic idea is to model the control problem as the interaction between an agent and a system. The agent obtains some observable from the system that are expected to carry information about an underlying and often hidden state and chooses an action from an action space. Then, a reward is obtained from the system giving a metric of how good the taken action was. Reinforcement Learning is a series of algorithms allowing to train such an agent by using the rewards given by the system.

One of these challenging problems is the control of micro-bunching instabilities (MBI) [6] in synchrotron light sources, where the interaction of the beam head with the wake field produced by the Synchrotron Radiation (SR) emitted from the tail leads to the development of substructures in the longitudinal phase-space. One successful attempt was already performed at SOLEIL [7], in this case using traditional control techniques based on chaos theory. The underlying idea of this feedback loop is to stabilize the system around pre-existing unstable equilibrium points.

* luca.scomparin@kit.edu

† now at SLAC, Menlo Park, California

One intriguing capability of RL is its great versatility: by changing the reward function different goals are achievable, even when they might not be characteristic of a given stable condition. For example, the emission of Coherent Synchrotron Radiation (CSR) could be enhanced or suppressed while setting an acceptable level of fluctuation in the emitted power. Moreover, the enhancement of a specific radiation frequency range could be achieved.

MODULAR ARCHITECTURE FOR FAST INFERENCE

One of the issues that can be encountered when implementing RL techniques with accelerators are latency limitations. Namely, the complete feedback loop (comprising beam diagnostic detector readout, feature extraction, observable evaluation with the agent and action taking) needs to be taken in a time frame comparable to the dynamics of the physics that needs to be controlled. In the case of the MBI, this imposes latency constraints in the order of the synchrotron periods, i.e. of a few tens of microseconds.

A fundamental requirement necessary in order to minimise deployment and testing time for different RL algorithms is a modularity oriented model. Such a system can be divided into four main parts. First, a detector readout interface (1) is needed to retrieve data with low-latency and high-throughput. This data stream from the detector is then fed into the feature extraction part (2), which produces higher-level observables that are then fed into the agent module (3) that chooses an action. The action needs then to be applied to the system, in this case the accelerator, through an action taking part (4), that can interface to a part of the machine control system, ideally with a low-latency connection. A schematic view of this system is shown in Fig. 1.

On top of this inference signal path two other systems are needed: a slow-control system and a training system. Both of these are less time-critical compared to the feedback path. The training system needs to keep track of the observables, of the actions taken, and of the rewards, so that this information can be retrieved during training to update the agents's parameters. Meanwhile, the slow-control allows the operator to set different parameters and tune the system based on the needs of the facility.

KINGFISHER

The different modules and signal paths described in the previous section have different computational requirements. For instance, fast but simple operations are required when interfacing with the readout electronics, while the agent

WEB-BASED APPLICATION FOR CABLE SIMULATION MODELS*

M. C. Paniccia[†], S. Clark, D. M. Gassner, R. Hulsart, P. Thieberger
Brookhaven National Laboratory, Upton, USA

Abstract

Signal attenuation in a coaxial cable increases with cable length, and the amount of attenuation and signal distortion is dependent on the signal's spectral frequency content. A model of these variations can help predict a signal's expected loss and distortion. This paper describes a free web-based application developed to provide accurate SPICE models for various coaxial cable types. The user can specify a length, select between different cable types, or upload a cable's attenuation curve, and receive a SPICE model for that cable. These simulation models have been used to assist the design and development of new instrumentation systems for the future Electron-Ion Collider (EIC).

INTRODUCTION

The new Electron-Ion Collider (EIC) will include over a thousand new beam position monitors (BPMs) and many other instrumentation systems spread throughout the complex. Signals generated at the various sensors must traverse cable lengths as great as 250 m. Understanding the signal loss and distortion as they propagate over these distances is a key aspect of the system design process. To assist in the design process, analog circuits are modeled with the Simulation Program with Integrated Circuit Emphasis (SPICE) [1]. The SPICE simulation provides a transient and steady-state response of the system allowing for the first-pass representation of expected performance. Modeling cables in SPICE poses a unique challenge as cable performance changes over distance and frequency content. Since most signals from instrumentation systems have a wide frequency content, it is imperative to accurately capture the frequency-dependent performance of the cabling.

A procedure for developing a SPICE simulation model for frequency-dependent cable loss is described in [2]. The frequency-dependent attenuation performance is simulated by creating a multistage passive filter with poles and zeros mapped along the cable's transfer function. A custom Python script was developed to implement the pole-zero approximation method and several simulation models were generated for different coaxial cables. To test the validity of the models, spare cable assemblies were tested in the lab with narrow pulses, and the SPICE model performance matched closely to the measured data. The Python scripts were integrated into a web application to make the cable simulation process accessible to the entire EIC team and the broader instrumentation community.

SPICE MODEL

The creation of the SPICE model starts with defining the cable's frequency-dependent attenuation characteristic curve. The characteristic curve acts like a filter's transfer function and defines the cable's response in the frequency domain. Cable manufacturers typically provide attenuation values at specific frequencies at a specified length; most often 100 ft or 100 meters. If not provided by the manufacturer, the characteristic curve can be measured using a network analyzer. Once established, the characteristic curve can be defined as an equation that can provide attenuation values for any given frequency. This equation takes the form of Eq. (1).

$$Atten = a_0 \sqrt{MHz} + a_1 MHz + a_2. \quad (1)$$

In generating the SPICE model, an equation for each cable type is determined using the least squares approximation of Eq. (1) to the attenuation versus frequency values provided by the manufacturer. The cable's characteristic curve is then scaled by the distance at which it was measured, assuming attenuation is proportional over distance and frequency. A pair of spare cables of different lengths were measured to verify this assumption using a network analyzer. The measurements were compared to the estimated attenuation curve using the proportional approximation and are shown in Fig. 1. For both cables, the proportional approximation proved to be conservative.

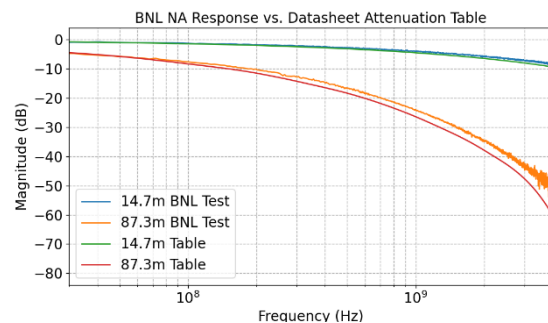


Figure 1: Comparison of LMR240 frequency-dependent attenuation characteristic curve and measured BNL network analyzer data.

The next step in the derivation of the SPICE model is to use the pole-zero approximation process described in [2]. This process recreates the characteristic curve for frequency-dependent attenuation by creating a circuit with a transfer function with a similar slope. The transfer function is created from multiple poles and zeros that are set along the characteristic curve. The poles and zeros are generated using resistors and capacitors configured in a low-pass filter. Multiple stages are connected using the SPICE Voltage

* Work supported by the US Department of Energy under contract No. DE-AC02-98CH10886.

[†] mpaniccia@bnl.gov

NOVEL PHOTOEMISSION TYPE OF X-RAY BEAM POSITION MONITOR FOR THE 'WHITE' UNDULATOR RADIATION*

P. Ilinski[†], MAX IV Laboratory, Lund University, Lund, Sweden

Abstract

A novel photoemission type of X-ray Beam Position Monitor (XBPM) for the 'white' undulator radiation is proposed. The XBPM employs beamline frontend fixed mask as a source of photocurrent signal. Signal spatial distribution and XBPM response were analyzed for various undulator radiation parameters.

INTRODUCTION

Photoemission blade type X-ray Beam Position Monitors (XBPM) [1] are standard for most synchrotron radiation facilities. The photoemission blade XBPMs are non-invasive and can provide high spatial resolution but encountering some drawbacks affecting their performance. Initially, the frontend (FE) XBPMs were developed as a standalone component, equipped with positioning stages. Signal response of the photoemission blade XBPM is quite vulnerable to the surface condition of the blades. Also, since operating with negative bias applied to the blade, a conductive deposit can be accumulated at insulator surfaces, leading to substantial increase of the dark current [2]. Operating without bias reduces the blade XBPM signal level.

Most of the time, the FE XBPM is located behind the fixed mask, which is a part of the FE and designed to absorb vast amount of the incident undulator radiation. Knowledge of undulator beam position relative to the FE fixed mask (FM) allows to reduce FM exit aperture and to achieve better beam alignment along the frontend. An XBPM, which is part of the FM was developed [3], it is based on detecting x-ray fluorescence from FM surfaces. Spatial calibration of the XBPM, which is fixed in space, can be performed by deflecting the undulator radiation beam [4]. This is a preferable way to spatially calibrate FE XBPM, since it corresponds to actual operation conditions, when the undulator beam is moving relative to the XBPM and not vice versa.

Proposed novel type of photoemission XBPM is part of the FM. It is detecting the photoemission produced at the FM surface under undulator radiation. The Photoemission Mask (PheM) XBPM will allow to combine XBPM and the frontend FM and to overcome some drawbacks of the photoemission blade XBPMs.

LAYOUT

Photoemission Mask XBPM consists of a fixed mask and detection part with four pickup electrodes, which are

hidden from undulator radiation (Fig. 1). The electrodes are collecting photoelectrons emitted from the fixed mask when exposed to the undulator radiation. The PheM XBPM can be a combination of upstream and downstream fixed masks with signal pickup part in between. In this case, the photocurrent signal will be collected from both fixed masks. These signals may be separated in case, if two sets of readout electrodes will be installed in between upstream and downstream masks. The PheM XBPM can also be a combination of upstream mask and downstream readout flange with pickup electrodes, such layout may be compatible with frontends already in operation. Since the fixed masks are electrically grounded, the electrodes need to be under positive potential to collect photoelectrons. In this situation the residual ions will not be attracted to the electrodes and therefore no conductive deposit will be developed at the insulator's surfaces.

Calculation of the PheM XBPM signal distribution was performed for the upstream fixed mask with the exit aperture of 11 mm by 11 mm and the downstream fixed mask with the exit aperture of 9 mm by 9 mm. The upstream fixed mask exit aperture dimensions correspond to the dimensions of the MAX-IV CoSAXS frontend upstream fixed mask. The downstream fixed mask dimensions were chosen not to obstruct the configuration of already installed blade type XBPMs at the CoSAXS frontend. Geometrical and electrostatic layouts can be further optimized for dedicated PheM XBPM design.

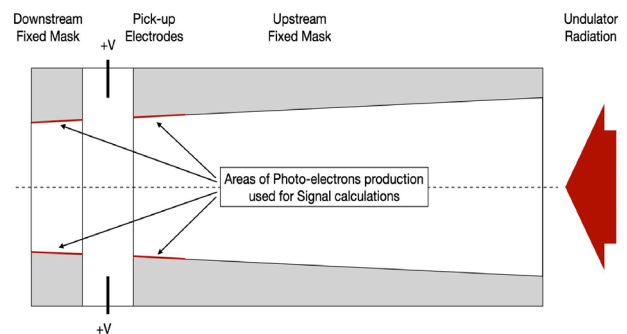


Figure 1: Layout of the Photoemission Mask XBPM.

RADIATION SOURCE

Radiation from planar and elliptical undulator radiation sources was used to calculate the PheM XBPM signal. The flux spectral density of MAX-IV CoSAXS planar undulator for $K=1.25$ is presented in Fig. 2 for various observation angles. As can be seen, at large observation angles, the PheM XBPM signal is generated mostly by the undulator harmonics with fundamental energies below 1 keV.

The wavelength of fundamental undulator harmonic is proportional to:

*Research conducted at MAX IV is supported by the Swedish Research council (contract 2018-07152), the Swedish Governmental Agency for Innovation Systems (contract 2018-04969), and Formas (contract 2019-02496)

[†]petr.ilinski@maxiv.lu.se

A NEW LUMINOSITY MONITOR FOR THE LHC RUN 3

S. Mazzone*, W. Andreazza, E. Balci, D. Belohrad, E. Bravin, N. Chritin,
 J. C. Esteban Felipe, T. Lefevre, M. Martin Nieto, M. Palm¹
 CERN, Geneva, Switzerland

¹presently at Terapet SA, Satigny, Switzerland

Abstract

The Beam RATE of Neutrals (BRAN) is a monitor that provides a relative luminosity measurement for the four LHC experiments. BRANs are used during operations as a tool to find and optimise collision and to cross-check experiments luminosity monitors. While each LHC experiment is equipped with BRANs, in this contribution we will focus on the new monitors installed for ATLAS and CMS that will replace the ageing gas chambers during LHC run 3. These will also serve as prototypes for the future High Luminosity LHC monitors that will need to sustain an even higher collision rate. A description of the BRAN as well as the first results obtained during the LHC Run 3 start-up will be presented.

INTRODUCTION

The BRANs are luminosity monitors installed on both sides of the four LHC experiments to measure the relative luminosity. The working principle is the detection of electromagnetic showers produced inside a target absorber by neutral particles (neutrons and high-energy photons) from the collisions. The detected signal I is thus proportional to the collision rate, that can be related to the luminosity \mathcal{L} through [1]

$$I \propto N = \sigma \mathcal{L} , \quad (1)$$

where N is the collision rate and σ the relative cross section. Neutral particles propagate in the direction of the colliding particles and can be intercepted at a sufficient distance from the Interaction Point (IP) when the two LHC beams are sufficiently separated by the D1 dipole. In the case of the Interaction Regions (IR) 1 and 5 - Atlas and CMS respectively - the BRANs are inserted inside the Target Absorber of Neutrals (TANs) at approximately 140 metres from the IP, in a position as close as possible to the maximum of the shower produced in the TAN.

BRANs are *relative* bunch by bunch luminosity monitors that are mostly used by LHC operators as a simple and reliable tool to find and optimise collisions and to cross-check the *absolute* luminosity monitors maintained by the LHC experiment that measure the actual instantaneous and integrated luminosities. As mentioned, the absolute calibration of the BRANs is not per se a requirement, the emphasis being on the stability, linearity and resolution. Table 1 contains a summary of the BRAN requirements. During the LHC runs 1 and 2, the BRANs installed in IR 1 and 5 were gas ionisation chambers [2] produced by Lawrence Berkeley

* stefano.mazzone@cern.ch

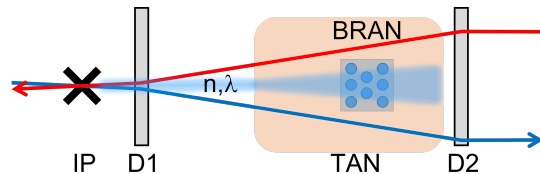


Figure 1: Layout of IR 1 and 5. BRANs are installed in the TANs approximately 140 metres from IP.

National Laboratory. While these detectors worked well through the LHC runs, they have been operating since 2009 in a high radiation environment and suffer from ageing components. In addition, these cannot be operated in the future High Luminosity (HL) run 4 of LHC as new absorbers with different geometry will replace the TANs to cope for the increased collision rate. It was therefore decided to develop new BRANs for IR 1 and 5 with the aim of replacing the gas chambers for LHC run 3 and to serve as a prototype to test materials and detection principles for the HL run 4. Two such detectors have been installed in February 2022 during the LHC year-end technical stop (YETS), at the right of IP1 and left of IP5. The two remaining BRANs are being assembled in view of an installation during the 2022-23 YETS. In this contribution we will describe the instruments and present the very first data available to date from Run 3 commissioning.

INSTRUMENT DESIGN

The principle of the new BRANs is the measurement of Cherenkov radiation produced in fused silica rods that are crossed by the showers produced by the TANs. Eight 603 mm long, 10 mm diameter fused silica rods are hosted in a mixed copper and aluminium enclosure that is inserted in the 100 mm wide TAN slot as shown in Fig. 2a. The rods are made of an ultra-pure, Hydrogen-free synthetic silica with low OH content. This type of material - Suprasil 3302 by Heraeus Quarzglas - was chosen among other types of fused silica that have been irradiated inside the IR1 TAN during the 2nd LHC run as it showed the minimum drop of transmission over the range 160-650 nm, attaining 20% of the transmission of the non-irradiated sample after being exposed to a dose of 0.8 MGy [3]. These results have been confirmed by a post run analysis of the spectral transmission of five rods performed in 2018 at the university of Illinois [4] showing that transmission of Suprasil in the visible range (400-600 nm) is practically unaffected by radiation exposure. As for the UV, all samples show a decrease of transmissivity particularly around 214 and 325 nm where

DIAMOND-II ELECTRON BEAM POSITION MONITOR DEVELOPMENT

L. T. Stant*, M. G. Abbott, L. Bobb, G. P. Cook, L. Hudson,
 A. F. D. Morgan, E. Perez-Juarez, A. J. Rose, A. Tipper
 Diamond Light Source, Oxfordshire, United Kingdom

Abstract

The UK national synchrotron facility, Diamond Light Source, is preparing for a major upgrade to the accelerator complex. Improved beam stability requirements necessitate the fast orbit feedback system be driven from beam position monitors with lower noise and drift performance than the existing solution. Short-term beam motion must be less than $2 \text{ nm}/\sqrt{\text{Hz}}$ over a period of one second with a data rate of 100 kHz, and long-term peak-to-peak beam motion must be less than $1 \mu\text{m}$. A new beam position monitor is under development which utilises the pilot-tone correction method to reduce front-end and cabling perturbations to the button signal; and a MicroTCA platform for digital signal processing to provide the required data streams. This paper discusses the challenges faced during the design of the new system and presents experimental results from testing on the existing machines.

INTRODUCTION

Diamond Light Source is a 3 GeV, 300 mA third-generation synchrotron located in Oxfordshire, UK. User operation began in early 2007 and since then a total complement of 33 beamlines have been commissioned. To further increase capabilities of the facility a new injector and storage ring will replace the existing machine, with the 18-month dark period scheduled for late 2026. This major upgrade, Diamond-II, will increase the energy to 3.5 GeV, reduce the horizontal emittance to 160 pm, and provide twice the number of straights [1].

As part of the Diamond-II upgrade, the storage ring electron beam position monitor (EBPM) processing electronics will be replaced¹. Several factors influenced this decision:

- Due to the higher closed-loop crossover frequency and lower latency requirements of the fast orbit feedback for Diamond-II, the data rate from the EBPM system must increase from 10 kHz to 100 kHz, which is not supported by the existing systems.
- At the time of the Diamond-II CDR [1], the state-of-the-art multiplex switching solution would have created many harmonics in the measurement data for the required data rate.
- The existing systems will be over 20 years old and most have been repaired at least once.

Table 1 summarises the requirements of the Diamond-II EBPM system.

* laurence.stant@diamond.ac.uk

¹ The existing LINAC and booster EBPM systems will be refurbished and upgraded as a future project.

Table 1: EBPM Requirements for Diamond-II

Parameter	Diamond-II
Number of EBPMs	252 (11/12 per cell)
Geometric factor k	7.3 mm
Short-term motion (<1 s)	
Commissioning (0.3 mA)	<130 nm/ $\sqrt{\text{Hz}}$
User beam (300 mA)	<2 nm/ $\sqrt{\text{Hz}}$
Long-term motion (<1 wk)	<1 μm pk-pk

The increasing adoption of the MicroTCA computing platform in the synchrotron community, combined with suitable technical resource available at Diamond Light Source, led to the choice of an in-house developed solution instead of an off-the-shelf product. The different parts of the EBPM system design will now be discussed.

BUTTON PICKUPS

Similar to Diamond, there will be two types of EBPM: primary EBPMs used for insertion device beam alignment will be located in straights on dedicated thermally stable pillars; and standard EBPMs located in the arcs will be mounted directly to the girders. Whereas the Diamond vessels were significantly wider in the horizontal dimension, the Diamond-II vessels are circular.

The button pickups are of a similar design to those used in the Diamond DDBA cell upgrade [2] and the ESRF design [3]. Due to the challenging manufacturing requirements of the button pickups, ongoing discussions with suppliers and other light sources have been necessary [4].

FRONT-END SYSTEMS

Analogue Front-End

Before digitisation, the signal from the button pickups must be filtered and amplified/attenuated by an analogue front-end. Typically, this unit will also include some form of compensation scheme to continuously correct the gain and phase variations between the EBPM channels. In Diamond, the compensation scheme chosen was multiplex switching located outside the vault. By moving the compensation inside the vault (i.e. closer to the buttons) it is possible to also correct for variations in cable gain and phase which have been shown to vary with temperature and humidity [5]. Due to promising results [6–9] and the avoidance of switching harmonics, the pilot tone compensation scheme was selected for use in the Diamond-II analogue front-end (D2AFE).

The D2AFE module (shown in Fig. 1a) contains four RF channels, each comprising of two stages of filtering, ampli-

PULSE-BY-PULSE PHOTON BEAM POSITION MEASUREMENTS AT THE SPring-8 UNDULATOR BEAMLINE*

H. Aoyagi[†], H. Osawa, K. Kobayashi, T. Fujita, S. Takahashi
 Japan Synchrotron Radiation Research Institute (JASRI/SPring-8), Hyogo, Japan

Abstract

A pulse-mode X-ray beam position monitor that enables pulse-by-pulse position measurement in the synchrotron radiation beamline of the synchrotron radiation facility was improved, and evaluation tests were performed. The monitor was equipped with blade-shaped detection elements utilizing diamond heatsinks to reduce stray capacitance, and a microstrip transmission line to improve high-frequency characteristics. The detection elements operate as photocathodes and generate single unipolar pulses with a full width at a half-maximum of less than 1 ns. This operation allows pulse-by-pulse measurement of the synchrotron radiation beam. To ensure operations at the undulator beamline in SPring-8, where the synchrotron radiation power is very intense, further improvements were introduced to the detecting elements to enhance heat resistance. The evaluation results of sensitivity and resolution in the pulse-by-pulse photon measurement and observation of beam oscillation during beam injection are discussed herein.

INTRODUCTION

We developed a pulse-mode X-ray beam position monitor (PM-XBPM) that enables pulse-by-pulse position measurements in the synchrotron beamline of SPring-8, a synchrotron radiation facility, and are working on practical applications. To improve the high-frequency characteristics, this monitor is equipped with diamond heatsinks to reduce the blade-shaped detecting elements' stray capacitance and a microstrip transmission line to match the impedance. The detection principle is the same as conventional X-ray beam position monitors (XBPMs), in which four blade-shaped detection elements are arranged vertically and horizontally, with the photon beam axis as the center of symmetry, and the current signal ratio of each detection element is read out as position information. The prototype was installed in a bending-magnet beamline (BM-BL), and evaluation tests were conducted. Thus, a unipolar pulse signal with a pulse length of 0.7 ns FWHM was generated, and a pulse-by-pulse beam position of the synchrotron radiation beam was observed [1].

To ensure the stable operation of the monitor in the insertion device beamline (ID-BL), where the synchrotron radiation power is extremely high, we aimed to enhance the heat resistance by modifying a diamond heatsink and a water-cooling holder [2]. By doubling the size of the diamond heatsink in the beam axis direction to 16 mm compared with the prototype, the contact area with the cooling base

was increased to enhance the thermal resistance. This improvement increased the photon-receiving area, which led to an increase in the current signal. Furthermore, the heat-transfer efficiency was enhanced by adopting a wedge-shaped copper plug.

We confirmed the basic performance of the modified pulse-mode XBPM at a BM-BL (BL02B1), which has a maximum power density of 1.5 kW/mrad² and an actual irradiation power density of approximately 0.1 W/mm². Subsequently, it was transferred to the ID-BL (BL35XU), which has a maximum power density of approximately 500 kW/mrad² and an actual irradiation power density of approximately < 25 W/mm², and evaluation tests were performed. This paper discusses the position sensitivity, resolution, and observation of the beam oscillation during a top-up injection.

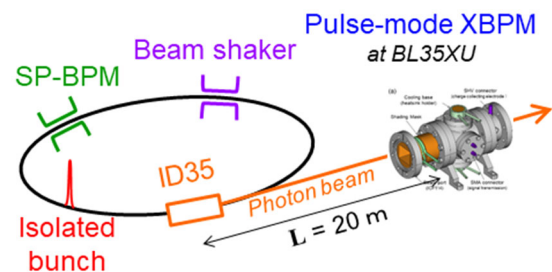


Figure 1: Setup of position sensitivity measurement.

POSITION SENSITIVITY

Perturbation by Beam Shaker and Amplitude Measurement by SP-BPM

Figure 1 illustrates the measurement system used for evaluating position sensitivity. A single isolated bunch was injected into the storage ring, and the bunch current was 0.95 mA. Betatron oscillations were excited horizontally and vertically using the bunch-by-bunch feedback (BBF) kickers at Cell 04 in the horizontal direction and a 0.9-m kicker at Cell 30 in the vertical direction. The perturbation frequency was set to 28.9 kHz ($\nu_x = 41.1382$) in the horizontal direction and 60.0 kHz ($\nu_y = 19.3257$) in the vertical direction. The excitation of the betatron oscillation was locked by a phase-locked loop (PLL) to automatically follow the tuning changes caused by the opening and closing of the ID gap and the bunch current. The perturbation amplitude was adjusted by the Dimtel iGp12 DAC output, and when the amplitude at the BPM of cell 21 reaches 100 μm , the DAC output is called "nominal kick power 100%." The kick angles corresponded to $\theta_x = 0.033 \mu\text{rad}$ and $\theta_y = 0.047 \mu\text{rad}$ under this condition. The stationary perturbation amplitude excited by radio frequency knockout

* Work supported by Japan Society for the Promotion of Science through a Grant-in-Aid for Scientific Research, No.18K11943 and No.21K12530.
[†] aoyagi@spring8.or.jp

BEAM POSITION MONITORING OF MULTI-BUNCH ELECTRON BEAMS AT THE FLASH FREE ELECTRON LASER

N. Baboi*, B. Lorbeer, H.-T. Duhme
Deutsches Elektronen-Synchrotron (DESY), Hamburg, Germany

Abstract

The superconducting FLASH user facility (Free electron LASer in Hamburg) accelerates 10 electron bunch trains per second, which are mostly used to produce high brilliance XUV and soft X-ray pulses. Each train usually contains up to 600 electron bunches with a typical charge between 100 pC and 1 nC and a minimum bunch spacing of 1 μ s. Various types of beam position monitors (BPM) are built in three electron beam lines, having a single bunch resolution of 2 – 100 μ m rms. This paper presents multi-bunch position measurements for various types of BPMs and built in at various locations. The dependency of the resolution on the beam offset is also shown.

INTRODUCTION

The Free electron LASer in Hamburg (FLASH) produces ultra-short intense XUV and soft X-ray pulses [1-3]. Beam diagnostic [4] is essential in obtaining and maintaining a high quality electron beam necessary for the self-amplified spontaneous emission effect responsible for producing the photon beams.

Beam Position Monitors (BPMs) are an important part of the beam diagnostics in FLASH. Many types of BPMs are built in along the ca. 250 m of the facility, being distributed in 3 electron beam lines. The BPM type at each location depends on the beam pipe and resolution requirements. Some types can detect bunches with a charge between ca. 10 to 1000 pC, and have a single bunch resolution of 2 to 15 μ m rms. Others need a higher charge, and have higher values for the resolution, but they are in most cases still in accordance with the local demands.

While the behavior of the BPMs is in general well understood, only the behavior of the first bunch has been so far studied in detail. In this paper we present the analysis of each bunch in long trains. The single bunch behavior for different bunch offsets is also shown.

The FLASH Facility

An overview of the FLASH layout is shown in Fig. 1 [3]. A photoelectric gun produces every 100 ms electron bunch trains with a length of up to 600 μ s and a repetition frequency of up to 1 MHz. TESLA superconducting structures accelerate them to an energy of up to 1.25 GeV. Two bunch compressors are used to reduce the bunch length to tens till hundreds of fs. The train is then split to the two undulator beamlines, FLASH1 and FLASH2, where photon pulses are produced. A third beam line splits off of FLASH2 and accommodates a laser-plasma experiment, FLASHForward [5]. Table 1 gives a summary of the main parameters of the electron and photon beams.

Note that currently the facility is at the end of an upgrade and refurbishment shutdown, with the main goals of increasing the energy, installing a laser heater, and a new bunch compressor [6].

Beam Position Monitors in FLASH

The different kinds of BPMs installed in the accelerator are able to measure the transverse position of each bunch within a train. Each type has several designs, depending on the beam pipe, whose diameter ranges from 10 to ca. 100 mm. There are button BPMs (one of the designs is described here [7]) and stripline BPMs [8], both types with electronics developed for FLASH [9]. Also there are cavity BPMs with electronics developed for the European XFEL [10] in the undulator section in FLASH2, as well as “cold” cavity BPMs in the accelerating modules [11].

The single bunch resolution has been evaluated for various charges and beam offsets. The method used for calculation is based on linear regression and is described in [12].

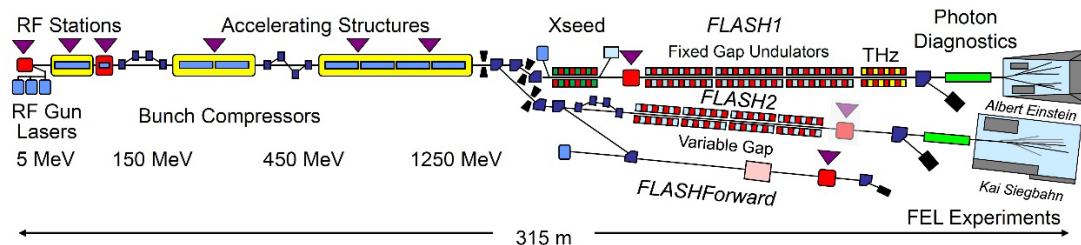


Figure 1: Schematic layout of FLASH [3].

* nicoleta.baboi@desy.de

ELECTRO-OPTICAL BPM DEVELOPMENT FOR HIGH LUMINOSITY LHC

A. Arteché*, S. M. Gibson†, John Adams Institute at Royal Holloway, University of London, UK
 T. Lefèvre, T. Levens, CERN, Geneva, Switzerland

Abstract

An Electro-Optic Beam Position Monitor (EO-BPM) is being developed as a high-frequency (up to 10 GHz) diagnostic for crabbing and Head-Tail intra-bunch detection at the HL-LHC. Following an earlier prototype at the SPS that demonstrated single-pickup signals, an upgraded design of an interferometric EO-BPM has been beam-tested at the HiRadMat facility for validation and characterisation studies. In the new design, the fibre-coupled Mach-Zehnder interferometer arms are modulated by lithium niobate waveguides integrated in an upgraded opto-mechanical arrangement that has been developed to produce a highly magnified image field replica of the passing Coulomb field. A new detection technique that is directly sensitive to the interferometric optical difference signal from opposite EO buttons has been applied to measure single-shot bunches for the first time. A transverse resolution study over a ± 20 mm range at 3 GHz bandwidth produced the first successful electro-optic bunch-by-bunch position measurement at the HiRadMat in-air extraction line. The results of this campaign show promise for an in-vacuum design that is in production for beam tests at the SPS during Run-3 of the LHC.

INTRODUCTION

The Electro-Optic Beam Position Monitor (EO-BPM) has been proposed as a high-frequency diagnostic for the High Luminosity Large Hadron Collider (HL-LHC), with an operational bandwidth that targets up to 6 – 10 GHz [1, 2]. Among the potential applications are the detection of crabbed-bunch rotation and as a higher bandwidth alternative to standard Head-Tail instability monitors [3].

A prototype of a single EO pickup with a lithium niobate (LN) crystal located 66.5 mm away from the beam was installed in the SPS in 2016, delivering the first EO acquisition of a proton-induced signal [4, 5]. The far location, the long bunch length, and the initial pickup design implied the detection of modulating fields below 1 kV/m, which represented a major challenge [6]. To enhance the signal strength, the prototype was replaced during the 2017 SPS run by a modified version that incorporated an electrode to concentrate the modulating field in the LN crystal, proving to be a good strategy [6, 7]. Since then, several improvements of the optical configuration and stability have been incorporated, transitioning towards a more compact and robust phase interferometer model [8, 9]. The culmination is the new opto-mechanical design tested at HiRadMat that, thanks to a refined electrode design, delivers a highly magnified im-

age replica E_z of the propagating Coulomb field E_C within a LN waveguide volume. This hot-spot mechanism enhances the modulating field E_z parallel to n_e by a significant factor, reaching 190 kV/m for a nominal SPS bunch, according to CST numeric simulations [10].

In combination with the upgraded pickup, a new optical detection technique is proposed as shown in Fig. 1. A Common Interferometric Point (IP-C) is generated when two optical paths combine after going through LN waveguides embedded in EO buttons placed on opposite sides of the pipe. Additionally on each side, one path through the crystal pickup combined with a simple bypass generates left and right side interferometers (IP-L & IP-R). While previous experiments at the SPS were based on the latter, this paper presents results from the common mode for first time.

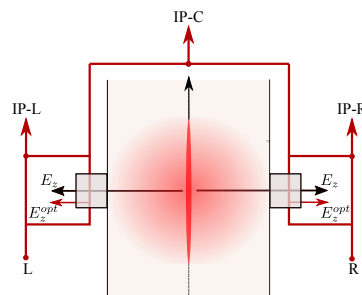


Figure 1: Triple interferometric layout of the EO-BPM.

The optical paths are linearly polarised in z at each LN waveguide, so E_z will activate the linear Pockels effect. This induces a time-profile optical modulation that is a replica of the passing bunch at IP-L & IP-R, and also at IP-C only when the beam is off-centre. Each interferometer has two output fibres from a 2×2 fused-coupler, so that each IP produces two opposite sign modulations: in-phase (+) and anti-phase (-). The IP-C detection allows us to correlate signal strength and transverse position using a single channel, and could also potentially deliver a straight intra-bunch measurement.

In summer 2021, the first interferometric EO-BPM system based on this promising fibre-coupled waveguide model was propitiously installed and tested at the HiRadMat facility. The proton bunch parameters for this SPS extraction line towards a target were similar to those for the nominal LHC bunch, typically $\sim 1.15 \cdot 10^{11}$ protons and $4\sigma \sim 1$ ns long Gaussian bunches. In-air characterisation tests of the transverse resolution were performed for single-shots and the results are presented in this paper. The ultimate goal of this campaign was to validate the common-mode detection technique and the new waveguide-based EO-BPM design under realistic beam conditions.

* alberto.artech@rhul.ac.uk

† stephen.gibson@rhul.ac.uk

DIAGNOSTICS WITH QUADRUPOLE PICK-UPS AT SIS18

Adrian Oeftiger*, Rahul Singh

GSI Helmholtzzentrum für Schwerionenforschung GmbH, Darmstadt, Germany

Abstract

The beam quadrupole moment of stored beams can be measured with a four-plate quadrupole pick-up. The frequency spectrum of the quadrupole moment contains not only the usual first-order dipole modes (the betatron tunes) but also the second-order coherent modes, comprising of (1.) (even) normal envelope modes, (2.) odd (skew) envelope modes and (3.) dispersion modes. As a novel diagnostic tool, the measured frequencies and amplitudes provide direct access to transverse space charge strength through the tune shift as well as linear coupling (and mismatch thereof), along with the benefit of a non-invasive beam-based measurement. Technically, quadrupole moment measurements require a pick-up with non-linear position sensitivity function. We discuss recent developments and depict measurements at the GSI SIS18 heavy-ion synchrotron.

INTRODUCTION

Quadrupolar pick-ups (QPU) in a beam line provide information about the coherent transverse second-order moments of a passing bunch of particles. These devices have often been used in studies measuring the beam emittance or injection mismatch of the optics functions [1–3], or the strength of space charge in synchrotrons [4–8]. The advantage is the non-invasive and thus non-destructive nature of measuring the quadrupolar moment S_{QPU} via induced currents in the four symmetrically arranged electrodes, in particular for inferring the transverse RMS emittances in comparison to destructive profile measurement methods like flying wire scans or secondary electron emission (SEM) grids. Typically, *time domain* oriented methods to determine the emittance from a measured quadrupolar moment demand well controlled experimental setups, where differential offsets in the quadrupolar moments need to be understood and controlled precisely while the strong dipole component in the signal needs to be suppressed. These challenges could possibly be the main reason why QPUs are typically not yet used as beam diagnostics in regular operation. A technically less demanding and thus potentially more rewarding approach in a synchrotron is to profit from the *frequency domain* and measure the bunch eigenmodes, where only the frequency content and not the absolute values of S_{QPU} matter.

The quadrupole spectrum of a circulating beam has a rich structure. Most often the two even transverse envelope modes of the oscillating $\sigma_{x,y}(s)$ are studied, most prominently for measuring the strength of space charge by determining the coherent tune shift of the envelope due to space charge defocusing. Past experiments mainly studied coasting beam conditions [4–7].

At the same time, space charge broadened resonances typically become an issue mostly under bunched beam conditions. A truly useful diagnostic tool for direct space charge strength quantification thus should be applicable to bunched beam. A recent study for the first time accomplishes this space charge measurement of bunched beams [8] at the CERN Proton Synchrotron (PS): since the envelope oscillations due to injection mismatch typically decohere very rapidly in bunches, they are much more challenging to measure than in coasting beams. As an alternative, the study establishes the quadrupole beam transfer function (Q-BTF) technique based on a transverse feedback system, which quadrupolarly excites the bunch in a frequency sweep while measuring the beam response in the QPU. Such measured “bands” of coherent envelope modes due to varying defocusing by space charge depending on the longitudinal line charge density are expected to reveal the maximum coherent envelope tune shift at the longitudinal peak line charge density.

Another notable finding from bunched beam Q-BTF measurements in Ref. [8] is the observation of the coherent dispersion mode. In Ref. [9] the connection of this mode to head-tail instabilities has been illuminated, as the dispersion mode locks onto the correlation between transverse displacement and longitudinal momentum. Furthermore, as also mentioned in Ref. [9], the space charge shift of the coherent dispersion mode frequency could in principle be used to quantify space charge as an alternative to envelope mode frequency shifts.

The quadrupole moment spectrum further contains the skew quadrupole resonances [9]. Their mode amplitude indicates injection mismatch with respect to linear coupling, which can be useful for a direct beam-based measurement. This approach again intrinsically includes space charge in contrast to conventional BPM-based methods such as the closest-tune approach $|C^-|$ [10], as dipole-moment-based measurements are insensitive to coupling contributions from space charge.

For bunched beam, the quantitative influence of chromatic detuning on the measured envelope bands has been raised as an open point, given its oscillatory nature due to synchrotron motion. Simulations in Ref. [8] demonstrate the significant widening of the measured envelope band width due to chromaticity. In this contribution we present new measurement results from the GSI SIS18 synchrotron, based on a recently established Q-BTF setup involving a quadrupole kicker and pick-up. While proton beams in CERN PS suffer from head-tail instabilities at intensities where space charge becomes relevant, (heavy-ion) beams in the SIS18 can reach significant space charge strength at lower intensities where head-tail instabilities play no significant role. SIS18 there-

* a.oeftiger@gsi.de

BEAM-BASED CALIBRATION OF SEXTUPOLE MAGNET DISPLACEMENT WITH BETATRON TUNE SHIFT

S. Takano^{†1}, T. Fujita, M. Takao, K. Fukami¹, M. Masaki, T. Watanabe¹, JASRI, Hyogo, Japan
H. Maesaka², K. Soutome², T. Hiraiwa, H. Tanaka, RIKEN SPring-8 Center, Hyogo, Japan
K. Ueshima, QST, Miyagi, Japan

¹also at RIKEN SPring-8 Center, Hyogo, Japan

²also at JASRI, Hyogo, Japan

Abstract

The alignment of sextupole magnets is one of the critical issues for the upcoming 4th generation light sources and future colliders to ensure enough dynamic aperture for stable operation and minimize deterioration of beam quality. We propose a beam-based calibration (BBC) method for the sextupole magnet displacement by observing the betatron tune shift. The beam position that makes the horizontal and vertical betatron tunes invariant to the sextupole strength marks the magnet center. The key is to increase the betatron coupling so that the vertical displacement of a sextupole from the beam results in a tune shift large enough for the calibration. The feasibility studies at SPring-8 successfully demonstrated the principle for calibrating both horizontal and vertical sextupole displacements in quantitative agreement with the theory.

INTRODUCTION

The alignment of sextupole magnets is one of the critical issues for the upcoming 4th generation light sources and future colliders. The misalignment and the beam offset in sextupoles should be within a few 10 μm to ensure enough dynamic aperture for stable operation and minimize deterioration of beam quality. A sextupole magnet horizontally displaced from the beam exerts a normal quadrupole (Q) field, and a vertically displaced one a skew Q field. We propose a beam-based calibration (BBC) method to measure the displacement of a sextupole magnet by observing the betatron tune shift. The beam position that makes the horizontal and vertical betatron tunes invariant to the sextupole strength marks the magnet center. We studied experimentally the feasibility of the proposed BBC for the sextupole magnet on the SPring-8 storage ring and successfully demonstrated the principle for calibrating both the horizontal and vertical displacements. In this paper, we overview the theoretical background related to the betatron tune-based BBC and elaborate on the results of feasibility studies at SPring-8.

THEORETICAL BACKGROUND

Magnetic Field of a Sextupole

Suppose that a beam passes through a sextupole magnet with offset (x_0, y_0) from the center of the magnetic field. When each particle in the beam moves $(\Delta x, \Delta y)$ around this

point, the magnetic field at the destination point is expressed in the forms

$$B_x = B''(x_0 + \Delta x)(y_0 + \Delta y), \quad (1)$$

$$B_y = \frac{B'''}{2} \{(x_0 + \Delta x)^2 - (y_0 + \Delta y)^2\}, \quad (2)$$

where B'' is the gradient of the sextupole magnet. Eqs. (1) and (2) can be rewritten in the forms

$$B_x = B''x_0y_0 + B''x_0\Delta y + B''y_0\Delta x + B''\Delta x\Delta y, \quad (3)$$

$$B_y = \frac{B'''}{2}(x_0^2 - y_0^2) + B''x_0\Delta x - B''y_0\Delta y + \frac{B'''}{2}((\Delta x)^2 - (\Delta y)^2). \quad (4)$$

The second and third terms in Eqs. (3) and (4) represent the normal and skew Q components in the magnetic field, respectively. Therefore, in a sextupole magnet, the beam passing through with a horizontal offset, $x_0 \neq 0$, undergoes a normal Q magnetic field, and the one passing through with a vertical offset, $y_0 \neq 0$, undergoes a skew Q field. The skew Q field in the sextupole magnet drives the linear coupling of the betatron motion that adds to the indigenous coupling driving term of the whole storage ring.

Betatron Tune Shift by a Displaced Sextupole

For the coupled betatron motion, if we define the difference between the fractional parts of unperturbed betatron tunes ν_x and ν_y as

$$\Delta \equiv \nu_x - \nu_y - q \quad (5)$$

with q an integer, the eigentunes in the normal coordinate ν_u and ν_v , which are observed in actual measurements instead of ν_x and ν_y , can be expressed as

$$\nu_{u,v} = \nu_{x,y} \mp \frac{1}{2}(\Delta - \sqrt{\Delta^2 + |c|^2}), \quad (6)$$

and

$$\nu_{u,v} = \nu_{x,y} \mp \frac{1}{2}(\Delta + \sqrt{\Delta^2 + |c|^2}), \quad (7)$$

for $\Delta \geq 0$ and $\Delta < 0$, respectively, where C is the coupling driving term (complex number) for the whole ring [1]. In what follows, we will address the case $\Delta < 0$ as in the studies reported in this paper.

[†] takano@spring8.or.jp

COLLIMATION AND MACHINE PROTECTION FOR LOW EMITTANCE RINGS*

J. Dooling[†], Y. Lee, M. Borland, A. Grannan, C. Graziani, R. Lindberg, G. Navrotsky
Argonne National Laboratory, Lemont, IL, USA
N. Cook, RadiaSoft, Boulder, CO, USA
D. Lee, University of California, Santa Cruz, CA, USA

Abstract

The reduced emittance and concomitant increase in electron beam intensity in Fourth Generation Storage Ring (4GSR) light sources lead to the challenging machine protection problem of how to safely dispose of the circulating charge during unplanned whole-beam loss events. Two recent experiments conducted to study the effects of 4GSR whole-beam aborts showed that damage to candidate collimator materials can be severe. This is a paradigm shift for SR light source machine protection. Typically the biggest threat to the machine is from CW synchrotron radiation. The choice of collimator material is important. High-Z, high-density materials such as tungsten may appear effective for stopping the beam in static simulations; however, in reality, short radiation lengths will cause severe destructive hydrodynamic effects. In our experiments, significant damage was observed even in low-Z aluminum. Thus unplanned, whole-beam aborts cannot readily be stopped in a single collimator structure. In this tutorial, alternatives such as multiple collimators and fan-out abort kicker systems will be discussed. Collimator design strategy and foreseen diagnostics for their operation will also be presented.

INTRODUCTION

The ultra-low emittance, high-intensity electron beams in Fourth Generation storage ring (4GSR) machines are capable of causing high-energy-density (HED) interactions on technical surfaces such as collimators or vacuum chamber walls. HED is defined as energy densities exceeding roughly 10^{11}J/m^3 [1]. Dose is defined as absorbed energy per unit mass, $D = E_a/\rho$. HED conditions represent an acute dose of 37 MGy in aluminum, 11.2 MGy in copper, and 5.2 MGy in tungsten. The term “acute” is somewhat ambiguous; here it implies the duration of the deposition is short. A useful rule-of-thumb is to compare the duration with a thermal diffusion time defined from the heat equation as $\tau_D = L^2/\alpha$, where L is a characteristic scale length of the absorbed energy distribution and α is the diffusivity. For systems undergoing rapid temperature or phase changes, α is a complex function of dose and time. For example, diffusivity and thermal conductivity change significantly

in aluminum as the material changes from solid to liquid phase [2]. Thermal conductivity falls further if the collimator enters a warm dense matter (WDM) regime [3]. Hence, sophisticated, self-consistent analysis may be required to properly capture material evolution under incident dose.

MACHINE PROTECTION

Third-generation storage ring light sources have typically not focused on protecting accelerator hardware from loss of the circulating electron beam; the effort has been and is still centered on protecting components from x-ray photons. Some measures have been taken such as shielding undulator permanent magnets from accumulated dose caused by high-energy electromagnetic showers; however, this exposure takes place over weeks and months and is not mechanically destructive. Attention to synchrotron photons is warranted given that insertion device beam lines generate kilowatts of beam power with power densities up to 600 kW/mrad^2 [4].

The Advanced Photon Source Upgrade (APS-U) Final Design Report (FDR) [4] states, “The machine protection system (MPS) protects the APS storage ring vacuum system from x-ray beam heating, loss of water cooling, and elevated vacuum levels.” On the other hand, documentation for high-energy experimental facilities such as the Electron Ion Collider (EIC) explicitly discuss the need for MPS to protect against beam strikes [5], “...the primary goal of the MPS is to protect the EIC accelerators from the possible damage caused by electron and proton beams.”

Two experiments conducted in the APS storage-ring (SR) [6] have led to the understanding that disposal of the electron beam during a whole beam dump—both planned and unplanned—must also be included in the function of the APS-U MPS. This language has been added to the MPS engineering specification document.

In the following subsections, we present a brief overview of MPS realizations at several accelerator facilities including APS-U. The selection is by no means comprehensive.

APS-U, Argonne National Laboratory

A schematic of the APS-U MPS topology is presented in Fig. 1. Twenty local MPS (LMPS) modules distributed around the ring feed the main MPS unit in the Main Control Room (MCR). Block diagrams for the logic paths are presented in Fig. 2. The top schematic depicts the Main logic block and the lower the local logic. Important subsystems to the MPS include the Front End Equipment Protection System (FE-EPS). The hierarchical architecture is common to

* This research used resources of the Advanced Photon Source (APS), one of the five U.S. Department of Energy (DOE) Office of Science user facilities and is based on work supported by Laboratory Directed Research and Development (LDRD) funding from Argonne National Laboratory, provided by the Director, Office of Science, of the U.S. DOE under Contract No. DE-AC02-06CH11357.

[†] dooling@anl.gov

THE DIAMOND BEAM LOSS MONITORING SYSTEM AT CERN LHC AND SPS

E. Calvo*, E. Effinger, M. Gonzalez-Berges, J. Martínez, S. Morales, B. Salvachua, C. Zamantzas
CERN, Geneva, Switzerland

J. Kral, Faculty of Nuclear Sciences and Physical Engineering (FNSPE), Prague, Czechia

Abstract

The Large Hadron Collider (LHC) and the Super Proton Synchrotron (SPS) accelerators are equipped with 17 pCVD diamond based Beam Loss detectors at strategic locations where their nanosecond resolution can provide insights into the loss mechanisms and complement the information of the standard ionization chamber type detectors. They are used at the injection and extraction lines of the LHC and SPS, to analyse the injection or extraction efficiency, and to verify the timing alignment of other elements like kicker magnets. They are used at the betatron collimation region and are being also explored as detectors to analyse slow extractions. The acquisition chain was fully renovated during the second LHC long shutdown period (from December 2018 to July 2022) to provide higher resolution measurements, real-time data processing and data reduction at the source as well as to integrate seamlessly to the controls infrastructure. This paper presents the new hardware platform, the different acquisition modes implemented, the system capabilities and initial results obtained during the commissioning and operation at the beginning of the LHC's Run 3.

INTRODUCTION

The LHC is currently equipped with 12 pCVD diamond beam loss detectors (dBLM), and 5 more are installed at the SPS. Their time response, in the order of a few nanoseconds, complements the information provided by the standard ionisation chambers, which deliver very sensitive but much slower measurements (from 40 μ s at LHC to 5 ms at SPS). Since the minimum LHC bunch spacing is 25 ns, pCVD detectors can provide bunch-by-bunch beam loss measurements. This time resolution is of particular interest at the injection and extraction regions, where the presence of unbunched beam or ghost bunches on the abort gap, can induce high and fast losses during the kicker ramps. This is the reason why half of the LHC diamond BLM detectors and most of the SPS detectors are located in those regions. The complete topology of the dBLM detectors can be seen in Fig. 1 where their locations are represented by green dots.

The second area of high interest equipped with three detectors per beam, is the LHC betatron collimation region, in IR7, where the LHC global aperture limit is located. On that area, bunch-by-bunch losses can be monitored along the full proton fill, and the loss distribution along the batches can provide additional information on the loss causes (electron cloud, long-range beam-beam interactions, etc) [1].

* eva.calvo.giraldo@cern.ch

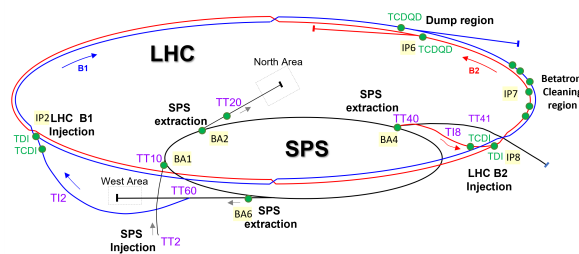


Figure 1: Location of diamond detectors at SPS and LHC.

This paper presents the recent changes that were implemented on the diamond BLM system installed in the CERN accelerator complex as well as some recent measurements to highlight their performances.

DIAMOND BLM HARDWARE

The diamond beam loss monitors consist of pCVD diamond detectors, 10 mm x 10 mm x 0.5 mm in size with gold electrodes of 8 mm x 8 mm on both sides. They are operated with a bias voltage of 500 V, which corresponds to an electric field strength of 1 V/ μ m. The detectors are connected to a splitter, which provides one DC and two AC outputs. Each of the two AC outputs is either amplified or in some cases attenuated in order to obtain two overlapped operational ranges, thus extending the full dynamic range. Amplifiers consist of either 20 or 40 dB gain, 2 GHz bandwidth, and can withstand up to 1 MGy TID [2].

These three elements are commercial components from CIVIDEC Instrumentation GmbH, and are mounted on a metallic support which positions the detector above or below the beam pipe, downstream of a collimator. Figure 2 shows a typical installation of one of those detectors installed by the end of one the SPS to LHC transfer lines. The acquisition



Figure 2: Photo of a dBLM detector installed at the end of the T18 LHC injection line.

COMMISSIONING BEAM-LOSS MONITORS FOR THE SUPERCONDUCTING UPGRADE TO LCLS*

Alan S. Fisher[†], G. W. Brown, E. P. Chin, C. I. Clarke, W. G. Cobau, T. Frosio, B. T. Jacobson, R. Kadyrov^{**}, J. A. Mock, Jino Park, E. Rodriguez, P. K. Roy, M. Santana Leitner, J. J. Welch
SLAC National Accelerator Laboratory, Menlo Park, CA, USA

Abstract

Commissioning of the 4-GeV, 120-kW superconducting linac, an upgrade to the LCLS x-ray FEL at SLAC, began in summer 2022, by accelerating a beam through the first cryomodule to 100 MeV. This autumn the beam will accelerate along the full linac, pass through the bypass transport line above the copper linac, and end at a new high-power tune-up dump at the muon shield wall. The first beam through the undulators is expected by early 2023, at a rate well below the full 1 MHz. A new system of beam-loss detectors will provide radiation protection, machine protection, and diagnostics. Radiation-hard optical fibres span the full 4 km from the electron gun to the undulators and their beam dumps. Diamond detectors cover anticipated loss points. These replace ionization chambers previously used with the copper linac, due to concern about ion pile-up at high loss rates. Signals from the new detectors are integrated with a 500-ms time constant and compared to the allowed threshold. If this level is crossed, the beam stops within 0.2 ms. We report on the initial commissioning of this system and on the detection of losses of both photocurrent and of dark current from the gun and cryomodules.

INTRODUCTION

SLAC removed the first km of its 3-km copper electron linac, completely emptying this part of the tunnel and the Klystron Gallery above it for the first time since construction in the 1960s. The LCLS-II Project replaced this with a new superconducting (SC) linac with 35 12-m-long cryomodules operating at $f_{RF} = 1.3$ GHz and two third-harmonic cryomodules. All have been installed in the first 700 m of this 1-km section of the tunnel (Fig. 1 of [1]).

In addition, two variable-gap undulators, for hard and soft x-rays, replaced the fixed-gap LCLS undulator. Both are in use with beam from the LCLS normal-conducting (NC) copper linac, in the third km. With a complex arrangement of bend magnets and kickers, one linac can share its rate between the two undulators, or the SC beam can go to one undulator and the NC beam to the other.

The SC linac, driven with continuous-wave (CW) RF power, will produce 4-GeV bunches with variable spacing at 1 MHz ($f_{RF}/1400$). The risk of damaging beam loss grows as the maximum operational beam power jumps from 500 W for the NC linac to 120 kW. A planned energy upgrade (LCLS-II-HE) will install more cryomodules with higher gradients, doubling the beam energy to 8 GeV and so doubling the beam power and the potential for damage.

* SLAC is supported by the U.S. Department of Energy, Office of Science, under contract DE-AC02-76SF00515.

[†] afisher@slac.stanford.edu

^{**} Present address: Apple Inc., Cupertino, California

The SC photoinjector is driven by CW RF at 186 MHz ($f_{RF}/7$) with a 1.3-GHz buncher. This source generates 750-keV electron bunches, which enter the first cryomodule (CM01) after 3 m. Each cryomodule has 8 RF cavities and operates at a temperature of 2 K.

At this time (early September 2022), photocurrent at 10 Hz passed through CM01 and reached energies from 80 to 100 MeV. The commissioning path then terminated the beam at collimator CYC01 (56 m from the cathode, Fig. 1), which was locked with its jaws closed. Alternatively, bunches have been kicked into the DIAG0 diagnostic line that can sample the full-rate beam at up to 120 Hz.

In October 2022, we plan to commission the 3.2 km path from the gun to the tune-up dump in the beam switchyard (BSY). Beam may travel through the undulators to their beam dumps for the first time by the start of 2023.

LONG BEAM-LOSS MONITORS

SLAC has depended on ion chambers [1] for loss measurements, to cover extended regions and points of known loss, such as beam stoppers or collimators. Simulations [1] have demonstrated that at high loss rates ions piling up in these devices may blind them to further losses. This consideration and others led to the adoption of new designs using Cherenkov emission in quartz optical fibres as Long Beam-Loss Monitors (LBLMs), and electron-hole pairs in diamond chips as Point Beam-Loss Monitors (PBLMs) [1]. This paper reports only on the LBLM performance during early commissioning through CM01, since most PBLMs are in the high-energy region that has not yet seen beam.

LBLM Design

As an electromagnetic shower from beam loss passes through the radiation-hard quartz optical fibre, it emits Cherenkov light traveling both upstream and downstream. A photomultiplier tube (PMT) is placed at the fibre's downstream end to detect this light, since our tests found 4 times more signal in this direction [1]. The PMT is in a rack-mounted chassis outside the tunnel, to be accessible and near the signal-processing electronics (Fig. 7 of [1]). At the fibre's upstream end, an LED emits weak light modulated at 0.8 Hz. A digital signal processor (DSP) detects this "self-check" or "heartbeat" using a sensitive filter based on a digital lock-in amplifier. This frequency is below any beam rate and is shared through the power line ($(60 \text{ Hz})/75 = 0.8 \text{ Hz}$) by the LED and DSP. The red-sensitive PMT (Hamamatsu H7422P-40) is housed in a Peltier-cooled module operating at 0°C to limit dark current [1].

COMMISSIONING OF THE LIBERA BEAM LOSS MONITORING SYSTEM AT SPEAR3*

K. Tian[†], S. Condamoor, J. Corbett, N. L. Parry, J. J. Sebek, J. Safranek, F. Toufexis
SLAC National Accelerator Laboratory, Menlo Park, CA, USA

Abstract

SPEAR3 is a third generation synchrotron radiation light source, which operates approximately 9 months each year with a very high reliability. The beam loss monitoring system in the storage ring has recently been upgraded to the modern Libera system from the original legacy hardware. During the initial stage of the new beam loss monitoring system deployment, it proved to be useful for a new lower emittance lattice commissioning in SPEAR3. In this paper, we will report progress in the Libera system commissioning in SPEAR3 and present some first results.

INTRODUCTION

In a high brightness synchrotron radiation light source, it is of great importance to monitor and reduce electron beam losses to improve machine performance and machine protection. As a result, besides various radiation detectors, many facilities also equip with a dedicated beam loss monitoring system to characterize the beam losses. The beam loss monitoring system in SPEAR3 was first deployed to conduct a precise measurement of electron beam energy in the storage ring by observing the resonant spin depolarisation of the beam [1]. The beam loss detector (BLD) was a NaI scintillator coupled to a photo-multiplier tube (PMT). The loss events captured by the scintillator were converted to analog signals and counted by a Struck 3820 scaler, which was integrated into the EPCIS control system and provided pulse counts as the loss rate. NaI detectors also proved to be beneficial for other accelerator physics experiments [2]. However, there were several drawbacks to the system. First, only one high voltage power supply (HVPS) delivered voltage to each PMT, which was not ideal because each detector could require different bias voltage for optimal performance. In addition, the data acquisition system relied on legacy NIM hardware for signal processing. They were not reliable and hard to maintain. As a result, we were motivated to upgrade the SPEAR3 BLM with modern technology. Inspired by successful experience from ESRF [3, 4] and SOLEI [5], we chose the commercial solution of Libera BLM system from Instrumentation Technologies [6].

HARDWARE DEPLOYMENT

The Libera beam loss monitoring solution consists of two main components, the BLD and the beam loss monitor (BLM). Similar to the original BLD in SPEAR3, the Libera

BLD is a PMT-based detector with a plastic scintillator, EJ-200 [7]. The PMT is from Hamamatsu with a built-in HVPS module. As shown in Fig. 1, the scintillator and the PMT are housed in a compact aluminium enclosure with a lead sleeve to shield the X-rays from the synchrotron radiation during operation. The typical response from the PMT for a loss event of the cosmic background detecting in the lab is also shown in Fig. 1 to illustrate the pulse response of the detector. The PMT output signal from the detector has several ns rising time and about 20 ns falling time. The

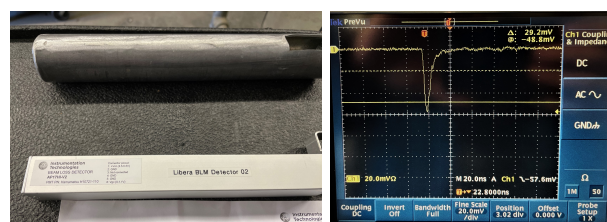


Figure 1: Libera BLD with the lead sleeve (left) and the analog signal for background cosmic ray detection (right).

Libera BLD essentially is a photo multiplier tube (PMT) with a built-in scintillator to convert an individual loss event to a fast analog pulse lasting for about 20 ns. On the other hand, the Libera BLM, each of which can support 4 BLDs, is the digital processing unit for the analog signals from loss events. The ADC of the BLM samples this analog signal at a sampling rate up to 125 MHz or a sampling period of 8 ns. As a result, an isolated beam loss event is converted to a digital peak being formed by about 3 sampling points. The bucket spacing of SPEAR3 is 2.1 ns, therefore, the Libera system is not able to resolve the beam loss with bunch-by-bunch resolution. However, this is still an improvement from the old system, which had a resolution of about 400 ns. Another benefit from the new system compared with the old one is power delivery and gain control from the BLM unit to the BLDs. In SPEAR3, the Libera BLM was integrated into the EPICS control system for easy configuration and control [8].

3 BLMs with 12 BLDs were acquired from the vendor with 9 BLDs installed in SPEAR3. These BLDs are distributed around the storage ring: 1 at the movable scrapers; 1 at a designated Touschek loss point at the center quadrupole at Girder 3 (3G QFC); 1 at the injection septum magnet; 1 at each of the four in vacuum undulators (IVUs); 1 at each of the two elliptical polarized undulators (EPUs). As shown in Fig. 2, the location for the BLD installation in SPEAR3 is limited due to the dense layout of the accelerator components. Most BLDs were installed horizontally in the beam plane so that the scintillator was close to the ring chamber

* Work supported by U.S. Department of Energy under Contract No. DE-AC02-76SF00515

[†] ktian@slac.stanford.edu

DESIGN OF HIGH DYNAMIC RANGE PREAMPLIFIERS FOR A DIAMOND-BASED RADIATION MONITOR SYSTEM

M. Marich*, S. Carrato, L. Vitale, University of Trieste, Trieste, Italy
G. Brajnik, G. Cautero, D. Giuessi, Elettra Sincrotrone Trieste, Trieste, Italy
L. Bosisio, A. Gabrielli, Y. Jin, L. Lanceri, INFN-Trieste, Trieste

Abstract

Regardless of the different accelerator types (light sources like FELs or synchrotrons, high energy colliders), diagnostics is an essential element for both personnel and machine protection. With each update, accelerators become more complex and require an appropriate diagnostic system capable of satisfying multiple specifications, that become more stringent as complexity increases. This paper presents prototyping work towards a possible update of the readout electronics of a system based on single-crystal chemical vapor deposition (scCVD) diamond sensors, monitoring the radiation dose-rates in the interaction region of SuperKEKB, an asymmetric-energy electron-positron collider. The present readout units digitize the output signals from the radiation monitors, process them using an FPGA, and alert the accelerator control system if the radiation reaches excessive levels. The proposed updated version introduces a new design for the analog front end that overcomes its predecessor's limits in dynamic range thanks to high-speed switches to introduce a variable gain in transimpedance preamplifiers, controlled by an ad-hoc developed FPGA firmware.

INTRODUCTION

SuperKEKB [1] hosts Belle II, designed for precision measurements of weak interaction parameters for finding New Physics beyond the Standard Model of particle physics [2]. The inner Belle II employs two types of detectors, namely microstrip and pixel sensors, which are silicon based [3]. The main concern is to reduce their performance degradation caused by radiations exceeding 20 Mrad (MGy). Indeed, the absorption, in short time intervals, of significant dose rates from the inner detector parts can cause their irreversible damage [4]. To reduce these risks, continuously monitoring radiation levels throughout the experiment and signalling abort requests is fundamental. The main abort signal is generated by the central control room after receiving abort requests from the local control rooms, indicating abnormal accelerator and/or beam conditions.

DIAMOND CONTROL UNIT

The current monitoring instrument named DCU (Diamond Control Unit) is an FPGA based system capable of handling up to 4 Diamonds Sensors for both electron and positron monitoring. The FPGA (Cyclone V GX 5CGXFC5C6F27C7N) is a high performance device equipped with 77K Programmable Logic Elements, part of

the Cyclone V GX Starter Kit. In this kit we can find a plethora of useful hardware components, such as an HSMC connector (to link other peripherals) and a 4 GB LPDDR2 memory. The memory is a key factor of the monitoring system, since, as we will see later on, the acquired data are processed and then saved.

Currently there are 7 DCUs (Diamond Control Unit) with 4 diamonds each, that are monitoring the High Energy Electron Ring (HER) and the Low Energy Positron Ring (LER). Mezzanine boards are used to connect the Cyclone V FPGA to the diamonds, each one developed for a particular task, such as analog to digital conversion, amplification and bias. Figure 1 shows the block diagram of the system and Fig. 2 is a picture of the assembled unit.

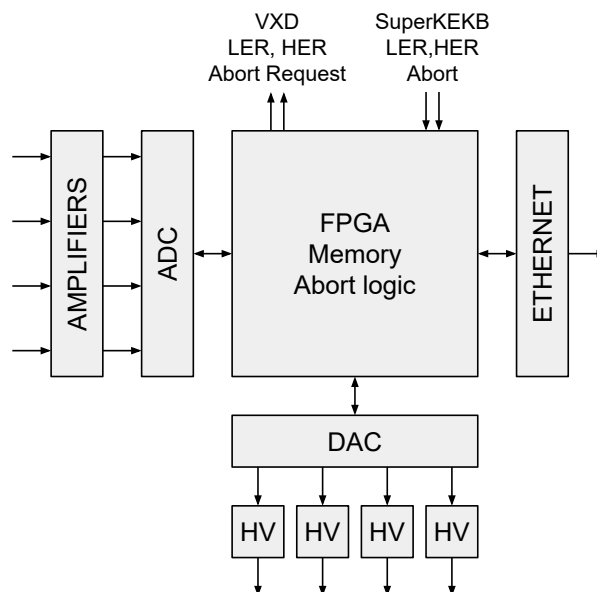


Figure 1: DCU block diagram.

Amplifier Board

It converts the input current in a voltage and filters the signals for each of the 4 channels. One important aspect of the transimpedance stage (TIA) is the variable gain obtained, as shown on the schematic (see Fig. 3), by switching between different feedback networks which are selected by FPGA controlled relays. The TIA's operational amplifier is an LTC6268, a low noise 500 MHz FET input amplifier with low input capacitance and low bias current. The filtering stage is implemented with an OPA211, low power, low noise density precision amplifier. The bandwidth is selected with

* marco.marich@elettra.eu

THE BEAM LOSS MONITORING SYSTEM AFTER LHC LONG SHUTDOWN 2 AT CERN

M. Saccani*, E. Effinger, W. Viganò, C. Zamantzas, CERN, Geneva, Switzerland

Abstract

Most of the LHC systems at CERN were updated during the Long Shutdown 2, from December 2018 to July 2022, to prepare the accelerator for High-Luminosity. The Beam Loss Monitoring system is a key part of the LHC's instrumentation for machine protection and beam optimisation by producing continuous and reliable measurements of beam losses along the accelerator. The BLM system update during LS2 aims at providing better gateway portability to future evolutions, improving significantly the data rate in the back-end processing and the software efficiency, and adding remote command capability for the tunnel electronics. This paper first recalls the Run 1 and Run 2 BLM system achievements, then reviews the main changes brought during LS2, before focusing on the commissioning phase of Run 3 and future expectations.

INTRODUCTION

The Large Hadron Collider (LHC) provided proton-proton collisions at a top energy of 8 TeV in Run 1 (11-2009 to 02-2013) and at 13 TeV during Run 2 (04-2015 to 11-2018). To achieve higher luminosity, the accelerator, as well as its injectors and experiments, underwent a first phase of upgrades during the Long Shutdown 2 (LS2), among which the improvement of cryogenic power, magnet diode, dump absorbers, and collimators. The LHC Run 3 started in July 2022 with a 13.6 TeV top energy and is expected to last 3 or 4 years, before LS3 brings a second phase of upgrades to allow 5x to 7x higher luminosity, as described in the High-Luminosity LHC (HL-LHC) preliminary design report [1].

The Beam Loss Monitoring (BLM) system is used for advanced beam diagnostics to tune beam parameters by char-

acterising loss patterns and locations. It is also a key part of machine protection. The system architecture, presented on Fig. 1, has been proposed in 2007 [2] to meet the LHC specifications [3]. The technical choices resulted in a highly reliable system, to protect the machine against excessive losses. Only a small deposition of the order of 100 mJ/cm³ out of the 320 MJ beam energy stored in the rings risks to provoke a magnet quench. To ensure safe operation, the beam shall be extracted in less than 3 LHC turns when excessive losses are detected.

The LHC BLM system consists of about 4000 detectors, covering all the critical loss locations around the ring, injection and extraction lines, cold superconducting magnets, collimators, etc. Those Ionisation Chambers (IC) are cylindrical tubes filled with N₂ and hosting electrodes polarized at 1.5 kV. Those electrodes collect the charges generated by the passage of secondary particles created by protons lost from the LHC beams [4]. The electrical current generated is acquired by Current to Frequency Converters (CFC) located in the tunnel. Measurements are digitised and optically transmitted every 40 μs to the surface. The back-end electronics located in 2 racks per LHC Interaction Point (IP) provides one Gy/s value per channel on 12 different time windows, ranging from 40 μs to 83.9 s. If one of these values exceeds a predefined threshold a beam dump is requested.

BLM PERFORMANCE IN RUN 1 & 2

During the first two LHC runs, the BLM system protected the machine and contributed to the tuning of the beam parameters [5]. This section reviews the system performance during this period and the modifications implemented based on experience and simulation models.

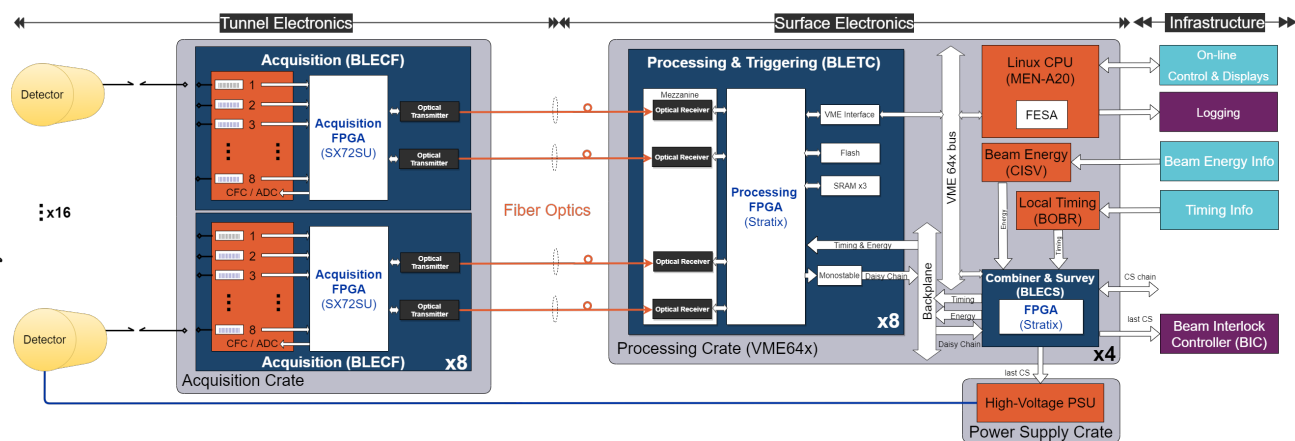


Figure 1: Schematic overview of the BLM system architecture in LHC.

* mathieu.saccani@cern.ch

Content from this work may be used under the terms of the CC BY 4.0 licence (© 2021). Any distribution of this work must maintain attribution to the author(s), title of the work, publisher, and DOI

BEAM LOSS MONITOR FOR POLISH FREE ELECTRON LASER (PoFEL): DESIGN AND TESTS*

R. Kwiatkowski[†], D. Zaloga, R. Nietubyc, J. Szewinski
 National Centre for Nuclear Research, Otwock, Poland

A. Wawrzyniak, National Synchrotron Radiation Centre SOLARIS, Krakow, Poland

Abstract

The Beam Loss Monitor (BLM) system is primarily used for machine protection and is especially important in the case of high energy density of accelerated beam, when such a beam could cause serious damages due to uncontrolled loss. PoFEL linear accelerator is designed with the beam parameters, which made BLM an essential system for machine protection. The design of BLM system for PoFEL is composed of several scintillation probes placed along and around the accelerator. The paper reports on design and first tests of prototype detector, which is planned to be used for PoFEL project. The prototype was tested in NCBJ and SOLARIS, using radioactive calibration samples and linear electron accelerator as a sources. We also present results of numerical investigation of radiation generated due to interaction of fast electrons with accelerator components.

INTRODUCTION

The motivation for using Beam Loss Monitoring system is the detection of unwanted events of fast charged particles escaping the designated path along the beamline. While not being incorporated directly into the vacuum system and beam instrumentation, the BLM is an important part of the high-energy accelerator, which could generate intense beams of high energies and power. The main role of the BLM is to protect the machine from damages (short- or long-term) caused by energetic particles hitting the vacuum components, and/or escaping vacuum pipe without puncturing them, and damaging sensitive equipment due to excessive radiation. Being important system for large facilities, the working principle of beam loss monitors could also be used for beam controlling and fine-tuning of its position and alignment.

THE PoFEL PROJECT

The PoFEL project, namely the construction of Free Electron Laser in Poland is in the preparation for a few years, and at in the present phase it have main features and components already fixed. It is driven by superconducting linear accelerator, based on TESLA SRF technology, and is designed to operate both in continuous

wave (cw) and long pulse (lp) mode. The generation of coherent light is planned in three branches, i.e. in the THz, IR and VUV range. The planned parameters of PoFEL electron beam are listed in Table 1.

Table 1: The Parameters of PoFEL Electron Beam (cw mode) [1-3]

parameter/position	Gun	VUV line	THZ line
Bunch charge [pC]	20-250	<100	250
Repetition rate [kHz]	50	50	50
Bunch length [ps]	2-10	0.1	<10
Beam energy [MeV]	4	<154	<979
Beam current [μ A]	12.5	5	12.5
Beam power [W]	-	770	940

BEAM LOSS TYPES

We could highlight two kind of losses, which lead to increased readout in the BLM system, i.e.: regular and irregular ones.

Regular Losses

Regular, controlled, losses are unavoidable part of accelerator operation and, therefore could be used for diagnostics purposes, like injection studies, energy tail measurements, lifetime limitations, etc. They occur usually as an effect of aperture changes or scattering on residual gas.

Irregular Losses

The irregular, uncontrolled, losses are events, which could lead to potentially hazardous situation and damage the equipment or vacuum components. Such losses could resulted from misaligned beam, leaks or obstacles in vacuum system, failures of beam control, or other accelerator parts. The severity of such an event varies from excess irradiation of nearby devices up to puncturing vacuum vessel wall, in case of prolonged exposition to electron beam.

DETECTORS FOR BLMs

Beam Loss Monitor, being in principle a detector of ionizing radiation, could be built using various types of components. The factors, deciding of device selection are, among others: intrinsic sensitivity; calibration procedures; radiation hardness; reliability; dynamic range; time resolution; size limitations; cost; saturation handling.

The BLM used worldwide are constructed using such detectors like: ionization chambers; PIN diodes; secondary emission monitors, scintillation detectors and cherenkov detectors. Each of the detectors have its char-

*The construction of PoFEL received funding from the European Regional Development Fund in the framework of the Smart Growth Operational Programme and Regional Operational Programme for Mazowieckie Voivodeship.

[†]email: Roch.Kwiatkowski@ncbj.gov.pl

EXPERIENCE WITH MACHINE PROTECTION SYSTEMS AT PIP2IT *

A. Warner[†], M. Austin, L. Carmichael, J.-P. Carneiro, B. Hanna, E. Harms, M. Ibrahim, R. Neswold, L. Prost, R. Rivera, A. Shemyakin, J. Wu, Fermilab, Batavia, IL, USA

Abstract

The PIP-II Injector Test [1] (PIP2IT) facility accelerator was assembled in multiple stages in 2014 – 2021 to test concepts and components of the future PIP-II linac that is being constructed at Fermilab. In its final configuration, PIP2IT accelerated a 0.55 ms x 20 Hz x 2 mA H⁺ beam to 16 MeV. To protect elements of the beam line, a Machine Protection System (MPS) was implemented and commissioned. The beam was interrupted faster than 10 μs when excessive beam loss was detected. The paper describes the MPS architecture, methods of the loss detection, procedure of the beam interruption, and operational experience at PIP2IT.

INTRODUCTION

PIP2IT is a prototype accelerator assembled as a testbed for developing and testing some of the novel and challenging technologies required to construct the Proton Improvement Plan-II (PIP-II) project at Fermilab [2]. The central element of PIP-II is the 2 mA, 800 MeV H⁺ linac which comprises a room temperature front end followed by an SRF accelerator. The PIP2IT (Fig. 1) was constructed in two phases. The first phase consisted of the room temperature portion of the machine, or Warm Front-end (WFE), which comprises a H⁺ ion source, a radio-frequency quadrupole (RFQ) and a transport line for delivering beam to the superconducting section of the accelerator at 2.1 MeV. In the second phase, it was appended by two cryomodules called a Half Wave Resonator (HWR) and a Single Spoke Resonator type1 (pSSR1).

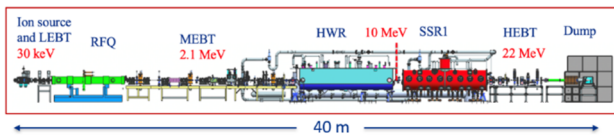


Figure 1: PIP2IT Accelerator Layout.

In the final PIP2IT operational scenario, a 5 mA, 0.55 ms x 20 Hz beam out of the RFQ was scraped transversely in the Medium Energy Beam Transport (MEBT), primarily with scrapers, and then half of the bunches was removed by a bunch-by-bunch chopping system in an aperiodic pattern required for the future injection into the Booster [3]. Then, the beam with 2 mA pulse current was accelerated in the HWR and pSSR1 cryomodules to 8 and 16 MeV, correspondingly, and transported through the High Energy Beam Transport (HEBT) to a beam dump. A machine protection system capable of inhibiting the beam within 10 μs in response to an acute beam loss, protecting

machine components from beam damage, and monitoring the machine configuration was developed.

MPS SCHEME

The PIP2IT MPS scheme tested several features that had been envisioned to be used at PIP-II.

- The main layer of protection is beam inhibiting by a small number (four) of devices that were carefully tested and administratively controlled. All of them are upstream of the RFQ.
- The global protection of the linac is performed by comparison of signals from pairs of current-sensitive devices. These devices (4 pairs) are administratively controlled.
- The second layer of protection, the local protection, controlled the beam loss to multiple electrically isolated electrodes in the MEBT.
- The third level was the readiness signals from the subsystems (vacuum, RF etc.).
- Finally, the beam could be operated only at specific combinations of beam intensities and machine configurations defining how far the beam can propagate. Each combination had its own table of the MPS parameters to control.

This hierarchy, on one hand, provided a robust protection, and, on the other hand, a significant flexibility in operation.

PROTECTION SYSTEM DESIGN

The machine protection system at PIP2IT was not a distributed system and was intended as a testbed for demonstrating the methods needed to protect accelerator components, adequately monitor beam current losses, develop the system logic, provide flexibility to beam measurements and to test hardware and tools required to build a larger scale distributed system for the PIP-II project.

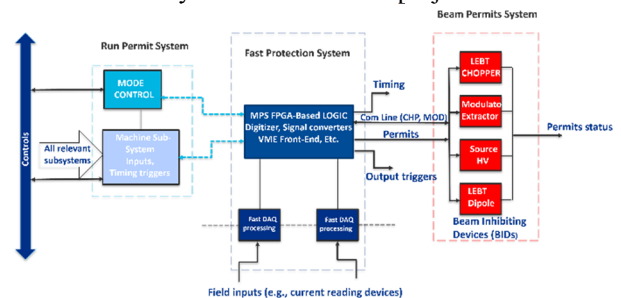


Figure 2: Simplified MPS concept.

The MPS ultimately received Ok/Not-Ok signals from subsystems and managed permits to Beam Inhibiting Devices (BIDs). Figure 2 shows the simplified block diagram. The Low Energy Beam Transport (LEBT) chopper was the primary BID that was cutting the beam off 150 ns after its

* This manuscript has been authored by Fermi Research Alliance, LLC under Contract No. DE-AC02-07CH11359 with the U.S. Department of Energy, Office of Science, Office of High Energy Physics
[†] warner@fnal.gov

DESIGN OF THE BEAM POSITION MONITOR FOR SOLEIL II

M. El Ajjouri, N. Hubert, A. Gamelin, F. Alves, Synchrotron SOLEIL, Saint-Aubin, France

Abstract

The Beam Position Monitors (BPM) for the SOLEIL low emittance upgrade project (SOLEIL II) are currently in the design phase. Efforts are put on the minimization of the heat load on the button by optimizing the longitudinal impedance and the BPM materials.

To validate the mechanical design and tolerances, a first prototype has been manufactured and controlled. This paper presents the mechanical design of the BPM, the metrology of the prototype and the lessons learned from this prototyping phase.

INTRODUCTION

SOLEIL is the French third generation light source routinely operated for external users since 2008 with electron beam emittance of 4 nm·rad at an energy of 2.75 GeV and a nominal current of 500 mA (uniform filling pattern). A low emittance upgrade project is currently in the Technical Design Report (TDR) phase. The reference lattice features a natural emittance of 84 pm·rad [1, 2]. It is based of alternating 7 bend and 4 bend achromats to minimize the displacement of the current source point and realignment of the beamlines, keeping the tunnel shielding wall unchanged. Main comparison lattice parameters are listed in Table 1.

Table 1: Main baseline TDR lattice parameters

	<i>SOLEIL</i>	<i>SOLEIL II</i>
Circumference (m)	354.1	353.9
Beam energy (GeV)	2.75	2.75
Beam current (mA)	500	500
Lattice Type	DBA	7BA/ 4BA
Straight section number	24	20
Natural emittance (pm·rad)	4000	84
RMS Nat. Bunch length (ps)	15	9
RF Voltage (MV)	2.8	1.8
RF Frequency (MHz)	352.2	352.4
Vacuum chamber size (mm)	70/25	12 round

BPM SPECIFICATIONS

SOLEIL II storage ring will be equipped with 180 BPMs: 7 per 4BA section, 10 per 7BA section and 4 additional BPMs in the two long straight sections (Fig. 1).

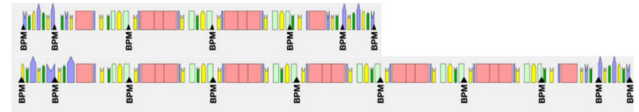


Figure 1: 4 BA cell (up) and 7 BA cell (down), and the beam position monitor location on the SOLEIL II lattice.

The main BPM specifications are listed in Table 2.

Table 2: Main Specification of the Beam Position Monitors

	<i>Time scale/freq.</i>	<i>Specifications</i>
Number of BPM		~180
BPM radius		16 mm
BPM resolution	@10 Hz @100 kHz TbT	1 μm@0.1 mA 50 nm@500 mA 100 μm@0.1 mA 1 μm@500 mA
Beam current dependence	0.1-20 mA in a single bunch	10 μm
Stability	One day One week	500 nm 1 μm
Absolute accuracy before BBA		<500 μs

BPM BLOCK MECHANICAL DESIGN

BPM Mechanical Integration

SOLEIL II vacuum chambers will have a drastically small inner diameter of 12 mm to allow high gradients in the quadrupoles and sextupoles. To keep the BPM body in the shadow of the bending magnets synchrotron radiation, their inner diameter will be enlarged to 16 mm. Systematic tapers upstream/downstream each BPM will ensure a smooth transition between the two pipe diameters.

A large part of the bending magnet synchrotron radiation power will be intercepted (and absorbed) by the vacuum chambers. To minimize the mechanical stress induced by the vacuum chambers during the thermalization of the machine, the straight section BPM will be isolated with bellows. In the arcs, due to high component density, only one bellow between two BPMs is foreseen. All the BPMs will be the fixed points of the vacuum chamber with rigid supports connected either to the ground (straight sections) or the girders (in the arcs).

To achieve the long-term stability requirements of 500 nm a day, 1 μm a week, and considering a temperature in the tunnel stabilized at ±0.1 °C, low thermal expansion stands will be considered in the straight sections. Invar is

DEVELOPMENT OF A NEW MEASUREMENT SYSTEM FOR BEAM POSITION PICKUPS IN THE LINAC AND BEAM ENERGY MEASUREMENT (TIME OF FLIGHT) IN THE MEBT FOR MedAustron

M. Repovz[†], M. Cerv, C. Kurfuerst, G. Muyan, S. Myalski, A. Pozenel, C. Schmitzer, M. Wolf
 EBG MedAustron, Wiener Neustadt, Austria
 A. Bardorfer, B. Baricevic, P. Paglovec, M. Skabar
 Instrumentation Technologies, Solkan, Slovenia

Abstract

The MedAustron Ion Therapy Centre is a synchrotron-based particle therapy facility which delivers proton and carbon beams for clinical treatment. Currently, the facility treats roughly 44 patients per day and is improving its systems and workflows to further increase this number. MedAustron was commissioned and is operational without fully integrated systems for measurements of “time of flight” (beam energy) in the MEBT and beam position in the LINAC. This paper presents the newly developed system for these use cases, which will improve the overall commissioning and QA accuracy. It will unify the hardware used for the cavity regulation in the injector low level radio frequency system LLRF and the synchrotron LLRF. It will furthermore be used for SYNC pickups, Schottky monitors and the RF knock-out exciter. The new system is based on the CotS MicroTCA platform, which is controlled by the MedAustron Control System based on NI-PXIe. Currently it supports fiber-optic links (SFP+), but other links (e.g. EPICS, DOOS) can be established. The modular implementation allows for integration with other components such as motors, amplifiers, or interlock systems and will increase the robustness and maintainability of the accelerator.

INTRODUCTION

After the Low Energy Beam Transfer (LEBT) line the beam is pulsed (with an electrostatic deflector) and accelerated with an RFQ and an Interdigital H-Mode Drift Tube Linac (IH-DTL) cavity (part of the linear accelerator) followed by the Medium Energy Beam Transfer (MEBT) line. Starting after the IH-tank and continuing along the complete MEBT line the Phase Probes (PHPs) for beam energy measurements are placed (4 locations in total) whilst to determine the beam position a Four-Button Probe is located at the entrance of the IH-tank.

These measurement devices are now integrated into a new system that has been developed in collaboration with Instrumentation Technologies.

The developed system description and operation will be elaborated, followed by the first measurement results and concluded by the advantages and disadvantages of the selected implementation as well some short information about the outlook.

[†] matjaz.repovz@medaustron.at

SYSTEM DESCRIPTION

For the readout electronics and data processing an off the shelf piece of hardware has been selected. One of the requirements was the need to use the same electronics for beam position measurement with the pickups in the LINAC, beam energy measurement (Time of Flight) as well as Injector LLRF [1].

The hardware selected is based on the MicroTCA.4 architecture for which Vadatech is the company that provides all the needed components. The crate foreseen to be used for the complete injector system is presented in Fig. 1 with all its connections.

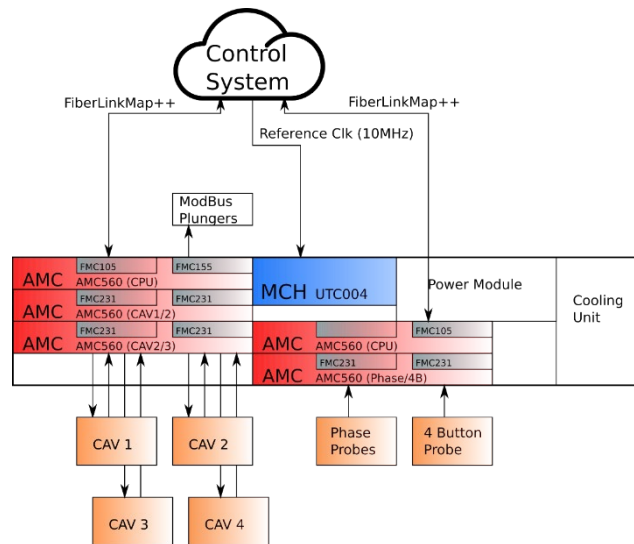


Figure 1: The MicroTCA crate and its connections.

For the four Phase Probes one FMC231 card [2] is needed and for the Four-Button Probe an additional

FMC231 card on the same AMC560 card [3] is required. For communication with the MedAustron control system a proprietary protocol on FiberLinkMap++ is used which goes via SFP+ optical connection on a second AMC560 card equipped with a FMC105 card [4]. The other AMC560 cards with an MC231 and an FMC105 are to be used for the injector low lever RF.

A CRYOGENIC RF CAVITY BPM FOR THE SUPERCONDUCTING UNDULATOR AT LCLS*

C. Nantista[†], P. Krejcik, A. Haase, SLAC National Accelerator Laboratory, Menlo Park, CA, USA.

Abstract

The new superconducting undulator beamline at LCLS requires the BPMs to be operated at cryogenic temperatures alongside the undulator magnets. They are used for beam-based alignment of the undulator magnets and quadrupole and require submicron resolution to achieve good FEL performance. This is to be achieved with X-band RF cavity BPMs, as is done now on the permanent undulator beamline. However, operating the cavities at cryogenic temperatures introduces significant challenges. We review the changes in RF properties of the cavities that result from cooling and how the design is changed to compensate for this. This includes a novel approach for employing a rectangular cavity with split modes to separately measure the X and Y position without coupling.

INTRODUCTION

A new superconducting undulator (SCU) is being installed on the hard x-ray undulator beamline (HXR) at the LCLS-II free electron laser at SLAC. The first two cryogenic modules will be installed at the end of the existing HXR permanent magnet undulator (PMU) beamline so that the FEL performance of the SCU can be measured and compared.

SCUs have been used extensively in storage rings as insertion devices but this will be the first time such a device is used in the x-ray FEL beamline at SLAC. An SCU has advantages in an FEL because of its tunability, and stronger magnetic fields in shorter period length undulators. These characteristics will generate brighter, shorter wavelength x-rays than a PMU, with a shorter FEL gain-length, resulting in a more compact beamline.

In order to realize these advantages it is necessary to install the SCU together with the other beamline components that integrate it into an FEL, including correction coils, phase shifter, quadrupole and BPM. All these components are considered necessary for the prototype module as well so that its performance can be quantitatively assessed. The BPM, which is the subject of this paper, is particularly important because it allows beam-based alignment (BBA) of the undulator beamline to be performed with sufficient precision to allow optimum FEL performance to be achieved. Submicron BPM resolution is required with bunch charges of 100 pC so that the BBA will result in full overlap of the electron and photon beams within micron tolerances.

The shorter gain length advantage of the SCU can only be exploited if all the beamline components are compactly arranged on the beamline without wasting any space with cold to warm transitions. That means that all components,

including the BPM, must be mounted inside the cryomodule and operated at liquid He temperatures, as shown in Fig. 1.

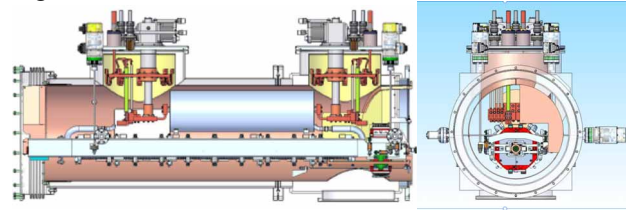


Figure 1: Cutaway and end views of the cryomodule containing the SCU and quadrupole (red) and BPM (copper) at the RH downstream end.

BPM DESIGN CONSIDERATIONS

The LCLS-II free electron laser at SLAC requires monitoring of the beam position with sub-micron level resolution in both x and y . At LCLS we have successfully used X-band RF cavity beam position monitors, or RFBPMs, of a unique configuration, illustrated in Fig. 2, whose design was developed over the last couple of decades [1-3]. It consists of two independent resonant cavities, dipole and reference, with signals coupled out through coaxial vacuum feed-throughs. A distinguishing feature benefiting sensitivity is the magnetic coupling of the dipole cavity fields into side waveguide stubs in a way that shields the pickups from the monopole mode [4].

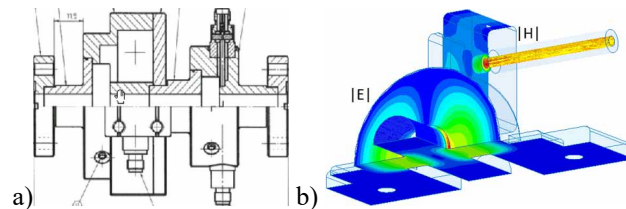


Figure 2: a) cutaway and external view of the LCLS room temperature RFBPM geometry and b) field simulation of dipole cavity coupling [5].

Several factors prevent us taking this RFBPM design and simply mounting it inside the cryomodule. First, the dimensional changes as it is cooled to 40°K produce a large shift in the resonance frequency that must be compensated by machining the cavity to different dimensions at room temperature. Note, that although the SCU coil must operate at 4.2°K, the adjacent components such as the quadrupole and BPM are only cooled to the temperature of the cryomodule thermal shield at 40°K.

The expansion coefficient also decreases exponentially with temperature, as shown in Fig. 3. The coefficient is so small below about 40°K that contraction effectively stops below that temperature, allowing us to accurately predict the machining dimensions at room temperature in order to

* Work supported by U.S. Department of Energy under Contract Numbers DE-AC02-06CH11357.

[†] nantista@slac.stanford.edu

FIRST APPLICATION OF A MULTIPROCESSING SYSTEM-ON-CHIP BPM ELECTRONICS PLATFORM AT SwissFEL

B. Keil†, R. Ditter, M. Gloor, G. Marinkovic, J. Purtschert
 Paul Scherrer Institute, Villigen, Switzerland

Abstract

We have developed a new BPM electronics platform based on a MultiProcessing System-on-Chip (MPSoC). This contribution introduces the first application of the platform at the Paul Scherrer Institute (PSI), which is the cavity BPM system for the SwissFEL soft X-ray undulator beamline called “Athos”, where a larger number of systems are now operational. Measurement results and differences to the predecessor system will also be presented.

INTRODUCTION AND MOTIVATION

PSI has several particle accelerator facilities, including, the High Power Proton Accelerator (HIPA), the Swiss Light Source (SLS), and SwissFEL, a hard X-ray free electron laser. The RF beam position monitors (BPMs) for the proton and electron beams of these accelerators [1-3] as well as the European X-ray FEL BPMs [4] have electronics - developed mainly by PSI - that were so far based on the VME64x form factor, with analog-to-digital converters (ADCs) using parallel data outputs.

However, for the BPMs of the latest SwissFEL undulator line called “Athos” [5] that generates soft X-rays as well as for future upgrades of SLS and HIPA BPMs, we decided to develop a new platform called “DBPM3”. It has a form factor tailored to future PSI BPM systems based on MPSoCs and ADCs with multi-gigabit serial interconnect. MPSoCs integrate several performant CPUs, rich FPGA fabric, various external interfaces and high-speed interconnect on a single chip, enabling the design of more compact and cost efficient BPM systems.

Table 1: PSI Accelerators and RF BPM Systems

PSI Facility	BPM Type	Frequency		FPGA/ASIC Type
		Beam	BPM	
HIPA	Coil	50 MHz	100 MHz	2x Virtex-2 Pro & DDC-ASICs
SLS	Button	500 MHz	500 MHz	DDC-ASICs
Swiss-FEL Linac ...	Cavity (Two Resonators)	2-bunch $\Delta T=28\text{ns}$ 100 Hz	3.3 GHz	2x Artix-7/ 1x Kintex 7
... Aramis Undulators ...			4.9 GHz	
... Athos Undulators		1-bunch 100 Hz	4.9 GHz	1x Zynq UltraScale+ MPSoC

In the following sections, we describe the hardware, software and firmware architecture of the DBPM3 platform.

Measurement results and commissioning experience of the first DBPM3 application, the Athos undulator cavity BPM system, are also presented. Besides Athos, we plan to use the DBPM3 platform also for the SLS 2.0 project [6], which is a major upgrade of SLS with a new low-emittance storage ring. Another application will be the upgrade of the 18 years old HIPA BPM electronics. Due to the smaller number of BPMs in Athos compared to SLS 2.0, Athos enabled us to get experience with the platform before producing larger quantities for SLS 2.0, where first beam is expected in 2025.

DBPM3 PLATFORM

Hardware

A DBPM3 unit has a 3 height unit (HE) 19” wide housing. As shown in Figs. 1 to 3, up to six single-width RF front-ends (RFFE or “daughterboards”) can be inserted from the rear side, or three double width RFFE (for SLS 2.0), or two with triple-width RFFE (for Athos). The number of BPMs per DBPM3 unit is four for Athos and three for SLS 2.0. The redundant power supply is also inserted from the rear side.

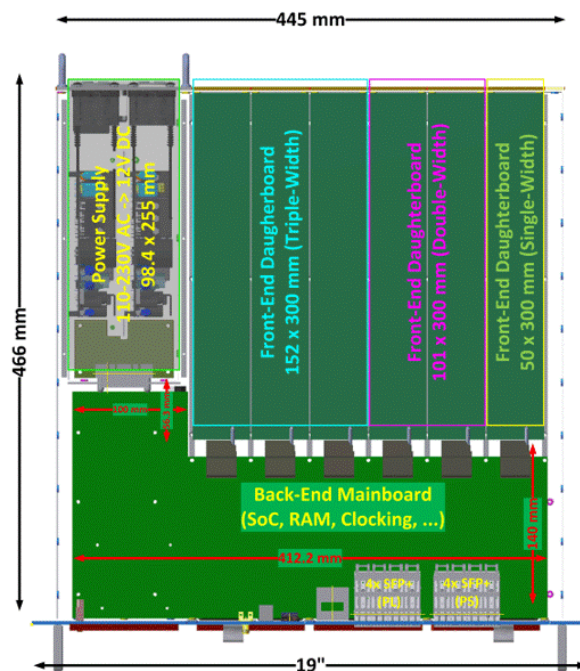


Figure 1: Top view of a DBPM3 unit with cover removed.

The digital back-end mainboard is mounted behind the front panel, having a direct coplanar 120-pin connectors to each daughterboard. The connector is self-centering, and

STANDARD BUTTON BPMs FOR PETRA IV

S. Stokov, M. Holz, G. Kube, D. Lipka, S. Vilcins
Deutsches Elektronen-Synchrotron DESY, Hamburg, Germany

Abstract

A new diffraction limited light source PETRA IV (DESY, Germany) with ultra-low emittance is currently being designed as an upgrade of the 3rd generation light source PETRA III. For transverse beam position measurements, beam position monitors (BPMs) will be used as an essential part of the beam diagnostic system. There will be a total of about 800 BPMs distributed along the 2.3 km storage ring. The inner diameter of the standard beam pipe, and therefore of most of the BPM chambers, will be 20 mm.

The primary purpose of the systems is to provide high-resolution measurements of the transverse position of the electron beam. By specification, the impact of the mechanical tolerances on the position readings should be below $150\ \mu\text{m}$ which is essential for the commissioning of the machine. To achieve this goal, the dependence of the accuracy of the beam position measurement on the tolerances of each manufactured part of the BPM was studied. This paper summarizes development and optimization of each part of the BPM by using EM simulations performed with CST Studio Suite.

INTRODUCTION

Similar to the PETRA III synchrotron ring, the standard button pickup electrodes BPMs will be used in PETRA IV. BPMs are the largest part of the PETRA IV diagnostic system. For the commissioning of the machine, an absolute beam position measurements accuracy of $\leq 500\ \mu\text{m}$ is required [1]. The following three main factors contributes to that number:

- manufacturing tolerances;
- tolerances from electronic part;
- tolerances from the BPMs alignment.

This article considers only the contribution of manufacturing tolerances to the accuracy of BPM measurement, which should not exceed the defined $150\ \mu\text{m}$.

DESIGN ASPECTS

During BPM development, the following goals were pursued:

- to have as few parts as possible to reduce the influence of the manufacturing tolerances on the beam position reading;
- compactness;
- ease of manufacture and assembly;
- reliability and ease of troubleshooting during operation.

Various shapes of the feedthroughs and buttons were considered, calculated, and simulated. The version of the BPM presented in this paper is currently being considered as the main candidate.

Assembly Overview

The final assembly of the BPM is shown in Fig. 1. Each BPM contains the main body and four feedthroughs with buttons. Before feedthroughs are inserted and welded to the main body, their electrical characteristics will thoroughly be measured to find pairs with equal characteristics. The overall dimensions of the BPM body are $72 \times 72 \times 31\ \text{mm}$. Additional cable holder will be attached to each BPM.

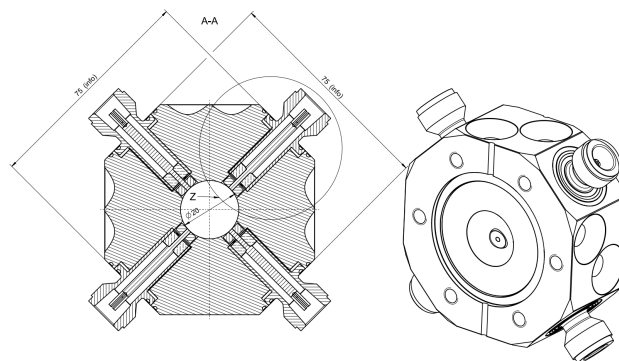


Figure 1: BPM assembly overview.

Feedthroughs with Buttons

Each feedthrough consists of the following parts:

- the body of the feedthrough with inner diameter of $7.5\ \text{mm}$ and attached to it N-type connector;
- the flat button without any skirt around it with a diameter of $7\ \text{mm}$ and a thickness of $3\ \text{mm}$ made of alloy C-22. The gap between the button and the insulator is $1\ \text{mm}$. When feedthrough is inserted into the main body, the gap between the button and the surrounding main body is $0.25\ \text{mm}$;
- the central pin with diameters of $3.04\ \text{mm}$ to match $50\ \text{Ohm}$ impedance. From one side it is connected to the button by laser welding and on the other, it forms a N-type female connector. The material is the same as that of the button - alloy C-22;
- the $5\ \text{mm}$ thick insulator;
- three channels on the outer surface of the assembled feedthrough to help vacuum pumping (see Fig. 2).

ELECTROMAGNETIC SIMULATION

Extensive electromagnetic simulations have been performed by the CST Studio Suite [2] to study how the manufacturing tolerances affect the signal and therefore the beam position measurements. The model from the CST Studio Suite used for the tolerance study is shown in Fig. 3. The beam parameters of the PETRA IV timing mode specified in Table 1 were used for all the simulations.

NEW GAS TARGET DESIGN FOR THE HL-LHC BEAM GAS VERTEX PROFILE MONITOR

H. Guerin^{*1}, R. De Maria, R. Kersevan, B. Kolbinger, T. Lefevre, M. T. Ramos Garcia,
B. Salvant, G. Schneider, J. W. Storey, CERN, Geneva, Switzerland
S. M. Gibson, Royal Holloway, University of London, Surrey, UK
¹also at Royal Holloway, University of London, Surrey, UK

Abstract

The Beam Gas Vertex (BGV) instrument is a novel non-invasive transverse beam profile monitor under development for the High Luminosity Upgrade of the LHC (HL-LHC). Its principle is based on the reconstruction of the tracks and vertices issued from beam-gas inelastic hadronic interactions. The instrument is currently in the design phase, and will consist of a gas target, a forward tracking detector installed outside the beam vacuum chamber and computing resources dedicated to event reconstruction. The transverse beam profile image will then be inferred from the spatial distribution of the reconstructed vertices. With this method, the BGV should be able to provide bunch-by-bunch measurement of the beam size, together with a beam profile image throughout the whole LHC energy cycle, and independently of the beam intensity. This contribution describes the design of the gas target system and of the gas tank of the instrument.

INTRODUCTION

With the foreseen High-Luminosity upgrade of the Large Hadron Collider (HL-LHC), knowledge of the beam emittance during the entire energy cycle will be critical for the machine commissioning. The Beam Gas Vertex (BGV) monitor being developed for this scope, proposes to use beam-gas inelastic hadronic interactions in order to provide a transverse beam size and beam profile measurement. As illustrated in Fig. 1, a noble gas is injected in a dedicated vacuum chamber to generate the beam-gas interactions. The tracks of issued secondary particles are detected by a forward tracking detector, located downstream of the gas target and outside the vacuum. Tracks and vertices are reconstructed with dedicated computing resources, and the beam size and profile are then inferred from the spatial distribution of reconstructed vertices. The instrument is being designed with the aim to achieve a beam size measurement accuracy $< 5\%$ and provide a bunch-by-bunch beam size measurement with a relative precision of a few percent within about 1 min, throughout the full energy cycle, and independent of the beam intensity.

A demonstrator device [1, 2] was installed and operated close to the Interaction Point 4 (IP4) of the LHC during Run 2 and demonstrated the feasibility of using beam-gas inelastic interactions to measure the beam size throughout the full LHC energy cycle and independently of the beam intensity, despite not being able to reconstruct interaction

* helene.chloe.guerin@cern.ch

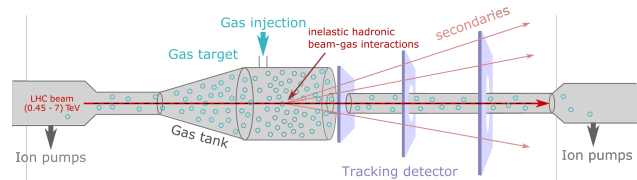


Figure 1: Sketch of the BGV instrument.

vertices. This limitation made the reconstruction of the beam profile impossible.

Following these results, work is ongoing to design the future instrument, which should be capable of vertexing to reach the above-mentioned specifications. A performance study based on Monte-Carlo simulation tools [3, 4] and track and vertex reconstruction analysis was carried out, in order to guide the BGV design.

The conclusions of this study lead to the choice of a compact tracker based on high resolution silicon pixel detectors. It was also decided to keep the distributed gas target system of the demonstrator, but to modify the dimensions of the vacuum chamber in order to reduce the longitudinal beam-gas interaction range and undesired radiation background, and to limit its beam impedance contribution in the LHC machine. This contribution presents the gas target and gas tank design of the future HL-LHC BGV instrument, and evaluates their impact on the machine operation.

GAS TARGET SYSTEM

Instrument Requirements

The BGV tracker was designed to detect tracks from inelastic beam-gas interactions occurring in a 1 m-long region along the beam axis and with an optimal distance of about 550 mm between the center of the gas target and the first detector plane. Most beam-gas interactions occurring outside this volume would not be used for the measurement and generate undesired background, increasing radiation levels in the LHC tunnel. Therefore, the requirements for the gas target design were to provide a uniform pressure distribution of about 1×10^{-7} mbar placed at the relevant distance from the tracker, with a quick pressure decrease outside it. Neon gas was chosen among other noble species in order not to saturate the chambers' non-evaporable getter (NEG) coating, and because remaining molecules after pumping wouldn't affect the sensibility of the leak detection systems, unlike helium and argon. Higher mass noble gases like krypton

FOCUS: FAST MONTE CARLO APPROACH TO COHERENCE OF UNDULATOR SOURCES

M. Siano*, B. Paroli, M. A. C. Potenza, Università degli Studi di Milano, Milan, Italy
G. Geloni, European XFEL, Schenefeld, Germany
D. Butti, T. Lefevre, S. Mazzoni, G. Trad, CERN, Geneva, Switzerland
U. Iriso, A. A. Nosyeh, L. Torino, ALBA-CELLS, Cerdanyola del Vallés, Spain

Abstract

We present *Fast Monte-Carlo approach to Coherence of Undulator Sources* (FOCUS), a new GPU-based code to compute the transverse coherence of X-ray radiation from undulator sources. The code relies on scaled dimensionless quantities and analytic expressions of the electric field emitted by electrons in an undulator. A consistent use of Fourier optics and statistical optics naturally leads to the core structure of the code, which exploits GPUs for massively parallel computations. We validate our approach by direct comparison with *Synchrotron Radiation Workshop* (SRW), evidencing a reduction in computation times by up to five orders of magnitude on a consumer laptop. Finally, we show examples of applications to beam size diagnostics.

INTRODUCTION

Computational tools are of fundamental importance at current synchrotron radiation facilities. The high complexity of modern X-ray beamlines and the need to properly characterize the emitted X-ray wavefronts as a function of the source parameters demand for accurate numerical codes.

To this aim, several software packages have been developed, based either on ray tracing or on wave optics [1–4]. Among them, *Synchrotron Radiation Workshop* (SRW) has been extensively validated at different facilities, and has become a reference in the accelerator and X-ray optics communities.

Simulations of the transverse coherence of X-ray beams are among the most challenging tasks and must rely on a statistical description of wave optics. The standard approach involves multi-electron simulations based on Monte Carlo sampling techniques. More recently, the coherent-mode decomposition method [5] has been applied to describe the transverse coherence properties of X-ray beams from undulator sources [6]. However, both methods are quite demanding in terms of computer resources and computation times.

Here we describe a new code, natively running on GPUs, to compute the transverse coherence of undulator X-ray radiation as a function of the electron beam parameters [7]. The code is named *Fast Monte Carlo approach to Coherence of Undulator Sources* (FOCUS) and relies on analytic expressions of the electric field obtained in free space. A consistent use of Fourier optics and statistical optics naturally leads to the massively parallel code implementation. FOCUS is written in C++ language accelerated with CUDA to harness the

compute capabilities of modern GPUs. Compared to multi-electron SRW simulations running with multi-threading parallelization, FOCUS achieves a remarkable reduction in computation times by up to five orders of magnitude on a consumer laptop. This enables fast and accurate characterization of the transverse coherence properties of the emitted X-ray beam as a function of the electron beam parameters.

THEORETICAL BACKGROUND

Let $\vec{E}(\vec{x}, z)$ be the slowly-varying envelope of the Fourier transform of the electric field (hereafter, simply the field) emitted by an ultra-relativistic electron moving through a planar undulator. Here $\vec{x} = (x, y)$ denotes transverse coordinates over an observation plane at a distance z from the undulator center. In the ultra-relativistic regime $\gamma \gg 1$, γ being the Lorentz factor, the field $\vec{E}(\vec{x}, z)$ is determined by solving paraxial Maxwell equations [8]. In addition, under the so-called resonant approximation, the vertical polarization component can be neglected and the vector field reduces to a scalar quantity [8]. For distances $z \gg L_w$, L_w being the undulator length, the following general expression for the horizontally polarized field is valid [8]:

$$\hat{E}(\hat{\theta}, \hat{z}) = \frac{e^{i\phi_s}}{\hat{z}} \text{sinc} \left(\frac{\hat{C} - \hat{\delta}_E}{2} + \frac{\zeta^2}{4} \right). \quad (1)$$

In Eq. (1) we have defined scaled quantities and dimensionless parameters as follows [8]:

$$\begin{aligned} \hat{E} &= -\frac{2c^2\gamma}{K\omega e A_{JJ,h}} E \\ \hat{x} &= \vec{x} \sqrt{\frac{\omega}{L_w c}} & \hat{z} &= \frac{z}{L_w} & \hat{\theta} &= \frac{\hat{x}}{\hat{z}} \\ \hat{l} &= \vec{l} \sqrt{\frac{\omega}{L_w c}} & \hat{\eta} &= \vec{\eta} \sqrt{\frac{\omega L_w}{c}} \\ \hat{C} &= 2\pi N_w \frac{\omega - h\omega_1}{\omega_1} & \hat{\delta}_E &= 4\pi N_w h \frac{\delta\gamma}{\gamma} \\ \phi_s &= \frac{\hat{z}}{2} \left| \hat{\theta} - \frac{\hat{l}}{\hat{z}} \right|^2 & \zeta &= \left| \hat{\theta} - \frac{\hat{l}}{\hat{z}} - \hat{\eta} \right|. \end{aligned} \quad (2)$$

In Eq. (2),

- ω is the angular frequency of the emitted radiation
- $\lambda = 2\pi c/\omega$ is the radiation wavelength

* mirko.siano@unimi.it

HL-LHC BEAM GAS FLUORESCENCE STUDIES FOR TRANSVERSE PROFILE MEASUREMENT

O. Sedlacek^{*12}, O. Stringer², C. Welsch², H. Zhang²

University of Liverpool, Liverpool, UK

M. Ady, A. R. Churchman, S. Mazzoni, M. Sameed, G. Schneider,
C. C. Sequeiro, K. Sidorowski, R. Veness, CERN, Geneva, Switzerland

P. Forck, S. Udrea, GSI, Darmstadt, Germany

¹also at CERN, Geneva, Switzerland

²also at Cockcroft Institute, Daresbury, Warrington, UK

Abstract

In a gas jet monitor, a supersonic gas curtain is injected into the beam pipe and interacts with the charged particle beam. The monitor exploits fluorescence induced by beam-gas interactions, thus providing a minimally invasive transverse profile measurement. Such a monitor is being developed as part of the High Luminosity LHC upgrade at CERN. As a preliminary study, the fluorescence cross section of relevant gases must be measured for protons at 450 GeV and 6.8 TeV (i.e. the LHC injection and flat top energies). In these measurements, neon, or alternatively nitrogen gas, will be injected into the LHC vacuum pipe by a regulated gas valve to create an extended pressure bump. This work presents the optical detection system that was installed in 2022 in the LHC to measure luminescence cross-section and horizontal beam profile. Preliminary measurements of background light and first signals are presented in this paper.

INTRODUCTION

During the Long Shutdown 3 (LS3, from 2026 to 2028) the Large Hadron Collider (LHC) will undergo a major upgrade to deliver higher luminosity [1], which will involve many new technologies including novel beam diagnostics. A gas jet monitor - Beam Gas Curtain (BGC) monitor - exploiting fluorescence is well-suited for such an environment as it provides non-invasive or minimally invasive profile measurements in the presence of high HL-LHC beam power and strong magnetic fields. The monitor [2–7] is based on a supersonic gas curtain propagating into the path of the beams at 45° that would allow an observation of the 2D transverse distributions from above. The beam excites the gas atoms through collisions which, after deexcitation, emit photons. The distribution of photons is then directly related to the distribution of the original beam. To optimize the detector it is important to know the light yield of the fluorescence process with working gases, such as neon and nitrogen, and protons at 6.8 TeV. Currently, the cross-sections at such high energies are extrapolated through many orders of magnitude from information found in literature at much lower energies [8]. To address this lack of data, an experiment was carried out in 2018 in the LHC to measure neon fluorescence yield at the LHC beam energies, but due to a high background and

a low cross-section, only the fluorescence caused by heavy lead ions at the injection energy was measured. Therefore, a new experimental setup was installed at the LHC with many improvements implemented in order to reduce synchrotron radiation background and to improve the sensitivity. The experimental setup is described in this paper, together with the first measurements performed during beam operation in 2022.

EXPERIMENTAL SETUP

A new imaging system was designed and installed at the LHC point 4 on the ‘Beam 1’ line (i.e. beam propagating clockwise) in a vacuum chamber equipped with a gas injection system with the aim of measuring the LHC beam-induced fluorescence yield of neon at 585 nm. Neon gas is injected at a pressure of 5×10^{-8} mbar to minimise its effect on the beam quality while providing enough gas atoms for the beam to collide with. The observed process is an emission line of neutral Ne which is due to the $2s^2 2p^5 ({}^2P_{1/2}^0) 3p^2 [1/2]_0 \rightarrow 3s^2 [1/2]_1$ transition at 585.4 nm [2, 9].

Figure 1 depicts the whole experimental setup including the camera module which measures the distribution of the emitted photons. An optical line is installed on top of a window flange, imaging the photons with an apochromatic triplet lens with an aperture of 40 mm and a focal length of 160 mm ideal for near-1:1 imaging conditions. The lens provides a high transmittance of approximately 80 % over the wavelengths of interest. In front of the sensor, a filter wheel is installed with one empty filter socket, one blocking filter and one 585 ± 10 nm filter. The blocking filter is a completely opaque screen stopping any photons from reaching the sensor and is used for background studies. The 585 ± 10 nm filter then allows the fluorescence signal to be measured while reducing other sources of background light. The fluorescence light is measured by a two-stage image intensifier reaching single-photon detection sensitivity [10].

The experimental chamber was installed during the 2021-22 LHC Year-End Technical Stop (YETS), in a position where low levels of synchrotron radiation are expected. To minimise the reflection of synchrotron radiation, the vacuum chamber was also blackened by amorphous carbon coating with a reflectivity of 14 %. An ultra-low reflectivity black

* Ondrej.Sedlacek@cern.ch

HIGH-RESOLUTION INTERFEROMETRIC BEAM-SIZE MONITOR FOR LOW-INTENSITY BEAMS

B. Alberdi-Esuain^{*,1}, J.-G. Hwang, T. Kamps¹

Helmholtz-Zentrum Berlin für Materialien und Energie, Berlin, Germany

¹also at Humboldt Universität zu Berlin, Berlin, Germany

Abstract

Plasma-based accelerator technology is reaching a mature state, where applications of the beam for medical sciences, imaging, or as an injector for a future large-scale accelerator-driven light source become feasible. Particularly, the requirements for beam injection into a storage-ring-based light source are very strict with regards to beam quality and reliability. A non-invasive diagnostics greatly helps to reduce the commissioning time of the machine. We present a device suitable for online, non-destructive monitoring of the transverse spot size of the injected beam. In order to measure lateral beam sizes with a few- μm resolution, the technique uses an interferometric regime of coherent synchrotron radiation that is enabled by a sub-femtosecond short bunch-length. Simulations of the photon flux and the retrieval of the beam spot-size are performed for different bandwidth filters in order to define the bandwidth acceptance. Results show the potential of the proposed system that achieves precise retrieval of the complex degree of coherence at an extremely low photon intensity similar to those expected towards the plasma-acceleration injectors.

INTRODUCTION

In the last years, the laser plasma-accelerator technology has advanced enough to produce charged-particle beams stably with ultra-low-emittances in 6D phase-space [1]. These achievements have enabled the application of plasma-accelerator technology for low-energy and high-quality injectors. Recent research evidence that the repetition rate of such a technique is not limited by plasma recovery time in the plasma cell, so it is promising to reach MHz repetition [2]. This feature opens a possibility to supersede the state-of-the-art injectors. Currently, there is an ongoing global effort aimed towards designing a compact plasma-wakefield accelerator as an injector for future large-scale accelerator-driven light sources such as Athena_e [3] or cSTART [4] for injection into ring-based light-sources, high-average-power plasma wakefield research with FLASHForward [5] or projects to apply this technology for free electron lasers directly [1]. These novel injectors can generate electron beams with an extremely low-emittance on the order of $\gamma\epsilon_{x,y} = 0.05 \text{ mm} \cdot \text{mrad}$ for pC to sub-pC bunch charges. The important beam parameters of these facilities are listed in Table 1.

Diagnostics techniques are following the steps forward of laser-plasma accelerators closely, particularly the non-

invasive spot-size measurement which inherently gives the beam emittance information. The characterisation of the electron distribution with the sufficient resolution is challenging due to the extremely small beam emittances and intensities in plasma-wakefield accelerators. Techniques that employ scintillation screens are widely used for similar beam conditions [6], but this deteriorates the beam quality noticeably or even it causes beam loss in the following section. On the other hand, synchrotron-radiation-based monitors is inadequate since light intensity by incoherent synchrotron radiation (ISR) is insufficient owing to the low electron intensity. However, the key feature of the laser-wakefield accelerators, temporally short bunch enables the arising of coherent synchrotron radiation (CSR) in the visible region, which enhances the photon flux significantly in a bending magnet. The photon flux by CSR provides sufficient intensity to place an interferometric beam size monitor (IBSM) which measures the lateral distribution of electrons by the spatial coherency of the interference pattern in the detector [7]. The use of the diffraction regime enhances the spatial resolution by two orders of magnitude, reaching μm -resolutions [8] and this has been applied to many storage-ring-based light sources [9–11]. By extension, we have designed and demonstrated the high-resolution IBSM for extreme beam conditions [12]. However, the detailed aspects of the bandwidth acceptance and beam spot-size retrieval are not fully discussed in the paper. Hence, numerical simulations for investigating the effect of bandwidth and for estimating the propagation of this error to the beam-size retrieval are explained. A scheme of the working principle of our design can be seen in Fig. 1.

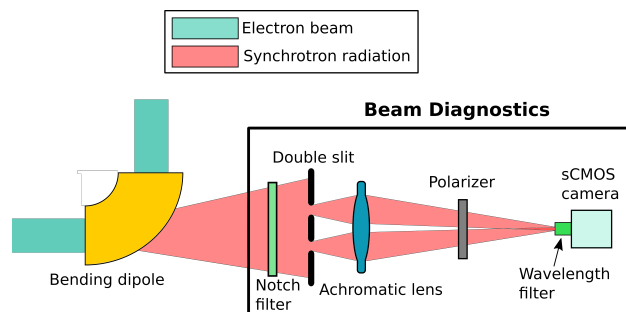


Figure 1: Schematic layout of the interferometry beam size monitor (IBSM) with a scientific complementary metal–oxide–semiconductor (sCMOS) camera for a plasma-wakefield accelerator.

* benat.alberdi_esuain@helmholtz-berlin.de

VISIBLE RANGE POLARIZED IMAGING FOR HIGH RESOLUTION TRANSVERSE BEAM SIZE MEASUREMENT AT SOLEIL

M. Labat*, A. Bence, A. Berlioux, B. Capitanio, G. Cauchon,
 J. Da Silva, N. Hubert, D. Pédeau, M. Thomasset
 Synchrotron SOLEIL, Gif-sur-Yvette, France

Abstract

SOLEIL storage ring is presently equipped with three diagnostics beamlines: two in the X-ray range (pinhole cameras) and one in the visible range. The visible range beamline relies on a slotted copper mirror extracting the synchrotron radiation from one of the ring dipoles. The extracted radiation is then transported down to a dedicated hutch in the experimental hall. Up to now, this radiation was split into three branches for rough monitoring of the beam transverse stability, bunch length measurements and filling pattern measurements. In the framework of SOLEIL's upgrade, we now aim at developing a new branch for high resolution beam size measurement using polarized imaging. This work presents the various modifications recently achieved on the beamline to reach this target, including a replacement of the extraction mirror, and preliminary results towards transverse beam size measurement.

INTRODUCTION

SOLEIL storage ring presently delivers synchrotron radiation to 29 beamlines. The stability of the delivered photon beams, a main figure of merit for users, relies on an accurate monitoring of the electron beam orbit and electron beam size / emittance at users source points. Presently, two beamlines in the X-ray range are dedicated to beam transverse size diagnostics, relying on pinhole camera systems. The high-resolution pinhole cameras' measurements are used in a feedback loop to maintain the vertical emittance within $\pm 5\%$. Despite the high reliability of those pinhole cameras, it would be reassuring to have an additional beam size measurement based on a different technique for redundancy and further verification of the absolute emittance value. This is the main reason why, for three years, we have been working on the upgrade of our third diagnostics beamline, the MRSV beamline (Visible Synchrotron Radiation Monitor) in the visible range, to implement an additional high-resolution beam size measurement based on π polarized imaging [2]. This development also turns to be of high interest in the perspective of SOLEIL-II: it might be indeed the only way to obtain, together with a pinhole camera, two beam size measurements with two different dispersion functions for energy spread retrieval. It is finally worth mentioning that, thanks to the high available photon flux on the MRSV beamline, beam size measurements should be achievable down to very low, ≈ 1 mA, currents (whereas pinhole cameras can't be operated below 10 mA) and could be run above the kHz

range at 500 mA (whereas pinhole cameras are limited to the 10 Hz range). This work presents the main steps of the upgrade of the MRSV beamline together with preliminary results.

GENERAL LAYOUT

The experimental layout of the MRSV beamline is presented in Fig. 1.

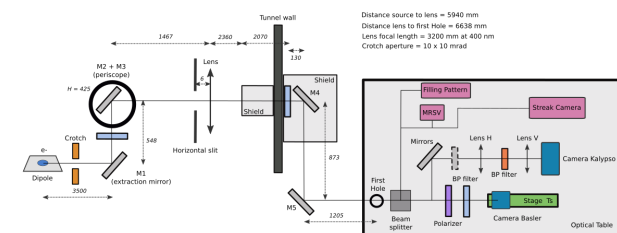


Figure 1: Layout of the MRSV beamline.

The Synchrotron Radiation (SR) of one of the ring dipoles (ANS-C01) is extracted using a slotted mirror, the slot being centered on the beam axis to let SR X-rays go through. The collected photons have a wavelength λ spanning from ≈ 190 to nearly 900 nm. The SR is then transported via a set of mirrors, including a periscope, down to a hutch in the experimental hall. On the beam path inside the tunnel are successively placed a slit and a lens. At the arrival on the optical bench in the hutch, the SR is split into several branches.

Initially, three branches were implemented (see pink boxes in Fig. 1): one with a fast diode for filling pattern measurement, one with a Streak Camera for bunch length measurement and one with a standard Ethernet camera for a coarse imaging of the beam at the source point. We added two new branches to test higher resolution / higher speed imaging systems for beam size retrieval at the source point of the MRSV beamline. We will focus in the following on the high resolution branch (see bottom branch in Fig. 1).

NEW EXTRACTION MIRROR

The initial extraction mirror was already a slotted mirror but without optimized cooling system. In standard operation at 500 mA, when the mirror was inserted in the *slot-insertion* mode, i.e. with its slot centered vertically on the SR fan, its temperature was continuously raising without reaching an equilibrium, preventing its safe use. A new design was therefore optimized in-house in order to guarantee a fast thermal equilibrium of the mirror at 500 mA and to ensure a surface

* marie.labat@synchrotron-soleil.fr

CORRECTIONS FOR SYSTEMATIC ERRORS IN TRANSVERSE PHASE SPACE MEASUREMENTS AT PITZ

C. Richard*, Z. Aboulbanine, G. Adhikari, N. Aftab, P. Boonpornprasert, G. Georgiev, M. Gross, A. Hoffmann, M. Krasilnikov, X.-K. Li, A. Lueangaramwong, R. Niemczyk, H. Qian, F. Stephan, G. Vashchenko, T. Weilbach, Deutsches Elektronen-Synchrotron DESY, Zeuthen, Germany

Abstract

The Photo Injector Test Facility at DESY in Zeuthen (PITZ) characterizes and optimizes electron sources for use at FLASH and European XFEL. At PITZ, the transverse phase space is measured using a single slit scan and scintillator screen method. With the trend in photoinjectors towards lower current and emittance, these measurements become increasingly influenced by systematic errors including camera resolution and scintillator response due to smaller spot sizes. This study investigates the effects and corrections of the systematic errors for phase space measurements at PITZ.

INTRODUCTION

The Photo Injector Test Facility at DESY in Zeuthen (PITZ) commissions and characterizes electron guns for use in Free Electron Lasers (FEL) at FLASH and European XFEL [1]. For FEL operation, the transverse emittance is a key parameter for optimizing the gain length [2]. To characterize the electron guns, PITZ measures the emittance using a single slit emittance scanners. These devices measure the transverse phase space by stepping a narrow slit through the beam to only allow particles at a given position to pass. The profiles of passed beamlets are measured with a camera capturing the signal on a downstream scintillator screen to measure the angular distribution [3]. The systematic errors in this system have previously been studied for the PITZ emittance scanners [4, 5] and it was found that one of the primary systematic errors in this system is the resolution of the camera. However, these studies focused on the effect of the camera resolution on full beam measurements not beamlet measurements and do not quantify the effects on the measured emittance. The effect of the slit width on the measured emittance has also been estimated [6, 7], but, for simplification, it was assumed the beam had no $x - x'$ coupling and the camera effects were excluded. In addition, previous studies do not propose corrections for the systematic errors and it is desired to correct for these errors so accurate emittance measurements can be made.

SYSTEMATIC ERRORS FROM SLIT SIZE

To measure the transverse position profile, the emittance scanner uses a $50 \mu\text{m}$ slit that is stepped across the beam. With this method, the measured profile is the convolution of the beam profile with the slit opening. Therefore, the measured rms beam size $\sigma_{x,m}$ can be corrected using

$$\sigma_{x,m}^2 = \sigma_{x,t}^2 + \sigma_s^2, \quad (1)$$

* christopher.richard@desy.de

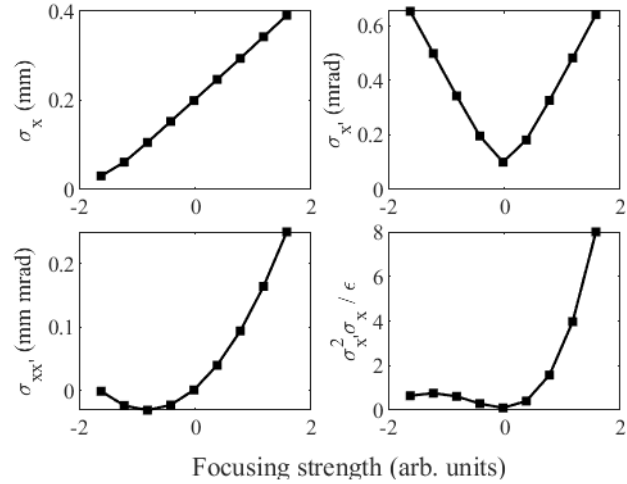


Figure 1: rms parameters of the synthetic optics scan used to test the correction methods. The geometric emittance is $0.02 \text{ mm}\cdot\text{mrad}$.

where $\sigma_{x,t}$ is the true rms beam size and $\sigma_s = 50 \mu\text{m}/\sqrt{12} \approx 14 \mu\text{m}$ is the rms size of the slit. This results in a $\sim 0.5\%$ increase in $\sigma_{x,m}$ when $\sigma_{x,t} \approx 0.15 \text{ mm}$ which is typical at PITZ and $\sim 5\%$ error when $\sigma_{x,t} \approx 0.05 \text{ mm}$. This also effects the measured geometric emittance measured rms emittance

$$\epsilon_m = \sqrt{\sigma_{x,m}^2 \sigma_{x',m}^2 - \sigma_{xx',m}^2}, \quad (2)$$

where $\sigma_{x,m}^2 = \langle x^2 \rangle$, $\sigma_{x',m}^2 = \langle x'^2 \rangle$, and $\sigma_{xx',m} = \langle xx' \rangle$ is a correlation term. The measured emittance can be corrected by the substitution $\sigma_{x,m}^2 \rightarrow \sigma_{x,m}^2 - \sigma_s^2$ into Eq. (2).

To study the effect on the measured emittance, a linear model of the emittance scanner was made in Matlab [8]. The model takes particles from an 4D input distribution and separates them into beamlets based on their x position replicate the slit mask. Each beamlet is then propagated through a drift length to the screen location and heat maps of the particle densities are made to replicate the screen response. To simulate beams with a range parameters similar to what is measured at PITZ, a Gaussian distribution is generated with geometric emittance $\epsilon_g = 0.02 \text{ mm}\cdot\text{mrad}$, put through a thin lens kick and a 30 cm drift length, then processed with the emittance scanner model. The resulting beam parameters at the start of the emittance scanner are shown in Fig. 1.

The measured, uncorrected rms emittance increases as the beam size decreases as expected from Eq. (1) and can be corrected (see Fig. 2). However, the emittance also significantly

SCINTILLATOR NON-PROPORTIONALITY STUDIES AT PITZ

A. Novokshonov*, G. Kube, S. Stokov

Deutsches Elektronen-Synchrotron DESY, Hamburg, Germany,

Z. Aboulbanine, G. D. Adhikari, N. Aftab, P. Boonpornprasert, G. Z. Georgiev,

J. D. Good, M. Gross, C. Koschitzki, M. Krasilnikov, X. Li, O. Lishilin,

A. Lueangaramwong, D. Melkumyan, F. Mueller, A. Oppelt, H. Qian,

F. Stephan, G. Vashchenko, T. Weilbach,

Deutsches Elektronen-Synchrotron DESY, Zeuthen, Germany

Abstract

A standard method to measure beam profiles is to use scintillating screens. Such technique is used e.g. at the European XFEL in order to overcome coherence effects in case of OTR based diagnostics. However, already during the XFEL commissioning, the standard screen material LYSO:Ce has revealed a new problem - non-proportionality effects. The reason is a high electron bunch density. Therefore it was decided to exchange LYSO:Ce by GAGG:Ce, as the material has not shown any signs of non-proportionality in a series of measurements at the XFEL. Nevertheless, further studies are ongoing. The last measurement campaign has been carried out at PITZ (DESY Zeuthen) which has two important advantages compared to the XFEL: (1) a higher bunch charge and (2) a lower electron energy. Five different scintillating materials have been investigated: LYSO:Ce, YAP:Ce, YAG:Ce, LuAG:Ce and GAGG:Ce. The present work comprises the results of the latest measurements.

INTRODUCTION

The European XFEL uses scintillating screens for standard beam profile diagnostics. $\text{Lu}_{2(1-x)}\text{Y}_{2x}\text{SiO}_5:\text{Ce}$ (LYSO) has been chosen as its resolution was the best compared to other materials [1, 2]. However, during the commissioning of the XFEL the measured emittances were larger than expected [3, 4]. In addition, bunches with charges above a few hundreds of pC showed a *smoke-ring* like shape with a drop of intensity right in the center. An example of such shape is shown in Fig. 1. It was supposed that this observation is caused by the scintillator material itself [5].

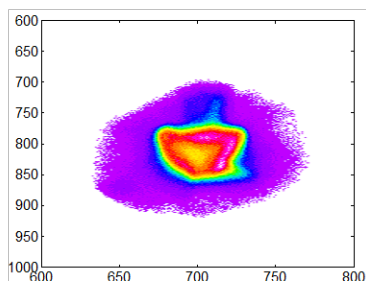


Figure 1: A typical picture received with the LYSO screen.

* artem.novokshonov@desy.de

This effect in principle is well-known in high-energy physics and is called *non-proportionality of scintillators* [6–8]. The more energy a particle loses per unit length in a scintillator volume, the less light output the scintillator will produce. In other words, the light output depends on the deposited energy density. In calorimetric measurements in high-energy physics it results in a non-proportional response [8] at different energies of an incoming particle, as the energy losses depend on its energy (see Fig. 2).

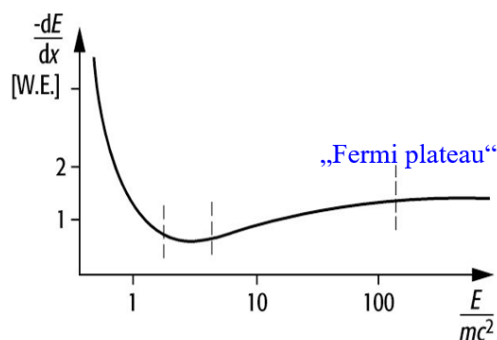


Figure 2: The dependence of particle energy losses in a media on the particle energy.

The effect is especially pronounced at low particle beam energies because the losses per unit length are largest, see Fig. 2. However, in the case of particle beam diagnostics for ultra-relativistic electron beams (as it is the case for the XFEL) the energy losses are smaller, characterized by the so called *Fermi plateau* in the energy loss curve Fig. 2. In addition, scintillators normally used for diagnostics purposes have thicknesses in the order of only a few hundreds of microns, hence the energy loss in the material is negligible compared to the total particle energy. As pointed out in Ref. [5], in this situation it is not the particle energy but the density of the impinging particles which leads to excitonic quenching effects, thus resulting in a non-linear light output. At the XFEL an electron bunch may contain up to 10^{10} particles with a typical size of $\sigma_x \times \sigma_y = 200 \times 200 \mu\text{m}^2$, and the energy density necessary for quenching is reached directly via the initial particle density. This is nicely demonstrated in Fig. 1 where the lowest light output is located exactly in the center of the beam, i.e. the region with the largest particle density.

COMMISSIONING OF THE TIMING SYSTEM AT ESS

A. Gorzawski*, G. Fedel, J. J. Jamroz, J. P. S. Martins, N. Milas
ESS, European Spallation Source, Lund, Sweden

Abstract

The European Spallation Source (ESS), currently under construction and initial commissioning in Lund, Sweden, will be the brightest spallation neutron source in the world, when its driving proton linac achieves the design power of 5 MW at 2 GeV. Such a high power requires production, efficient acceleration, and almost no-loss transport of a high current beam, thus making design and beam commissioning of this machine challenging. The commissioning runs of 2021 and early 2022 were the first where the master timing system for the linac was fully available. As a consequence of that, the beam actuators and beam monitoring equipment relied fully on timing events sent across the machine, not only to be triggered to act but also to get the configuration. In this paper, we describe the timing system as available today, present how we define and create the beam pulses using the available parameters. We also present planned future upgrades and other outlook for the system.

INTRODUCTION

ESS is a collaboration of 17 European nations and its objective is to be the world's most powerful spallation neutron source [1]. The neutrons are produced by a 5 MW proton beam hitting a solid, rotating tungsten target at a distance of 600 m from the ion source. The ESS linac, the driver of the protons onto the target, requires site-wise synchronisation in order to accelerate the desired beam through its components. The production of the proton beam begins with the ion source providing the pulse of protons with an optimized current and of a given length [2]. Later, the two choppers (LEBT and MEBT) shape the pulse to the desired pulse length. The acceleration is given by the radio-frequency cavities pulsing at the correct moment. The overall repetition rate is a consequence of the definition of the arbitrary number of consecutive set of timing events (cycles), that are pre-loaded before the ion source starts producing the beam. Last but not least, the beam pulse current is primarily controlled by the IRIS settings, and does not belong to the timing system.

The combination of the three beam parameters, i.e. beam repetition rate, beam pulse length and beam current defines the envelope of the accelerator working point defined as a beam mode. At any time of the machine operation, the Fast Beam Interlock System (FBIS [3]) with Beam Current Monitors (BCMs) is supervising the compliance to the beam mode, i.e. asserting if the produced beam pulse belongs to the allowed parameter space. Pulse timing information distributed to the BCMs containing the planned beam pulse

position in the cycle has therefore also a machine protection purpose.

Figure 1 shows schematic of the ESS linac. The actuators are located within the beginning of the line (e.g. source and choppers), at the very end of the line (target raster magnets), and along the full linac (RF stations). The proton beam instrumentation devices, e.g. Beam Current Monitors (BCMs), Beam Position Monitors (BPMs), Faraday Cups (FCs) and Beam Loss Monitors (BLMs) are located along the line.

The ESS distributed control system is based on Experimental Physics and Industrial Control System (EPICS [4]). The full synchronisation is provided by a distributed timing system with its own network infrastructure, and it is operated within a *Beam Production* environment. The entire timing system is configured with the pre-created timing tables, that consists a definition of supercycles, namely sequenced definitions of what the RF/actuators and instrumentation do in the given cycle. This paper summarises the efforts put in the beam commissioning of the Normal Conducting Linac, i.e. from the ion source to the DTL1 FC.

TIMING SYSTEM

The main role of the ESS timing system is to generate, acquire and distribute RF ≈ 704.42 MHz based timing signals:

- Synchronous clock, mostly RF/8 = 88 MHz.
- Machine synchronous and asynchronous events.
- Trigger events as a derivative of timing events.
- Data bus (a.k.a. data buffer) with beam and machine parameters.
- Absolute time reference.
- Orchestrate EPICS record processing and acquisition.

In addition, those features are utilized for troubleshooting of different distributed subsystems. The timing hardware is based based on Micro Telecommunications Computing Architecture (MTCA [5]). The detailed concept was described in [6]. Figure 2 presents the timing system topology. The Timing Master (TM) is the main timing system gateway for the operation control while event receivers (EVRs) embedded within TDMS perform synthesis of the received information into the timing signals required by a particular subsystem.

Supercycle Engine

The ESS machine ticks in ≈ 71.43 ms cycles (≈ 14 Hz). The cycles can be added together making a meaningful supercycle, so a collection of cycles. The operation team defines each supercycle and a certain supercycle is played during different site acceptance tests, or site integration tests, or the ESS production operation. The ESS machine ticking is produced by the ESS in-house EPICS module called Supercycle

* arek.gorzawski@ess.eu

SIMULATION AND MEASUREMENTS OF THE FAST FARADAY CUPS AT GSI UNILAC

R. Singh^{*1}, S. Klapproth², P. Forck¹, T. Reichert¹, A. Reiter¹, G. Rodrigues³

¹GSI Helmholtz Center for Heavy Ion Research, Darmstadt, Germany

²Technische Hochschule Mittelhessen, Friedberg, Germany

³Inter University Accelerator Center, New Delhi, India

Abstract

The longitudinal charge profiles of the high intensity heavy ion beam accelerated at the GSI UNILAC up to 11.4 MeV/u can differ significantly in consecutive macropulses. Variations in bunch shape and mean energy were also observed within a single macro-pulse. In order to have an accurate and fast determination of bunch shape and its evolution within a macro-pulse, a study of fast Faraday Cup designs is underway at GSI. In this contribution, we present CST particle in cell (PIC) simulations of radially coupled co-axial Fast Faraday Cup (RCFFC) and conventional axially coupled FFC (ACFFC) design. The simulation results are compared to the measurements performed under comparable beam conditions primarily with RCFFCs. A rather large impact of secondary electron emission is observed in simulations and experiments. The biasing of the FFC central electrode as a mitigation mechanism on the measured profiles is discussed.

INTRODUCTION

Measurement of longitudinal beam parameters such as kinetic energy, the energy spread, and spread in particle time of arrival with respect to the RF is essential in linear accelerators (LINACs). Kinetic energy measurements are performed using the Time of Flight (ToF) between two or more phase probes (also referred as pick-ups/BPMs) and are routinely done at several locations along the UNILAC. The correlated distributions of beam energy spread and time of arrival with respect to RF phase or “phase spread” with respect to synchronous particle form an ellipse in longitudinal phase space. Typical strategy of determining full longitudinal phase space ellipse is by measuring one of the projection of longitudinal phase space under controlled longitudinal optics settings [1]. The problem of longitudinal emittance determination is thus reduced to precise measurement of the longitudinal charge distribution. The measurement of phase/time of arrival spread also referred to as “longitudinal charge distribution” or often just “bunch length” or “bunch shape” and is typically more accessible for direct measurements. Fast Faraday cups (FFCs) are variants of the regular Faraday cups optimized for measuring fast time varying charge distributions. In order to measure short bunch signals in ns regime, the FFC structures are carefully designed to match the signal termination impedance along with measures for suppression of field dilution and secondary electrons.

In this upcoming section, we will show the simulations of two FFC designs, a) in the first design, the beam is radially coupled into a coaxial cable via a blind hole [2] which is compared with a second design b) the traditional and commercially available axially coupled tapered co-axial cable design [3]. The simulation details and signals induced by beam in the FFC structure in presence of secondary electron emission are discussed. In the following section, measurements with ion beam performed with these FFCs are discussed.

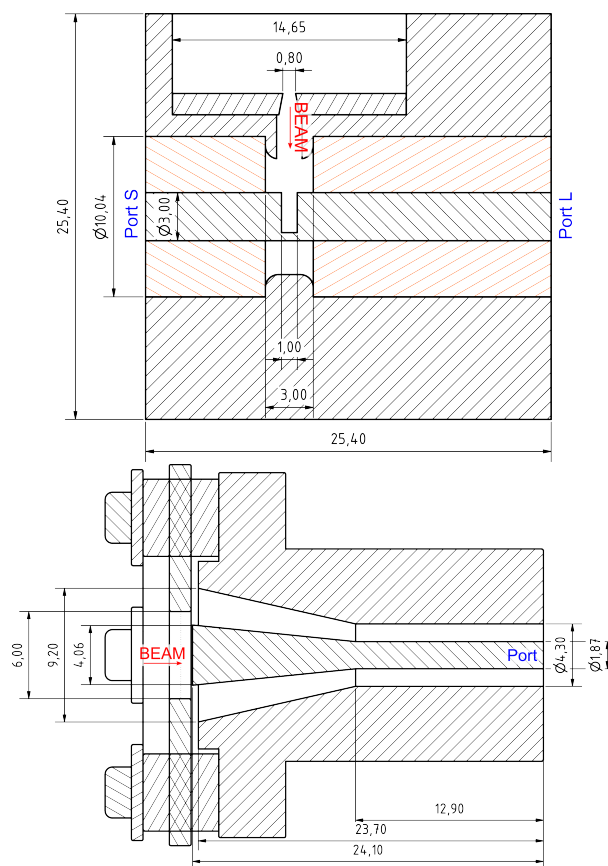


Figure 1: Schematic of the two co-axial FFCs investigated in this manuscript. (Top) Radially coupled FFC and (bottom) Axially coupled FFC. The beam incidence and port for signal coupling are indicated.

SIMULATIONS

Both FFC designs are shown in Fig. 1 which are simulated with the PIC solver of CST EM Studio and ion beam as input.

* r.singh@gsi.de

COHERENT DIFFRACTION RADIATION FOR LONGITUDINAL ELECTRON BEAM CHARACTERISTICS

R. Panaś*, NSRC SOLARIS, Kraków, Poland
A. Curcio, CLPU, Villamayor, Spain
K. Lasocha, Jagiellonian University, Kraków, Poland

Abstract

For the need of diagnostics of the longitudinal electron beam characteristics at the first Polish free electron laser (PoIFEL) project, a Coherent Diffraction Radiation (CDR) system is being developed and tested. It will allow for non-destructive bunch length measurement based on the power balance of CDR radiation collected by Schottky diodes in different ranges of (sub-)THz radiation. The first tests and measurements will be performed at the end of the SOLARIS synchrotron injector linac, where the beam has been already characterized and aligned. In this paper the theoretical background of the measurement, calculations and first experimental achievements will be presented.

COHERENT DIFFRACTION RADIATION

Electromagnetic radiation is emitted when a beam of charged particles accelerates or changes medium of propagation (abruptly or continuously in terms of the local electromagnetic susceptibility) [1, 2]. If the emitted wavelength is comparable or greater than the bunch length, the radiation is said "coherent" because the contributions from the single particles within the beam interfere constructively and the bunch emits as a whole. In that case the emitted radiation power is proportional to the square of the bunch form-factor and increases with decreasing bunch length. For bunch lengths on the picosecond scale variations in the peak current can be easily monitored by GHz-THz detectors like Schottky diodes [3, 4]. For shorter bunches far-infrared diagnostics are needed, for example spectrometers [5]. If the goal is to infer a relative information of the bunch compression, then a source of coherent radiation coupled to a power-detector can provide this information, since for a detected frequency which is high-enough the amount of detected power scales with the shortness of the emitting bunch. Coherent radiation can be coupled out of the beamlines through suitable transparent windows, eventually transported in air into power-detectors. For the diagnostic purposes of the PoIFEL project [6], Coherent Diffraction Radiation (CDR) will be exploited, which allows for non-destructive bunch length measurements. Diffraction radiation is the radiation that a bunch of particles emits when crossing two regions of limited size with different index of refraction [7]. This can be accomplished if the beam passes through a hollow disk of dense material. If the disk surface is metallic the radiation is emitted from localized layers of that surface, in such a way that the beam properties are imprinted into the

emitted radiation at the transition plane and can be exploited for diagnostics. The fact that the disk is hollow allows for the beam not to be scattered and the emittance be preserved (the field lines polarize the radiator even if the particles do not propagate inside it). The spectral angular distribution of energy emitted backward in the form of diffraction radiation from a perfectly conducting round disk, with an internal and external radius equal to respectively a and b , can be described with the following formula [8, 9]:

$$\frac{d^2I}{d\omega d\Omega} = |F(\omega)|^2 \times \frac{Q^2}{(4\pi^3\epsilon_0 c^5 \beta^4 \gamma^2)} \times \left| \int_a^b d\rho \rho K_1\left(\frac{\omega\rho}{\beta\gamma c}\right) J_1\left(\frac{\omega\rho}{c \sin\theta}\right) e^{\frac{j\omega^2\rho^2}{2c^2}} \right|^2, \quad (1)$$

where Q denotes the bunch charge, ϵ_0 is vacuum permittivity, c is the velocity of light, β is the ratio of particle velocity and the velocity of light and γ is the Lorentz factor. The quantity $F(\omega)$ is called *bunch form factor* and strictly depends on the shape of the electron bunch. An example of spectral-angular distribution of emitted CDR energy is shown in Fig. 1.

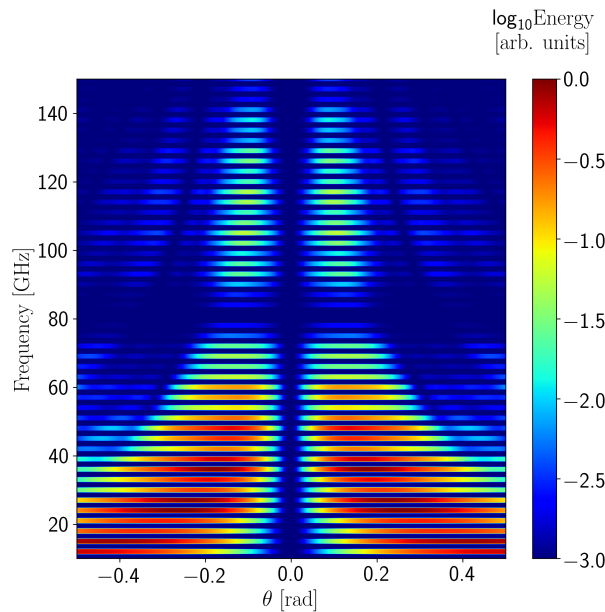


Figure 1: CDR spectral-angular distribution for the SOLARIS injector bunch repetition pattern and beam energy of 550 MeV. The radiator diameter has been set to 5 cm with 1 cm diameter hole for non-destructive diagnostics.

* roman.panas@uj.edu.pl

ZnO(In) SCINTILLATION LIGHT SPECTRA INVESTIGATION FOR HEAVY ION DETECTOR APPLICATION^{*†}

M. Saifulin^{1,‡}, P. Boutachkov, C. Trautmann¹, B. Walasek-Höhne

GSI Helmholtz Center for Heavy Ion Research, Darmstadt, Germany

P. Rodnyi, I. Venevtsev, Peter the Great Polytechnic University, St. Petersburg, Russia

E. Gorokhova, JSC S.I. Vavilov State Optical Institute, St. Petersburg, Russia

¹also at Technical University Darmstadt, Darmstadt, Germany

Abstract

ZnO-based ceramics are known as promising scintillators exhibiting light emission in the ultraviolet (UV) spectral region (~390 nm) and ultrafast decay times (<1 ns). They are of great interest for applications in scintillation counters and screens at high-energy heavy ion accelerators. In this contribution, the deterioration of scintillating properties of ZnO-based ceramics subjected to heavy ion exposure at high doses is investigated. The scintillation light spectra of ZnO(In) as a function of fluence for 4.8 MeV/u ⁴⁸Ca and ¹⁹⁷Au ions were studied. We observed that the deterioration of the scintillation intensity with increasing fluence follows the Birks-Black model.

INTRODUCTION

Zinc oxide is a multi-functional material with many applications due to its interesting properties [1, 2]. In particular, since the 1960s it has been known as a promising scintillation material that exhibits sub-nanosecond fast light emission at room temperature [3–5]. Previously, pure and doped ZnO has been produced in various forms (powder, thin films, single- and poly-crystals, and ceramics) with the purpose of detecting different types of ionizing radiation [6–9].

Recent studies and technological advances have made it possible to produce bulk pieces of indium- and gallium-doped zinc oxide ceramics (ZnO(In) and ZnO(Ga)) by uniaxial hot pressing in vacuum [10, 11]. These scintillating ceramics become highly interesting for heavy-ion radiation detection at accelerator facilities like GSI and the future FAIR facility in Darmstadt, Germany [12]. ZnO(In) and ZnO(Ga) scintillators are considered as promising candidates to substitute plastic scintillator BC400 commonly used for beam intensity monitoring and spill micro-structure characterization at SIS-18 synchrotron, where ion beams from proton to uranium with energies from 150 MeV/u to 4.5 GeV/u can be obtained.

As a part of a research and development project for a radiation-resistant fast scintillation detector, we report on the performance and in-situ characterization of ZnO(In) ceramics scintillation light spectra change as a function of ion fluence.

^{*} The results presented in this contribution are based on the work performed before the 24th of February, 2022.

[†] DLR funded this work within the ERA.Net RUS Plus Project RUS_ST2017-051.

[‡] m.saifulin@gsi.de (corresponding author)

ZnO(In) SCINTILLATION SPECTRA

The investigated ZnO(In) ceramic samples were produced in the form of 8 mm × 8 mm × 0.4 mm size plates at the Joint Stock Company “Research and Production Corporation S.I. Vavilova” (St. Petersburg, Russia). The samples were produced with 0.046 at % In³⁺ doping concentration. Samples density estimated from mass and volume measurements was 4.66 g/cm².

In-situ characterization of scintillation light spectra was performed using 4.8 MeV/u energy ⁴⁸Ca and ¹⁹⁷Au ions from UNiversal Linear ACcelerator (UNILAC) of the GSI Helmholtz Center for Heavy Ion Research GmbH (Darmstadt, Germany) [13]. The irradiations were carried out at room temperature in vacuum at a beam incidence angle of 45° with respect to the sample surface.

Scintillation light was collected with a lens placed in front of the ion-incident surface of the sample. The collected light was transferred via a light guide to an Ocean Optics QE-Pro spectrometer. The acquired spectra were corrected for dark counts and normalized by the number of ions that hit the sample during the spectrum acquisition.

Figure 1 shows how the scintillation light spectrum of ZnO(In) ceramic sample changes as a result of 4.8 MeV/u ⁴⁸Ca ion irradiation. The spectra have only one emission

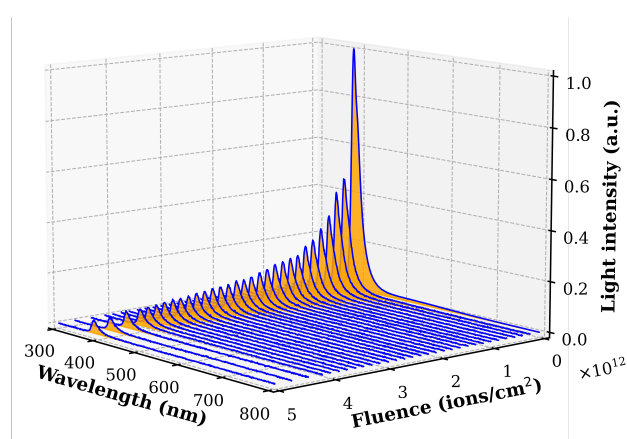


Figure 1: Spectra of ZnO(In) ceramic as a function of 4.8 MeV/u ⁴⁸Ca ion fluence.

band in the ultraviolet (UV) light region with a maximum at around 387 nm. The observed peak corresponds to the near-band-edge emission (NBE) known for scintillation decay times less than nanosecond. With increasing fluence, the

BEAM INTENSITY MEASUREMENT IN ELENA USING RING PICK-UPS

O. Marquversen[†], D. Alves, CERN, Geneva, Switzerland

Abstract

A bunched beam intensity measurement system for the CERN Extra Low ENergy Antiproton (ELENA) ring, using a cylindrical shoe-box electrostatic pick-up from the existing orbit system, is presented. The system has been developed to measure very challenging beam currents, as low as 200 nA corresponding to intensities of the order of 10^7 antiprotons circulating with a relativistic beta of the order of 10^{-2} .

In this work we derive and show that the turn-by-turn beam intensity is proportional to the baseline of the sum signal and that, despite the AC-coupling of the system, the installed front-end electronics, based on a charge amplifier, not only guarantees the preservation of the bunch shape (up to a few tens of MHz), but also allows for an absolute calibration of the system. In addition, the linearity of the intensity measurements and their independence with respect to average beam position is evaluated using a standard electromagnetic simulation tool. Finally, experimental measurements throughout typical antiproton deceleration cycles are presented and their accuracy and precision are discussed.

THE MEASUREMENT SYSTEM

This newly developed intensity measurement system is an add-on to the Extra Low ENergy Antiproton (ELENA) ring orbit system [1], using the already available sum signal from one ring Pick-Up (PU). In terms of hardware, the add-on consists of an Analog to Digital Converter (ADC) mounted on a PCIExpress bus [2] integrated in a front-end computer installed in the CERN control system, in order to digitise the PU sum signal.

ELECTROSTATIC PICK-UP AS A CHARGE MONITOR

As an alternative, or a complement, to the standard beam current transformers, an electrostatic orbit PU can be used to measure the intensity of bunched beams, either in a beam line or in a ring.

The Charge Found from the Output Voltage

The beam intensity can be found from the integrated output voltage from an electrostatic PU:

The charge Q , induced in the inner surface of a cylindrical PU is given by

$$Q = Q_b = \rho V \quad (1)$$

where ρ is the beam charge density [charge/m³], V is the volume enclosed by the PU and Q_b is the portion of the beam charge contained in this volume.

The current density, J is given by

$$J = \frac{i}{A} = \rho \beta c \quad (2)$$

where i is the beam current, A its transverse area and βc its speed. Combining Eq. (1) and Eq. (2) we get

$$Q = \frac{i}{\beta c A} V = \frac{L}{\beta c} i \quad (3)$$

where L is the length of the PU.

The current i_z , drawn from the PU (as shown in Fig. 1), can be written as

$$i_z = \frac{dQ_b}{dt} = \frac{1}{\beta c} \cdot L \cdot \frac{di_b}{dt} \quad (4)$$

This current is split in two in the load impedance, Z , which is assumed to consist of a resistor, R , in parallel with a capacitor, C_L . C_L is in parallel with the pick-up capacitance, C_{pu} , and can be combined into a single capacitance, C , thus including both the PU and the load.

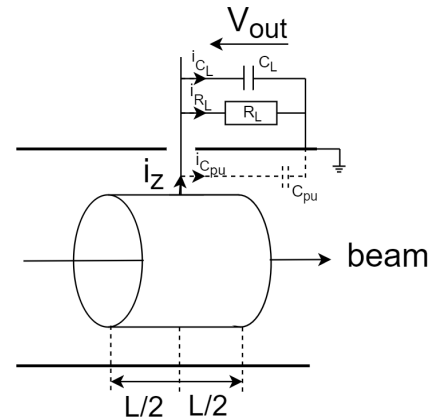


Figure 1: A circular electrostatic pick-up.

Ohm's law is used to get the voltage on the output, V_{out} :

$$i_z = i_R + i_C \quad (5)$$

where:

$$i_R = \frac{V_{out}}{R} \quad \text{and} \quad i_C = \frac{dQ_C}{dt} = C \frac{dV_{out}}{dt} = RC \frac{di_R}{dt}$$

The transfer function can be calculated by combining Eqs. (4) and (5) and differentiating assuming sinusoidal inputs to obtain:

$$\frac{i_R}{i_b} = \frac{L}{\beta c} \cdot \frac{j\omega}{1+j\omega RC} \quad (6)$$

The V_{out} on the load is found by multiplying the current, i_R , with the resistance, R (Ohm's law):

$$V_{out} = R \cdot i_R = \frac{L}{\beta c} \cdot \frac{j\omega RC}{1+j\omega RC} \cdot i_b \quad (7)$$

Equation (7) is a standard first order high pass transfer function.

A bunched beam in a circular accelerator will have a periodic spectrum consisting of all harmonics (H) of the revolution frequency, where the amplitude ratio between harmonics will be dependent upon bunch shape as indicated in Fig. 2.

[†] ole.marquversen@cern.ch

THE CRYOGENIC CURRENT COMPARATOR AT CRYRING@ESR*

L. Crescimbeni[†], D. M. Haider[†], A. Reiter, M. Schwickert, T. Sieber
GSI Helmholtz Centre for Heavy Ion Research, Darmstadt, Germany
H. De Gersem, N. Marsic, W. F. O. Mueller, TU Darmstadt, Darmstadt, Germany
M. Schmelz, R. Stolz, V. Zakosarenko³, Leibniz IPHT, Jena, Germany
F. Schmidl, Friedrich-Schiller-University Jena, Jena, Germany
T. Stoehlker^{1,2}, V. Tympel, Helmholtz Institute Jena, Jena, Germany
¹also at GSI Helmholtz Centre for Heavy Ion Research, Darmstadt, Germany
²also at Institute for Optics and Quantum Electronics, Jena, Germany
³also at Supracon AG, Jena, Germany

Abstract

The Cryogenic Current Comparator (CCC) at the heavy-ion storage ring CRYRING@ESR at GSI provides a calibrated non-destructive measurement of beam current with a resolution of 10 nA or better. With traditional diagnostics in storage rings or transfer lines a non-interceptive absolute intensity measurement of weak ion beams ($< 1 \mu\text{A}$) is already challenging for bunched beams and virtually impossible for coasting beams. Therefore, at these currents the CCC is the only diagnostics instrumentation that gives reliable values for the beam intensity independently of the measured ion species and without the need for tedious calibration procedures. Herein, after a brief review of the diagnostic setup, an overview of the CCC operation with different stored ion beams at CRYRING is presented. The current reading of the CCC is compared to the intensity signal of various standard instrumentations including a Parametric Current Transformer (PCT), an Ionization Profile Monitor (IPM) and the Beam Position Monitors (BPMs). It could be shown that the CCC is a reliable instrument to monitor changes of the beam current in the range of nA.

INTRODUCTION

The non-destructive and absolute monitoring of ion beams with an intensity in the order of nA plays an essential role in accelerator facilities that produce slowly extracted ions for nuclear physics research or rare isotopes and antiprotons in storage rings. In general, for coasting beams standard diagnostic systems are not able to provide measurements in the range of nA without major efforts. Even then, the instruments that can provide some information in this range have problems to deliver the high precision and reliability that is required (e.g. Schottky [1]), or are destructive, at least partially, reducing severely the possibility of using them as monitoring devices in storage rings (e.g. Faraday Cups and Secondary Electron Monitors) or are limited to bunched beams (BPM, Integrating Current Transformer).

The Cryogenic Current Comparator (Fig.1) is a superconductive device that can measure currents in the order of nA detecting the magnetic field of the beam itself. The CCC uses a DC Superconducting Quantum Interference Device (SQUID) as a highly sensitive magnetometer, shielded from external magnetic fields thanks to an elaborate superconductive magnetic shielding, to provide absolute high-precision measurement of low-intensity currents while being non-destructive and easy to calibrate.

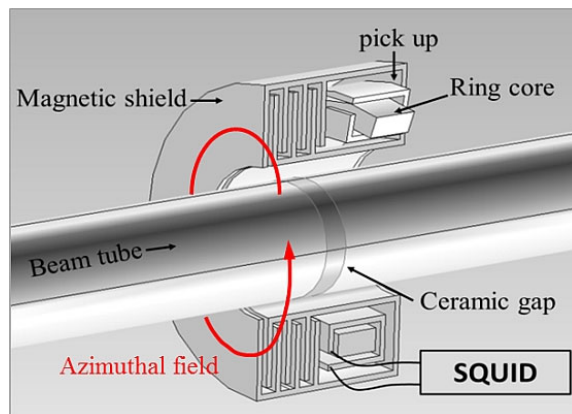


Figure 1: Schematic view of the CCC.

Five CCCs are planned to be installed in the FAIR facility and, in preparation, a prototype was installed in the heavy-ion storage ring CRYRING@ESR at GSI to be tested with beam. The prototype is based on the FAIR-Nb-CCC-XD [2] that is part of the family of CCC-XD that has been developed for the use with large beam-lines diameters (e.g. at Antiproton Decelerator at CERN [3]) and that was adapted to the beamline dimensions at FAIR ($\varnothing 150 \text{ mm}$). At CRYRING, the CCC was operated with several different ion species (D^+ , O^{6+} , Nb^{78+} , Pb^{78+} , U^{91+}) and various beam conditions (e.g. coasting/bunched) with beam intensities between 5 nA and 20 μA to demonstrate the detector performance that can be expected for FAIR.

COMMISSIONING IN CRYRING

The CCC detector is allocated in a newly manufactured beamline cryostat developed in collaboration with ILK Dresden[§] to fulfil the needs of the installation at FAIR [4]. The SQUID sensor of the CCC is a highly sensitive magnetometer and is susceptible to external perturbations.

*Work supported by AVA – Accelerators Validating Antimatter the EU H2020 Marie-Curie Action No. 721559 and by the BMBF under contract No 05P21SJRB1.

[†]l.crescimbeni@gsi.de, d.haider@gsi.de

[§]ILK Dresden gGmbH, Dresden, Germany

[¶]Model PT415 from Cryomech Inc, Syracuse, NY, USA

DIFFERENTIAL CURRENT TRANSFORMER FOR BEAM CHARGE MONITORING IN NOISY ENVIRONMENTS

H. Maesaka^{†, 1}, T. Inagaki¹, RIKEN SPring-8 Center, Sayo, Hyogo, Japan
K. Yanagida, H. Dewa, JASRI, Sayo, Hyogo, Japan
K. Ueshima, QST, Sendai, Miyagi, Japan
¹also at JASRI, Sayo, Hyogo, Japan

Abstract

We designed and produced a new differential current transformer (CT) for electron beam current and charge measurement in noisy environments, such as near a high-power pulse generator. This differential CT has four pickup wires coiled at equal intervals (90 degrees) on a toroidal core. Each coil has two turns and the midpoint of the coil is connected to the body ground so that a balanced differential signal is generated. A beam pipe with a ceramics insulation gap is inserted into the toroidal core to obtain a signal from a charged-particle beam. The four balanced differential signals are transmitted through a Category-6 twisted pair cable and fed into an amplifier unit. The four signals are then summed by the amplifier and digitized by an MTCA.4 high-speed AD converter. We produced differential CTs and installed them into the new injector linac of NewSUBARU. Before the installation, we confirmed basic performances such as the beam current sensitivity of 1.24 V/A, wide frequency response of up to 100 MHz, etc. The beam test was performed at the new linac of NewSUBARU and beam charge measurement performance, common-mode noise cancellation, etc. were evaluated. The differential CTs have been utilized for stable beam charge monitoring in the NewSUBARU linac.

INTRODUCTION

Reliable monitoring of the charge and current of a particle beam is important for most particle accelerators. A current transformer (CT) is often used as a non-invasive beam charge and current monitor. The signal output of a CT is usually designed as a single-ended coaxial line. If a single-ended CT is located near a pulsed high-power component, a common-mode noise can be overlapped with a beam signal and the noise can deteriorate the measurement accuracy.

To mitigate the noise from the high-power component, a differential CT was proposed and utilized in the X-ray free-electron laser, SACLA [1, 2]. This differential CT has four single-turn coils around a toroidal magnetic core, where two coils generate positive signals and the other two generate negative signals. A common-mode noise can be canceled out by subtracting the positive and negative signals. Since each signal output is a single-ended coaxial line, however, a preamplifier or a balun near the differential CT is required to transform two differential single-ended signals into a balanced differential line for long signal transmission.

A new 3 GeV light source project, NanoTerasu [3, 4], was proposed and it is now being constructed in Sendai, Japan. Before the construction of NanoTerasu, a new injector linac for the NewSUBARU storage ring [5] was constructed as a prototype of the NanoTerasu linac [6]. One of the most important design concepts of these accelerators was low-cost and easy maintainability. A differential CT should also be low-cost and the number of components in the system should be as small as possible. Therefore, we designed a new differential CT that did not need a preamplifier near the CT.

DESIGN

A new differential CT aims to extract a balanced differential signal directly from a coil. Therefore, we designed a CT having two-turn pickup coils wound on a toroidal magnetic core and the midpoint of each coil is grounded. A schematic view of the new differential CT is shown in Fig. 1. Four pickup coils are attached to a toroidal core at equal intervals (90 degrees) and a beam pipe with a ceramics gap is inserted into the core. The toroidal core is Fine-met FT-3KM F7555G supplied from Hitachi Metals, which has enough permeability as high frequency as 1 GHz. An 11 Ω resistor is attached to each coil in parallel to attenuate a beam signal. The signals from pickup coils are extracted from four LEMO 0S302 series 2-pin connectors. A photograph of the differential CT is shown in Fig. 2. The four balanced differential signals are transmitted to a readout electronics by a Category-6 (CAT6) S/FTP cable for Ethernet, which has good high-speed signal transmission characteristics and a reasonable price.

The beam current sensitivity of each turn of the pickup coil is 0.125 A/A since the number of total turns is 8. The voltage sensitivity of the output to the beam would be 12.5 V/A without any parallel resistors since the characteristic impedance of the balanced differential line is 100 Ω . Since the sensitivity of around 1 V/A is easy to deal with for us, an 11 Ω metal-film resistor (± 0.1 % accuracy) is inserted in parallel with the pickup coil to attenuate the signal amplitude. The sensitivity is reduced by a factor of 0.099 and the current and voltage sensitivity are finally decreased to 0.0124 A/A and 1.24 V/A, respectively, which corresponds to -35 dB relative to the beam current.

The readout electronics consists of an amplifier unit and a high-speed digitizer. The block diagram of the amplifier unit is shown in Fig. 3. The S/FTP cable from a differential CT is received by an M12 X-coded connector, which is more reliable than an RJ-45 modular connector. Common-

[†] maesaka@spring8.or.jp

LHC SCHOTTKY SPECTRUM FROM MACRO-PARTICLE SIMULATIONS

C. Lannoy^{1,*}, D. Alves, N. Mounet, CERN, Geneva, Switzerland
 K. Lasocha, Institute of Physics, Jagiellonian University, Kraków, Poland
 T. Pieloni, EPFL, Lausanne, Switzerland
¹also at EPFL, Lausanne, Switzerland

Abstract

We introduce a method for building Schottky spectra from macro-particle simulations performed with the PyHEADTAIL code, applied to LHC beam conditions. In this case, the use of a standard Fast Fourier Transform (FFT) algorithm to recover the spectral content of the beam becomes computationally intractable memory-wise, because of the relatively short bunch length compared to the large revolution period. This would imply having to handle an extremely large amount of data for performing the FFT. To circumvent this difficulty, a semi-analytical method was developed to compute efficiently the Fourier transform. The spectral content of the beam is calculated on the fly along with the macro-particle simulation and stored in a compact manner, independently from the number of particles, thus allowing the processing of one million macro-particles in the LHC, over 10 000 revolutions, in a few hours, on a regular computer. The simulated Schottky spectrum is then compared against theoretical formulas and measurements of Schottky signals previously obtained with lead ion beams in the LHC.

INTRODUCTION

Schottky signals contain information on various beam and machine parameters, such as momentum spread, betatron tune, synchrotron frequency and chromaticity, among others. The basic theory of Schottky signals predicts how all of these parameters express themselves in the recorded signal, after it is transformed to the frequency domain. This topic is treated in detail in a classical work by Boussard [1]. The developed theory is however limited only to the simplified beam dynamics and does not include, e.g., collective effects and beam interaction with the vacuum chamber through impedance. Due to the complex theoretical description of such effects, it is most suitable to study their impact on Schottky spectra using multi-particle simulations, as done in [2], where the effect of space charge was investigated.

Obtaining a Schottky spectrum from multi-particle simulations in the case of the CERN Large Hadron Collider (LHC), is particularly challenging computationally due to the highly sparse characteristic of the current signal produced by a single bunch. While discretising the current signal in time, and applying the FFT algorithm to retrieve the spectral content of the beam is manageable for smaller accelerators, typically having smaller revolution periods and longer bunches, like the CERN Proton Synchrotron (PS), this is unfortunately intractable memory-wise for the LHC. As a conservative estimate, for the LHC revolution frequency

$f_0 \approx 11245.5$ Hz, if we sample a 1 ns long bunch with 100 points (which corresponds to a sampling frequency of 100 GHz) over 10 000 turns, we would have to store an array of $10^{11+4}/f_0 \sim 10^{11}$ signal samples¹ or around 1 TB of data, hence the need of an alternative approach.

The study presented herein is based on simulations performed with PyHEADTAIL [3, 4], a macro-particle code that can be used to track turn-by-turn the six-dimensional phase space evolution of a bunch, possibly including the effects of direct space charge and beam-coupling impedances (although this capability is not yet used for this study). The following section will present the method used to post-process the data from PyHEADTAIL and reconstruct the Schottky spectra, while the third section will compare the simulation results against theoretical formalisms and measurements from LHC ion beams.

METHOD

To simulate Schottky spectra one generates a set of macro-particles following an initial phase-space distribution, and then tracks turn-by-turn the macro-particles using the machine optics. The Schottky spectra are computed using an analytical Fourier transform, performed turn-by-turn at the same time as the tracking.

Longitudinal and Transverse Phase Space

An accurate description of the longitudinal phase space is necessary since the average Schottky spectrum explicitly depends on the distribution of synchrotron oscillation amplitudes [1]. For LHC lead ion bunches, the synchrotron oscillation amplitudes $\hat{\tau}$ approximately follow a Rice distribution [5]. The amplitude of the momentum deviation $\widehat{\Delta p}$ can be deduced from $\hat{\tau}$ by substituting Eq. (4) in Eq. (11) from [6], which yields

$$\widehat{\Delta p} = \frac{p_0}{|\eta|} \hat{\tau} \left(1 - \frac{(h_{rf} \omega_0 \hat{\tau})^2}{16} \right) \Omega_0,$$

with p_0 the reference momentum, η the slippage factor, Ω_0 the nominal angular synchrotron frequency², h_{rf} the radio frequency harmonic and ω_0 the angular revolution frequency of the LHC. The initial position with respect to the synchronous particle z and momentum deviation Δp of each

¹ Most of these will be zeros and while Sparse Fourier Transform algorithms exist, these are only applicable to sparse output signals.

² By nominal synchrotron frequency we mean the synchrotron frequency of the synchronous particle, for which the synchrotron amplitude vanishes.

* christophe.lannoy@cern.ch

FIRST RF PHASE SCANS AT THE EUROPEAN SPALLATION SOURCE

Y. Levinsen*, M. Akhyani, R. Baron, E. Donegani, M. Eshraqi, A. Garcia Sosa,
H. Hassanzadegan, B. Jones, N. Milas, R. Miyamoto, D. Noll, I. Vojtkovic, R. Zeng
European Spallation Source, Lund, Sweden
F. Grespan, INFN, Italy
I. Bustinduy, ESS-Bilbao, Bilbao, Spain

Abstract

The installation and commissioning of the European Spallation Source is currently underway at full speed, with the goal to be ready for first neutron production by end of 2024. This year we accelerated protons through the first DTL tank. This included the RFQ, 3 buncher cavities in the medium energy beam transport as well as the DTL tank itself as RF elements. At the end of the DTL tank we had a Faraday cup acting as the effective beam stop. This marks the first commissioning when RF matching is required for beam transport. In this paper we discuss the phase scan measurements and analysis of the buncher cavities and the first DTL tank.

INTRODUCTION

The European Spallation Source (ESS) is designed as the world brightest neutron source, driven by a 5 MW proton beam that is accelerated to 2 GeV. The proton linac driver consists of a normal conducting (NC) front end that brings the beam energy to around 90 MeV, followed by a superconducting (SC) section and finally a beam transport to the rotating tungsten target wheel. The linac features a very long beam pulse length of 2.86 ms, with a 14 Hz repetition rate. The NC radiofrequency (RF) and hence beam bunch frequency is at 352.21 MHz. The two last SC families operate at twice that frequency, 704.42 MHz.

The first beam commissioning of the ESS linac commenced in 2018-19, including the ion source (IS) and the low energy beam transport (LEBT) [1, 2]. The second stage of commissioning started in the fall of 2021, included the radio-frequency quadrupole (RFQ) and the medium energy beam transport (MEBT). This run continued with some minor interruptions until the next step which sent beam through the first drift tube linac (DTL) tank, starting at the end of May 2022 and continuing until mid July. For this stage the buncher cavities in the MEBT were also made available, which marked the first time beam-based RF matching was possible and necessary.

In this paper we will discuss the initial experience in matching the RF phase and amplitude using the phase scan technique primarily for the buncher cavities and also for the first DTL tank. A more general overview of the MEBT characterisation is presented in [3]. Prerequisites for this work is also to have good diagnostics [4], and a well functioning timing system [5]. For the bunchers, the primary signal to look at is the beam position monitor (BPM) phase response. For the DTL we have transmission scans as well as the response signals of the internal BPMs in the tank.

* yngve.levinsen@ess.eu

SIMULATIONS

Our primary simulation software is TraceWin [6], as well as OpenXAL [7] meant primarily for online modelling though usable for any simulation where an envelope model is sufficient. That essentially translates to effects where a linear space charge model is sufficient. In both cases, each gap in the bunchers and DTL is modeled as a drift-kick-drift.

RF phase scans are performed by modulating the amplitude and phase of an RF element, and monitoring the Time of Flight (ToF) of the beam downstream of the element. In general the absolute value of the ToF is not known, so most commonly one then instead looks at the change in BPM phase signal(-s) and compares with model expectation.

For modelling RF cavities one often refers to the transit time factor (TTF), which follows

$$T = \frac{1}{\int E_z dz} \left[\int E_z \cos \omega t dz - \tan \phi \int E_z \sin \omega t dz \right]. \quad (1)$$

Here E_z is the longitudinal on-axis field amplitude that generally depend on z , and ω is the RF frequency. V_0 is the integrated field amplitude E_z . ϕ is the relative phase arrival of the particle. The time t is a function of z through the speed of the particle. Through the TTF we can then get the simple formula for the the net energy gain traversing the cavity, which becomes

$$\Delta W = qV_0 T \cos \phi, \quad (2)$$

where q is the charge of the particle, and V_0 is the integrated field (denominator of (1)). For $\phi = 0$ we then have what we call “on crest” acceleration, which gives the maximum energy gain, but then with no longitudinal focusing. In fact there is even defocusing on half of the bunch, since particles arriving early (or late) and would need a higher energy kick to “catch up” instead get a lower energy kick falling further behind the synchronous particle.

Buncher cavities run at $\phi = -90^\circ$, which provides no acceleration but maximum longitudinal focusing. These are rather simple cavities generally speaking, providing sine-like signatures in phase space downstream that are relatively easy to analyse (differing for example from DTL signatures). As we can understand from Eq. (1), even if the net energy gain is zero, the transit time still depends on the amplitude of the cavity. This can be understood from the fact that the cavity has a finite size and the particle is travelling slower than the speed of light. If $\phi = -90^\circ$, the particle arrives at the entrance of the cavity early and experience a slight deceleration. In the middle of the cavity there is no acceleration, while in the second half there is a comparatively positive acceleration

BEAM CHARACTERIZATION OF SLOW EXTRACTION MEASUREMENT AT GSI-SIS18 FOR TRANSVERSE EMITTANCE EXCHANGE EXPERIMENTS

J. Yang^{1,*}, P. Boutachkov, P. Forck, T. Milosic, R. Singh, S. Sorge
GSI Helmholtzzentrum für Schwerionenforschung GmbH, Darmstadt, Germany
¹also at Goethe Universität, Frankfurt am Main, Germany

Abstract

The quality of slowly, typically several seconds, extracted beams from the GSI synchrotron SIS18 is characterized with respect to the temporal spill stability, the so-called spill micro structure on the 100 μ s scale. A pilot experiment was performed utilizing transverse emittance exchange to reduce the beam size in the extraction plane, and the improvement of spill micro structure was found. Important beam instrumentation comprises an Ionization Profile Monitor for beam profile measurement inside the synchrotron and a plastic scintillator at the external transfer line for ion counting with up to several 10^6 particles per second and 20 μ s time slices. The performant data acquisition systems, including a scaler and a fast Time-to-Digital Converter (TDC), allow for determining the spill quality. The application of the TDC in the measurements and related MAD-X simulations are discussed.

INTRODUCTION

Temporary beam stability within 100 μ s of the slowly extracted beam from the GSI SIS18 synchrotron is crucial for fixed-target experiments. Beam instrumentation plays an essential role in the slow extraction investigation into searching for better methods that could mitigate the spill micro structure.

SIS18 has a circumference of 216.72 m and a beam rigidity of up to 18 Tm. Tune-swept slow extraction is regularly performed. The third-order resonance excited by the sextupolar field is fed by increasing the strength of two fast quadrupoles. The extracted beam, referred to as a spill, has a temporal variation on time scales of micro-to-milliseconds, which is also called spill micro structure [1]. The reason is related to the power supply ripples which act on the quadrupole magnet, leading to the unintended variation of the machine tune [2]. The spill micro structures are mitigated if the machine tune during the extraction is set closer to the resonance tune, which results in a larger spread of the transit times [3]. That can be achieved not only by proper lattice settings, e.g. lower sextupole strengths but also by reducing the beam size (emittance) in the extraction plane. The latter is applied for this study. Since the beam is injected into the synchrotron by horizontal multi-turn injection, the horizontal emittance is significantly larger than the vertical emittance. One of the possible techniques to get a smaller beam is to benefit from the transverse emittance exchange effect to re-

duce the beam size at the extraction plane under a suitable emittance exchange condition [4]. The emittance exchange effect has already been successfully observed at SIS18 due to residual skew quadrupole components, described in [5]. It was executed by utilizing linear horizontal-vertical betatron coupling while the horizontal tune Q_x crosses the coupling resonance in a short time. The resonance in SIS18 is defined by $Q_x = Q_y + 1$. Tune-swept slow extraction measurement with transverse emittance exchange was performed using a $E = 300$ MeV/u Ar¹⁸⁺ coasting beam [6]. By performing emittance exchange, beam size at the extraction plane was reduced, and the improvement of the spill micro structure was found.

Essential beam instrumentation was used for different purposes in the slow extraction experiment utilizing emittance exchange: firstly, an Ionization Profile Monitor (IPM) [7] was used for the observation and measurement of the beam profiles during the transverse emittance exchange; secondly, a plastic scintillator [8] was used for particle counting while performing slow extraction; moreover, data acquisition systems were used to characterize the spill signals, including a scaler [9] and a fast Time-to-Digital Converter (TDC) [10].

This contribution will present the application example of the above-mentioned beam instrumentation used in the recent slow extraction investigation utilizing transverse emittance exchange. The experiment results concerning spill characterization and related simulations are discussed in detail.

MEASUREMENTS

Beam Profile

The online observation of the transverse emittance exchange effect is essential in the investigation and ensures the beam size condition for the following slow extraction.

During the emittance exchange process, tune crossing was executed by moving the horizontal tune from 4.17 to 4.2995 within 40 ms; meanwhile, the vertical tune was kept constant at 3.24. The resultant horizontal emittance reduction and vertical emittance increase were observed by the IPM [7], which is installed inside the SIS18 synchrotron ring for beam profile measurement. The profile readout period of the IPM is 10 ms. The signals from the detector within 50 μ s were integrated and formed one profile data. By calculating the widths of beam profiles, beam size evolution along with the time in one acceleration cycle was obtained. The emittance exchange effect was evidently demonstrated in Fig. 1. It

* Jia.Yang@gsi.de

DEEP NEURAL NETWORK FOR BEAM PROFILE CLASSIFICATION IN SYNCHROTRON

Michał Piekarski*,¹, NSRC SOLARIS, Jagiellonian University,
¹also at AGH University of Science and Technology, Kraków, Poland

Abstract

The main goal of National Synchrotron Radiation Centre (NSRC) Solaris is to provide scientific community with high quality synchrotron light. To achieve this, it is necessary to constantly monitor many subsystems responsible for beam stability and to analyze data about the beam itself from various diagnostic beamlines. In this work a deep neural network for transverse beam profile classification is proposed. Main task of the system is to automatically assess and classify transverse beam profiles based solely on the evaluation of the beam image from the Pinhole diagnostic beamline at Solaris. At the present stage, a binary assignment of each profile is performed: stable beam operation or unstable beam operation / no beam. Base model architecture consists of a pre-trained convolutional neural network (CNN) followed by a densely-connected classifier and the system reaches accuracy at the level of 94.10%. The model and the results obtained so far are discussed, along with plans for future development.

INTRODUCTION

Solaris is a third generation light source (shown in Fig. 1) operating at the Jagiellonian University in Kraków, Poland [1]. This advanced and complex scientific infrastructure offers new highly innovative research opportunities for areas including physics, medicine and nanotechnology. Currently at Solaris five experimental beamlines offering various techniques, e.g.: photoemission electron microscopy, X-ray absorption spectroscopy, ultra angle-resolved photoemission spectroscopy or multi-scale X-ray and multimodal imaging, are available to the scientific community whereas another three are already at advanced level of construction and commissioning. Moreover, Solaris is also a National Cryo-EM Centre, with two latest generation cryo-electron microscopes enabling life science researchers to unravel life at the molecular level [2].

Synchrotron control system is large, distributed and controls hundreds of devices and reads measurement and diagnostic data out of thousands. Moreover, due to a complexity of physical phenomena that occurs during the operation i.e. electron injection, beam tuning and beam decay, it is often difficult to quickly determine the reason of beam instabilities or its lost. Manual inspection performed even by an experienced operator is not able to extract full information from hundreds of diagnostic signals, which carry a lot of important information about the state of the machine. The purpose of this work is to present a system that could help operators in detecting potential threats and, in the future,



Figure 1: NSRC Solaris [3].

to serve as a tool for predicting anomalies, beam loss or equipment failure.

The use of artificial intelligence (AI) techniques, including machine learning and neural networks, for signal analysis, prediction or anomaly detection has a long history. As the accelerators serve as an interesting research area also here we observe a huge interest in the anomaly detection area where new methods are developed, validated and deployed to solve existing problems regarding the operation of synchrotron radiation systems. Classic neural networks or machine learning frameworks take advantage of archived data of beam position in the storage ring in order to determine the appropriate orbit correction to minimize the proposed cost function [4, 5]. The problem of anomaly detection and failure prediction in the accelerator control systems has also been discussed during the ICALEPCS or IBIC conferences and different approaches has been proposed [6, 7]. Finally, various applications of artificial intelligence based systems has been identified in the fields like beam stabilization, autonomous operation, optimisation and performance improvements [8–10]. Since there is such a high demand on a precise and reliable AI-based systems I propose a deep neural network (DNN) for transverse beam profile classification as a support tool for operators.

BEAM PROFILE CLASSIFICATION SYSTEM

In this section a transverse beam profile classification model based on deep, convolutional neural network is presented. Main idea behind it is to use Pinhole diagnostic beamline beam profiles and employ transfer learning methods to build suited classifier on top of the pre-trained architecture.

* michal.piekarski@uj.edu.pl, piekarski@agh.edu.pl

NEURAL NETWORK INVERSE MODELS FOR IMPLICIT OPTICS TUNING IN THE AGS TO RHIC TRANSFER LINE

J. P. Edelen, N. M. Cook, J. Einstein-Curtis, RadiaSoft LLC, Boulder, CO, USA
 K. A. Brown, V. Schoefer, BNL, Upton, NY, USA

Abstract

One of the fundamental challenges of using machine-learning-based inverse models for optics tuning in accelerators, particularly transfer lines, is the degenerate nature of the magnet settings and beam envelope functions. Moreover, it is challenging, if not impossible, to train a neural network to compute correct quadrupole settings from a given set of measurements due to the limited number of diagnostics available in operational beamlines. However, models that relate BPM readings to corrector settings are more forgiving, and have seen significant success as a benchmark for machine learning inverse models. We recently demonstrated that when comparing predicted corrector settings to actual corrector settings from a BPM inverse model, the model error can be related to errors in quadrupole settings. In this paper, we expand on that effort by incorporating inverse model errors as an optimization tool to correct for optics errors in a beamline. We present a toy model using a FODO lattice and then demonstrate the use of this technique for optics corrections in the AGS to RHIC transfer line at BNL.

INTRODUCTION

Machine learning (ML) has seen a significant growth in its adoption for widespread applications. In particle accelerators, ML has been identified as having the potential for significant impact on modeling, operation, and controls [1, 2]. These techniques are attractive due to their ability to model nonlinear behavior, interpolate on complicated surfaces, and adapt to system changes over time. This has led to a number of dedicated efforts to apply ML, and early efforts have shown promise.

For example, neural networks (NNs) have been used as surrogates for traditional accelerator diagnostics to generate non-interceptive predictions of beam parameters [3, 4] or for a range of machine tuning problems utilizing inverse models [5]. When used in conjunction with optimization algorithms, neural networks have demonstrated improved switching times between operational configurations [6]. Neural network surrogate models have also been demonstrated to significantly speed up multi-objective optimization of accelerators [7]. Additionally, ML has been of interest for anomaly detection for root cause analysis [8] and for outlier detection, using large data-sets of known good operational states [9], using autoencoders.

In this work we seek to apply ML methods — for both tuning and anomaly detection — on the AGS to RHIC transfer line at Brookhaven National Laboratory. Specifically, we employ the use of inverse models for these applications. The application of inverse models for anomaly detection

is a burgeoning area of research in many other fields that has not seen much attention in particle accelerators. Here we present our work towards implementing inverse models to detect errors in quadrupoles using only beam position monitors and corrector data. We will demonstrate the utility of this approach using a toy model, and then show how it scales to a larger system such as the AGS to RHIC transfer line. We will then show results of training inverse models using data from the machine and discuss future work for this effort.

FODO BENCHMARK

Before applying our technique to the ATR line, we first demonstrate the efficacy of our technique using a toy problem. Here we consider a linear system comprised of two quadrupoles, four beam position monitors and two correctors that operate in both the horizontal and vertical plane. The training data consisted of 5000 examples simulated by randomly changing corrector strength and the initial beam position. The model was trained to predict the corrector setting for a given set of BPM readings. The network architecture was optimized as a function of the number of layers as well as the nodes per layer to improve training loss without over-fitting. Figure 1 shows the model prediction compared to the ground truth for each of the correctors (kickers). The relationship is almost perfectly linear in all cases, indicating the model is well trained.

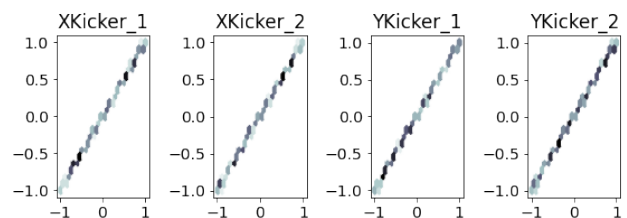


Figure 1: Real corrector setting on the x-axis with inverse model output result on the y-axis. The plots show a well-trained inverse model.

To evaluate the neural network against standard linear model benchmarks, we trained a linear model using the same data as the neural network. We also introduced different sextupole strengths to the lattice in order to understand the impact of a simple nonlinearity on the system. The linear model was compared to the neural network model for each case. Figure 2 shows the RMS prediction error on the test data for each of the correctors and the aggregate error which is computed as the sum of the squares of the individual corrector errors.

PHOTON POLARIZATION SWITCH AT ALBA

L. Torino*, G. Benedetti, F. Fernández, U. Iriso, Z. Martí, J. Moldes, D. Yezpe
 ALBA-CELLS, Cerdanyola del Vallès, Spain

Abstract

The polarization of the synchrotron radiation produced by a bending magnet can be selected by properly choosing the vertical emission angle. At beamlines this can be done by moving a slit to block unwanted polarization: this method is time consuming and not very reproducible. Another option is to fix the slit position, generate a local bump with the electron beam, and vary the emission angle at the source point such that the sample is illuminated with the desired polarization. At ALBA, we have implemented this option within the Fast Orbit Feedback, which allows to perform the angle switch in less than one minute without affecting other beamlines. This report describes the implementation of this technique for the dipole beamline MISTRAL at the ALBA Synchrotron.

INTRODUCTION

Some experimental techniques, such as imaging in the magnetic domain, take great advantage from using different polarizations of synchrotron radiation. At ALBA, the MISTRAL beamline is devoted to these technique and a fast and reliable polarization selection mechanism is demanded.

The polarization of the synchrotron radiation produced by a bending magnet is distributed as a function of the emission angle, as depicted in Fig. 1. Until last year, polarization was

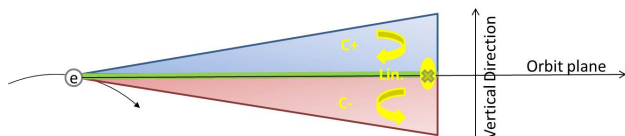


Figure 1: Synchrotron radiation produced by an electron beam passing through a bending magnet: the polarization is different according to the emission angle (C+: Circular Positive, C-: Circular Negative, Lin.: Linear).

selected by means of movable slits. This process works fine but creates problem of optics stability related with heat-load of components: when changing the mask position, a different part of the optics is enlightened and time for thermalisation is needed for thermal stabilization. Moreover, since the radiation follows a different optical path, the sample location also had to be adjusted, making the process unpractical and time consuming.

Another approach, already experimented at PSI [1], is to generate bumps with the electron beam. Doing this the radiation follows always the same optical path, and the desired polarization can be selected without varying the position of the slit.

* Itorino@cells.es

At ALBA, we decided to implement the Polarization Switch for the MISTRAL beamline within the Fast Orbit FeedBack (FOFB) architecture.

SWITCHING MECHANISM

In order to switch the polarization of synchrotron radiation, the idea is to create bumps at the MISTRAL source point so to locally change the direction of the orbit plane. In this way, when switching polarization, the position of the electron beam is kept while the angle changes, allowing to select a different polarization. Figure 2 shows the bump necessary to obtain positive and negative circular polarization.

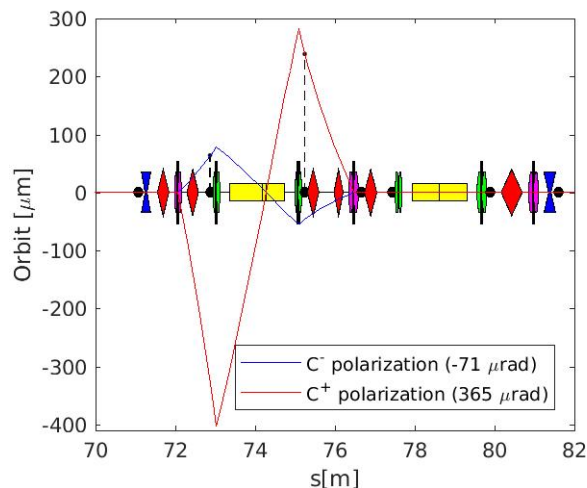


Figure 2: Bump to select different polarization at MISTRAL source point: negative polarization in blue, positive polarization in red. The dashed line represents the position of BPMs involved in the bump. The asymmetry is due to the initial alignment of the beamline.

At ALBA, before the switching mechanism was implemented, it was not possible to generate such a bump during normal operation since a FOFB system is running to keep the distortion with respect to the golden orbit lower than 1 μm RMS.

At the beginning, the choice of not changing the FOFB code was taken, and thus an online modification to the golden orbit was discarded. The other option was then to displace offsets of BPMs involved in the bump to "trick" the FOFB system to actually produce it.

The formula to obtain the beam position x from a BPM button is:

$$x = k_x \frac{\Delta}{\Sigma} - \delta x$$

MULTI-DIMENSIONAL FEEDFORWARD CONTROLLER AT MAX IV

C. Takahashi*, A. Freitas†, V. Hardion, M. Holz, M. Lindberg, M. Sjöström, H. Tarawneh
 MAX IV Laboratory, Lund, Sweden

Abstract

Feedforward control loops are used in numerous applications to correct process variables. While feedforward control loops correct process variables according to the expected behavior of a system at any given setpoint, feedback loops require measurements of the output to correct deviations from the setpoint. At MAX IV, a generic multi-dimensional input and output feedforward controller was implemented using TANGO Control System. This paper describes the development and use cases of this controller for beam orbit and optics corrections at MAX IV.

INTRODUCTION

MAX IV Laboratory is a fourth-generation light-source facility comprised of a 3 GeV storage ring, a 1.5 GeV storage ring, and a linear accelerator that serves as a full-energy injector to the rings and as a driver for the Short Pulse Facility. Yearly, the laboratory receives around 1000 users from academia, research institutes, industry, and government agencies through user access programs. With this, MAX IV has consistently delivered to users at 300 mA and 400 mA, on the 3 GeV and 1.5 GeV storage rings respectively.

The MAX IV distributed control system is composed of a three-layer architecture, in which TANGO [1] is the distributed control framework used on the middle layer to interface the equipment available in the facility and supervise their operation. The critical tasks are handled by dedicated hardware, and, from the client layer, Python and Matlab scripts can be used to interact with TANGO.

TANGO allows the implementations of devices to interface with real-world equipment and also to act on them according to a desired logic. In this context, TANGO devices can be used to implement controllers that read signals and actuate on other devices. Controllers act on system output in order to guarantee its stability and robustness by compensating for disturbances in the system. In this context, the controller can either react to errors on the output signal/setpoint or react to the input disturbance against an expected value. The first category is named feedback control, and the last one is feedforward control. While feedback control is more common in the literature and has obvious importance in stabilizing the system and satisfying its robustness requirements, feedforward control is required when large disturbances occur on a well-tracked system [2]. At MAX IV, the beam orbit and optics fall under the second category. These systems are controlled and have excellent tracking performance; however, they are subject to disturbances determined by insertion devices (ID) undulators positions. Thus, it became

necessary to implement a Multi-Dimensional Feedforward device to compensate that.

The first section of this paper will describe the general multi-dimensional feedforward device implemented at MAX IV, and the second section will detail some of its applications on the accelerator.

FEEDFORWARD CONTROL

Generally, feedforward control measures the disturbances on the input beforehand and adjusts the manipulated variable in order to minimize the deviation on the controlled variable [3]. Furthermore, when the effects of the disturbances can not be eliminated by the feedback loop alone, the feedforward controller can improve the overall performance of the system [2]. In this context, an ideal feedforward compensator could be derived by multiplying the transfer function of the disturbance by the inverse of the process variable; however, this realization is frequently unfeasible, unstable, or non-causal [4]. Therefore, different feedforward devices implementations have been proposed in the literature. The TANGO feedforward device implemented at MAX IV has a minimalist approach to a multi-dimensional controller.

Overall, it is necessary that the systems are already stable and tracked before using a feedforward strategy. In this context, feedforward controllers are often used jointly with a closed loop feedback control [2, 4]. Figure 1 presents a generic diagram of a feedforward-feedback control loop in which the feedforward controller compensates the disturbances. Hence, disturbances do not travel through the whole control path, minimizing the risks of oscillations and over-corrections.

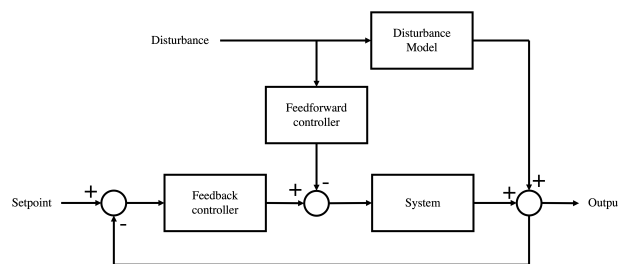


Figure 1: Block diagram of feedforward-feedback control system.

The ideal feedforward controller should compensate the disturbance according to its transfer function. Given that, $D(s)$ and $Y(s)$ are, respectively, the disturbance and the system output, $G_c(s)$ and $G_f(s)$ are the feedback and feedforward controllers and $G_p(s)$ represents the transfer function of the disturbance, then the control loop transfer function is given by Eq. (1). This equation should be zero to reject the

* carla.takahashi@maxiv.lu.se

† aureo.freitas@maxiv.lu.se

FAST ORBIT FEEDBACK UPGRADE AT SOLEIL

R. Broucquart[†], N. Hubert, Synchrotron SOLEIL, Gif-Sur-Yvette, France

Abstract

In the framework of the SOLEIL II project, the diagnostics group must anticipate ahead of the dark period the upgrade of important system like the BPM electronics, the timing system and the Fast Orbit Feedback (FOFB). The FOFB is a complex system that is currently embedded in the BPM electronics modules (eBPM). A new flexible stand-alone platform is under conception to follow the future upgrades of surrounding equipment, and to allow the integration of future correction schemes. In this paper we will present the current status of technical decisions, tests and developments.

CONTEXT

SOLEIL II aims at outstanding performances on the beam physics, qualified with renewed instrumentations. Most of the equipment linked to the FOFB will have to be updated to either accommodate these new performances (corrector magnets and their power supplies) or because they have reached obsolescence (BPM electronics, timing system).

The eBPMs (Libera Electron) currently host a major part of the FOFB system: 1) they are linked with a fast dedicated network to exchange the measured positions in all bpm location, 2) they compute the correction to apply from the given response matrix and 3) they communicate with the corrector magnet Power Supplies Controller (PSC) to apply the correction on beam.

These features have been embedded in the FPGA located inside those electronics. Most are custom developments or integration of the Diamond Light Source Communication Controller (DLS CC) [1]. This entanglement makes it difficult to upgrade the eBPMs, having to deal with two major applications: position monitoring and FOFB.

As FOFB system are very dependent on the machine layout, boundary systems and stabilization strategy, it has been decided to keep this system as an in-house development. To ease the integration, our strategy is to first segregate the FOFB system on a new dedicated platform. This platform will be interfaced with current eBPMs, PSC and timing system. It will evolve with the upgrade of each of these boundary systems.

On a feature perspective, the initial goal is to reproduce the actual features, operation control interface and performances. Future features will then be added: augmented monitoring, special mode of operation for fast lattice parameters measurements, new correction scheme... With the evolution of boundary systems and features in mind, a new modular FOFB system has been proposed.

SPECIFICATIONS AND GOALS

- Functionalities reproduced: With the new FOFB system platform, obtain the same service as provided currently.
- Increased performances: Communication latency and data rate will be improved, and with the leverage of a reduced latency of the future eBPMs, it will unlock a larger correction bandwidth. Performances evolution are given in Table 1.
- Follow machine evolution: SOLEIL II will bring down beam dimensions and thus stability requirements. With new correctors magnets and power supplies, the FOFB system shall attain lower stability dimensions.
- Offer new features: The new platform will allow new monitoring and fast lattice parameters measurement, such as fast response matrix identification or fast beam based alignment.

Table 1: FOFB Performances Evolution

	Actual FOFB	Future FOFB
# BPM	122	~180
# Corrector	50 H & V	To be defined
Data rate	10 kHz	100 kHz
Correction BW	150 Hz	1 kHz
Latency (communication and computation)	100 μs	10 μs
Stability	10 % of beam size 20 μm H ; 0.8 μm V	5% of beam size 50 nm H & V

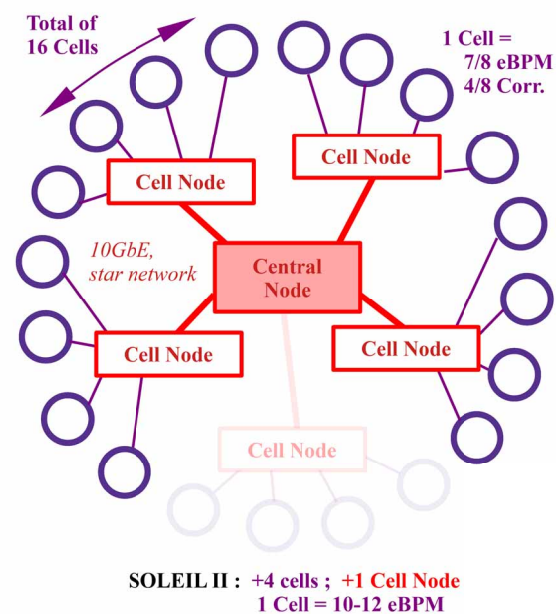


Figure 1: Network Topology.

[†] romain.broucquart@synchrotron-soleil.fr

REQUIREMENTS AND STATUS OF PETRA IV FAST ORBIT FEEDBACK SYSTEM

S.H. Mirza*, A. Alov, H.T. Duhme, B. Dursun, A. Eichler, S. Jablonski,
J. Klute, F. Ludwig, S. Pfeiffer, H. Schlarb, B. Szczepanski

Deutsches Elektronen-Synchrotron DESY, Hamburg, Germany

G. Rehm, Helmholtz-Zentrum Berlin für Materialien und Energie/BESSYII, Berlin, Germany

Abstract

PETRA IV is the upcoming low-emittance, 6 GeV, fourth-generation light source at DESY Hamburg. It is based upon a six-bend achromat lattice with additional beamlines as compared to PETRA III. Stringent stability of the electron beam orbit in the ring will be required to achieve a diffraction-limited photon beam quality. In this regard, the requirements and the proposed topology of the global orbit feedback system are discussed for expected perturbations. An initial analysis based upon system requirements, design and modelling of the subsystems of the orbit feedback system is also presented.

INTRODUCTION

Multi-bend achromat (MBA) lattice design in fourth-generation light sources provides the possibility of achieving a high degree of transverse coherence and brightness of photon beams by generating extremely low emittance electron beams. But the effort must be complemented by the transverse orbit stability against dipolar perturbations arising within the ring and from ground motion. Moreover, the transverse orbit stability requirement has drastically increased in the fourth-generation light sources also due to the smaller size of the electron beam in both transverse planes.

The upcoming PETRA IV of DESY Hamburg, which is an upgrade of the existing ring of PETRA III will have a six-bend achromat lattice [1] with additional beamlines having transverse beam position and pointing angle stability requirement of 5% to 10% of the electron beam size and divergence, respectively. A fast orbit feedback (FOFB) system is being developed to achieve disturbance rejection up to 1 kHz on the closed orbit. The main strategy for designing the FOFB system is to identify the requirements and design the subsystems around these requirements using lattice-based simulations.

The required performance criteria for the fast orbit correction is defined by the beam size and divergence at insertion devices (given in Table 1).

Even a generally accepted target of keeping RMS variation of electron beam position and pointing angle to 10% of RMS beam size and divergence [2] requires stabilization of 297 nm and 100 nrad (RMS) in the vertical plane of PETRA IV. The beam size and divergence are given with $\sigma = \sqrt{\beta\epsilon + \sigma_E^2\eta^2}$ and $\sigma' = \sqrt{\frac{\epsilon}{\beta}}$, where ϵ and β are the emittance and beam size, respectively. The energy spread

* sajjad.hussain.mirza@desy.de

Table 1: Electron Beam Parameters at IDs

Parameter	Value
$\beta_{x,y}$ (m), standard cell	2.2
$\beta_{x,y}$ (m), flagship IDs	4
Nat. emittance $\epsilon_{x,y}$ (pm rad)	20, 4
Beam size $\sigma_{x,y}$ (μm), standard cell	6.6, 2.97
Beam div. $\sigma'_{x,y}$ (μrad), standard cell	3.02, 1.34
Beam size $\sigma_{x,y}$ (μm), flagship IDs	8.9, 3.98
Beam div. $\sigma'_{x,y}$ (μrad), flagship IDs	2.23, 1.0

σ_E and the dispersion η is assumed to be zero at the location of IDs. The reuse of the old tunnel of PETRA III will come with relatively larger static and dynamic errors [3]; a stability task force was formed to model the error spectrum. The ground motion is expected to be below 100 Hz, but a disturbance rejection bandwidth of 1 kHz is targeted to achieve reasonable attenuation on the lower side of the frequency spectrum where most of the disturbances are expected. This is necessary to achieve the above-mentioned stability criteria, which further requires a latency-optimized system. The update rate of the closed loop is planned to be 130 kHz (equal to the revolution frequency) to reduce the latency in the closed loop. In this case, the betatron frequencies ($\nu_x = 23.43$ kHz and $\nu_y = 35.156$ kHz) cannot be disregarded in the FOFB modelling, because they are within the Nyquist sampling frequency and they may be in the region where the sensitivity function (transfer function from disturbance to output) could have a magnitude larger than 1.

This contribution discusses the proposed topology for the global FOFB system. In addition, analytical modeling of the subsystems is presented, which plays an important role in their design and in identifying the technical challenges to achieve 1 kHz disturbance rejection for SISO simulation.

PROPOSED TOPOLOGY FOR THE FOFB SYSTEM

FOFB system for PETRA IV is planned to perform orbit correction for the full range of disturbance spectrum, i.e. from quasi-DC to high frequency (1 kHz). The slow correctors distributed along the ring will correct large and slow orbit offset drifts. The FOFB system will correct fast perturbations referenced to the orbit maintained by slow correctors during machine commissioning. A total of 789 beam position monitors (BPMs) and 322 fast correctors in the vertical plane, and 200 fast correctors in the horizontal plane will

INVESTIGATING THE TRANSVERSE DYNAMICS OF ELECTRON BUNCHES IN LASER-PLASMA ACCELERATORS

A. Koehler^{*,1}, German Aerospace Center (DLR e.V.), Fassberg, Germany
¹previously at Helmholtz-Zentrum Dresden – Rossendorf, Dresden, Germany

Abstract

The demonstrations of GeV electron beams and FEL radiation driven by a centimeter-scale device illustrate the tremendous progress of laser-plasma accelerators. In such applications, beam divergence and size, along with beam energy and charge, are critical parameters of electron beams. An insight on the transverse parameters and their dynamics such as beam decoherence can be obtained by diagnostics complemented by betatron radiation detectors. This talk will also provide a brief overview of recent techniques for accessing the transverse phase space.

INTRODUCTION

Relativistic electron sources represent an important tool in basic and applied sciences. The best examples are synchrotron light facilities and free-electron lasers (FELs), in which electrons produce extremely short and bright flashes of light as they pass through periodic structures. This radiation allows us to study ultrashort processes and nonequilibrium states in biology, chemistry, and materials science. However, the radiofrequency technology generally used limits the maximum electron current and thus the available radiation intensity due to its accelerating structures. Ultimately, this leads to huge, expensive accelerators that can only be made available to a small group of users. In contrast to conventional accelerators, plasma accelerators produce highly relativistic electrons of up to several GeV at much shorter acceleration lengths of only a few millimeters. Because of the high beam currents enabled by the plasma medium, they are ideally suited for driving FELs, as demonstrated recently [1, 2].

Plasma accelerators can be driven by intense laser radiation, e.g. in laser wakefield acceleration (LWFA) schematically shown in Fig. 1. In LWFA, a high-intensity laser pulse propagates through an underdense plasma of density n_e , exciting plasma waves of frequency $\omega_p = \sqrt{n_e e^2 / (m_e \epsilon_0)}$. Here, e , m_e and ϵ_0 are the elementary charge, the electron mass, and the vacuum permittivity, respectively. The waves are excited by the ponderomotive force of the laser pulse, which displaces electrons from high intensity regions. At relativistic laser intensities, the electrons are completely pushed from the high intensity regions by the laser pulse. Due to their large mass, the ions remain behind and form a plasma cavity or a so-called bubble [3]. Electrons in a plasma cavity experience a longitudinal accelerating electric field and gain the energy γ . In the transverse plane, the plasma's electric and magnetic fields continuously focus

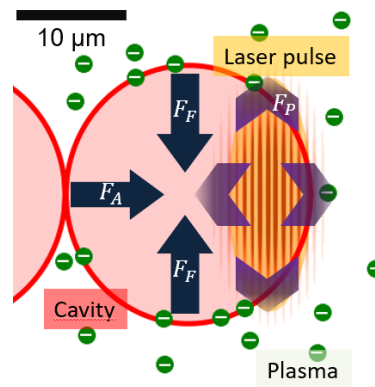


Figure 1: Schematic of LWFA. The laser pulse moves from left to right. F_P , F_F and F_A are the ponderomotive force of the laser pulse and the focusing and accelerating forces of the cavity on injected electrons, respectively.

the electrons and cause them to oscillate at the betatron frequency $\omega_\beta = \omega_p / \sqrt{2\gamma}$ and wavelength λ_β . The resulting betatron radiation enables the study of beam dynamics inside the plasma as well as it provides a broadband, ultrashort x-ray source [4].

The characteristics of betatron radiation can be compared with radiation from undulators and wigglers [5]. The dimensionless wiggler parameter for LWFA depends on the betatron radius r_β as

$$K = 2\pi\gamma \frac{r_\beta}{\lambda_\beta}. \quad (1)$$

The betatron radius is the amplitude of the electron orbit during acceleration. The betatron radiation spectrum is synchrotron-like and is described by the critical energy $E_c = 3\gamma^2 K h \omega_\beta$, where h is the Planck constant.

Typical LWFA operating at plasma densities of $1 \times 10^{19} \text{ cm}^{-3}$ possesses plasma wavelengths of $10 \mu\text{m}$. When the accelerated electrons reach energies of about 250 MeV at typical r_β of $1 \mu\text{m}$, then $K \approx 10$ indicates the wiggler regime and the emitted spectrum has a critical energy of about 10 keV.

The paper is structured as follows: First, a basic setup for LWFA is shown, including commonly utilized betatron diagnostics. Then, very briefly, betatron decoherence is introduced. Finally to a short summary, laser-acceleration methods of other particles are mentioned.

* Alexander.koehler@dlr.de

ANGULAR-RESOLVED THOMSON PARABOLA SPECTROMETER FOR LASER-DRIVEN ION ACCELERATORS

C. Salgado-López*, J. I. Apiñaniz, A. Curcio, D. de Luis, J. L. Henares,
J. A. Pérez-Hernández, L. Volpe, G. Gatti
Centro de Láseres Pulsados (CLPU), Villamayor (Salamanca), Spain

Abstract

Laser-plasma driven accelerators have become reliable sources of low-emittance, broadband and multi-species ion beams, presenting cut-off energies above the MeV-level. We report on the development, construction, and experimental test of an angle-resolved Thomson Parabola (TP) spectrometer for laser-accelerated multi-MeV ion beams which is able to distinguish between ionic species with different q/m ratio. The angular resolving power is achieved due to an array of entrance pinholes and it can be simply adjusted by modifying the geometry of the experiment and/or the pinhole array itself. The analysis procedure allows for different ion traces to cross on the detector plane, which greatly enhances the flexibility and capabilities of the detector. A full characterization of the TP magnetic field has been implemented into a relativistic code developed for the trajectory calculation of each beamlet. High repetition rate compatibility is guaranteed by the use of a MCP or plastic scintillator as active particle detector. We describe the first test of the spectrometer at the 1 PW VEGA 3 laser facility at CLPU, Salamanca (Spain), where up to 15 MeV protons and carbon ions from a 3-micron laser-irradiated metallic foil are detected. A second set of experimental measurements is shown, where highly magnified traces are obtained which leads to a possible transversal beam emittance estimation.

INTRODUCTION

Since the invention of the Chirped Pulse Amplification [1], the range of accessible light intensities on focus for ultrabright lasers has only increased. Such enhancement paved the way for laser-plasma particle accelerators (LPA), mainly focused on ions [2] and electrons [3]. The applications of such accelerated beams profit from the low-emittance and ultrashort duration of the beams, well-fitted characteristics for practical employments. Specifically, since the demonstration of collimation and monochromatisation of LPA multi-MeV ion beams [4, 5], their potential employments have attained plenty of attention, including ultrafast proton probing [6], isochoric heating of dense plasmas [7], fast ignition of inertial confinement fusion reactions [8] and medical purposes [9] among others.

Due to the specific LPA beam characteristics, one of the most widely used diagnostics for laser-driven ion accelerators are Thomson Parabola (TP) spectrometers [10]. First developed by Thomson in 1907, they are in-line diagnostics which sort the particles depending on their energy, momen-

tum and charge-to-mass ratio. The latter is specially useful in LPA scenario where the acceleration of multi-species beam is frequent. The main drawback of TPs is the incapability of deconvolving the spatial distribution of the measured beam as only a particular angle of the beam with an insignificant spread is evaluated because of the use of an entrance pinhole mask. Previous studies with different detectors, focused on analysing the spatial structure of the beams, showed that the most common laser based ion acceleration mechanism, the Target Normal Sheath Acceleration or TNSA [2], emits extraordinarily low-emittance beams from a source with a diameter as big as a few hundreds of micrometers and a total beam divergence of 20° . In order to retrieve spatial information about the beam other methods could be use, as stacks of radiochromic films or scintillators [11] which nevertheless fail when attempting to have fine spectral resolution. We present a multi-pinhole Thomson Parabola spectrometer, which combines sharp spectral and angular accuracy, besides the ionic species sorting capability.

DESIGN

Thomson Parabola spectrometers work according to magnetic and electric sector spectrometer principles. The entrance pinhole selects a beamlet composed by ions with specific q/m . Parallel (or anti-parallel) magnetic (B) and electric (E) dipoles deflect the ions in orthogonal directions. Such particles are detected in a two-dimensional spatially resolved particle-sensitive detector. In paraxial approximation with perfect fields, the particles will draw a parabolic trace onto the detector (given simply by Lorentz force) as

$$y^2 = \frac{q B^2 l_2 l_3}{m E} x, \quad (1)$$

where l_2 dipole length, l_3 the particle free-flight distance after the deviation, being the fields parallel to the x-axis. As seen, different charge-to-mass ratio particles will describe different traces and the position of the particle onto the trace will describe its kinetic energy.

We propose a modification of the basic TP design which consist on the substitution of the entrance pinhole by a mask in which several pinholes are drilled. The array of holes chops the incoming beam into several beamlets which are simultaneously detected, resulting in a tomography-like spectral measurement with tunable spatial-resolved information [12]. Figure 1 shows the basic device design.

Previous works [13–15] showed similar measurement strategies but most of the cases dismissing the electric field (and therefore the q/m differentiation) or limited their detec-

* csalgado@clpu.es

LINAC4 LASER PROFILE AND EMITTANCE METER COMMISSIONING

A. Goldblatt*, F. Roncarolo, J. Tagg, O. Andreassen, CERN, Geneva, Switzerland
 T. Hofmann, Bobst Mex SA, Lausanne, Switzerland

G. E. Boorman, A. Bosco, S. M. Gibson, John Adams Institute, Royal Holloway, United Kingdom

Abstract

The CERN LINAC4 is now equipped with two laser profile and emittance meters, a basically non destructive measurement of the transverse beam profile, not limited by the beam power density. The light of a pulsed laser is transported through optical fibers and focused into the 160 MeV/c H^- beam. The interaction of this laser “wire” with the H^- ions detaches electrons that are collected by an electron-multiplier, while the resulting H^0 particles, after being separated from the main H^- beam by a dipole magnet, are recorded by a diamond strip detector, located a few meters away from the interaction point. The transverse beam emittance and profile are reconstructed from the laser by a stepped scan through the H^- beam. After several years of feasibility tests and prototyping, this paper presents the details about the final hardware implementation, operational aspects, and the 2022 experimental results.

INTRODUCTION

Since 2019, when being connected as injector to the Proton Synchrotron Booster (PSB), LINAC4 serves as source of all CERN proton beam formats. While its predecessor LINAC2 was producing 50 MeV/c protons, LINAC4 accelerates H^- ions up to 160 MeV/c which are converted into protons – via a thin stripping foil – during injection into the four rings of the PSB. During the construction and commissioning of the LINAC4, a novel laser-based system was developed to measure the transverse beam profile and emittance in a non destructive way. After several years of design and testing, two systems were installed in strategic locations, both receiving 160 MeV/c H^- beams. The instrument operates on the *photo-detachment* principle, i.e. a laser-based stripping of the weakly coupled, second electron of the H^- ion, described in detail in [1–4]. The light of a pulsed laser is transported through optical fibers and focused to a cross section of about 140 μm diameter into the H^- beam. For each LINAC pulse, approximately 7% of the ions interacting with the laser are fully stripped. As depicted in Fig. 1:

- at the interaction point (IP) the detached free electrons are bent by a short dipole (weakly affecting the main beam) into an electron-multiplier tube (EMT).
- the neutral H^0 particles are measured on a diamond strip detector a few meters downstream, after being separated from the H^- beam by a main linac dipole.

The laser is scanned in well defined increments horizontally (H) or vertically (V) through the H^- beam. Correlating

* aurelie.goldblatt@cern.ch

the laser positions at the IP with the EMT and diamond detector signals allows the reconstruction of the beam profile and emittance, respectively, similar to a classical slit-grid emittance-meter.

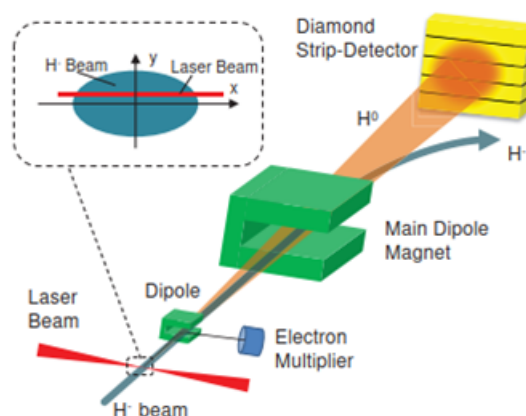


Figure 1: Concept of the laser emittance meter.

HARDWARE IMPLEMENTATION

It was decided to implement two systems to guarantee redundancy, and also to be complementary. The first system was installed at the end of the linac, before the first horizontal bend to the PSB transfer line. Here the beam emittance is dominated by the the beam size wrt. the dispersion. The second system is located between two main dipole magnets in the transfer line, where the H^0 background due to beam gas stripping is low. The distance between the H^0 detectors and the laser IP, 4.5 and 7 m, was chosen to have a convenient phase advance for sampling the angles of the emittance ellipse, like performed in slit-grid emittance-meters. The laser source, located in a dedicated hutch in the LINAC4 klystron hall, consists of an infrared laser with adjustable power, frequency and pulse length, with characteristics detailed in Table 1. The beam quality factor ensures a small beam diameter and long *Rayleigh* range at the interaction point, which is crucial to achieve a good resolution. The laser beam is transported from the surface to the interaction points in the LINAC4 tunnel through large mode area optical fibers with a special end-facet, designed to withstand the laser power density. Each of the two instruments receives two fibers of 30 and 70 m length to reach the two IP locations, for horizontal and vertical laser scans.

The diamond strip detector is composed of two motorized sensors, each having 28 channels with a pitch of 0.34 mm. They were produced by a polycrystalline chemical vapor deposition (pCVD) method and are radiation tolerant. Two

A HIGH PERFORMANCE SCINTILLATOR ION BEAM MONITOR*

D. S. Levin[†], University of Michigan, Ann Arbor, MI, USA

P. S. Friedman, Integrated Sensors LLC, Palm Beach Gardens, FL, USA

T. Ginter, Michigan State University, East Lansing, MI, USA

C. Ferretti, A. Kaipainen, N. Ristow, University of Michigan, Ann Arbor, MI, USA

Abstract

A high-performance Scintillator Ion Beam Monitor (SBM) provides diagnostics across an extremely wide range of isotopes, energies, and intensities employing a machine-vision camera with two novel scintillator materials moveable into/out of the beam without breaking vacuum. Scintillators are: 1) a semicrystalline polymer material (PM), film, 1 – 200 μm thick; and 2) a 100 – 400 μm thick opaque sheet consisting of a hybrid of an *inorganic-polymer* (HM) hybrid matrix. The SBM was demonstrated at the Facility for Rare Isotope Beams (FRIB, East Lansing, MI) providing real-time beam profile and rate analysis spanning more than five orders of magnitude *including visualization of single ion signals*. It may replace FRIB reference detectors: a phosphorescent beam viewer, a Faraday cup, a microchannel plate, and a silicon detector.

INTRODUCTION

Ion beam laboratories such as the Facility for Rare Isotope Beams (FRIB) feature many experimental beam lines requiring extensive, and potentially very expensive beam tuning. For example, the 2023 FRIB operating budget is nearly \$100M [1], distributed over some 3100 active beam hours suggests an hourly beam operating cost on the order of \$30k. Other facilities such as ANL, JLab, BNL/NASA require high performance scintillator detectors for charged particle counting over a wide dynamic range. High usage costs put a premium on technologies that enable the beam to be imaged, focused and otherwise tuned for research use with minimal time overhead and maximum versatility and spatial precision. The Scintillator Ion Beam Monitor system[‡] (SBM) hardware/software beam detector and analysis suite is designed to meet these requirements. This article describes the SBM and recent experiment results.

The SBM hardware employs a machine-vision camera combined with a fast, large aperture lens and two proprietary thin scintillator materials. The scintillators mount on a multi-target cassette controlled by a robotic arm that allows them to be swapped or translated in/out of the beam without breaking vacuum. This detector is fabricated in a six-way stainless steel cross (6WC) composed of the three orthogonal transepts and can be configured directly into a high vacuum beamline. Figure 1 shows the 6WC mounted on a support stage for positioning

in a beam, and a cross-sectional view showing the ladder or cassette of scintillator targets. A high resolution (megapixels), low-noise (2.4 photoelectrons RMS/ADC bin) CMOS sensor collects the scintillation light along the vertical branch line through a clear port window with a fast ($f/0.9$) lens. The field of view and depth of field are sufficient to image the entire target region.

Scintillators

Two types of proprietary scintillators are employed in the SBM: (1) Polymer Material (PM) – a semicrystalline polymer developed as a resilient thin film primarily for packaging applications. It was discovered to be an intrinsic scintillator with superior physical properties and higher light-yield than most plastic scintillators based on polyvinyltoluene and/or polystyrene. Because PM is semicrystalline, it has a “hazy” appearance. The PM-scintillator is highly radiation damage resistant. It produces a much stronger photodetector signal in our 6WC than other plastic scintillators tested such as BC-400 [2]. Various scintillator thicknesses from 200 μm to 1 μm have been tested. These thin films are particularly attractive for transmissive applications such as external beam radiation therapy (EBRT) where it is necessary for the imaging target to remain in the beam during treatment; (2) Hybrid Material (HM) is an *inorganic-polymer* material, is non-hygroscopic, is radiation damage resistant, is available in both thin and large area sizes, and can generate up to order of magnitude stronger signals per unit thickness than CsI(Tl). These large signals are attributed primarily to the photon transport; photons do not internally reflect and are emitted readily from the surface. The HM photon yield itself per energy deposited might be similar to CsI(Tl), in the range of 48000 – 65000 photons/MeV [3, 4]. Being polycrystalline in nature, it is visually opaque and incapable of total internal reflection, thus resulting in (1) a higher percentage of photons escaping from the film surface, (2) reduced back surface reflection and more accurate beam imaging and dosimetry. Two types of HM (HM₁ and HM₂) are included for SBM use, differentiated by their dopants, light yields, and decay times in the μs versus ms range respectively.

EXPERIMENTAL RESULTS

The SBM has been evaluated experimentally in various laboratories and with different radiation sources. Initial tests focused on scintillator performance using low-rate alpha and beta sources (²⁴¹Am, ⁹⁰Sr). Beam tests at FRIB using a 3 MeV/n ⁸⁶Kr beam in Sept. 2021, were followed at the Michigan Ion Beam Lab (MIBL) with high intensity 1 – 5 MeV protons, and at the Notre Dame Radiation

* Work supported by SBIR Phase-II award from the DOE Office of Science to Integrated Sensors, LLC (Award No. DE-SC0019597).

[†] dslevin@umich.edu

[‡] An Integrated Sensors patented product

AN X-RAY BEAM PROPERTY ANALYZER BASED ON DISPERSIVE CRYSTAL DIFFRACTION

N. Samadi[†], C. Ozkan Loch, G. Lovric, Paul Scherrer Institut (PSI), Villigen PSI, Switzerland
 X. Shi, Advanced Photon Source, Argonne National Laboratory, Lemont, USA

Abstract

The advance in low-emittance X-ray sources urges the development of novel diagnostic techniques. Existing systems either have limited resolution or rely heavily on the quality of the optical system. An X-ray beam property analyzer based on a multi-crystal diffraction geometry was recently introduced. By measuring the transmitted beam profile of a dispersive Laue crystal downstream of a double-crystal monochromator, the system can provide a high-sensitivity characterization of spatial source properties, namely, size, divergence, position, and angle in the diffraction plane of the system at a single location in a beamline. In this work, we present the experimental validation at a super-bending magnet beamline at the Swiss Light Source and refine the method to allow for time-resolved characterization of the beam. Simulations are then carried out to show that the system is feasible to characterize source properties at undulator beamlines for fourth-generation light sources.

INTRODUCTION

Fourth-generation synchrotron facilities [1-3] have brought the needs and challenges in developing advanced source property diagnostics. A complete characterization of the source position, angle, size, and divergence is critical for not only the electron source study but also the beamline experiment optimization. Many efforts have been dedicated to searching for the best diagnostic tools with different approaches, such as direct imaging [4-6], interferometry-based [7-9], and dispersion-based methods [10, 11]. Since each technique has advantages and limitations, we have concluded in a recent review [12] that the combination of multiple techniques may be advantageous.

Most recently, an X-ray beam property analyzer (XBPA) based on a multi-crystal diffraction geometry has been proposed and demonstrated to measure source properties with high resolution and sensitivity [13], showing great potential for X-ray beam quality characterization at next-generation light sources. Here, we first review the theoretical model of the XBPA system, followed by an experimental demonstration at a super-bending magnet beamline at the Swiss Light Source (SLS), performed with an ultra-fast detector. Finally, we summarize the simulation results of the XBPA for analyzing the source properties of an undulator beamline, as proposed in the course of the SLS upgrade.

XBPA SYSTEM DESCRIPTION

The XBPA system together with the physical model and fundamental equations is described in detail in [13]. A

schematic is shown in Fig. 1. The XBPA system uses a crystal monochromator (e.g., a double-crystal monochromator (DCM) is the most commonly used) to generate a narrow-bandwidth (in the order of $\Delta E/E \approx 10^{-4}$) beam with the energy spread in the diffraction direction (e.g., vertical direction for a vertical deflecting monochromator), as shown in Fig. 1(a). The flat beam downstream of the monochromator is a near-Gaussian profile, as shown in Fig. 1(b), that contains the source angle and divergence information. By placing a Laue crystal in the dispersion geometry tuned to the central energy of the monochromator, a small spatial portion of the beam will be diffracted away, leaving a valley in the transmitted beam profile, as shown in Fig. 1(c). The width and location of the valley contain the source position and size information. By analyzing both the flat and transmitted beam profiles, the spatial properties of the photon source in the diffraction direction can be fully extracted.

When the source has a fixed position, but the beam is tilted by an angle, the flat beam will move vertically according to the angle and the source-to-detector distance. However, the Laue-transmitted beam valley location will not move, as the monochromator will select out the same energy from the angular distribution of the source, or the central energy line (dashed line in Fig. 1) will not move. On the other hand, if the source is fixed in angle but moves vertically in position, not only the flat beam will move vertically, but the valley position will also move vertically the same amount as the source motion (i.e., a parallel vertical shift of the dashed central energy line in Fig. 1). Thus, there is a simple relationship between the vertical source angle (y'_s) and position (y_s) and the measured flat beam location

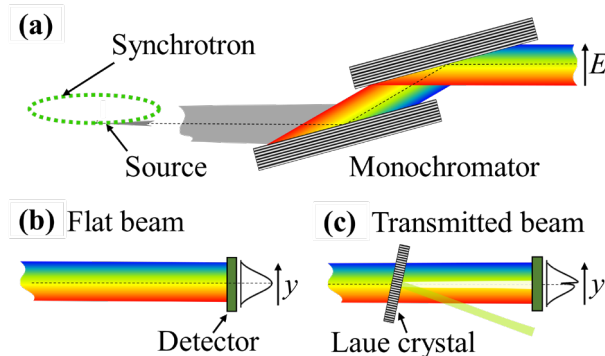


Figure 1: Schematic of the XBPA system containing the crystal monochromator, the Laue crystal in dispersion geometry downstream of the monochromator, and the detector. (a) shows a double-crystal monochromator geometry, (b) and (c) show the flat beam without the Laue crystal and the transmitted beam with the Laue crystal tuned to the central energy of the monochromator, respectively.

[†] nazanin.samadi@psi.ch

BEAM STABILITY IN THE MAX IV 3 GeV STORAGE RING

J. Breunlin*, G. Felcsuti, MAX IV Laboratory, Lund University, Sweden

Abstract

The MAX IV Laboratory, inaugurated in 2016, hosts a 3 GeV ultra-low emittance storage ring, a 1.5 GeV storage ring and a linear accelerator driven Short Pulse Facility to deliver synchrotron radiation to scientific users. A Stability Task Force has been assigned to ensure the delivery of stable beams since early on in the design phase of the laboratory and is continuing its work in an ongoing and multi-disciplinary effort. Measurements of the electron beam stability resulting from the passive stabilization approach taken for the two storage rings will be presented, as well as figures of beam stability with the Fast Orbit Feedback system in operation. Each ID beamline in the 3 GeV storage ring is equipped with a pair photon beam position monitors that are currently used to complement the electron beam position monitors. In the light of the city development around the MAX IV campus, maintaining the good mechanical stability of the laboratory has to be seen as an ongoing effort. A number of studies are being performed to identify possible risks and to decide where measures need to be taken.

INTRODUCTION

The MAX IV 3 GeV storage ring, is optimized for the production of high-brightness X-rays and features a 20-fold seven-bend achromat lattice reaching a bare lattice emittance of 328 pm rad [1, 2]. The emittance coupling is adjusted for a routine delivery beam with a vertical emittance of 8 pm rad. All user beamlines use insertion devices (IDs). The RMS electron beam sizes in the source points are 52.0 μm horizontally and 4.0 μm vertically when considering the horizontal emittance reduction by ID radiation damping.

In order to achieve our overall stability goal, a beam stability better than 10 percent of the RMS beam size, the tolerances on magnet stability of 20 nm to 30 nm RMS displacement had been defined during the project phase [3]. This is achievable also because the very good initial 'green field' ground vibration levels have not increased significantly by the presence of the laboratory.

This paper shows examples of the work of the MAX IV Stability Task Force covering mechanical stability topics and floor vibration, the orbit stability of the stored electron beam, the role of orbit feedback systems, as well as position and angle stability studies with the synchrotron radiation (SR) beam from IDs.

MECHANICAL STABILITY

Mechanical stability at MAX IV is in general achieved by passive systems [3]. While internal vibration sources are easily controlled by passive isolators, disturbances originating outside the borders of the facility must be dealt with

differently: by careful design of the support structures, and by early involvement in planned projects near the laboratory. A few examples are mentioned below.

During the design phase of the facility, the main mechanical stability concern was heavy traffic on the nearby motorway (distance approx. 120 m). Here the special floor structure designed to mitigate traffic-related disturbances together with the implementation of a policy ensuring stiff foundations (by prescribing a goal for the lowest resonance frequencies for structures supporting accelerator and beamline components) turned out to be very successful. Even though vibration peaks due to heavy traffic are clearly observable in the floor of the laboratory (see the correlation between vibration peak count and heavy vehicle count in Fig. 1), as of today, only minor disturbances to beamline operations have been related to traffic. The vibration levels caused by motorway traffic are typically used as a reference to evaluate the impact of future projects in the vicinity of the laboratory.

MAX IV was one of the first buildings in Brunnsög, a quickly developing district of Lund where office buildings, research facilities and residential homes for 40 000 inhabitants will be built the coming decades. As the city is growing around the MAX IV Laboratory, the nature of addressing mechanical stability changes. The main focus has been shifted from ensuring proper design towards influencing potentially vibration-generating projects planned in close proximity to our operations. In practice, our concerns regarding mechanical stability are raised in early planning phase through discussions with policymakers and urban developers about the location and design of their projects. For instance, track vibration isolation of a new tramway line close to the laboratory was implemented thanks to the cooperation with the municipality, and as a result, no detectable influence has been observed on the accelerator since the tram has been in operation since the end of 2020.

Currently, we are involved in the decision on where to introduce speed bumps on nearby roads. To minimize the risk of disturbing ambient vibrations at the laboratory, tests were conducted in collaboration with the municipality to determine safe distances for different bump profiles, vehicle weights, and speeds, see Fig. 2.

ELECTRON BEAM STABILITY

The Slow Orbit Feedback (SOFB) system is designed to correct the electron orbit at repetition rates up to 10 Hz in order to handle slow drifts [4]. A total of 200 beam position monitors (rf-BPMs) are available in each plane as well as 200 horizontal and 180 vertical corrector magnets. The targeted orbit stability is achievable with the SOFB only during operation (see Fig. 3); a result of the excellent passive stability of the storage ring. Integrated up to 1 kHz

* jonas.breunlin@maxiv.lu.se

ADAPTIVE FEEDFORWARD CONTROL OF CLOSED ORBIT DISTORTION CAUSED BY FAST HELICITY-SWITCHING UNDULATORS

M. Masaki[†], S. Takano¹, T. Watanabe¹, T. Fujita, H. Dewa, T. Sugimoto¹, M. Takeuchi
JASRI, Hyogo, Japan

H. Maesaka², K. Soutome, T. Fukui, H. Tanaka, RIKEN SPring-8 Center, Hyogo, Japan

K. Kubota, SPring-8 Service Co. Ltd., Hyogo, Japan

¹also at RIKEN SPring-8 Center, Hyogo, Japan

²also at JASRI, Hyogo, Japan

Abstract

We developed a new correction algorithm for closed orbit distortion (COD) based on adaptive feedforward control (AFC). The AFC system integrated into the SPring-8 storage ring has proved to be effective in suppressing the fast COD with repetitive patterns caused by helicity-switching undulators. The scheme aims to counteract error sources by feedforward correctors at the position or in the vicinity of error sources to avoid a potential risk of unwanted local orbit bumps, which is known to exist for the global orbit feedback. The new option, AFC, is especially advantageous when an error source causes an angular fluctuation of photon beams such as a fast orbit distortion near undulators. The AFC provides a complementary capability to a so-called fast global orbit feedback (FOFB) for coming next-generation light sources where ultimate light source stability is essentially demanded.

INTRODUCTION

Storage-ring-based light sources have become essential facilities for photon sciences and related applications including industrial purposes. One of the key advantages for light source users is the brightness of light, which is also related to the degree of transverse coherence. However, high photon beam stability is also essential for successful developments, along with high brightness. In modern or future light sources, the pointing stability of photon beam should be sufficiently smaller than the electron beam size to achieve the inherent light source performance. Beam orbit disturbances in a storage ring can be caused by a variety of error sources. For examples, (i) mechanical motions of magnets or vacuum chambers due to ground motion, cooling water, (ii) electro-magnetic noise of magnet power supplies or RF sources, (iii) magnet pole gap or phase motions, polarization switching kickers of insertion devices (IDs). These disturbances can be suppressed by orbit feedback and feedforward controls, or elimination of the error source itself. In the case that the error sources are unknown, slow or fast global orbit feedback can be an effective countermeasure. On the other hand, when the error sources are known, an ideal solution is to remove the error source itself, but not feasible for all sources. For an example, in the case of ID-derived orbit disturbance due to gap motion or fast switching kicker, feedforward corrections are often used without removing

the error sources. The feedforward counter kicks in the vicinity of the error kicks are very effective.

In the SPring-8 storage ring, two twin-helical undulators (THUs) with fast kicker systems: ID23 and ID25 [1, 2] were installed for periodic photon helicity switching in X-ray magnetic circular dichroism experiments at beamlines. Orbit variations due to periodic excitation of the kicker magnets on demand from user experiments have been observed for years, even though ID23 and ID25 are equipped with fast corrector magnets for feedforward corrections to suppress them. The periodic orbit fluctuations, which are synchronized with the kicker excitation, gradually grew up to 10 μm (RMS) or more because of the deterioration with time of feedforward correction accuracy.

To address this issue, based on a fundamental orbit correction strategy to directly counteract an error source to be corrected, we have taken the following points into consideration: (i) the error sources are identified at the two THUs, (ii) the feedforward correction is already equipped, and (iii) the degradation rate of the correction accuracy is slow. We have introduced, instead of a conventional fast global orbit feedback, a new COD correction algorithm based on adaptive feedforward control (AFC) [3], in which the feedforward tables are dynamically updated. The COD variations originating in the two error sources (ID23 and ID25) are independently suppressed by the new AFC system. Our goal for the orbit stabilization is to suppress the COD fluctuations of less than 1 μm RMS during the kicker excitation in a transparent manner where experimental users cannot observe any periodic disturbance.

HELICITY-SWITCHING UNDULATORS OF SPRING-8

Schematics of the THU installed in the SPring-8 storage ring are illustrated in Fig. 1. The twin helical switching system consists of the two helical undulators for right- and left-handed circular polarizations, placed on the upstream and downstream sides, respectively. Five kicker magnets make the dynamical horizontal orbit bumps (orbit A and B as shown in Fig. 1) alternately, for periodic optical helicity switching. The switching-frequency for ID23 is 1 Hz; ID25 can be switched at either 1 or 0.1 Hz. When the electron beam orbit is switched to the orbit A, the radiation from the upstream undulator propagates horizontally off-axis and is

[†] masaki@spring8.or.jp

RF SYSTEM-ON-CHIP FOR MULTI-BUNCH AND FILLING-PATTERN FEEDBACKS*

P. Baeta[†], B. Keil, G. Marinkovic, Paul-Scherrer-Institut (PSI), Villigen, Switzerland

Abstract

We have evaluated an RF System-on-Chip (RFSoc) as a platform to implement the multi-bunch (bunch-by-bunch) feedback and the filling pattern (single bunch charge) measurement system for the Swiss Light Source (SLS) upgrade project, the SLS 2.0. This paper presents the status and first results of a preliminary design of the feedback systems using an RFSoc evaluation board, including test measurements at the SLS.

INTRODUCTION

The Swiss Light Source (SLS) is a synchrotron light source at Paul Scherrer Institute (PSI), and it has been in user operation since June 2001. The SLS beamlines cover research areas such as, but not exclusively, atomic and molecular science, material science, environmental and earth science, and life and medical science. To preserve the high scientific output of SLS, PSI plans an upgrade of SLS, the SLS 2.0. The SLS storage ring will be replaced, and an innovative magnet lattice with reverse bends will provide up to 60-fold higher brightness for hard X-rays [1]. Moreover, aging systems of the SLS will be exchanged, including the storage ring multi-bunch feedback (MBFB) and filling pattern feedback (FPFB). In this context, an RF System-on-Chip (RFSoc) from Xilinx/AMD [2] has been evaluated as a possible solution to substitute the existing technology of the MBFB and FPFB systems in operation at the SLS [3, 4]. The RFSoc integrates multi-core CPUs, FPGA fabric, high-speed analog-to-digital (ADC), and digital-to-analog data converters (DAC) with several Giga-samples per second (Gs/s) on a single chip. We have used the ZCU111 kit from Xilinx/AMD to evaluate the RFSoc [2]. The ZCU111 evaluation board features an RFSoc with eight 12-bit 4 Gs/s ADCs, eight 14-bit 6.5 Gs/s DACs, a 4-core 64-bit, and a 2-core 32-bit ARM CPU. In addition, the RFSoc provides various data storage and communication interfaces, including multi-gigabit links and Ethernet.

The following sections of the paper describe the implementation of a three-dimensional multi-bunch feedback (MBFB) and the measurement of the relative charge in each bunch (filling pattern) at the SLS storage ring with the RFSoc, using RF beam position monitor (BPM) signals.

HARDWARE

Figure 1 shows the hardware setup installed in the SLS storage ring for developing and testing the MBFB and filling pattern measurement using the RFSoc. A BPM with four capacitive button electrodes is connected to RF hybrids, generating: The sum signal, S, proportional to the bunch charge; the horizontal, X, and vertical, Y, signals proportional to the product of transverse bunch position

offset and charge. The ZCU111 is the core component of the system. The device acquires and samples the X, Y, and S signals with its ADCs, and generates the correction signals with its DACs. The correction signals are amplified and drive the MBFB kickers. In addition, acquired signal S is used to measure the filling pattern.

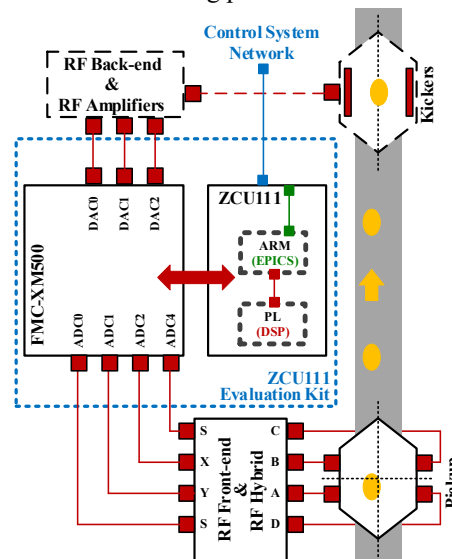


Figure 1: Hardware block diagram of the RFSoc-based multi-bunch feedback and filling pattern measurement.

The current MBFB system at SLS, presented in [3], has been in operation since 2006. The system has a commercial RF front-end (RFFE), which mixes the BPM signals from 1.25-1.5 GHz range down to baseband. The RFFE provides to ADCs: The transverse position signals, X and Y, and the phase signal for the longitudinal position, S. The signals X, Y, and S are sampled each by an 8-bit 500 Mega-samples per second (Ms/s) ADC. The signals are processed on a Virtex-2 FPGA with firmware implemented in VHDL at PSI. The driving signals for the transverse and longitudinal MBFB kickers are generated each by an 8-bit 500 Ms/s DAC. Each DAC directly drives the RF power amplifiers of transverse strip line kickers for X and Y channels. The longitudinal plane has an analog upconverter to transform the baseband (0-250 MHz) DAC signal to 1.25-1.5 GHz for the power amplifier of the longitudinal kicker.

The primary goal of the first MBFB implementation on the RFSoc was to facilitate the comparison with the current SLS system. Therefore, the new RFSoc firmware is functionally compatible with the analog signal conditioning of the current system. Consequently, the new and existing MBFB system electronics can be exchanged or even operated in parallel, enabling live switching between the two systems using combiners/splitters.

At SLS, the current FPFB measures the bunch charge with an avalanche photodiode (APD), using synchrotron

[†] pedro.baeta@psi.ch

DUAL CHANNEL FMC HIGH-VOLTAGE SUPPLY

W. Viganò **, J. Emery, M. Saccani, CERN, Geneva, Switzerland

Abstract

The Beam Loss Monitoring (BLM) detectors and electronics are installed in the CERN accelerators to provide measurements of the beam loss and to protect from excessive losses. The majority of the BLM detector types require voltage biasing up to 2000 V_{DC} with a possibility to generate patterns to verify the connection chain from the detectors to the front-ends.

Currently, the power supply solution consists of Components Off-The-Shelf (COTS) large format power supplies with additional custom electronics and various interconnections to provide monitoring and remote control. For this reason, a market search has been done to identify a high reliability module suitable for dedicated BLM installations composed of a few detectors. The outcome of this market survey has justified the need to design a low-cost custom board, compatible with the CERN infrastructure and different detector types, as well as easily customizable to cover various installation architectures and needed voltage ranges.

The main characteristics of the developed board are: autonomy and full remote control; common hardware for different applications with a change of the DC/DC converter and a few components; smaller size than what is currently used as High-Voltage (HV) power supplies; multiple different high voltage or low voltage outputs for specific applications with the default design consisting of two positive high voltage outputs and one low voltage output; μ V voltage sensing and mA current sensing capabilities; protection against overvoltage.

INTRODUCTION

The present article describes the design and test methodologies adopted to build and validate a dual channel high voltage supply in a FMC form factor. It will be used to bias BLM diamond detectors and mobile installations of ionization chambers and other beam instrumentation detectors in the CERN accelerators.

Next chapters highlight the effort put on the safety and operability aspects of the design related to the small form factor as well as the versatility and adaptability of the card for multiple use cases and applications.

DEVELOPMENT STRATEGY

Specifications

The first phase of the design focused on collecting specifications from all BLM systems at CERN, which are based mainly on ionization chambers with various dimensions and shapes, diamond detectors and silicon photomultipliers.

The outcome of the investigation is summarised in Table 1. A development baseline was defined to be a common platform for most of the BLM detectors with a board able to generate two high-voltage outputs and one low voltage output settable in a pre-defined range.

To minimize the development time, and to make the board compatible with several other platforms, the FPGA Mezzanine Card (FMC) form factor has been selected.

The CERN Beam Instrumentation Group has developed and already produced a large quantity of Intel Arria V based VME64x carrier for one High Pin Count (HPC) FPGA Mezzanine Card (FMC, VITA 57) called VFC-HD [1].

The additional requirements for FMC High-Voltage Supply were to keep the standard front panel width of 4HP, use SHV connector for high-voltage outputs and LEMO connectors for low voltage outputs. As an additional feature, it should be possible to plug adjacent boards into a VME crate without any risk of electrical discharges.

Table 1: Default Version Specifications

Version	Min Voltage [V]	Max Voltage [V]
V1	+175	+1734
V2	-175	-1734
V3	+5	+10

IMPLEMENTATION

Electronic Design

An XP Power AG Series DC/DC converter is the core component in the developed design. The AG Series is a broad line of ultra-miniature DC to HV DC converters that sets an industry standard in high-voltage miniaturization. Module are available in three categories of input voltages: 5 V, 12 V and 24 V. We have decided to use the 12 V series as default because it is the best compromise between the voltage and current level for the VME standard. Nevertheless, the FMC board is designed to be compatible with the 5 V series as well. The AG Series offers modules with positive or negative output voltages ranging from 100 V to 6000 V. The FMC High-Voltage Supply board is designed to work safely up to 2000 V. A possible extension up to 3000 V is still under evaluation.

Figure 1 shows a block diagram of the high-voltage interface. From the FMC connector, the mezzanine receives the +12 VDC power rail for the HV DC/DC converters and the +3.3 VDC power rails to the digital circuitry. A power enable digital signal is used to control, using Pulse Width Modulation (PWM), the +12 V_{DC} rail making it possible to adjust the main HV DC/DC accordingly, with the XP Power AG series that works at 12 V_{DC} or at 5 V_{DC}, while the voltage regulator is fine-

* william.vigano@cern.ch

AN LHC PROTECTION SYSTEM BASED ON FAST BEAM INTENSITY DROPS

M. Gasior, T. Levens, CERN, Geneva, Switzerland

Abstract

The Large Hadron Collider (LHC) is protected against potentially dangerous beam losses by a distributed system based on some four thousand beam loss monitors. To provide an additional level of safety, the LHC has been equipped with a system to detect fast beam intensity drops and trigger a beam dump for potentially dangerous rates. This paper describes the architecture of the system and its signal processing, optimized to cope with dump thresholds in the order of 0.01% of the circulating beam intensity. The performance of the installed system is presented based upon beam measurements.

INTRODUCTION

The LHC Beam Charge Change Monitor (BCCM), also called the dI/dt system, is specified to trigger beam dumps for beam losses exceeding thresholds in six integration windows in two beam energy ranges, as summarised in Table 1. The integration window lengths, expressed in units of the LHC revolution period T_r ($\approx 89 \mu\text{s}$), have been chosen to correspond to integration periods of the Beam Loss Monitoring (BLM) system. The BCCM is required to operate for beam intensities from 5×10^9 elementary charges (q_0) for a single pilot bunch, up to $6 \times 10^{14} q_0$ for ≈ 2800 physics beam bunches of $2.1 \times 10^{11} q_0$, resulting in the intensity dynamic range of $\approx 10^5$ and the beam signal dynamic range of ≈ 40 . Thus, the smallest beam dump threshold of $0.5 \times 10^{11} q_0$ for the longest integration window in the high energy range corresponds to an intensity change of $\approx 0.008\%$. Such challenging beam dump threshold levels and the required operational reliability have proved to be very difficult to satisfy at the same time. The BCCM system design described in this paper was preceded by a few prototypes and the experience gained at each stage contributed to the improving performance.

The initial prototype of the system was based on signals from Fast Beam Current Transformers (FBCTs), with 16-bit ADCs sampling at 160 MHz and IQ narrowband processing of the 40 MHz beam component implemented in an FPGA [1]. A mayor limitation of the first prototype was the beam sensor itself, as its readings were beam position dependent [1]. This triggered a development of a new technology, resulting in Wall Current Transformers (WCTs) [2], which removed the beam position dependence problem [3] and finally replaced the FBCTs. Then the WCT signals were used in the next version of the BCCM and the signal processing was updated. However, this version had not achieved the required reliability to work as an LHC protection system without triggering false dumps. Finally, the architecture of the BCCM was revised and the system was completely rebuilt according to the design described in this paper.

Table 1: BCCM Beam Dump Threshold Levels in $10^{11} q_0$

Beam energy	Integration window lengths in T_r units					
	1	4	16	64	225	1125
$< 0.5 \text{ TeV}$	6	6	6	6	6	6
$\geq 0.5 \text{ TeV}$	3	3	3	3	2	0.5

The most fundamental change in the new BCCM is the source of the beam signal, where the WCT has been replaced by the sum signal of a beam position monitor (BPM). This way the development of the BCCM became independent of the beam intensity measurement system, which is critical for the LHC operation and therefore any changes to its parameters were very difficult. This was previously posing serious limitations during the development of the BCCM. The BPM also provides larger signals than the WCM, which contributes to the improved noise performance of the present system.

The signal processing now used in the BCCM provides a few improvements and simplifications:

- the fast beam signals are rectified, allowing the system bandwidth to be strongly limited by low-pass filters already before the ADC;
- in consequence, the beam synchronous ADC sampling could be lowered to 40 MHz, allowing to use high signal-to-noise ratio ADCs and facilitating the digital signal processing;
- the idea of one revolution digital delay line was introduced: the beam signal changes are calculated as plain differences of one revolution period integrals, allowing simple, reliable and efficient signal processing;
- the ADC sampling phase does not need to be adjusted to the beam signal, increasing the simplicity and robustness of the system operation.

The new LHC BCCM system based on the mentioned features is described in the following sections and its performance illustrated with beam measurements.

SYSTEM ARCHITECTURE

The block diagram of the BCCM is shown in Fig. 1, along with signals sketched in key nodes of the system. The signals from four electrodes of a BPM are first processed by 80 MHz non-reflecting low-pass filters (NRLP), amplified by RF amplifiers (RFA) and then combined to remove their beam position dependence. The resultant signal is rectified by an envelope detector (ED), which allows subsequent strong low-pass filtering, essential to limit the system bandwidth and in consequence noise. The filtered signal is digitised by a 16-bit ADC (LTC2204) sampling at 40 MHz derived from the 400 MHz LHC RF frequency. The ADC samples are processed by an FPGA

INFLUENCE OF THE BEAM INDUCED IRRADIATION ON THE CRITICAL CURRENT PHENOMENA IN SUPERCONDUCTING ELEMENTS

J. Sosnowski, NCBJ, Świerk, Poland

Abstract

In the constructions of the modern accelerators, of free electrons as is in the case of FEL-s or ionized particles as in LHC working in CERN, the ionized beam is guided by the magnetic field generated in electromagnets, more and more frequently wound up using superconducting wires. The beam's induced irradiation arises in these accelerators, which influences the properties of the superconducting elements, as wires, current leads or shields, which issue is discussed in the present paper. It is shown in which way the irradiation damages the subtle structure of superconducting materials, leading to columnar defects formation in 2D HTc superconductors. It is analysed theoretically how these nano-structural defects influence the critical current properties of the superconducting materials. In the paper is developed energetic approach, of the Ginzburg-Landau type in lowest order approximation, to the process of capturing of the magnetic pancake vortices in HTc superconductors. Various initial positions of the captured vortices are analysed, movement of them through the potential barrier leads to electric field generation. The dependence of the potential barrier on transport current is analysed. Influence of the irradiation effects on the current-voltage characteristics of superconductors are investigated then and critical current values detected, as the function of irradiation intensity, size of created then nano-defects and physical parameters such as critical temperature and elasticity forces. This analysis has therefore physical meaning and should be useful also for prediction the proper work conditions of accelerators with superconducting elements.

INTRODUCTION

Nowadays it is intensively developed nuclear accelerators technology, to which belong also linear constructions of the FEL-s type. In these facilities more and more frequently there are applied superconducting materials [1], including the HTc superconductors too. They are used in solenoids generating magnetic field, forming the electron beam at FEL-s facilities but also as current leads, resonant cavities, shields and various correctional coils, guiding the beam along the appropriate track. Before applying these new materials in accelerating machines, we should therefore to establish the sensitivity of their properties to irradiation, which appears especially in nuclear accelerators. This issue is just the subject of paper.

In the paper is discussed how irradiation arising in modern accelerating devices, caused by primary beam of ionized particles circulating in synchrotrons or electrons beam in linear FEL-s machines, will influence the current carrying properties of superconducting elements. For the case of FEL-s linear accelerators beside primary beam, in which

irradiation is created by moving electrons, occur too the secondary beams, composed beside all from neutrons, γ -rays, positrons and photonic bunches. They are created during collisions of electrons with walls of accelerators.

These investigations are especially relevant for HTc superconductors, which are characterised by the subtle planar structure of 2D type, very sensitive therefore to the defects concentration. These defects are created just by the irradiation caused by the ionic or electrons beam guided in accelerators lines. For that 2D structure the ionic bombardment can lead to the columnar defect creation. At an aim of describing mathematically the influence of the irradiation, creating the nano-sized defects on superconducting elements, it has been developed the model oriented on the energy variation analysis during the dynamic interaction of nano-defects with the magnetic vortices. They are generated by external magnetic field or current flow. This general model has been applied to the defects induced by irradiation as well as mechanically formed defects, such as dislocations arising especially during the winding procedure of the superconducting coils.

BEAM IRRADIATION EFFECTS IN SUPERCONDUCTORS

Irradiation in superconducting accelerators although caused by rather small volume of ionized beam has significant influence on superconducting elements just because the superconductivity is very subtle effect. It is second order effect in perturbation range, which for many years was not explained theoretically therefore by scientists. So it can be expected that irradiation of the superconducting materials will have large influence on their properties, which concerns especially the low dimensional superconductors as two-dimensional HTc superconductors based on CuO₂ planes but also will apply to the quasi one-dimensional A15 type superconductors. This class of materials is characterized by three linear, perpendicular chains of the atoms of the transition metals. Beam irradiation of these materials, for instance Nb₃Sn wires, will lead to damage of the chains responsible for their superconducting properties. Critical temperature is then really decreasing. Also HTc superconductors, reaching already room temperature are more and more attractive from the point of view of application them in nuclear physics devices. World record of the critical temperature belongs now to the hydrogen sulphide and exceeds already room temperature. $T_c = 14^\circ\text{C}$ at H₂S + CH₄, unfortunately under very high pressure at 267 GPa. But this world record for highest T_c should be still confirmed. Second on this list is lanthanum - hydrogen compound of the composition LaH₁₀ at pressure of the 170 GPa, with critical temperature of -23°C [2]. To the

UPGRADE OF THE BPM LONG TERM DRIFT STABILIZATION SCHEME BASED ON EXTERNAL CROSSBAR SWITCHING AT PETRA III

G. Kube, F. Schmidt-Föhre, K. Wittenburg
Deutsches Elektronen-Synchrotron DESY, Germany
A. Bardorfer, L. Bogataj, M. Cargnelutti, P. Leban, M. Oblak, P. Paglovec, B. Repič
I-Tech, Solkan, Slovenia

Abstract

PETRA IV at DESY will be an upgrade of the present synchrotron radiation source PETRA III into an ultra low-emittance source with beam emittance of about 20 pm rad which imposes stringent requirements on the machine stability. In order to measure beam positions and control orbit stability to the required level of accuracy, a high resolution BPM system will be installed which consists of about 800 monitors with the readout electronics based on MTCA.4. In order to fulfill the requested long-term drift requirement ($< 1 \mu\text{m}$ over 7 days), also the BPM cable paths have to be stabilized because of the PETRA-specific machine geometry. To achieve this, the crossbar switching concept was extended such that the analogue switching part is separated from the read-out electronics and brought as close as possible to the BPM pickup. While first measurements were presented before, meanwhile the system has undergone a major revision, especially the external switching matrix changed from a prototype setup to a system close to the final design. This contribution summarizes the latest measurements from PETRA III, demonstrating the high performance of the external stabilization concept.

INTRODUCTION

The PETRA IV project at DESY (Hamburg, Germany) aims at the construction of a diffraction limited ultra-low emittance light source operating at 6 GeV. The storage ring will be installed in the existing 2.3 km PETRA tunnel, thus it will follow the geometry of the old PETRA collider with 8 octants made of arcs, each hosting nine hybrid six bend achromatic (H6BA) cells which are connected by long straight section as shown in Fig. 1. Given the constraints on the DESY campus, only three octants will host beamlines (named OCTU in Fig. 1). Therefore, the facility will reuse the existing PETRA III experimental halls and will build a new one covering two octants of the ring in the West. The remaining octants (named OCTA) will host damping wigglers (DWs) in order to reduce the H6BA lattice emittance from approx. 43 pm rad down to the target value of 20 pm rad. The PETRA IV design operational parameters are summarized in Table 1, more information about the project and its actual status can be found e.g. in Refs. [1, 2].

The small PETRA beam emittance translates directly into much smaller beam sizes of 7 μm in both planes at the insertion device source points, thus imposing stringent requirements on the machine stability. In order to measure beam positions and control orbit stability to the requisite level of

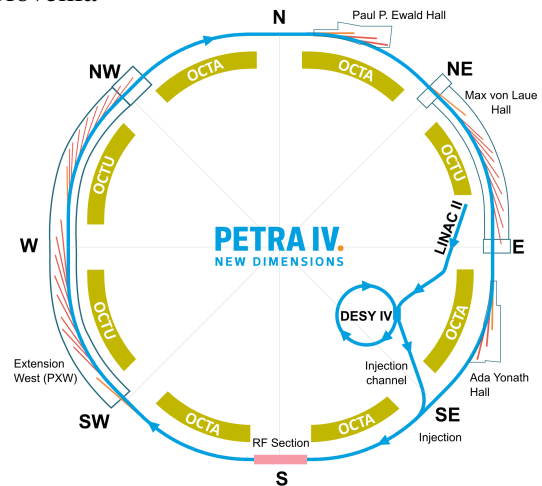


Figure 1: Layout of the PETRA IV facility. Existing experimental halls (Max von Laue, Peter P. Ewald, and Ada Yonath) will be reused, an additional experimental hall in West will be constructed.

Table 1: PETRA IV Main Parameters

Parameter	Value
energy	6 GeV
circumference	2304 m
emittance (with DWs)	20 pm rad
rel. energy spread (with DWs)	0.91×10^{-3}
momentum compaction	3.3×10^{-5}
$\beta_{x,y}$ at IDs	2.2 m, 2.2 m

accuracy, a high resolution BPM system will be installed which consists of 787 individual monitors with the readout electronics based on MTCA.4 as technical platform. In Table 2 the BPM readout specifications are summarized.

As pointed out in Ref. [3], the specific PETRA IV machine geometry has to be taken into account in order to fulfil the requested long-term drift specification. This requires an additional stabilization of the BPM cable paths. Different drift compensation schemes are available and reviewed in Ref. [4]. As outcome of tests performed at PETRA III [3, 5] and of the discussion in Ref. [6] it was decided to use the principle of external crossbar switching where the analogue switching part is separated from the read-out electronics and brought as close as possible to the BPM pickup. Based on this idea DESY and the company I-Tech started a cooperation within the PETRA IV Technical Design Report (TDR) phase. Objectives are development and tests of a MTCA.4

PRELIMINARY EVALUATION OF THE MTCA.4 BPM ELECTRONICS PROTOTYPE FOR THE PETRA IV PROJECT

P. Leban, M. Cargnelutti, A. Bardorfer, M. Oblak, B. Repic, L. Bogataj, P. Paglovec
 Instrumentation Technologies (I-Tech), Slovenia

G.Kube, F.Schmidt-Föhre, K.Wittenburg, Deutsches Elektronen-Synchrotron DESY, Germany

Abstract

Within the PETRA IV project at DESY, the synchrotron radiation source PETRA III will be upgraded into a low-emittance source. The small beam emittance and reduced beam size imply stringent requirements on the machine stability. To meet the requirements on position measurement and orbit stability, a high-resolution BPM system will be installed in the new machine, with about 800 BPMs and MTCA.4-based readout electronics.

In the TDR phase of the project, I-Tech and DESY are cooperating on the realization of a BPM prototype that will demonstrate the feasibility of reaching the PETRA IV requirements. Several analog, digital and SW parts are taken from the Libera Brilliance+ instrument and are reused in the MTCA.4 BPM prototype, with some innovations. One of them is the separation of the RF switch matrix used for long-term stabilization: placing it near the BPM enables also the long RF cables to be stabilized. An 8 channel RTM board, able to acquire signals from two BPMs was developed and is also tested.

This paper presents an overview of the BPM electronics prototype and the promising test results achieved in the Instrumentation Technologies' laboratory with the first boards produced.

PERFORMANCE REQUIREMENTS

The PETRA IV performance requirements for the BPM electronics are presented in Table 1.

Table 1: Performance Requirements for the PETRA IV BPM Electronics

Parameter	Requirement
Resolution on single bunch/turn	< 20 μm RMS (0.5 mA)
Resolution on closed orbit	< 200 nm RMS (at 200 mA in 1600 bunches, 300 Hz bandwidth)
Beam current dependence	$\pm 2 \mu\text{m}$ (0 to -60 dBm range)
Long-term stability at room temperature (25°C)	< 1 μm (6 days, ± 1 K)
FOFB latency	≤ 3 turns

PROTOTYPE DESCRIPTION

The PETRA IV project requirements [1] for the BPM electronics performance could not be met with the

commercially available Libera instrumentation entirely. A characteristic of the machine are the long RF cable paths between the BPM and the BPM electronics which can extend over 150 metres, up to 200 metres. The compensation mechanism in the Libera Brilliance+ instrument is not capable to compensate the disturbances along the cables which makes position readout sensitive to environmental and mechanical factors. To fulfill the 1 μm long-term stability over 6 days ($\Delta T = \pm 1$ K), the RF cables must be compensated well.

Another project-specific requirement is that the BPM electronics hardware should be based on the MTCA.4 standard, with a combination of modules provided either by DESY, by commercial suppliers or developed specifically. In the time frame of the TDR phase of the project, I-Tech developed the RTM module which contains the RF front-end, analog signal conditioning components and the A/D converters. The module connects to the DESY's AMC module [2]. In each of the machine cells, all the BPM electronics, including the Fast-Orbit-Feedback (FOFB) and timing cards, are foreseen to be installed in a single 12-slot chassis. Due to space constraints, a high density of RF channels per BPM module was preferred. Taking into account other constraints, such as power consumption and cooling capabilities, the final RTM design includes 8 RF channels with standard SMA-F connectors and 2 additional RJ-45 connectors. The A/D converters are dual-channel 125 MHz/16 bit and are driven by the clock provided through the HW or SW PLL on-board the RTM module. The reference clock is locked to the turn-by-turn clock of PETRA IV provided by the timing system.

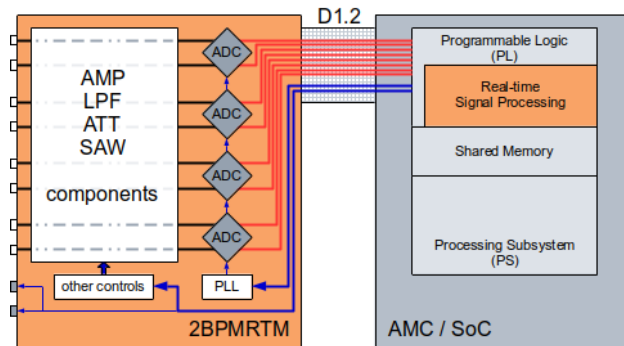


Figure 1: RTM and AMC modules used for the prototype system.

A general-purpose AMC module was used for the development phase and it utilizes a high-performance Zynq Ultrascale+ (ZUP) System-on-Chip (SoC) with 1 GB shared memory for the programmable logic (PL). According to the architecture, only the PL of the SoC is

DETECTION OF A DC ELECTRIC FIELD USING ELECTRO-OPTICAL CRYSTALS

A. Cristiano*¹, M. Krupa, CERN, Geneva, Switzerland
 R. Hill, University of Huddersfield, UK
¹also at University of Huddersfield, UK

Abstract

Standard Beam Position Monitors (BPM) are intrinsically insensitive to beams with no temporal structure, so-called DC beams, which many CERN experiments rely on. We therefore propose a novel detection technique in which the usual BPM electrodes are replaced with electro-optic (EO) crystals. When exposed to an electric field, such crystals change their optical properties. This can be exploited to encode the electric field magnitude onto the polarisation state of a laser beam crossing the crystal. An additional EO crystal, placed outside the vacuum chamber, can be used to control the system's working point and to introduce a sinusoidal modulation, allowing DC measurements to be performed in the frequency domain. This contribution presents the working principle of this measurement technique, its known limitations, and possible solutions to further increase the system's performance. Analytical results and simulations for a double-crystal optical chain are benchmarked against the experimental data taken on a laboratory test bench.

INTRODUCTION

Most high-energy particle accelerators rely on radiofrequency cavities to boost bunches of particles to the desired energy. The power spectral density of such beams extends to high frequencies. However, some physics experiments require particle beams without any temporal structure [1], e.g. the future Search for Hidden Particle (SHiP) experiment at CERN [2]. Since DC particle beams do not induce signals in commonly used Beam Position Monitors, other methods are used to observe their transverse position. Indirect measurements can be performed with Schottky monitors [3], but they require some integration time. On the other hand, screen-based BPMs [4] interact with the particle beam and unavoidably affect its parameters which can deteriorate the beam. To address these issues, a novel BPM based on electro-optical crystals and suitable for measurement of DC beams (EO-DC-BPM) is under development at CERN.

Under an electric field exposure, EO crystals' properties change linearly due to the Pockels effect [5]. This variation can be encoded into the polarisation state of a laser beam crossing the crystal and later decoded through interferometric or amplitude demodulation techniques. The fast response of the Pockels effect makes EO crystals suitable for high frequency diagnostic tools. A high-frequency EO BPM capable of detecting variations of the transverse position within a bunch of a particle beam is currently under development for

the HL-LHC project [6]. However, EO crystals are dielectric and in a presence of a DC or quasi-DC electromagnetic field, free charge carriers move to their boundaries and create an internal electric field obstructing the external field. This reduction of the modulation depth leads to a measurement error and has limited the use of EO materials to measurements above 20 Hz [7], unless the space charge is avoided through mechanical rotary stages [8].

Until now, the EO-DC-BPM development has focused on studying the feasibility of using an optical chain based on EO-crystals for measurements of the intensity of an electrostatic field in frequency domain. A proof-of-concept test bench has been designed to scrutinize the experimentally obtained results against those expected from simulations.

ELECTRO-OPTIC DC FIELD SENSOR

The EO-DC-BPM consists of four identical optical branches arranged symmetrically around the vacuum chamber. Each branch accommodates a chain of two electro-optical crystals. One crystal is placed inside the vacuum chamber and couples to the electrostatic field of the particle beam. The other crystal remains outside and is externally modulated with a sinusoidal field to move the measurement to the frequency domain. On top of the modulation signal, a DC bias is used to tune the system and to compensate crystal drifts which can lead to measurement error.

A conceptual overview of a single optical branch of the EO-DC-BPM is shown in Fig. 1. The sensor is composed of two EO crystals made of Lithium Niobate (LiNbO_3) which was chosen due to its large EO coefficients, low conductivity [9] and high radiation hardness [10] compared to other EO materials. The optical axes of the crystals are aligned with the z -axis. A linearly polarised laser beam traverses the crystals along the y -axis and oscillates in x - z plane.

The input polariser fixes the laser beam's polarisation at 45° with respect to the x -axis. The laser beam then enters

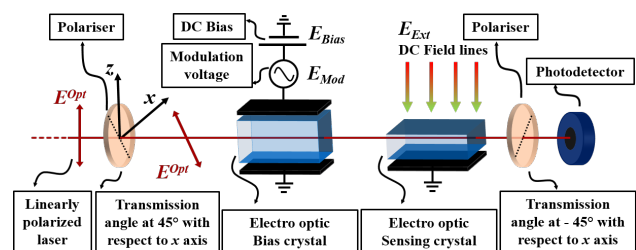


Figure 1: Schematic view of one optical branch of the EO-DC-BPM.

* antonio.cristiano@cern.ch

HL-LHC BPM SYSTEM DEVELOPMENT STATUS

M. Krupa*, I. Degl'Innocenti, D. Gudkov, G. Schneider, CERN, Geneva, Switzerland
D. R. Bett, University of Oxford, UK

Abstract

The demanding instrumentation requirements of the future High Luminosity LHC (HL-LHC) require 44 newly designed Beam Position Monitors (BPM) to be installed around the ATLAS and CMS experiments in 2026–2028. Three BPM types are now in pre-series production, with two more variants under design. Close to the collision point, a set of cryogenic directive coupler BPMs equipped with a brand new acquisition system based on nearly-direct digitization will resolve the position of the two counter-rotating LHC beams occupying a common vacuum chamber. Other new button and stripline BPMs will provide not only the transverse beam position, but also timing signals for the experiments, and diagnostics for the new HL-LHC crab cavities. This contribution summarizes the HL-LHC BPM specifications, gives an overview of the new BPM designs, reports on the pre-series BPM production status and plans for series manufacturing, outlines the foreseen acquisition system architecture, and highlights the first beam measurements carried out with the proof-of-concept electronics for the directive stripline BPMs.

INTRODUCTION

The High Luminosity LHC (HL-LHC) project aims to significantly boost the LHC performance with a series of major upgrades scheduled to take place in 2026–2028 [1]. Most notably, the two regions housing the large ATLAS and CMS experiments will be overhauled including a complete replacement of the low-beta Inner Triplets (IT) with higher gradient focusing magnets to produce an even smaller beam size at the Interaction Points (IP) where the LHC beams collide. Further increase of the instantaneous luminosity will be possible thanks to crab cavities (CC) installed on each side of ATLAS and CMS. The CC installed upstream from the IP will tilt each circulating bunch transversely such that at the IP it collides head-on with the counter-rotating bunch. The CC on the other side of the IP will reverse this tilt to cancel out any transverse oscillation outside of the crabbing region between two CCs.

SYSTEM OVERVIEW

The HL-LHC ITs will require a set of new Beam Position Monitors (BPM) to reliably control the orbit of extraordinarily small beams. Moreover, additional specialized BPMs are needed near the CCs to tune and monitor the crabbing process as well as to watch for any beam instabilities [2]. In total, 44 new BPMs of 5 types will be installed as part of the HL-LHC project. Figure 1 shows the arrangement of the new BPMs on each side of the IP in the HL-LHC era.

* michal.krupa@cern.ch

The six BPMs closest to the IP (BPMQSTZA and BPMQSTZB types) are installed inside the continuous cryostat of the new HL-LHC IT where both counter-rotating beams will circulate in a common vacuum chamber. Therefore, these BPMs must be able to distinguish the position of each beam independently. Such a feature, referred to as directivity, is typical of directional coupler BPMs in which the passing beam induces signals on four long antennas (commonly called striplines) parallel to the beam motion axis [3]. The striplines are connectorised on each end and are designed such that the majority of the beam signal couples only on the upstream port with a much smaller (around 5%) parasitic signal leaking to the downstream output. To further reduce the cross-talk between the two beams, the HL-LHC directional couplers will be installed in locations where bunches of both beams arrive at different times with the temporal separation ranging from 3.9 ns (approximately 3 times larger than the bunch length) up to 10.5 ns depending on the BPM location. The measurement error due to the presence of the other beam will also be reduced through digital signal processing with a new dedicated fast-sampling data acquisition system [4]. All HL-LHC directional coupler BPMs will operate at a cryogenic temperature within the 60–80 K range. Moreover, the BPMQSTZB type BPMs will be equipped with shielding blocks made out of tungsten to decrease the ionizing dose received by the nearby superconducting magnets [5].

Further away from the IP, after the separation-recombination dipoles, both beams circulate in separate vacuum chambers. A standalone double-aperture cryogenic dipole will be equipped with two capacitive button BPMs (one per beam, BPMQBCZA/B type) installed within the magnet's cryostat and operating at 4.5–20 K. The signals of these BPMs will be measured by the currently used LHC BPM data acquisition system [6].

The remaining three room-temperature BPMs installed after the CCs will not become part of the main LHC BPM system but will instead serve very special users. The two BPTQR type BPMs will replace the initially foreseen APWL pick-ups as the main diagnostic monitors for the crab cavities. These BPMs will be connected to dedicated electronics and will combine three different BPMs in a single unit:

- a set of capacitive buttons for phasing the CCs with the beam and for filtering the CC antenna signal,
- a pair of 94 mm-long stripline antennas for the CC amplitude and noise feedback at the 800 MHz component,
- a pair of Electro-Optical (EO) buttons [7] or a pair of 400 mm-long stripline antennas for wideband measurements of beam instabilities introduced by the CCs.

The detailed BPTQR design is not yet frozen, and some technical decisions (e.g. the choice between EO buttons and stripline antennas) will be taken in the following years.

CAVITY BPM ELECTRONICS FOR SINBAD AT DESY

B. Lorbeer*, M. Werner, T. Lensch, I. Kroupchenkov, H. T. Duhme, S. Vilcins, D. Lipka
Deutsches Elektronen-Synchrotron DESY, Hamburg, Germany

Abstract

The SINBAD (Short and INnovative Bunches and Accelerators at DESY) R&D accelerator is planned for studying new concepts for high gradient electron beam acceleration and the generation of ultra-short electron bunches. The accelerator called ARES (Accelerator Research Experiment At DESY) is composed of S-band accelerating structures. In order to achieve the goal of very short electron bunches the electron beam charges generated in the RF (radio frequency) Gun can vary in a range from 200 pC down to 500 fC. A new type of high resolution cavity BPM (beam position monitor) has been developed to measure the beam position with good resolution at small charge down to 500 fC. One key component in the BPM system are the custom RF front-end receiver electronics to meet the resolution requirements in the required charge range. The entire BPM system with a focus on the system design requirements and the MicroTCA based RF electronics are presented in this paper.

INTRODUCTION

The S-band electron linear accelerator ARES at DESY in Hamburg, Germany is build for studying novel acceleration techniques including a beam manipulation testbed, accelerator components and concepts for autonomous accelerator operation. Its target parameters are an energy of 50 MeV-155 MeV, a charge of 0.5 pC-200 pC. A single electron bunch at the rate of 50 Hz is generated by an RF-Gun in which the electrons are released from a cathode by making use of a photocathode laser. The machine has already been successfully commissioned and first experiments have been carried out [1–4]. The diagnostics include eight high resolution in-house developed cavity BPM (beam position monitors) which are distributed at significant locations along the 50 m long machine [5]. An overview of the machine with two BPMs currently under test is shown in Fig. 1.

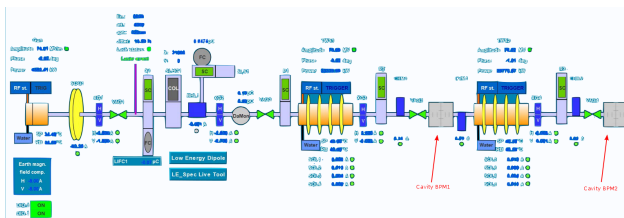


Figure 1: Extraction from ARES Linac operation panel with two cavity Beam Position Monitors.

The key specification of the cavity BPM system are position measurements at bunch charges from 500 fC up to

1 nC. The challenging requirement in precision and accuracy at the smallest charge is 5 μm in a measurement range of 100 μm while averaging over 25 bunches. The single bunch resolution requirement over a range of 700 μm is 35 μm [6].

CAVITY BEAM POSITION MONITOR

In order to determine the bunch charge and position of the electron bunch in the beam-pipe a monopole and two dipole excited modes in the cavity are necessary [7, 8]. The excited monopole mode shows a proportionality to the electron bunch charge and two excited dipole modes deliver proportionalities to the horizontal and vertical position of the electron bunch. The measured voltages are $V_{mon} \propto q$ and $V_{dipole} \propto x_{pos}, y_{pos}$ respectively. The realization of the cavities for measuring the amplitudes of monopole and dipole modes are based on a tedious design procedure of the vacuum chamber which includes electromagnetic field simulation and tolerance studies before it could be produced. More details can be found in [9]. A simplified electromagnetic simulation model of the cavity is shown in Fig. 2.

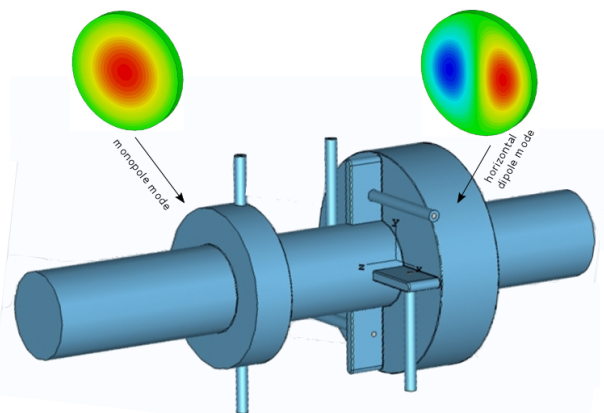


Figure 2: Simulation model of Cavity Beam Position Monitor. Monopole and dipole modes have symmetric ports to maintain symmetric fields around the beam axis. The measurement system only uses one of the ports and the other is terminated with 50 Ohm.

The mono and dipole cavity geometries have been chosen to be compatible with existing BPM monitors already installed at the E-XFEL and FLASH at DESY, Hamburg, Germany. Both machines operate with high repetition rates of the electron bunch of up to 4.5 MHz. Therefore a loaded quality factor of around 70 has been a feasible choice to avoid an overlap of subsequent bunches. The design procedure also aimed for high sensitivities of monopole and dipole cavities to deliver sufficient signal power at very low charges.

* bastian.lorbeer@desy.de

XFEL PHOTON PULSE MEASUREMENT USING AN ALL-CARBON DIAMOND DETECTOR

C. Bloomer^{*,1}, L. Bobb, Diamond Light Source Ltd, Didcot, UK
M. E. Newton, University of Warwick, Coventry, UK
W. Freund, J. Grünert, J. Liu, European XFEL, Schenefeld, Germany
¹also at University of Warwick, Coventry, UK

Abstract

The European XFEL can generate extremely intense, ultrashort X-ray pulses at MHz repetition rates. Single-crystal CVD diamond detectors have been used to transparently measure the photon beam position and pulse intensity. The diamond itself can withstand the power of the beam, but the surface electrodes can be damaged since a single pulse can already exceed the damage threshold of the electrode material. Presented in this work are pulse intensity and position measurements obtained at the European XFEL using a new type of all-carbon single-crystal diamond detector developed at Diamond Light Source. Instead of traditional surface metallisation, the detector uses laser-written graphitic electrodes buried within the bulk diamond. There is no metallisation in the XFEL X-ray beam path that could be damaged by the beam. The results obtained from a prototype detector are presented, capable of measuring the intensity and 1-dimensional X-ray beam position of individual XFEL pulses. These successful measurements demonstrate the feasibility of all-carbon diagnostic detectors for XFEL use.

INTRODUCTION

The European XFEL is a radiation source characterised by ultrashort pulse duration, high pulse intensities, high repetition rates, and almost complete transverse coherence. Individual pulses can contain up to 4 mJ of energy, delivered in a pulse that is less than 100 fs long [1,2]. It is important to monitor the XFEL pulse parameters such as intensity, beam size, and beam centroid position. Pulse-by-pulse capabilities are extremely useful as individual pulses vary considerably due to the stochastic nature of the light generation process in an XFEL. Making such measurements “transmissively”, enabling the majority of the pulse energy to pass through the beamline into the instrument for the user experiment, is an increasingly important part of normalising data for fluctuations of the photon pulse parameters. Obtaining pulse-by-pulse X-ray beam size and position measurements in particular is extremely difficult, and there are very few techniques available that can achieve this. A general overview of XFEL beamline diagnostics can be found in Ref. [1].

On-line diagnostics that can be safely placed in the X-ray beam path and withstand the beam powers can be challenging to develop. Any beam instrumentation needs to be designed to survive the single-shot and multi-bunch beam intensities, while also making measurements of the X-ray beam without

interfering with the beam delivery and user experiments. The peak power is sufficient to damage many materials placed in the beam path. Because of the extremely short pulse lengths, thermal transport does not remove any heat from intercepting diagnostics during the pulse duration itself, even for extremely good heat conductors such as copper or diamond [3], a factor exacerbated by the high repetition rate of the XFEL pulses in the MHz range. Under a sufficiently focused X-ray beam, most materials placed directly in the beam path will suffer ablation, and the upper layers of the material will vaporise due to absorption of energy from a single XFEL pulse. For this reason, instruments made of low atomic number materials such as diamond are useful, as photon absorption is lower resulting in lower absorbed power densities.

Single-crystal CVD diamond detectors show great promise for XFEL beam diagnostics. Compared to other detector materials, diamond has superior radiation tolerance, excellent thermal conductivity, and fast response times (i.e. fast charge carrier drift velocities). CVD diamond has found many uses at XFEL beamlines: as a scintillator screen material for beam profile imaging (when appropriately doped) [4], as a foil to generate backscattered photons for simple position or intensity monitoring [5], and most recently as solid-state ion-chamber flux intensity monitors [6, 7]. The diamond itself can withstand the power of the beam, but the pulses can deposit sufficient energy into the detector that surface electrodes and other metallisation in the beam path may be damaged by the radiation.

Presented in this work are proof-of-principle pulse intensity and position measurements obtained at the European XFEL using a new type of all-carbon single-crystal diamond detector developed in collaboration between University of Warwick and Diamond Light Source.

DETECTOR DESIGN

The detector used for this work utilises laser-written graphitic electrodes, instead of traditional surface metallisation. These are fabricated using an ultrashort pulse laser technique. At the laser focal point there is sufficient energy deposited into the diamond that a local phase transition can take place: electrically non-conductive diamond is converted into conductive graphite. Diamond detectors using such electrodes were first demonstrated in the early 2010s [8].

These buried graphitic electrodes offer several advantages that make them more resistant to damage than surface metallised electrodes. Firstly, they very closely match the sur-

* chris.bloomer@diamond.ac.uk

PSF CHARACTERIZATION OF THE ALBA X-RAY PINHOLES

U. Iriso, Z. Martí, A. A. Nosych, ALBA Synchrotron, Cerdanyola del Vallès, Spain
A. Cazorla, ICMAB, Campus UAB, Bellaterra, Spain
I. Mases, CERN, Geneva, Switzerland

Abstract

ALBA is currently equipped with two X-ray pinhole cameras for continuous beam size monitoring using the synchrotron radiation from two different bending magnets. The first pinhole was installed on day-1 and it is working properly since 2011 as the work-horse for the ALBA emittance measurements. The second one has been commissioned in early 2021 for redundancy purposes. This paper summarizes the exercises to characterize the Point Spread Function (PSF) of both pinhole cameras using analytical calculations, SRW simulations, and experimental measurements.

INTRODUCTION

Measuring the transverse beam size and emittance of the electron beam is an essential tool to control the machine performance. Since the ALBA commissioning in 2011, this was carried out using an X-ray pinhole camera located in FE34 [1]. During the last years, at ALBA we have performed other means to infer the beam emittance based on the Synchrotron Radiation Interferometry (SRI) [2] or Heterodyne Near Field Speckles (HNFS) [3]. Nevertheless, we found the X-ray pinhole camera as a more robust set-up, and so we have finally decided to install a second unit for redundancy purposes, this time located in FE21 - almost on the opposite side of the storage ring.

In a pinhole (see Fig. 1), the source image (the electron beam) is amplified at the image plane by a factor $X = L_2/L_1$, where L_1 is the distance between the source point and the pinhole, and L_2 corresponds to the distance between the pinhole and the image plane (YAG screen).

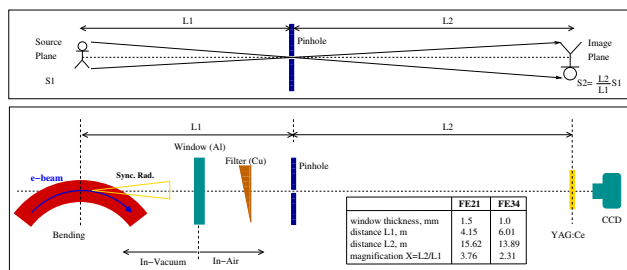


Figure 1: Top: general working principle of a pinhole imaging system. Bottom: sketch of the X-ray pinhole cameras at ALBA, with the geometrical parameters of FE21 and FE34.

But imaging with a pinhole requires a thorough characterization of the pinhole Point Spread Function (PSF, or σ_{PSF} in the following), which is the beam size measured at the image plane corresponding to a point-like source. If σ_e is the electron beam size, the size measured at the YAG screen

in Fig. 1 is affected by the σ_{PSF} by:

$$\sigma_{\text{YAG}}^2 = (X\sigma_e)^2 + \sigma_{\text{PSF}}^2. \quad (1)$$

This paper summarizes the exercises to characterize the PSF of both ALBA pinhole cameras using analytical calculations, SRW simulations [4], and experimental measurements using the beam lifetime. For reference, Table 1 lists the main beam parameters for both pinholes.

Table 1: Twiss Parameters at FE21 and FE34, and Main Operation Parameters of ALBA

	FE21	FE34
hor beam size, μm	55	60
ver beam size, μm	24	27
hor beta function, m	0.52	0.435
ver beta function, m	22.83	25.82
hor dispersion, mm	20.1	37.1
ver dispersion, mm	7.0	11.5
energy spread, %	$1.05 \cdot 10^{-3}$	
emittance, nm-rad	4.6	
coupling, %	0.5	
energy, GeV	2.98	

BEAMLINER SETUP

Both ALBA set-ups (see Fig. 1, bottom) follow the classical design in other light sources [5]: the source point (a bending dipole in both cases) emits synchrotron radiation, and the visible and soft X-rays part are filtered out by an Aluminium window. Furthermore, the Al-window separates vacuum from in-air components. Next a Copper filter whose length can be varied between 0 mm and 5 mm is used to attenuate or harden the X-rays before they hit the pinhole. This is a μm size hole, which is properly aligned using a motorized stage (see next sub-section). Finally, an imaging system consisting in a YAG screen with an optical set-up transforms the X-rays into visible light to form the image and obtain the beam size.

The paper focuses on the cases with and without the use of Cu filter. By optimizing the contrast in Control Room during normal operation conditions, we work with a Cu thickness of 0.3 mm. In order to compare the Cu filter effect, the paper focus the study on four cases:

- FE21, 1.5 mm of Al
- FE21, 1.5 mm of Al, and 0.3 mm of Cu
- FE34, 1.0 mm of Al
- FE34, 1.0 mm of Al, and 0.3 mm of Cu

SECONDARY ELECTRON EMISSION (SEM) GRID FOR THE FAIR PROTON LINAC

J. Herranz, Proactive R&D, Sabadell, Spain

T. Sieber, P. Forck, GSI, Darmstadt, Germany

I. Bustinduy, A. Rodriguez Paramo, ESS Bilbao, Zamudio, Spain

A. Navarro Fernandez, CERN, Geneva, Switzerland

Abstract

New SEM-Grid has been developed for FAIR Proton Linac, the instrument consists of 2 harps fixed together in an orthogonal way. This SEM-Grid will provide higher resolution and accuracy measurements as each HARP consists of 64 tungsten wires 100 μm in diameter and 0.5 mm pitch. Each wire is fixed to a ceramic PCB with an innovative dynamic stretching system, this system assures wire straightness under typical thermal expansion due to beam heat deposition. Simulation calculations of electric field distribution have been performed, three main parameters have been optimized, wires distribution, quantity of polarization electrodes and distance between electrodes and wires. The design and production of the SEM-Grid has been performed by the company Proactive R&D that has counted on the expertise of ESS-Bilbao to define safe operation limits and signal estimation by means of a code developed specifically for this type of calculations. Preliminary validations of the first prototypes have shown excellent mechanical and electrical behaviour. After the successful beam test validations performed in June 2022, final series of the SEM-Grid will be produced to be installed on FAIR proton LINAC.

FAIR PROJECT INTRODUCTION

The FAIR [1] facility at GSI will provide antiproton and ion beams of worldwide unique intensity and quality for fundamental physics research.

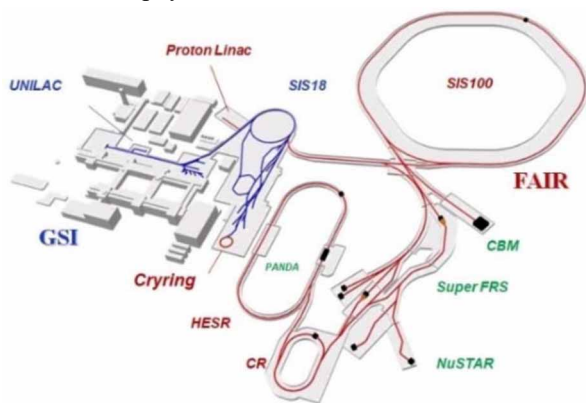


Figure 1: Layout of the FAIR facility.

The accelerator facility of FAIR, shown in Fig. 1, will include three linear accelerators, the existing UNILAC (for which a refurbishing program is currently on the way), a superconducting cw-Linac, designed mainly for intermediate energy experiments [2], and the new proton Linac (pLinac) [3]. The UNILAC and pLinac will be the

main injectors of SIS18, which will in turn be an injector for SIS100, the central accelerator component of FAIR.

The pLinac consists of a novel so called ‘Ladder’ RFQ [4] followed by two $\sim 10\text{ m}$ sections of Cross Bar H-driфтtube accelerator (CH) structures [5]. The first section includes six CH modules, which are pairwise rf-coupled (Coupled CH or CCH). The second section consists of three separate modules, each connected to its own klystron. The pLinac will deliver a current up to 70 mA with a macropulse length of 35 μs (at max. 4 Hz) and a typical bunch length of 100 ps. The design energy is 68 MeV. Figure 2 shows a schematic of the pLinac and its beam instrumentation.

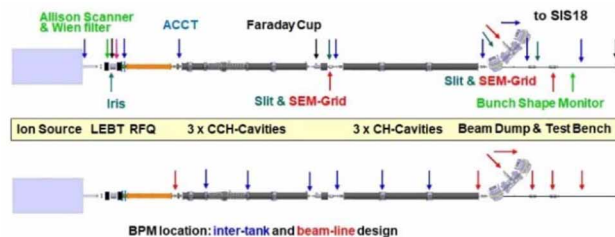


Figure 2: Schematic of the FAIR pLinac, side view, showing the location of diagnostics (upper) and BPMs, divided in cavity (inter-tank) and beamline BPMs (lower).

The overall diagnostics concept and layout of pLinac has been described in various reports, e.g. [6]. Because of the compact structure of the two CH sections, diagnostics (except BPMs) will be concentrated in the LEBT, in the MEBT behind the RFQ and in a diagnostics/rebuncher (so called SD) section between the CCH and CH parts of the pLinac. Additional beam diagnostics elements are placed in the transfer line to SIS18 as well as in a straight line to the beam dump.

Special care has been taken for the design of the SEM Grids. We expect a 1σ beam radius of 1.5 mm in the ‘‘worst case’’, therefore the wire pitch cannot be larger than 0.5 mm to obtain realistic profiles. Moreover, a stretching mechanism is required to compensate for thermal expansion, even if the grids are operated in a ‘‘grid protection mode’’ at reduced duty cycle. Any kind of plating on the tungsten wires must be considered carefully because of possible melting and agglutination during irradiation.

SEM GRID DESIGN

The working principle of SEM grids is based on secondary electrons, which are released from the grid wires upon ion beam impact. The resulting current distribution

EMITTANCE DIAGNOSTICS AT PETRA IV

M. Marongiu*, G. Kube, M. Lantschner, A. Novokshonov, K. Wittenburg
 Deutsches Elektronen-Synchrotron DESY, Germany

Abstract

The PETRA IV project will be a Diffraction Limited Light Source designed to be the successor of PETRA III, the 6 GeV 3rd generation hard X-Ray synchrotron light source at DESY in Hamburg. It will operate at a beam energy of 6 GeV with a design emittance of 20/4 pm rad. For a precise emittance online control, two dedicated diagnostics beamlines will be built up to image the beam profile with synchrotron radiation in the X-Ray region. With two beamlines, it will be possible to extract both the transverse beam emittances and the beam energy spread. Both beamlines will be equipped with two interchangeable X-Ray optical systems: a pinhole camera system to achieve high dynamic range and a Fresnel Diffraction system for high resolution measurements in the range 1-18 μm. This paper describes the planned setup and deals with the possible limitations.

INTRODUCTION

The PETRA IV project [1] will be a Diffraction Limited Light Source designed to be the successor of PETRA III, the 6 GeV 3rd generation hard X-Ray synchrotron light source at DESY in Hamburg. It will operate at a beam energy of 6 GeV with a design emittance of 20/4 pm rad instead of the 1300/10 pm rad currently obtained in PETRA III. The machine will be installed in the same tunnel of the current operating one. Table 1 summarizes the main parameters of PETRA IV and PETRA III.

Table 1: Main Parameters of PETRA IV Compared with the Values Currently in Use at PETRA III

Parameters	PETRA IV	Petra III
Energy (GeV)	6	6
Circumference (m)	2304	2304
Current (mA)	80/200	100/120
Number bunches	80/1600	40/480
Emittance (pm rad)		
Horizontal	<20	1300
Vertical	<4	10
# Undulator beamlines	30	21 (26)

For a precise emittance online control, two dedicated diagnostics beamlines will be built up to image the beam profile with synchrotron radiation in the X-Ray region. With two beamlines in locations with different dispersion, it will be possible to extract both the transverse beam emittances and the beam energy spread. The emittance sensitivity required is 0.5 pm rad which translates in a beam size sensitivity requirement of 100 nm.

* marco.marongiu@desy.de

It will be also required to have a high dynamic range measurement; therefore, each beamline will be equipped also with an X-Ray pinhole camera system (XPC) to measure beam size above 15 μm. Figure 1 shows a sketch of the designed beamline. The overall beamline length of about 50 m derives from the requirement to place the detector part outside the accelerator tunnel.



Figure 1: Beamline sketch of the emittance measurement.

Different locations for the beamlines have been considered and, due to geometric constraints, it has been chosen a canted section using as a radiation source a 3 Pole Wiggler (3PW) with a peak magnetic field of around 0.8 T. Table 2 shows the main beam parameters at the beamline locations.

Table 2: Main beam parameters at the possible beamlines locations. The last column represents the relative dispersion contribution to the emittance. The 3 pole wiggler (3PW) considered has a peak magnetic field of around 0.8 T.

Rad. Source	β_x m	β_y m	σ_x μm	σ_y μm	D. %
3PW	4.6	4.6	9.6	4.3	0.04
3PW	2.6	2.6	8.1	3.3	10.3

X-RAY FRESNEL DIFFRACTOMETRY

In order to achieve a high resolution measurement, the X-Ray Fresnel diffraction technique [2] (XFD) has been considered. Optimizing opportunely a single slit width (A), a double-lobed pattern emerges and the depth of its median dip is correlated to the source size (i.e. the dip becomes shallow with the increase of the source size). Figure 2 shows a sketch of the technique: the choices of the distance of the slit to the source point (L), the distance from the slit to the observation point (R) and the observing wavelength (λ) determine the slit width. The only requirement for the light

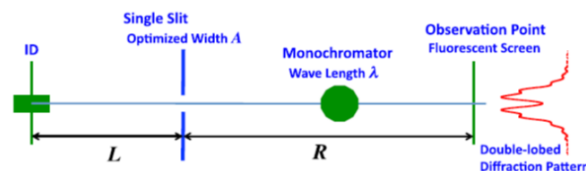


Figure 2: Sketch of the XFD measurement [2].

MERITS OF PULSE MODE OPERATION OF RESIDUAL GAS IONIZATION PROFILE MONITOR FOR J-PARC MAIN RING*

Kenichirou Satou[†], Susumu Igarashi, and Yoichi Sato, J-PARC/KEK, Tokai, Japan

Abstract

The measurement accuracy of the ionization profile monitor (IPM) of J-PARC main ring (MR) depends on the flatness and stability of the gain of the position-sensitive microchannel plate (MCP). The flatness of the MCP deteriorates after long-term operation; the gain of the central area selectively decreases as the integrated output charge increases. The beam-based calibration, where the local bump shifts the beam and the reconstructing beam profiles determine the gain distribution, is used to calibrate the flatness. The immediate gain drop occurs when the output current from the MCP becomes comparable to the bias current is problematic. This gain drop depends on the bias voltage and the output current; thus, it is difficult to calibrate. A pulsed HV module of 30 kV, which collects ionized electrons and ions, was installed to solve these problems. The pulse mode operation can modulate the averaged output current from the MCP to improve gain stability. Profiles of the intense beam up to $3.3E13$ particles per bunch were measured and compared with those measured by destructive profile monitors in beam transport lines 3–50 BT, and the Abort line. Estimated emittances were consistent at $\pm 20\%$.

INTRODUCTION

The idea of detecting ionized electrons or ions generated by the interaction with residual gas to measure a beam profile was reported in the mid-1960s [1, 2]. The residual gas ionization profile monitor (IPM) has been widely used in proton and hadron synchrotrons because of its non-invasiveness to the beam since it does not insert solid material or gas into the beam. A small rate of nuclear collision with residual gas particles is preferable to a high-power proton synchrotron on its low beam power loss and thus lower induced remnant dose.

The first IPM system in KEK was used at KEK-PS [3], where the system collected positive ions using an external electric field (E_{ex}). These ions were detected using a microchannel plate (MCP). Similar monitors were designed for the J-PARC main ring (MR) and installed in 2008 [4-6]. These were operated in the ion collection using an intensive E_{ex} of 50 kV across 130 mm-size cage electrodes at the maximum. A horizontal type IPM (D2HIPM) and a vertical type IPM (D2VIPM) were installed in a straight line named *Ins_B*, where the horizontal dispersion function is zero. However, another horizontal type IPM (D3HIPM) is installed in the arc section, named *Arc_C*, where the horizontal dispersion function was non-zero. The Twiss parameters at these IPMs are $(\beta_x, \beta_y, \eta_x) = (12.1 \text{ m}, 27.3 \text{ m}, 0 \text{ m})$,

(13.1 m, 21.6 m, 0 m), and (8.4 m, 15.5 m, 2.0 m) for D2VIPM, D2HIPM, and D3HIPM, respectively. The MCPs are a two-stage type with 32 multi-strip anodes of 2.5 mm (in width), a glass tube with 15 μm in diameter, and an effective area of 30 mm \times 80 mm. The resistances are 112 M Ω for D2HIPM and 120 M Ω for D2HIPM, respectively.

A fast data-taking system has realized the turn-by-turn (TxT) measurement. The TxT profiles are used widely in correction of dipole and quadrupole injection mismatches [7]. However, it was strenuous to measure beam emittance due to the strong beam space charge (E_{sc}) of MV/m level, signal purity contaminated with secondary electrons, and MCP's dynamic gain deterioration that occurred several msec after the electron multiplication occurred.

We modified the original DC type IPM to a gated IPM, where the pulsed E_{ex} is applied to switch the system in $\sim 20 \mu\text{s}$ to solve the MCP's dynamic gain deterioration. The remaining sections describe this IPM system for J-PARC MR and the merits of pulse mode operation. Finally, the estimated accuracy of the system checked with the multi-ribbon profile monitors (MRPMs) in beam transport lines is presented.

IPM IMPROVEMENTS

At the initial stage of beam commissioning, where the beam intensity is 1/10 of the designed intensity of 4E13 ppb, three IPM systems were designed to collect positive ions with strong E_{ex} [4-6].

The dipole magnets were installed only in the D2HIPM to collect electrons against strong E_{sc} to measure an intense beam of several E13 particles per bunch (ppb) [8]. The guiding dipole field of $B_g = 0.2 \text{ T}$ was applied parallel to the vertical component E_{ext} , which was used to direct the electrons to the MCP. The B_g and the horizontal E_{sc} (E_{sc-x}) component produce an $E \times B$ drift motion, which converts the transversal kick by the E_{sc-x} to the longitudinal drift motion.

Measuring only the ionized electrons, which are ~ 1000 electrons per bunch, is challenging. The contaminant of secondary electrons degenerates the signal purity and the measurement accuracy. To subdue the secondary electrons generated by the ion's impacts on the electrodes, we applied a simple idea of using a window on cage electrodes to collect the ions and demonstrated it first on IPM for the CERN PS [9]. This structure is called an ion trap. Applying the same idea subdues the secondaries onto the MCP detector and improves signal purity significantly [10].

It is necessary to check the difference in signal intensity between the ion and electron collection to check the signal purity; besides the detection efficiency of MCP, which is 10%–60% for electrons and 60%–85% for ions, in the case

* Work supported by Accelerator and Beamline Research and Technology Development for High-Power Neutrino Beams in the U.S.-Japan Science and Technology Cooperation Program in High Energy Physics.

[†] email address: kenichirou.satou@j-parc.jp

EXPERIMENTAL INVESTIGATION OF GOLD COATED TUNGSTEN WIRES EMISSIVITY FOR APPLICATIONS IN PARTICLE ACCELERATORS

A. Navarro*, M. Martin, F. Roncarolo, CERN, Geneva, Switzerland

Abstract

The operation of wire grids and wire scanners as beam profile monitors can be heavily affected, both in terms of measurement accuracy and wire integrity, by the thermal response of the wires to the energy deposited by the charged particles. Accurate measurements of material emissivity are crucial, as Radiative Cooling represent the most relevant cooling process. In this work, we present a method for emissivity measurements of gold-coated tungsten wires based on calorimetric techniques. The dedicated electrical setup allowed transient and steady state measurements for temperatures up to 2000 K. A theoretical description of the measurement technique will be followed up by the electrical set up description and a detailed discussion about the measured results and uncertainties.

INTRODUCTION

Wire grids are examples of thin target detectors extensively used in particle accelerators for transverse beam profile measurements [1]. Depending on the the detector characteristics and beam parameters (intensity, energy, transverse and longitudinal beam size) the operation of the monitor can result in thermo-mechanical stresses, potentially perturbing the measurement accuracy and degrading the monitor integrity. To prevent these circumstances, a thorough understanding of the particle-detector interactions is of critical importance.

For simulating the particle-detector interaction and predict detector material heating and damage, a finite difference program has been implemented [2]. Uncertainties in the material properties such as melting (or sublimation) temperatures, heat capacity, thermal conductivity and/or emissivity, can induce large uncertainties in the simulation results. For published values in the scientific literature of the emissivity of tungsten wires (commonly used in particle accelerators), large uncertainties can be found. Figure 1 shows some examples of reported emissivity values as a function of the temperature.

To reduce the uncertainties of the thermal evolution models, we decided to experimentally measure the emissivity of gold-coated tungsten wires, widely used at CERN for wire grid detectors. Many techniques can be used for measuring the emissivity [3–5]. Each method has its own inherent advantages and drawbacks. The calorimetric method was used for the measurements reported in this paper. This methods gives information about the total hemispherical emissivity. The main advantage of this method is that it can measure

small sample ($\sim \mu\text{m}$) sizes and it does not require expensive or sophisticated equipment. It is a direct absolute method, so no standard emissivity reference is necessary. Some disadvantages are: it is time consuming because it is typically performed in steady state; the sample needs to be placed under vacuum (typically 10^{-5} bar) to avoid convective losses; the measurement of the surface temperature is a big source of uncertainty.

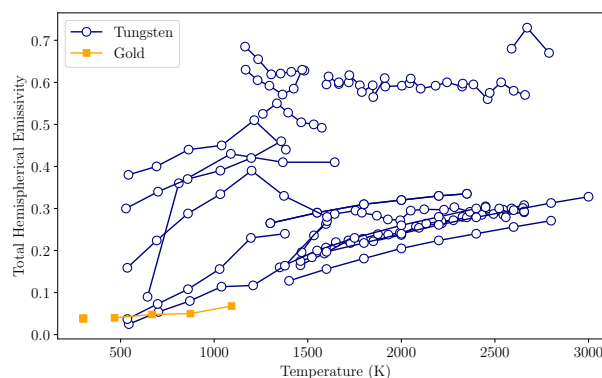


Figure 1: Examples of reported emissivity measurements for Gold and Tungsten. From Ref. [6].

SPECIFICS OF THE CALORIMETRIC METHOD

The calorimetric method is based on studying the energy balance of the sample material at a certain temperature, which is maintained via joule effect. For a temperature T , the resistance of a wire, with a wire length $l(T)$, can be calculated by:

$$R(T) = \frac{\rho(T)l(T)}{S_f}, \quad (1)$$

where S_f is the section of the wire assumed to be constant over its length. $\rho(T)$ is the resistivity of the material and $l(T)$ is the length of the sample, and they are both dependent on the material temperature. As a first approximation, $l(T)$ can be modeled as a linear increase, $\Delta l(T) = l_0 \alpha_l (T - T_0)$, where α_l is the coefficient of thermal expansion. It is difficult to give a simple mathematical description of the variation of the resistivity with temperature, as it is very much material dependent. Tabulated values of the resistivity as a function of temperature can be found in literature.

Once thermal equilibrium is reached for a specific intensity, the average temperature of the sample can be determined by measuring the resistance and comparing it to the known values of R/R_0 for the material. The energy balance of the

* araceli.navarro.fernandez@cern.ch

ASSESSING THE PERFORMANCE OF THE NEW BEAM WIRE SCANNERS FOR THE CERN LHC INJECTORS

S. Di Carlo*, W. Andreazza, D. Belohrad, J. Emery, J.C. Esteban Felipe, A. Goldblatt, D. Gudkov, A. Guerrero, S. Jackson, G.O. Lacarrere, M. Martin Nieto, A.T. Rinaldi, F. Roncarolo, C. Schillinger, R. Veness
European Organization for Nuclear Research (CERN), Geneva, Switzerland

Abstract

Reliably measuring the transverse beam profile in the LHC injector chain is essential for the operation of the CERN accelerator complex. This report aims to assess the reliability, stability, and reproducibility of a new generation of beam wire scanners developed at CERN in the framework of the LHC Injectors Upgrade (LIU). The study includes data from over 60000 scans performed in 2021 and 2022, with a particular focus on reproducibility, investigation of optimal operational settings to ensure a large dynamic range, and evaluation of absolute accuracy through comparison with other instruments present in the injectors.

INTRODUCTION

The LHC Injectors Upgrade (LIU) [1] program started in 2010 with the purpose of improving the beam performance throughout the injector chain, in order to satisfy the specifications required by the High Luminosity LHC (HL-LHC) project, and was completed in 2021. In parallel to the improvement of the beam parameters, it was necessary to design various pieces of beam diagnostics instrumentation for the injectors: the LINAC4, the Proton Synchrotron Booster (PSB), the Proton Synchrotron (PS), and Super Proton Synchrotron (SPS). Following several years of design and testing of prototypes during the LHC Run2 (2015-2018) [2–6], the new beam instrumentation suite was installed during the second LHC Long Shutdown (LS2) in 2019 and 2020, while commissioning with beam started in 2021. This paper focuses on the description of the new LIU beam wire scanner (LIU BWS) design, giving a general overview followed by a more detailed evaluation of the performance at their particular location in each of LHC injectors involved: PSB, PS, and SPS.

THE LIU BEAM WIRE SCANNER

A BWS is an instrument designed to measure the transverse beam profile [7]. A thin wire passes through the beam producing a shower of secondary particles that are measured with a detection system. The rate of secondary particles is correlated with the position of the wire, allowing for the reconstruction of the 1-dimensional transverse profile of the beam, usually measured in the horizontal or vertical plane. Figure 1 shows a schematic of the LIU BWS working principle and architecture.

* salvatore.di.carlo@cern.ch

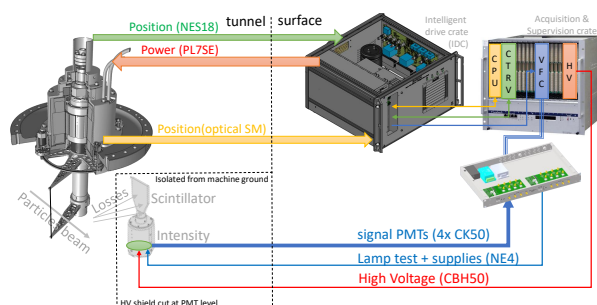


Figure 1: Schematic of the LIU BWS working principle and architecture [8]. The kinematic unit (the movable part of the scanner) and the detector measuring the secondary showers are placed in the accelerator's tunnel. These items are shown on the left side of the schematic. On the right side, we have the stand-alone control unit and the VME acquisition system, which are located in the service area on the surface. The CTRV is a CERN VME Timing Receiver board, while the VFC is the VME FMC Carrier board. The cables connecting tunnel and surface electronics are quite long, in some cases up to 150 m.

Upgrade Motivations

The design of a new LIU BWS was necessary in order to adequately measure the transverse profile of the new high intensity and brightness beams required by the HL-LHC project. The limitations of the present, old BWS are thoroughly discussed in previous works [9, 10] and here we briefly discuss some of the main shortcomings. The old wire scanners in the LHC injectors were either rotational (PSB, PS, SPS) or linear (SPS). The linear scanners in the SPS had strong limitations on beam intensity due to their low speed (1 m/s), leading to possible wire sublimation. For the rotational scanners the precision on the position of the wire was never better than 100 μm and was significantly degraded by electronic noise on the potentiometer reading, mechanical play, and vibrations [11]. From the operational point of view, the old wire scanners also required the operator to define the optimal working point for each measurement, which consisted of setting the detection parameters, i.e. the photo-multiplier tube (PMT) bias voltage and attenuation filter, before a beam profile could be measured. This often resulted in lengthy sessions of measurements. For the LIU BWS it was decided to design a unique standardised system, both, in terms of hardware and software, to satisfy the specifications of each of the LHC injectors. The LIU BWS is rotational, can be operated without need of selecting an op-

MODELING AND EXPERIMENTAL EVALUATION OF A BUNCH ARRIVAL-TIME MONITOR WITH ROD-SHAPED PICKUPS AND A LOW-PI-VOLTAGE ULTRA-WIDEBAND TRAVELING WAVE ELECTRO-OPTIC MODULATOR FOR X-RAY FREE-ELECTRON LASERS*

A. Kuzmin[†], E. Bründermann, C. Eschenbaum, C. Koos, A. Kotz, A.-S. Müller, G. Niehues, A. Schwarzenberger, Karlsruhe Institute of Technology KIT, Karlsruhe, Germany
B. E. J. Scheible^{1,‡}, A. Penirschke, Technische Hochschule Mittelhessen, Friedberg, Germany
M. K. Czwalińska, H. Schlarb, Deutsches Elektronen-Synchrotron DESY, Hamburg, Germany
W. Ackermann, H. De Gerssem, Technische Universität Darmstadt, Darmstadt, Germany
¹also at Technische Universität Darmstadt, Darmstadt, Germany

Abstract

X-ray Free-Electron Laser (XFEL) facilities, such as the 3.4 km European XFEL, require long-range synchronization that necessitate the use all-optical links with electro-optic bunch arrival-time monitors (BAM). Current BAM systems achieve a resolution up to 3.5 fs for 250 pC bunches. Precise bunch arrival timing is essential for experiments, which study ultra-fast dynamical phenomena with highest temporal resolution. Future experiments will crucially rely on femtosecond pulses from bunch charges well below 20 pC. State-of-the-art BAMs are not allowing accurate timing for operation with such low bunch charges. Here, we report on the progress in the development of an advanced BAM based on rod-shaped pickups mounted on a printed circuit board and ultra-wideband travelling-wave electro-optic modulators with low operating voltages. We perform modeling and experimental evaluation for the fabricated pickups and electro-optic modulators and analytically estimate timing jitter for the advanced BAM system. Additionally, we discuss an experimental setup to demonstrate joint operation of new pickups and wideband EO modulators for low bunch charges less than 5 pC.

INTRODUCTION

X-ray Free-Electron Laser (XFEL) operation depends on a synchronization system with high timing stability and fs-precision [1]. Furthermore, precise bunch arrival timing between FEL and external laser pulses is essential for experiments, which study ultra-fast dynamical phenomena with highest temporal resolution [2]. For this reason, an all-optical synchronization system is implemented in several facilities, e.g. the 3.4 km long European XFEL [3].

This synchronization system is based on a pulsed optical reference, which is emitted by a commercial laser oscillator locked to the main oscillator for medium and long-term stability [1]. The reference laser pulses are distributed to different end-stations, e.g. electro-optic (EO) bunch arrival-time

monitors (BAMs), via actively length-stabilized all-optical fiber links [1]. The BAM stations allow for precise arrival-time measurements by coupling to transient fields of every single bunch with cone-shaped pickups [1, 4, 5]. A bipolar radio-frequency (rf) pulse is fed to an electro-optic modulator (EOM) where the rf pulse is matched with the optical reference pulse [4]. The laser amplitude is modulated linearly to the arrival-time deviation, which can be determined afterwards in the data acquisition electronics [4].

The current BAMs achieve single bunch arrival-time measurements with a resolution of 3.5 fs for 250 pC bunches [6]. Experiments will crucially rely on fs pulses from bunch charges well below 20 pC. Therefore, an updated BAM for bunch charges lower than 5 pC is targeted. In this contribution the progress made in the two sub-projects is compiled and the overall improvement is estimated. Additionally, possibilities of the experimental demonstration are discussed.

NEW BAM DESIGN

In an ongoing project two components of the BAMs have been redesigned. The first objective was to update the pickups in order to increase the voltage signal by a factor of 10. The second objective was to develop and test a new electro-optical modulator which would allow further increase of timing resolution of a BAM. The new EOM has to be simultaneously broadband and has to feature low π -voltage.

Pickups

The state-of-the-art 40 GHz-pickups were shaped as a cone to reduce ringing and reflections by a constant line impedance [5]. In simulations they achieve 15 mV pC⁻¹ ps⁻¹ as normalized signal slew rate (SR), which is a decisive characteristic for the overall BAM sensitivity. The signal slope could be increased significantly by switching to an open-coax design with prolonged inner conductor, because of an increased active surface and reduced distance to the bunch [7]. Further improvement was found by implementation of these pickups in form of a rod mounted on a printed circuit board (PCB), their four signals are combined and fed to a common vacuum feedthrough [7]. This design surpassed the goal of 150 mV pC⁻¹ ps⁻¹ in simulations [7].

* Work supported by the German Federal Ministry of Education and Research (BMBF) under contract No. 05K19VKB and 05K19RO1.

[†] artem.kuzmin@kit.edu

[‡] bernhard.scheible@iem.thm.de

INSTALLATION AND COMMISSIONING OF THE PULSED OPTICAL TIMING SYSTEM EXTENSION

F. Rossi*, M. Ferianis, Elettra Sincrotrone Trieste S.C.p.A., Trieste, Italy

Abstract

At the FERMI FEL user facility, a fully optical timing system has been operated, to synchronize it, since the start of machine commissioning, back in 2009. In the past years the system has been progressively extended to support more clients. The latest upgrade is focusing on the pulsed subsystem which provides the phase reference to remote lasers and the bunch arrival monitor diagnostic stations. In origin the pulsed subsystem had a capacity to feed simultaneously six stabilized fiber links. The upgrade to the original layout makes it possible to install up to eight new additional links. Here we will describe the new setup and the results achieved in terms of short- and long-term stability.

INTRODUCTION

FERMI [1] is a fourth generation light source, a seeded Free Electron Laser (FEL), operating as a user facility in Trieste, Italy. A state-of-art all optical timing and synchronization system [2] has been deployed implementing a hybrid architecture as a combination of pulsed and continuous wave techniques.

The pulsed optical timing subsystem generates and delivers with 10 femtosecond precision the reference to all phase critical FERMI clients, like lasers and longitudinal diagnostics. The installation started with two links in 2009 and, since then, has been progressively updated to the current configuration serving a total of six clients.

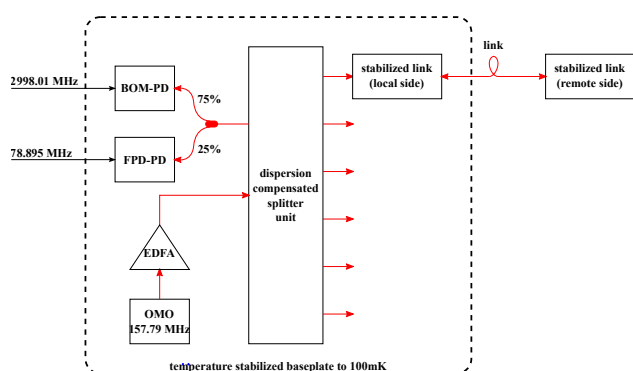


Figure 1: Block diagram of the original pulsed timing subsystem.

The block diagram of the subsystem originally installed is shown in Fig. 1. The optical master oscillator (OMO) is a soliton fiber laser working with a repetition rate of 157.79 MHz, i.e. one nineteenth of the 2998.01 MHz microwave frequency of the reference master oscillator (RMO). The OMO is phase locked to the RMO signal by a Balanced

Optical Microwave Phase Detector (BOM-PD), while the ambiguity of the zero crossing selection is solved by using a Fast Photodiode Phase Detector (FPD-PD). The signal from the OMO, amplified by a single Erbium Doped Fiber Amplifier (EDFA), is delivered at the output ports of a splitter along a dispersion-compensated path. This one is entirely implemented in fiber and guarantees short pulses at the input of a stabilized link which is built around a balanced cross-correlator (BOCC). Six ports are dedicated to timing distribution purposes, other two are used to seed the phase detectors and, finally, one is reserved for the extension. Each splitter output port dedicated to the timing distribution provides pulses at 40 mW average power, while the full width at half maximum (FWHM) is about (165 ± 9) fs.

A progressive extension of the pulsed optical timing subsystem is expected in the coming years to feed new clients with the phase reference. To fulfil the installation requests of additional timing clients in FERMI (e.g. new bunch arrival monitor stations or a user laser oscillator) we have started working towards an upgrade of the original subsystem.

THE SLAVE SUBSYSTEM

The extension of the pulsed subsystem has been implemented by Cycle GmbH [3]. The design follows the same architecture of the original subsystem so the optical signal coming from a second port of the OMO is again amplified and split. The upgrade makes it possible to add up to eight new stabilized pulsed links to the timing system. The optical signal is mainly routed in fiber; along the path there is a minimal free-space section described below. One of the design requirements was to maintain mechanical and optical compatibility with the link stabilization units installed in the past.

The overall block diagram of the extended pulsed system is shown in Fig. 2. The part described in the previous section is called “master” while the new devices are hereafter indicated as “slave”. In fact the slave is locked to the master to remove residual timing drifts among the two splitters output ports. The key element of the tracking loop is a phase detector implemented by means of a BOCC. The error signal is used to drive an actuator – a combination of a fiber piezo stretcher and a motorized translation stage – to keep the pulses coming out from the outputs of the master and slave splitters synchronized. Part of the actuator block is also a manual free-space delay line used to align in time the pulses and set the zero-crossing of the BOCC in the dynamic range of the control loop.

There are two fiber interconnections between the master and slave subsystems at ports A and B. The former is included in the controlled path of the tracking system while

* fabio.rossi@elettra.eu

STATUS OF A MONITOR DESIGN FOR SINGLE-SHOT ELECTRO-OPTICAL BUNCH PROFILE MEASUREMENTS AT FCC-ee

M. Reißig*, E. Bründermann, S. Funkner, B. Härer, G. Niehues, M. M. Patil, R. Ruprecht, C. Widmann, A.-S. Müller, Karlsruhe Institute of Technology, Karlsruhe, Germany

Abstract

At the KIT electron storage ring KARA (Karlsruhe Research Accelerator) an electro-optical (EO) near-field monitor is in operation performing single-shot, turn-by-turn measurements of the longitudinal bunch profile using electro-optical spectral decoding (EOSD). In context of the Future Circular Collider Innovation Study (FCCIS), a similar setup is investigated with the aim to monitor the longitudinal bunch profile of each bunch for dedicated top-up injection at the future electron-positron collider FCC-ee. This contribution presents the status of a monitor design adapted to cope with the high-current and high-energy lepton beams foreseen at FCC-ee.

INTRODUCTION

The future electron-positron collider FCC-ee is a planned high-energy, high-intensity accelerator located at CERN with approximately 100 km circumference and a beam energy up to 180 TeV [1]. To optimize luminosity, it will be operated with a top-up injection, which requires a detailed monitoring of the bunch profiles. In the frame of the Future Circular Innovation Study (FCCIS), a diagnostics tool for single-shot bunch-by-bunch measurements of the longitudinal bunch profile is under development at KIT. The design of this monitor is based on the electro-optical (EO) near-field monitor at the Karlsruhe Research Accelerator (KARA), which is able to perform turn-by-turn single-shot bunch profile measurements [2].

Bunch Profile Measurements at KARA

The EO near-field monitor at KARA offers turn-by-turn single-shot bunch profile measurements during an operation mode for short bunches. To resolve the bunch profile of single electron bunches with a length of 10 ps, a technique called electro-optical spectral decoding (EOSD) is used. Figure 1 shows the principle of an EOSD measurement at KARA in three consecutive steps.

In the first step, the electron bunch profile is encoded into the polarization of the chirped laser pulse. The electron's electric field changes the refractive index of the GaP (EO) crystal according to the Pockels effect. However, the change in refractive index in GaP depends on polarisation and propagation direction, because it is an anisotropic material. Therefore, the crystal becomes birefringent, which changes the polarization of the laser pulse from linear to elliptical in proportion to the electric field strength. The result is a modulation of the laser polarization that depends on the bunch charge density.

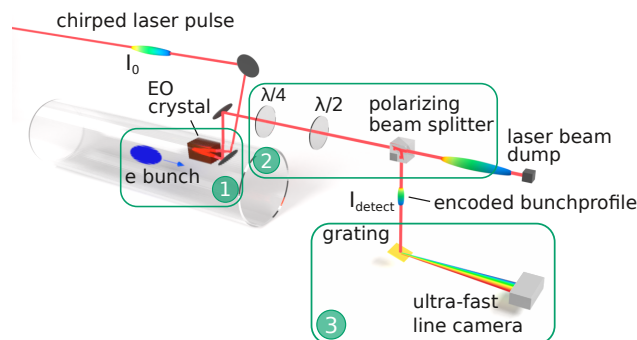


Figure 1: Scheme of the EO near-field setup at KARA. Adapted from [4].

In the second step, the bunch profile, which is now encoded in the laser polarization, is converted to an intensity modulation. This is achieved by a polarizing beam splitter (PBS), which only forwards light with a certain linear polarization to the spectrometer. A $\lambda/4$ - and a $\lambda/2$ -waveplate are set up in front of the PBS in a near-crossed configuration. This way, only very little light is transmitted if the laser pulse is not modulated and linearly polarized, but the transmitted intensity increases approximately linearly with the modulation of the polarisation.

In the third step, the intensity modulation of a single laser pulse is measured with a spectrometer containing the KIT-built, ultra-fast line camera KALYPSO [3]. In the spectrometer, the chirped laser pulse is refracted on a grating, which fans out the laser pulse according to the wavelength. The line camera then measures the laser intensity at different wavelengths, which corresponds to the longitudinal electron bunch profile.

Challenges for EO at FCC-ee

Simulations of the EO monitor at KARA for FCC-ee beam parameters showed, that there will be two major challenges that need to be tackled [5].

First, the operation mode for production of Z bosons at a collision energy of 90 GeV features a bunch length of $\sigma_{\text{FCCee Z}} = 15.4$ mm, which is very large compared to the typical length during measurements at KARA of around $\sigma_{\text{KARA}} \approx 3$ mm. The monitor at KARA is designed for short bunches. The laser pulse passes the crystal twice: first against the bunch direction (upstream) and after reflection at the back of the crystal, the laser pulse travels parallel to the bunch (downstream). Only the downstream modulation of the laser contributes to the bunch profile measurement, the upstream modulation is treated as a disturbance. For short bunches, the up- and downstream modulations do not

* micha.reissig@kit.edu

STUDIES ON RADIALLY COUPLED FAST FARADAY CUPS TO MINIMIZE FIELD DILUTION AND SECONDARY ELECTRON EMISSION AT LOW INTENSITIES OF HEAVY IONS*

G. Rodrigues^{1,†}, K. Mal¹, S. Kumar¹, R. Singh², C.P. Safvan¹, R. Mehta¹

¹Inter University Accelerator Centre, Aruna Asaf Ali Marg, New Delhi, India

²GSI Helmholtzzentrum für Schwerionenforschung GmbH, Darmstadt, Germany

Abstract

Fast Faraday Cups (FFCs) are interceptive beam diagnostic devices used to measure fast signals from sub-nano-second bunched beams and the operation of these devices is a well-established technique. However, for short bunch length measurements in non-relativistic regimes with ion beams, the measured profile is diluted due to field elongation and distortion by the emission of secondary electrons. Additionally, for short bunches with a low “signal to noise ratio” envisaged in the High Current Injector at the Inter University Accelerator Centre, the impedance matching of the EM structure puts severe design constraints. This work presents a detailed study on the modification of a radially-coupled coaxial FFC. The field dilution and secondary electron emission aspects are modelled through EM simulations and techniques to minimise these effects are explored.

INTRODUCTION

In the upcoming High Current Injector (HCI) Programme [1, 2] at New Delhi, India, there is an urgent need for developing diagnostics for longitudinal measurements which are critical for the successful operation of the High Current Injector. The operation of Faraday cups for intensity measurements is well established where the suppression of the emitted secondary electrons is carried out using a superimposed electric field, such that the emitted secondary electrons are retarded and recaptured [3]. For longitudinal charge profile measurements of short bunches (≤ 5 ns), it is critical to avoid impedance discontinuities in the Faraday cup structure until frequencies up to few GHz. Modified Faraday cup designs tailored to measure longitudinal charge distributions [3, 4] are called Fast Faraday Cups (FFC) [5]. Early FFC designs were tapered extension of coaxial cables allowing for full beam deposition on the central conductor while maintaining 50 Ω characteristic impedance [3, 6]. Following that, alternative FFC designs based on radial coupling in the central conductor [5] of a co-axial cable and microstrip based designs [4, 7] have been used in various accelerator laboratories. Recently [8], two FFC designs, one using a Radially-Coupled Coaxial Fast Faraday Cup (RCFFC) and a conventionally axially coupled FFC (ACFFC) were simulated with ion beams and compared with the measurements under similar beam conditions. A strong distortion in the longitudinal charge profile measurement due to secondary electrons is observed. External DC biasing of the central conductors minimises the

distortion to a large extent. Most studies available in the literature are focused mainly on electromagnetic characteristics, i.e. targeting impedance mismatch aspects. However, there are additional challenges for short bunched beam measurements in non-relativistic regimes; a) the field elongation and b) distortion by the emission of secondary electrons. In this study, we will present a design modification of a Radially-Coupled Coaxial Fast Faraday Cup (RCFFC) considering the existing beam conditions at the High Current Injector Programme, which is presently under commissioning stages at the Inter-University Accelerator Centre (IUAC), New Delhi. The primary drawback of the original design is the low “signal-to-noise” ratio due to the narrow beam limiting aperture of 0.8 mm along with the need for precise beam alignment with long averaging times for the measurement. The second challenge is the delayed signal induction due to emission of secondary electrons. The major modifications in our adapted design is to counter these challenges and are discussed in this contribution.

EM SIMULATIONS OF A MODIFIED RCFFC

The characteristic impedance (Z_{coax}) of a coaxial transmission line is defined with the following parameters [9], ϵ and μ as the permittivity and permeability of the material respectively, with r_1 and r_2 being the radii of the inner and outer conductor, respectively. The non-TEM mode with the lowest cut-off frequency (f_c) is TE_{11} and the cut-off frequency given by the standard known relation. Since the width of the co-axial line cannot be arbitrarily increased, a conical taper between a thin and a thick co-axial line was chosen. In order to minimise the reflection at the transition of coaxial and conical lines, it is necessary to design in such a way that the characteristic impedances of both the lines have the same impedance of 50 Ω . CST Microwave Studio [10] was used to design the RCFFC assembly with the interfacing option to the transmission line at the desired characteristic impedance of 50 Ω . Figure 1 shows the cross-sectional view of the model of the RCFFC, which consists of a metallic cube with two N-type connectors positioned concentrically. The collimating aperture of diameter 2 mm is chosen based on the relatively lower beam intensities of heavy ions available at the upcoming High Current Injector Programme. A rod of diameter 6 mm was inserted between the central electrodes of the connectors and tapered down to 3 mm, being the diameter of the standard N-type connector pin.

* Work supported by VAJRA

† gerosro@gmail.com

OPTIMIZATION STUDY OF BEAM POSITION AND ANGULAR JITTER INDEPENDENT BUNCH LENGTH MONITOR FOR AWAKE RUN 2

C. Davut^{*,1,2}, G. Xia¹, University of Manchester, Manchester, UK
O. Apsimon¹, University of Liverpool, Merseyside, UK
P. Karataev, Royal Holloway, University of London, London, UK
S. Mazzoni, T. Lefevre, CERN, Geneva, Switzerland
¹also at Cockcroft Institute, Daresbury, UK
²also at CERN, Geneva, Switzerland

Abstract

In this paper, a study using the Polarization Current Approach (PCA) model is performed to optimize the design of a short bunch length monitor using two dielectric radiators that produce coherent Cherenkov Diffraction Radiation (ChDR). The electromagnetic power emitted from each radiator is measuring a different part of the bunch spectrum using Schottky diodes. For various bunch lengths, the coherent ChDR spectrums are calculated to find the most suitable frequency bands for the detection system. ChDR intensities measured by each detector are estimated for different impact parameters to explore the dependence of bunch length monitor on beam position and angular jitter. It is found that, in the present configuration, the effects of beam position and angular jitter are negligibly small for bunch length measurement.

INTRODUCTION

In recent years, coherent Cherenkov Diffraction radiation (ChDR) has become a suitable candidate for non-invasive longitudinal bunch profile diagnostics with successful experimental validations [1, 2]. Although, the exact solutions of the electromagnetic problems are often not known, and detailed computer simulations require extensive time and resources, the properties of the radiation are often derived from simplified models, that assume specific assumptions on the radiator shape [3].

The emission characteristics of ChDR can be calculated by Polarization Current Approach (PCA) which describes simultaneously generated DR and ChDR as a solution to the “vacuum” set of macroscopic Maxwell’s equations [4]. Among the other theoretical models, PCA introduces some limitations on the longitudinal size of the radiator when calculating of the spectral-angular distribution of ChDR that makes it a powerful tool to calculate expected radiation yield and directivity of ChDR cone [5].

Considering a relativistic charged particle with energy $\gamma = 1/\sqrt{1 - \beta^2}$ moving rectilinearly at a distance b from a prismatic dielectric target, such as in Fig. 1, the particle field flattened into a plane perpendicular to its motion having a relation between its components $E_{\perp} \gg E_{\parallel}$ and $H \approx E$ for $\beta = v/c \sim 1$. The Fourier component of E_{\perp} is spatially restricted in a circle with a radius which is called the effective field

radius $l = \gamma \beta \lambda / 2\pi$, where λ is the radiation wavelength. Hence, the following the condition should be satisfied :

$$l \gtrsim b. \quad (1)$$

In this case the dielectric medium will be polarised and the polarization radiation will be emitted [6].

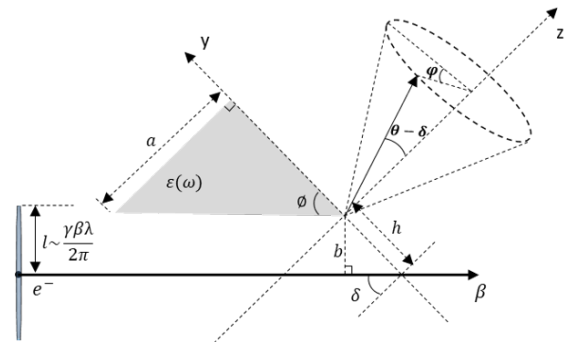


Figure 1: The geometry of ChDR emission by a relativistic charged particle moving rectilinearly at a distance b from the bottom surface of a prismatic dielectric target.

Therefore the spectral-angular distribution of ChDR can be calculated by Polarization Current Approach (PCA), as described in [4], in terms of its vertical and horizontal components with respect to particle trajectory and after the radiation is refracted out at the exit surface of the prism.

$$\frac{d^2 W}{d\omega d\Omega} = S_e(\omega) = \frac{d^2 W_{\perp}}{d\omega d\Omega} + \frac{d^2 W_{\parallel}}{d\omega d\Omega}. \quad (2)$$

The total radiation intensity generated by an electron bunch can be described by

$$S(\omega) = S_e(\omega) [N + N(N - 1)] F(\omega), \quad (3)$$

where $S(\omega)$ is the experimentally measured spectrum, $S_e(\omega)$ is the theoretically calculated single electron spectrum, N is the number of electrons within the bunch and $F(\omega)$ is the longitudinal bunch form factor [7]. As an important feature of the radiation spectrum, the domination of the longitudinal bunch form factor on the radiation spectrum indicates how far the radiation intensity extends in the frequency range. The amplitude of the longitudinal form factor

* can.davut@manchester.ac.uk

CREATION OF THE FIRST HIGH-INDUCTANCE SENSOR OF THE NEW CCC-Sm SERIES*

V. Tympel^{†,1}, T. Stoehlker^{1,2}, Helmholtz Institute Jena, Jena, Germany
 D. Haider, M. Schwickert, T. Sieber

GSI Helmholtz Centre for Heavy Ion Research, Darmstadt, Germany

L. Crescimbeni, F. Machalet, T. Schönau³, F. Schmidl, P. Seidel

Institute of Solid State Physics (IFK), Jena, Germany

M. Schmelz, R. Stolz, V. Zakosarenko⁴, Leibniz-IPHT, Jena, Germany

¹also at GSI Helmholtz Centre for Heavy Ion Research, Darmstadt, Germany

²also at Institute for Optics and Quantum Electronics, Jena, Germany

³also at Leibniz Institute of Photonic Technology, Leibniz-IPHT, Jena, Germany

⁴also at Supracon AG, Jena, Germany

Abstract

Cryogenic Current Comparators (CCC) for beamlines are presently used at CERN-AD and in the FAIR project at CRYRING with 100 mm and 150 mm beamline diameter, respectively, for non-destructive absolute measurement of beam currents in the amplitude range of below $10 \mu A_{pp}$ (current resolution $1 nA_{pp}$). Both sensor versions (CERN-Nb-CCC and FAIR-Nb-CCC-XD) use niobium as a superconductor for the DC-transformer and magnetic shielding. The integrated flux concentrators have an inductance below $100 \mu H$ at 4.2 Kelvin. The new Sm-series (Smart & Small) is designed for a beamline diameter of 63 mm and is using lead (Pb) as superconductor. The first implemented sensor (IFK-Pb-DCCC-Sm-200) has two core-based pickup coils ($2 \times 100 \mu H$ at 4.2 K) and hence the option to use two SQUID units. During construction, some basic investigations such as on noise behaviour (fluctuation-dissipation theorem, white noise below $2 pA_{rms}/\sqrt{Hz}$) and the magnetic shielding in terms of L_{core} - $C_{meander}$ -resonance and additional mu-metal shielding were undertaken. These results are presented herein. Finally, a current resolution of $0.5 nA_{pp}$ was achieved without additional shielding measures in laboratory environment.

INTRODUCTION

Cryogenic Current Comparators (CCC) measure the azimuthal magnetic field of a charged particle beam non-destructively. By using superconducting components such as magnetic shielding, DC transformer, and SQUIDS, a current resolution in the nA range can be achieved [1]. After the development of large CCCs for the CERN Antiproton Decelerator (CERN-Nb-CCC) [2] and FAIR-project (FAIR-Nb-CCC-XD) [3], both with a current pulse resolution $>1 nA$, some new concepts are currently being tested on smaller size CCCs - the so-called Small & Smart series (CCC-Sm, $<1 nA$).

PICKUP COILS

To increase system availability and enable comparison experiments, the setup is carried out with two superconductive pickup coils (Dual-core CCC or DCCC). Standard Magnetec M-616 cores [4] were used for the first DCCC-Sm (see Fig. 1), which achieve an inductance of about $100 \mu H$ in a package of three cores per coil (see Fig. 2).

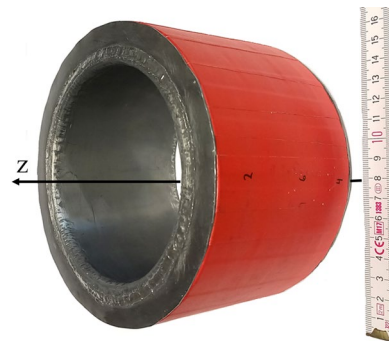


Figure 1: Pickup coil #1, one full-faced single-turn coil made of lead through three M-616 cores with z-axis as later beam direction.

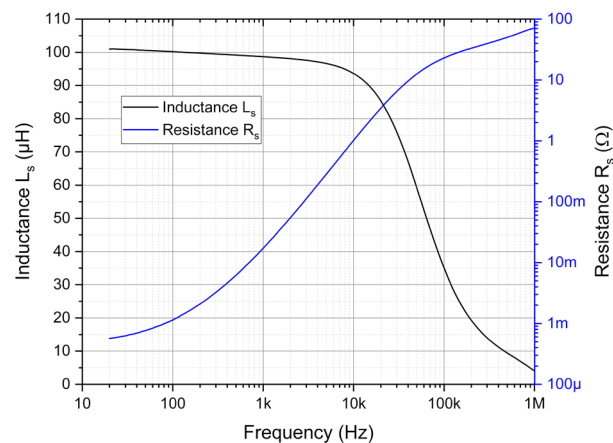


Figure 2: Pickup coil #1, serial inductance L_s and serial resistance R_s measured at 4.2 K.

* Work supported by the BMBF under contract No. 5P21SJRB

† volker.tympel@uni-jena.de

BOOSTER FILLPATTERN MONITOR

F. Falkenstern, J. Kuszynski, G. Rehm
Helmholtz-Zentrum Berlin, Germany

Abstract

The "Booster Fillpattern Monitor" is used to measure currents in each individual electron bunch in the booster of the BESSY II machine.

The booster with its circumference of 96 meters has space for max. 160 electron bunches. The distance between the electron bunches of 60 cm (96 m / 160) is determined by the RF Master Clock $\sim 499,627$ MHz. In practice, fill patterns of a one to five equally spaced bunches are in use.

The fill pattern monitor digitizes electrical pulses generated from a strip line using a broadband ADC. The sampling frequency is selected as an integer fraction of the bunching frequency, acquiring the full fill pattern over a number of turns.

Experiments performed at BESSY II demonstrate the performance of the setup and will be discussed.

INTRODUCTION

The BESSY II electron storage ring (SR) is a third-generation light source operating at an energy of 1.7 GeV with a stored current of 300 mA in the top-up mode [1]. The top-up injection in the SR allows almost constant synchrotron light for the users at the beamlines.

For injection into the BESSY II SR a full energy fast cycling booster synchrotron is used. Injection at full energy offers a lot of advantages for a high brilliance synchrotron radiation. It ensures a shot filling time, ion trapping etc. [2].

In the SR, electrons might be stored in any pattern consisting of up to 400 buckets (Fig 1).

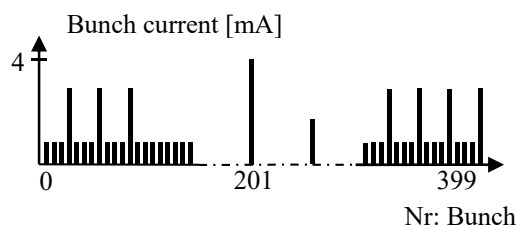


Figure 1: The typical fillpattern at storage ring BESSY II.

The injection of electrons in these buckets is managed from the TopUp engine [3]. It is possible to fill one to five buckets in the SR simultaneously. For this, the information from the fill pattern monitor (BunchView) in the SR is used [4].

The TopUp engine analyses this information and starts injection in the SR for filling the lost electrons in the emptiest bunches.

REQUIREMENTS

For the permanent optimization of the storage ring and the safe operation of the BESSYII machine, the reliably working injection into the storage ring is of great importance. In case of failure of injection system (Linac, Booster etc.), the beam in the storage ring is in decay mode. During the lifetime of about 8 hours, only half of the electrons remain in the storage ring after 8 hours. Most users at beamlines need constant synchrotron light (constant current in the SR) for their experiments. Therefore, the demands for diagnostics in this area have grown significantly. The booster fill pattern monitor was developed because of these increased demands on diagnostic capabilities.

REQUIREMENTS TO THE SYSTEM

The bunch resolved measurements have a large demand on the bandwidth of the RF signal, which makes acquisition and digitization difficult. Suppressing the signal noise with narrow analog filters is not possible. Improving the signal-to-noise ratio is then only possible by averaging of sampling data with digital processing. This requires many sample points from the analog (real) beam signals. For the bunch signals, which are repeated every turn, like the signals in the storage ring, it is mostly possible. In the booster, the circulated bunches are repeated during the booster period, but the induced bunch signal can vary a lot because of the acceleration of the electron buckets. Thus, averaging is not possible over many revolutions.

The second requirement is a sophisticated synchronization. The system needs a low jitter sample clock that is derived from the master clock (MC), revolution trigger and the start trigger of the booster. The measurement system can trigger internally (on the bunch signal) or externally on the start signal. While in operation it is mostly triggered by the external booster start trigger.

The third demand is the memory requirement of samples with high sample rate. It takes 35 ms to accelerate the electrons in the booster to the point of extraction. With the high sampling rate, it requires many megabytes of FIFO memory. As the FPGA card only allows a small FIFO memory, the external RAM memory would have to be declared as FIFO.

SETUP

The measuring system generates a current filling pattern in the booster every second. The external 1 Hz trigger starts recording data. The bunch signals (Fig. 2) are generated by a set of striplines (in the vacuum tube) and combined with the RF combiner (Fig 3).

SECONDARY EMISSION MONITOR SIMULATION, MEASUREMENTS AND MACHINE LEARNING APPLICATION STUDIES FOR CERN FIXED TARGET BEAMLINES

L. Parsons França^{1,2,3,*}, F. Roncarolo¹, F. M. Velotti¹, M. Duraffourg¹, C.P. Welsch^{2,3},
H. D. Zhang^{2,3}, E. Kukstas^{2,3}
¹CERN, Geneva, Switzerland
²Cockcroft Institute, Daresbury, UK
³University of Liverpool, UK

Abstract

The CERN fixed target experimental areas have recently acquired new importance thanks to newly proposed experiments, such as those linked to Physics Beyond Colliders (PBC) activities. Secondary Emission Monitors (SEMs) are the instruments currently used for measuring beam current, position and size in these areas. Guaranteeing their reliability, resistance to radiation and measurement precision is challenging. This paper presents the studies being conducted to understand ageing effects on SEM devices, to calibrate and optimise the SEM design for future use in these beamlines. These include feasibility studies for the application of machine learning techniques, with the objective of expanding the range of tools available for data analysis.

INTRODUCTION

The TT20 beamline at CERN carries the 400 GeV/c beam from the SPS towards the fixed target experiments in the North Area (Fig. 1). The slow extracted beam is de-bunched¹, with total intensity ranging from a few 10^{11} (during machine setup and development) to a few 10^{13} protons (during physics), diluted along spills lasting between 1 to 5 seconds. The choice of instrumentation for beam position, size and intensity measurements is at the moment restricted to SEMs and scintillating screens [1].

SEM monitors generally consist of metallic wires or thin foils, intercepting the beam. As the beam passes through these surfaces some particles interact, transferring energy to the material [3]. If the electrons in the metal receive enough energy to escape the Fermi level, they are released, in a process known as Secondary Emission (SE), theoretically described by E. J. Sternglass [4].

The number of electrons emitted per incident proton is defined as the Secondary Emission Yield (SEY) and can be written as [5]:

$$SEY = 0.01L_s \frac{dE}{dx}|_{el} \left[1 + \frac{1}{1 + (5.4 \cdot 10^{-6} E/A_p)} \right]. \quad (1)$$

It depends on the kinetic energy of the projectile (E), the electronic energy loss ($\frac{dE}{dx}|_{el}$), the mass of projectile (A_p) and the characteristic length of diffusion of low energy electrons

* luana.parsons.franca@cern.ch

¹ The SPS RF is switched off at flat top, before extraction

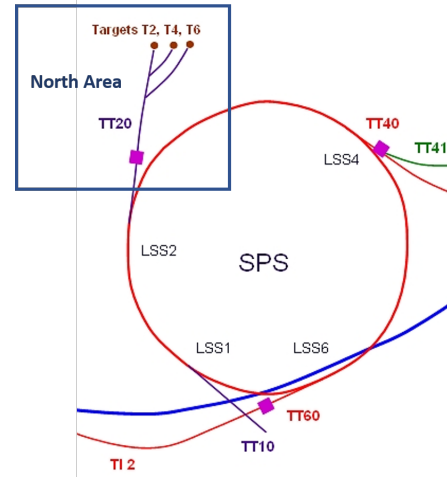


Figure 1: Schematic representation layout of SPS and North Area beamlines, sourced from [2].

(L_s), given by:

$$L_s = (3.68 \cdot 10^{-17} NZ^{1/2})^{-1}, \quad (2)$$

which varies according to the number of atoms per unit volume (N) and the atomic number (Z).

The signal measured by the SEM (N_{SEM}) is proportional to the number of protons (N_p), related via a calibration factor (C_f):

$$C_f = \frac{N_p}{N_{SEM}}. \quad (3)$$

This calibration factor is linked to the SEY and other properties, such as the electronics gain. More detailed information on this can be found in [6].

There are over 100 SEM monitors in the SPS complex, with varying *filling factors*, used for measuring different beam properties; *single foils* (labelled as BSI) for beam intensity; *split foils* (BSP or BSM) for beam position; and *scanning single bands* (BBS) or *multiple band grids* (BSG) for both beam position and size. All of them are equipped with the same Data Acquisition System (DAQ), publishing the spill signals every 20 ms.

Given the nature of SE processes, like the SEY dependence on material properties (e.g. oxidation, vacuum conditioning, radiation damage, etc...) and the low particle fluxes to be

OPERATIONAL AND BEAM STUDY RESULTS OF MEASUREMENTS WITH THE TRANSVERSE FEEDBACK SYSTEM AT THE CANADIAN LIGHT SOURCE

S. Martens*, T. Batten†, D. Bertwistle, M. J. Boland‡,¹
 Canadian Light Source, Saskatoon, Canada

¹also at University of Saskatchewan, Dept. of Phys. and Eng. Phys., Saskatoon, Canada

Abstract

A transverse bunch-by-bunch feedback system has been installed in the storage ring at the Canadian Light Source (CLS) to counteract beam instabilities. The 2.9 GeV electron storage ring is 171 m in circumference with 13 insertion devices currently installed, each contributing to the impedance of the ring and lowering the instability threshold. The new Transverse Feedback System (TFBS) provides improved bunch isolation, higher bandwidth amplification and diagnostics to study, understand and damp these instabilities. This paper will show and overview of the system setup, examples of operational performance and results of the diagnostic capabilities, including tune feedback, grow/damp measurements, and excite/damp measurements.

SYSTEM OVERVIEW

The Canadian Light Source storage ring is a third generation light source. Current standard operation uses 220 mA of stored electron current in the ring. The storage ring uses a compact lattice consisting of twelve double-bend achromat cells [1]. A table of storage ring parameters is listed in Table 1 [2]. Recent improvements have allowed the ring to transition from a fill-decay operation to a top-up operation, keeping the beam current consistent. The storage ring is subject to coupled bunch instabilities that arise via interaction between the vacuum chamber and the stored electron current. Changes over time to the configuration of the storage ring have impacted the growth of these instabilities. To improve diagnostics and stability for the beam, the existing Transverse Feedback System (TFBS) was upgraded to include Dimtel Equipment to identify and mitigate against coupled bunch instabilities.

Table 1: CLS Ring Parameters

Circumference	170.88 m
Beam Energy	2.9 GeV
Beam Current	220 mA
Periodicity	12 Cell
RF Frequency	500 MHz
Harmonic Number	285
Momentum Compaction	0.0038

* Stephen.Martens@lightsource.ca

† Tonia.Batten@lightsource.ca

‡ mark.boland@lightsource.ca

OPERATIONS

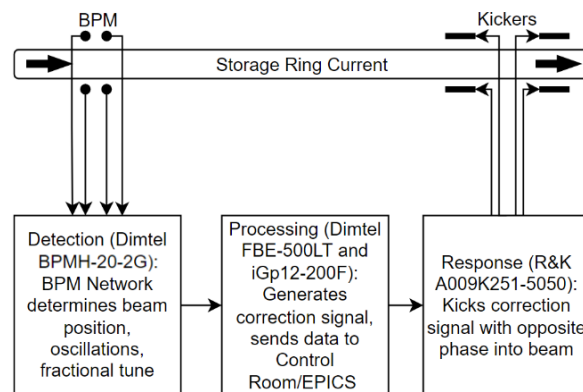


Figure 1: Transverse Feedback System Diagram and Hardware.

The Dimtel TFBS is currently in use in the storage ring to provide active damping against coupled bunch instabilities. In addition, it is used to provide bunch cleaning, tune measurements, tune feedback and diagnostics for beam instabilities in experiments.

TFBS Description

The TFBS uses three main elements depicted in Fig. 1. It uses a beam position monitor for detection, a network unit and processing system for analysis, and a kicker network for response. The four button BPM sends data to a hybrid RF-passive network unit which produces horizontal, vertical, and sum outputs. These signals are sent to the Bunch-By-Bunch Feedback front/back end unit and three 500 MHz processing units. The BPM signals are converted into a series of correction signals and sent to the response system which uses four broad-band RF power amplifiers and two kicker assemblies [3]. The 500 MHz RF signal is also input into the system to synchronise the timing [4]. The correction signal is applied to the beam to mitigate the instability identified by the processing system.

Tune Measurement and Feedback for Operations

The betatron tune of a synchrotron corresponds to the oscillation frequency of transverse motion within the ring. The number of complete oscillations within a single revolution of the ring is the integer tune, while the fractional oscillation corresponds to the fractional oscillation after a single turn [5]. The fractional tune can be measured by the

ORBIT CORRECTION UPGRADE AT THE CANADIAN LIGHT SOURCE

T. Batten*, M. Bree†, J. M. Vogt‡, Canadian Light Source, Saskatoon, Canada

Abstract

The Canadian Light Source is a 3rd generation synchrotron that began user operations in 2005 and now supports 22 operational beamlines. The previous orbit correction system was experiencing an increasing number of failures associated with obsolete hardware. This system was upgraded to improve machine reliability and performance, as well as to support new diagnostic capabilities.

OVERVIEW

The orbit correction system is responsible for maintaining the orbit of the stored electron beam. It reads the beam positions at various points around the storage ring, computes the deviation of the beam from its ideal location, and then calculates and distributes new setpoints to the orbit corrector magnets. As the complexity of the machine increases with the addition of insertion devices, the speed and accuracy of this setpoint distribution becomes even more critical to quickly damp down perturbations in the stored beam so that a stable orbit is maintained.

OLD SYSTEM

The previous system used versa mezzanine eurocard (VME) based hardware to read beam positions and to distribute orbit correction magnet setpoints. The VME cards were obsolete and showing increasing signs of failure. The beam position readings were averaged onboard, which restricted the diagnostic capabilities, and the setpoints were not distributed in parallel, which limited the correction rate.

The software used to support this system had multiple layers, hosted on a variety of machines, in a number of different languages. Furthermore, the computer that hosted communication with the orbit correction hardware was running an obsolete operating system with a customized compile environment, on hardware that was becoming increasingly difficult to service or replace. As a result, implementing changes or diagnosing problems was challenging.

NEW SYSTEM

The upgrade eliminated all of the obsolete hardware and dramatically increased the diagnostic capabilities. The new orbit correction system exposes all of the raw data which is now used to analyze performance and identify potential issues.

Hardware

The new orbit correction system, shown in Fig. 1, incorporates D-tAcq analog to digital converters (ADC) [1,2] to read

* tonia.batten@lightsource.ca

† michael.bree@lightsource.ca

‡ johannes.vogt@lightsource.ca

beam position monitor (BPM) positions and custom built nuclear instrument modules (NIM) that use PoLabs single board controllers (SBC) [3] to support parallel distribution of magnet power supply setpoints.

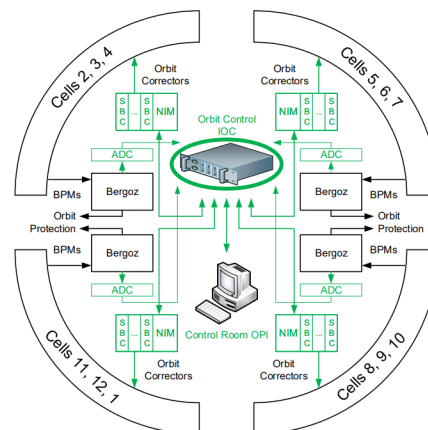


Figure 1: New orbit correction system architecture.

Software

The new software is running on more robust hardware, using a Scientific Linux 7 operating system, as shown in Fig. 2. This allows cores to be dedicated to specific tasks to ensure fast and predictable response times. In addition to simplifying the architecture, the new software is both dynamically configurable and easily extensible.

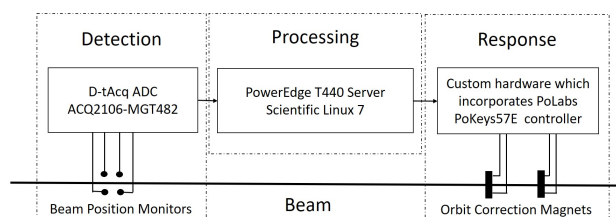


Figure 2: Orbit correction block diagram.

ENHANCEMENTS

The new diagnostic capabilities include:

Extensible Architecture

The architecture of the new software makes maintenance, support, and enhancement efforts more efficient. It supports dynamic saving and reloading of configuration and machine parameters for easy adjustment and machine recovery in the case of a hardware failure or a power outage.

CONCEPTUAL DESIGN OF THE TRANSVERSE MULTI-BUNCH FEEDBACK FOR THE SYNCHROTRON RADIATION SOURCE PETRA IV

S. Jablonski, H.T. Duhme, B. Dursun, J. Klute, S. H. Mirza, S. Pfeiffer, H. Schlarb
 Deutsches Elektronen Synchrotron (DESY), Hamburg, Germany

Abstract

PETRA IV will be a new, fourth-generation, high-brilliance synchrotron radiation source in the hard X-ray range. To keep the emittance low at high beam current an active feedback system to damp transverse multi-bunch instabilities is required. The particular challenge to the system is the very low-noise, while maintaining high bandwidth, which is defined by the 2 ns bunch spacing.

In this paper, we present the conceptual design of the transverse multi-bunch feedback (T-MBFB) system and technical challenges to fulfill the performance requirements. An overview is given on the hardware and the method for detecting and damping the coupled-bunch oscillations. Using modern high-speed ADCs enables direct sampling of pulses from beam pick-ups, which removes the necessity for down-converters. Powerful digital signal processing allows not only for the effective feedback implementation, but also for developing versatile tools for the machine diagnostics.

REQUIREMENTS FOR T-MBFB

The T-MBFB must be able to damp the coupled-bunch oscillations for two PETRA IV operation modes, i.e. brightness mode (maximum 3840 bunches, 2 ns bunch spacing, total current of 200 mA) and timing mode (80 bunches, 96 ns bunch spacing, total current of 80 mA). To suppress the possible oscillation modes, the feedback acts

on each bunch (bunch-by-bunch, turn-by-turn system), which requires at least 500 MHz flat magnitude and linear phase detector electronics. The frequencies of the horizontal and vertical betatron oscillations are ~ 23.4 kHz and ~ 35.2 kHz, respectively [1].

PETRA IV is planned to have much lower horizontal electron beam emittance (< 20 pm rad in the brightness mode [2]) than PETRA III. The detector resolution must be finer than $1 \mu\text{m}$ to not degrade the beam emittance [1]. For ± 1 mm expected transverse motion range, the required minimum SNR of the detector is 60 dB. In a direct sampling detector scheme, the detector noise is dominated by the intrinsic noise of the ADCs, which is discussed later in the subsection on the RFSoc digitizer.

Another requirement is the feedback damping time τ of the multi-bunch instabilities, which was defined to be not worse than 20 turns in any operation mode and for the worst case, i.e. when the synchrotron chromaticity Q' is zero [1]. However, such a damping time is only required for a relatively small transverse oscillation amplitude at the pick-up, i.e. $A_p < 200 \mu\text{m}$.

Additionally, the bunch charge in the timing mode is considerably higher than in the brightness mode, therefore, the MBFB system must have a wide dynamic range and an overvoltage protection to ensure high performance and high reliability for both machine setups.

The T-MBFB requirements and some of the PETRA IV design parameters are summarized in Table 1.

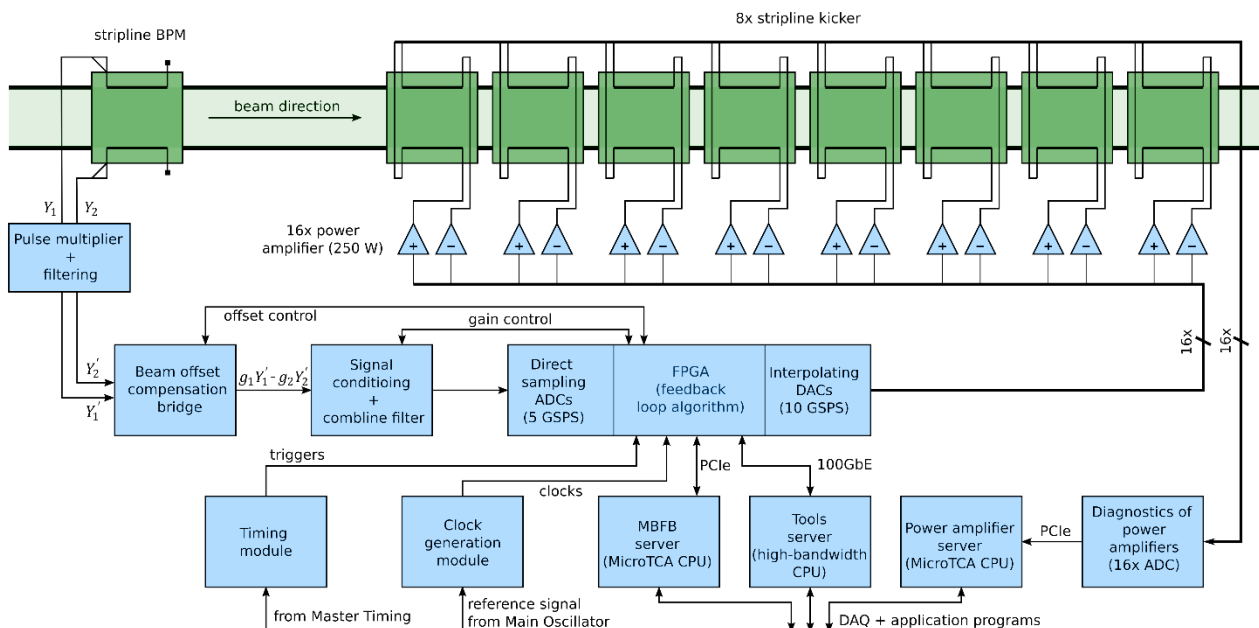


Figure 1: Simplified block diagram of the vertical transverse multi-bunch feedback (T-MBFB).

Content from this work may be used under the terms of the CC BY 4.0 licence (© 2021). Any distribution of this work must maintain attribution to the author(s), title of the work, publisher, and DOI

MEASUREMENTS FOR EMITTANCE FEEDBACK BASED ON RESONANT EXCITATION AT DIAMOND LIGHT SOURCE

S. T. Preston*, T. Olsson, A. Morgan†, L. Bobb, Diamond Light Source, Oxfordshire, UK

Abstract

In the Diamond storage ring, the vertical emittance is kept at 8 pm rad by an emittance feedback which modifies the strengths of skew quadrupoles. A new feedback using a stripline kicker to control the vertical emittance by exciting the beam resonantly at a synchrotron sideband is planned to avoid modification of the optics. This is crucial for the anticipated Diamond-II upgrade of the storage ring, which will have a much smaller equilibrium emittance than the existing machine. A larger coupling is therefore needed to keep the vertical emittance at the same level, potentially reducing the off-axis injection efficiency and lifetime. Measurements of the beam oscillation and emittance have been performed at the existing storage ring to characterise the effects of chromaticity and impedance on the optimal excitation frequency, where the emittance is increased significantly while the beam oscillation is kept low. The implications for simulating the emittance feedback for the Diamond-II storage ring are also discussed.

INTRODUCTION

The vertical emittance of the Diamond Light Source storage ring is kept constant during user operation by a feedback system to maintain the source brightness, spot size and coherence as conditions in the machine change [1]. Before each machine run, the optics are corrected using LOCO [2], giving a vertical emittance on the order of a few pm rad. The emittance is then measured using two pinhole cameras and increased to 8 pm rad by changing the strengths of the skew quadrupoles in the ring [1]. This results in changes of the optics such as betatron coupling and vertical dispersion. Although not a concern for the existing ring, it could negatively affect the off-axis injection efficiency and lifetime for the planned Diamond-II storage ring, which will reduce the equilibrium emittance from 2.7 nm rad to 160 pm rad with open insertion devices and 120 pm rad with closed [3]. The required coupling to reach the same level of vertical emittance will then be considerably higher.

A new emittance feedback that does not affect the optics is therefore under development. Inspiration comes from the pulse picking by resonant excitation (PPRE) method operated at BESSY-II [4, 5], where the emittance of a single bunch is increased by driving the beam at a synchrotron sideband. The purpose is to extract single bunch light for timing users while operating with a multi-bunch fill pattern. At Diamond, the plan is to drive all the bunches and use a feedback system to adjust the excitation amplitude to keep the emittance constant.

* shaun.t.preston@gmail.com

† alun.morgan@diamond.ac.uk

Measurements at different excitation frequencies have been done at the existing Diamond storage ring. The optimal frequency and implications for predicting the behaviour of the Diamond-II storage ring are discussed. The new emittance feedback is also presented along with future plans.

THE DIAMOND MULTI-BUNCH FEEDBACK SYSTEM

The transverse multi-bunch feedback system (TMBF) for the Diamond storage ring is developed in-house. It uses a beam position monitor (BPM) to detect turn-by-turn bunch-by-bunch data and stripline kickers to apply excitation to the beam. More details about the hardware can be found in [6–8]. The system can apply multiple concurrent excitations to user defined groups of bunches, down to the level of a single bunch. In user operation, it is used both to damp coupled-bunch instabilities and for low gain frequency sweeps to measure the betatron and synchrotron tunes for tune feedback. During machine development, it is also used to drive the beam for instability studies.

FEEDBACK IMPLEMENTATION

The emittance feedback is implemented using the TMBF system for excitation and the existing pinhole cameras for measurement. An additional excitor is used to drive the beam at one of the synchrotron sidebands. In practice, this is realised by using a numerically controlled oscillator (NCO), whose amplitude and frequency can be adjusted as needed.

In order to implement the feedback, an additional control loop was added, which adjusts the amplitude of the NCO in order to maintain a target value of emittance. As in the existing emittance feedback system, the change in beam size is monitored by two pinhole cameras and the emittance calculated using this data.

To improve the effectiveness of the technique, tune tracking is also implemented. The purpose of tracking is to allow the excitation to follow the jitter in tune, which causes the excitation to stay on the peak of the desired sideband. This is achieved by using a phase-locked loop which monitors a single tracking bunch.

Interference can be reduced by turning off the TMBF system tune sweep for the tracking bunch and a few bunches either side and not applying an emittance excitation to them. These bunches only need a fraction of the charge of the others for sufficient lifetime without an emittance increase.

The feedback has run successfully in dedicated development time and is being integrated into the existing control system, which will allow switching between the existing skew quadrupole and sideband excitation methods for user operation.

CONTROL SYSTEM SUITE FOR BEAM POSITION MONITORS AT MAX IV

Áureo Freitas*, Carla Takahashi, Mirjam Lindberg, Robert Lindvall, Robin Svärd, Vincent Hardion
MAX IV Laboratory, Lund, Sweden

Abstract

MAX IV is a fourth generation synchrotron facility at Lund, Sweden. It is composed of a full energy linear accelerator and two storage rings with 1.5 GeV and 3 GeV, which requires hundreds of beam position monitors. In this context, Libera Single Pass E and Libera Brilliance+ are employed as BPM instruments. This paper will present an overview of the control system suite used in the facility, including the communication, data acquisition and storage pipelines, monitoring, configuration and software maintainability.

INTRODUCTION

MAX IV Laboratory [1] is a fourth generation light source located at Lund, Sweden. The accelerator complex consists of a 3 GeV, 250 m long full energy linac, two storage rings of 1.5 GeV and 3 GeV, and a Short Pulse Facility. During 2022 a total of sixteen beamlines are receiving light [2].

TANGO Controls is a toolkit for building distributed object based control systems. The distributed object in TANGO Controls is called a device and is created as an object in a container process called a device server. The device server implements the network communication and links to the configuration database and clients. TANGO device servers and clients can be written in Python, C++ or Java. TANGO comes with a full set of tools for developing, supervising, monitoring and archiving [3].

The TANGO Controls toolkit has been used to build the control systems for large and small physics experiments like synchrotrons, lasers, wind tunnels and radio telescopes, and it has been chosen as the Control System at MAX IV Laboratory.

CONTROL SYSTEM AT MAX IV

The control system at MAX IV Laboratory is distributed and consists of an estimated 370 servers, running 24,000 TANGO devices and providing 500,000 control points. The accelerator control system has a unique TANGO database and contains 200 servers. The servers are hosted in virtual machines running Linux operating systems and, for some applications, the TANGO servers are hosted in industrial computers and embedded systems. Figure 1 represents a small zoom of the control system complexity and interconnections.

Deploying and maintaining such big systems requires proper workflows and tools. MAX IV has been using Ansible [4] to manage and deploy its full control system, both software and infrastructure, for quite some time with great

success. All required software (i.e. TANGO devices) is packaged as RPMs (Red Hat Package Manager) making deployment and dependency management easy [5].

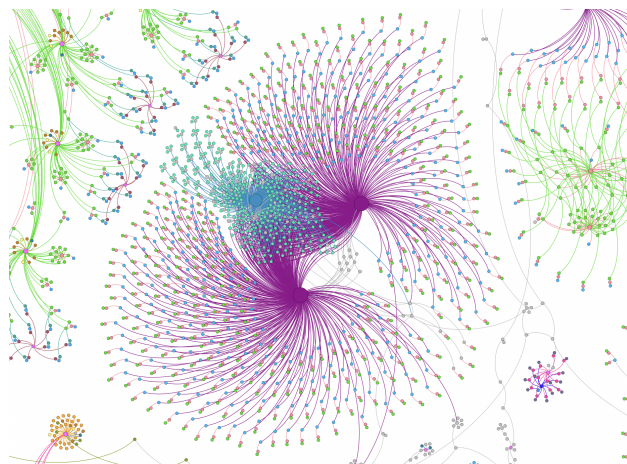


Figure 1: Zoom of the MAX IV 3 GeV storage ring control system. The two big pink stars represent the slow orbit feedback for the horizontal and vertical planes. The big blue star represents the Libera manager device.

BEAM POSITION MONITORS AT MAX IV

MAX IV uses a commercial solution for beam position monitors from I-Tech [6] with a custom firmware for internal needs. There are a total of 72 Libera Brilliance+ units in use in the storage rings, providing 236 beam position monitors (and an extra BPM for 3 GeV ring transfer line): 200 units in the 3 GeV ring and 36 units in the 1.5 GeV ring. For the linac, there are a total of 21 Libera Single Pass E units providing 48 beam position monitors.

Libera Brilliance+ features high precision position measurement of the electron beam in the booster or storage ring. Its digital signal processing supports programmable bandwidth and can facilitate all position measurements required in various regimes: pulsed, first turns, turn-by-turn and regular closed orbit. Acquisitions can be carried out simultaneously on all data paths: from raw ADC acquisition, turn-by-turn acquisition, slow acquisition to fast acquisition [7].

The instrument is based on the MTCA.0 modular technology and hosts up to 4 RAF (BPM) modules, one EVRX (timing) module and GDX (control) module in a single crate. The GDX module is used for the fast orbit feedback and to provide a continuous 10 kHz data streaming. This data is stored temporarily in a data storage cluster and is accessi-

* aureo.freitas@maxiv.lu.se

A MODERN ETHERNET DATA ACQUISITION ARCHITECTURE FOR FERMILAB BEAM INSTRUMENTATION*

R. Santucci[†], J. Diamond, N. Eddy, A. Semenov, D. Voy, Fermilab, Batavia, IL, USA

Abstract

The Fermilab Accelerator Division, Instrumentation Department is adopting an open-source framework to replace our embedded VME-based data acquisition systems. Utilizing an iterative methodology, we first moved to embedded Linux, removing the need for VxWorks. Next, we adopted Ethernet on each data acquisition module eliminating the need for the VME backplane in addition to communicating with a rack mount server. Development of DDCP (Distributed Data Communications Protocol), allowed for an abstraction between the firmware and software layers. Each data acquisition module was adapted to read out using 1 GbE and aggregated at a switch which up linked to a 10 GbE network. Current development includes scaling the system to aggregate more modules, to increase bandwidth to support multiple systems and to adopt MicroTCA as a crate technology. The architecture was utilized on various beamlines around the Fermilab complex including PIP2IT, FAST/IOTA and the Muon Delivery Ring. In summary, we were able to develop a data acquisition framework which incrementally replaces VxWorks & VME hardware as well as increases our total bandwidth to 10 Gbit/s using off the shelf Ethernet technology.

INTRODUCTION

The current framework of the Fermilab complex, regarding data acquisition, consists of three key areas: hardware platforms, embedded systems, and software. Of the large number of systems, many consist of a VME based platform with a variety of different VxWorks based crate controllers [1]. This architecture has proven extremely reliable; however, it has seen a technical debt build up. Aging crate hardware and stale software has led to rising maintenance costs as new requirements are needed to meet intensity goals and as new projects come online. To meet these new goals, each challenge was worked on iteratively, addressing each bottleneck in the full hardware/software life cycle. The primary hardware hurdle was removing the need of the VME back plane along with a VxWorks based crate controller. Moving to a Linux rack mount server and adopting a 10 GbE network, allowed us to increase bandwidth and decrease complexity in our systems. This was driven by the adoption of Ethernet on each digitizer. The Distributed Data Communication Protocol (DDCP) was developed to abstract an Ethernet field bus interface for the digitizers. This hardware abstraction layer, utilizing the POSIX socket API, allowed

for easy adoption and network communication during development. Alongside aging hardware has been software stagnation. This stagnation, was largely driven by the complexity of individual systems with no common platforms. The move to Linux has allowed for the adoption of many new software technologies many of which utilize open-source communities. By transitioning to off the shelf Ethernet, we have been able to drastically increase our data throughput. Installations at the Fast/IOTA complex, the PIP2IT Test stand, as well as the current roll out to the Muon delivery ring have seen lower user complexity as a direct cause and effect from higher bandwidth. Future development will see the adoption of MicroTCA, standard socFPGA modules, and a common software suite to allow for easy adoption to more systems.

HARDWARE PLATFORMS

VME and VxWorks

Current Instrumentation front-ends utilize many different platforms, the primary being VME with a VxWorks RTOS. These systems have been in use ranging from 5 – 30 years. Although reliable, the cost to maintain these systems has become prohibitive. Crate controllers, (MVME500, MVME2400, MVME2401, MVME2434) have either seen drastic price increases or are no longer in production / available. Digitizer stockpiles are dwindling with no clear path to acquire more. Code bases have stagnated as it is prohibitive to update systems to modern compilers. The learning curve of VxWorks makes it difficult to train new developers on aging systems. In addition, data bandwidth requirements have shifted to need larger and larger amounts of data. Limited to a theoretical backplane speed of 40 MB/s (VMEbus IEEE-1014) adopting Ethernet was a less costly transition to increase bandwidth.

MicroTCA.4

Work is underway to transition from VME to the MTCA.4 platform for instrumentation [2]. In addition to modern crate standards, this platform provides Ethernet fabric on the backplane which is managed by the MTCA Carrier Hub (MCH) with a 10 Gbit uplink. The MTCA.4 standard also provides for a Rear Transition Module (RTM) which can be used to integrate analog signal conditioning which was typically done in an external crate for the VME systems.

Custom Digitizer

The hardware used to transition the DAQ from VME to Ethernet is a custom 8 channel 250 MS/s 16 bit digitizer board developed at Fermilab in 2016. A block diagram of the module is shown in Fig. 1. The board was originally targeted for VXS with Ethernet on the backplane. Unfortunately, this

* This manuscript has been authored by Fermi Research Alliance, LLC under Contract No. DE-AC02-07CH11359 with the U.S. Department of Energy, Office of Science, Office of High Energy Physics.

[†] rsantucc@fnal.gov

ENeXAr: AN EPICS-BASED TOOL FOR USER-CONTROLLED DATA ARCHIVING

J. F. Esteban Müller*, European Spallation Source ERIC, Lund, Sweden

Abstract

ENeXAr is a data archival tool for EPICS-based systems. It is intended as a complement for traditional data archiving solutions, to cover use cases for which they are usually not designed: mainly for limited-duration high-data rates from a subset of signals. The service is particularly useful for activities related to machine commissioning, beam studies, and system integration testing. Data acquisition is controlled via PV Access RPC commands and the data is stored in standard HDF5-based NeXus files. The RPC commands allow users to define the acquisition parameters, the data structure, and the metadata. The usage of EPICS RPC commands means that the users are not required to install additional software. Also, acquisitions can be automatized directly from EPICS IOCs.

INTRODUCTION

Most accelerator facilities rely on data archiving services that continuously acquire and store data from all the signals that need to be monitored.

At ESS, our control system is based on EPICS [1] and we use the Archiver Appliance [2] for archiving data related to the machine operation.

There are use cases, however, when traditional data archivers are not optimal. For example, during system testing, machine commissioning activities, beam studies, or when troubleshooting issues with a particular device, users may require to acquire different signals than those regularly stored in the archiver. Often, these sets of signals contain long arrays (waveform records), which would be very costly to continuously archive for all systems, in terms of required network bandwidth and storage. However, acquiring only a subset of them for a limited period of time poses no issues.

Traditionally this is done using scripts, in which case the user needs to take care of acquiring the data using the EPICS libraries and storing the data. This results in different systems using a variety of file formats that make data analysis more complex.

The purpose of ENeXAr is to facilitate data acquisition and storage, by defining a set of commands that allow users to run an automatic data collection that saves the data in central storage, together with user-defined metadata. The only requirement for users is to have an EPICS base installation.

SOFTWARE ARCHITECTURE

ENeXAr is implemented in Python and it uses the pyepics [3] and p4p [4] packages for EPICS Channel Access and PV Access support, respectively.

* JuanF.EstebanMuller@ess.eu

Figure 1 shows a schematic view of its architecture. Clients send commands to the ENeXAr service via Remote Procedure Calls (RPC), using the PV Access protocol. There are also status PVs to monitor the service. ENeXAr processes the commands, some of which will trigger a data acquisition from EPICS IOCs. The connection to the IOCs can use either the PV Access (PVA) or Channel Access (CA) protocols.

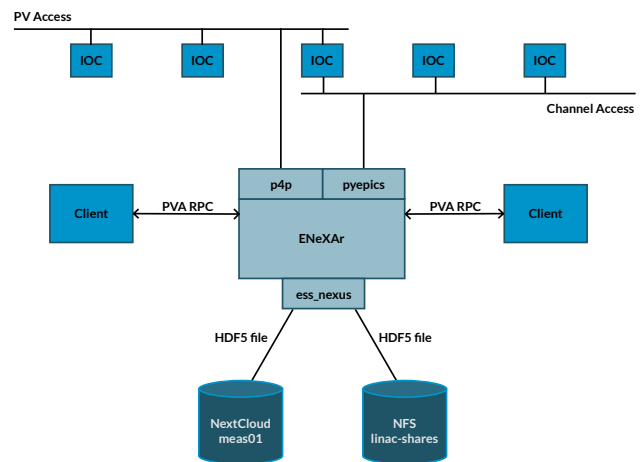


Figure 1: The architecture of the ENeXAr service. On the top, the IOCs produce data that is acquired by ENeXAr through EPICS using the pyepics and p4p epics modules. Clients send commands to the service using PV Access RPC calls. On the bottom, it is shown examples of storage backends that can be used.

The service runs on several processes using the Python multiprocessing library. The main limitation is that write operations to a single HDF5 file should always originate from the same process, since the h5py libraries do not allow for parallel write operations. As we will see later, that can be a performance bottleneck, although not very serious.

The acquisitions are then saved into the file storage backend. The data is formatted using the NeXus [5] convention and saved as HDF5 [6] files. Files are created using the ess-nexus Python package [7]. Files are not indexed and the directory structure inside the storage backend is completely managed by the users.

Multiple instances of ENeXAr can be deployed in the same network, provided that they use a different prefix for the PV names used for commands and status. That allows, for example, for each instance to use a different storage backend, or as a means for balance the load in the service.

USAGE

As stated above, the user controls the data acquisition via EPICS RPC calls, which can be generated by any EPICS7-

APPLICATION OF MACHINE LEARNING TOWARDS PARTICLE COUNTING AND IDENTIFICATION

S. Engel^{1,*}, R. Singh^{2,†}, P. Boutachkov²

¹ University of Essex, Colchester, England

² GSI Helmholtz Centre for Heavy Ion Research, Darmstadt, Germany

Abstract

An exploration into the application of three machine learning (ML) approaches to identify and separate events in the detectors used for particle counting at the GSI Helmholtz Centre for Heavy Ion Research was performed. A shape-based template matching algorithm (STMF), Peak Property-based Counting Algorithm (PPCA) and convolutional neural network (CNN) were tested for counting the number of particles accurately without domain-specific knowledge required to run the currently used algorithm. The three domain-agnostic ML algorithms are based on data from scintillation counters commonly used in beam instrumentation and represent proof-of-principle for an automated particle counting system. The algorithms were trained on a labelled set of over 150 000 experimental particle data. The results of the three classification approaches were compared to find a solution that best mitigates the effects of particle pile-ups. The two best-achieving algorithms were PPCA and CNN, achieving an accuracy of over 99%.

INTRODUCTION

As charged particle beams pass through a scintillation counter, it induces the excitations in the scintillation material which relaxed with emission of photons. These photons are amplified using photo multiplier tubes (PMT) which outputs a voltage pulse measured over time. The shortest pulse lengths are typically of the order of few ns given by the scintillation process itself. The transportation of these pulses from the radiation environment to the detection electronics is about 50-100 m, which further increases the pulse length due to cable dispersion. As the rate of particles arriving at the scintillator increases so does the probability for signal pile-ups, an overlap of sequential pulses. Due to complex slow extraction process from the particle accelerators and sub Poissonian particle distribution [1], non-negligible percentage of signal pile-ups occur at most particle arrival rates. These complex, hard-to-count, peak shapes change in a non-linear fashion. The interference causes difficulties in using conventional computing methods to accurately count particles, although strategies to mitigate them using hardware [2] and software solutions [3, 4] have been explored. Notably several ML approaches have been developed with some success by relying on domain-specific knowledge and feature engineering specific to the detector [3–5].

Other more general ML approaches rely on 2D data and/or data with multiple features [6], demonstrating domain-

specific knowledge is not necessary to provide satisfactory results. Specifically, CNN's prove to be the ideal conventional ML solution because of their robustness and the ability to create a domain agnostic, end-to-end discriminating model which eliminates unnecessary domain-specific pre-processing [7].

DATA COLLECTION AND TRANSFORMATION

The major portion of the training and testing data consisted of high-resolution experimental data of 1.5×10^5 peaks collected at the SIS18 synchrotron at GSI with a sampling rate of 2.5 GSa/s. The data was labelled by fine-tuning the present particle counting algorithm. Therefore, only labeled data with a low extraction rate of up to 3×10^5 particles per second could be used.

Low-resolution data was generated by downsampling the high-resolution data collected at (2.5×10^9) samples per second as seen in Fig. 1. Data was downsampled by a factor of s to test the accuracy at various resolutions.

The high-resolution data was bootstrapped by combining an offset copy of a time series with the original to create more complex shapes representative of data with a higher rate of particles.

The validation data of 416 peaks was experimentally collected by firing a laser at the scintillation counter at precisely set intervals to selectively generate various pile-up shapes.

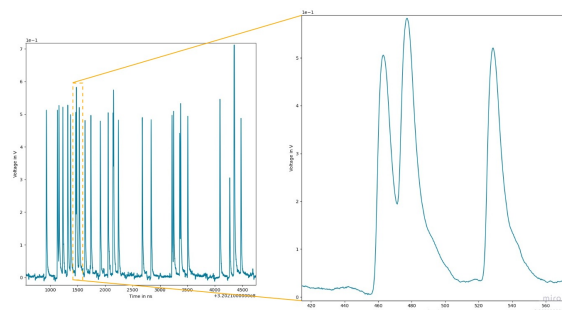


Figure 1: Graph showing a section of a time series with a close-up of a peak

TIME SERIES CLASSIFICATION USING SUPERVISED MACHINE LEARNING

1. Shape-based Template Matching Framework (STMF)
2. Peak Property-based Counting Algorithm (PPCA)
3. Convolutional neural network (CNN)

* samuel-engel@outlook.com

† r.singh@gsi.de

CONTROL SYSTEMS OF DC ACCELERATORS AT KAHVELab

T. B. Ilhan*, A. Caglar, D. Halis, Yıldız Technical University, Istanbul, Turkey
A. Adiguzel, S. Oz, İstanbul University, İstanbul, Turkey
H. Cetinkaya, Dumlupınar University, Kutahya, Turkey
E. Elibollar, M. F. Er, A. Inanc, V. E. Ozcan, Boğaziçi University, İstanbul, Turkey
U. Kaya, İstinye University, İstanbul, Turkey
A. Ozbey, İstanbul University-Cerrahpaşa, İstanbul, Turkey
G. Turemen, TENMAK-NUKEN, Ankara, Turkey
N. G. Unel, University of California (UCI), California, USA

Abstract

KAHVE Laboratory has two functional particle sources: thermal electrons and ionized hydrogen. Each of these are followed by DC acceleration sections, for obtaining an electron beam to accelerate electrons MeV energy level and for providing protons to the radio frequency quadrupole accelerator which are being built. So far both systems have keV energy levels. Both systems employ LabVIEW based GUIs to interact with the user and to control and monitor the DC power supplies. The vacuum gauges, turbomolecular pumps, stepper motors and high voltage power supplies are all controlled with PLCs. The equipment under high voltage, are monitored and controlled via Arduino based wifi and bluetooth wireless communication protocols. The proton beamline has additional devices for beam diagnostics which are being commissioned like pepper pot plate, scintillator screen and faraday cup. Both systems are being standardized before MeV energy level for generalize to national labs which are working on detectors and accelerators. We believe such a setup could be a low budget control and readout example for modern small experiments and educational projects.

INTRODUCTION

The proton accelerator at KAHVELab utilizes a 20kV high voltage power supply units (PSU), two low voltage PSUs, one four-channel low voltage PSU, two turbomolecular pumps, two vacuum gauges, three pneumatic cylinders with PLC and PC control combined all in one LabVIEW GUI as shown in Fig. 1. The system extracts 20keV proton beam from microwave discharge ion source. Upgrade process of the ion source with permanent magnets and the addition of a 800 MHz RFQ is on going. After the RFQ, the beam energy will be 2 MeV.

The electron accelerator at KAHVELab uses 60kV high voltage PSU, two four-channel low voltage PSUs, one low voltage PSU, two turbomolecular pumps, two vacuum gauges, two stepper motors, PLC and PC control combined, all in one LabVIEW GUI as shown in Fig. 2. It produces a 50keV electron beam using thoriated tungsten thermionic cathode. This project was supported by TUBITAK Project No: 117F462. Different cathode types, welding and hardening processes are successfully tested.

* taha.batuhan.ilhan@cern.ch, kahvelab@gmail.com

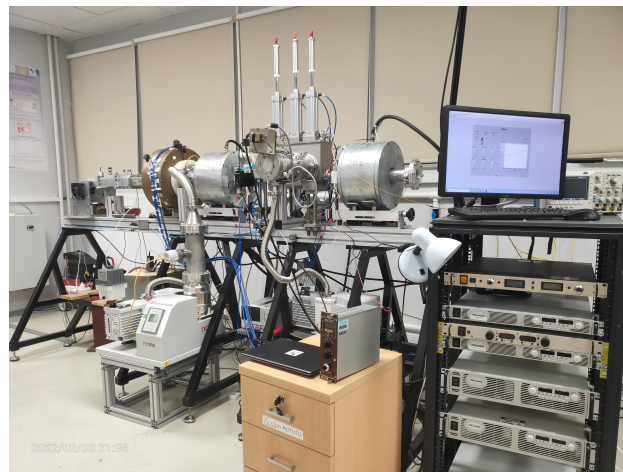


Figure 1: The Proton Accelerator at KAHVELab.

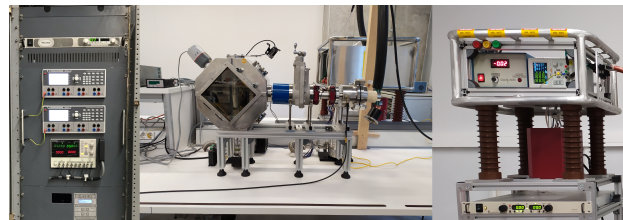


Figure 2: The Electron Accelerator at KAHVELab.

CONTROL SYSTEM DEVELOPMENT OF PROTON ACCELERATOR

The system [1] employs PLC and PC for controlling devices and automation at the moment. PC used for user interface and serial communication with devices which can not be controlled directly with PLC yet. Devices like vacuum gauges and pneumatic cylinders need digital and analogue signals for control. Also, PLC's have the ability to serial control of devices like turbomolecular pumps and power supplies. While developing a control system for these accelerators we found out LabVIEW is very easy for testing an instrument but not so much to build a stable control system. We therefore implemented a LabVIEW GUI controlled PLC system which is more stable than pure LabVIEW option. PLC's also has the benefit of providing digital and analogue signals. Unfortunately devices like PSUs or vacuum pumps do not have drivers for PLC's and we had to write one for each such device.

NOVEL FAST RADIATION-HARD SCINTILLATION DETECTOR FOR ION BEAM DIAGNOSTICS*

P. Boutachkov[†], M. Saifulin¹, C. Trautmann¹, B. Walasek-Höhne
GSI Helmholtz Center for Heavy Ion Research, Darmstadt, Germany

E. Gorokhova, JSC S.I. Vavilov State Optical Institute, St. Petersburg, Russia

P. Rodnyi, I. Venevtsev, Peter the Great Polytechnic University, St. Petersburg, Russia

¹also at Technical University Darmstadt, Darmstadt, Germany

Abstract

Novel radiation-hard scintillators were developed in the last years based on indium-doped zinc oxide ceramic with an extremely short decay time below a nanosecond. Fast counting detectors and fast screens were considered as potential beam diagnostic applications of this material. At the GSI/FAIR facility, scintillation detectors are commonly used for measuring the intensity and detailed time structure of relativistic heavy ion beams. The scintillating material is inserted directly into the beam path. Signals from individual ions are counted, providing systematic-error-free beam intensity information. Standard scintillators require frequent maintenance due to radiation damage. To address this limitation, a large area ZnO radiation-hard detector prototype was developed. The prototype detector operates at orders of magnitude higher irradiation levels, at higher counting rates and has better time resolution compared to a plastic scintillator. In addition, the novel detector material opens the possibilities for applications in other beam diagnostic systems, for example, scintillation screens for transverse profile measurements. Therefore, ZnO scintillation ceramics are of general interest for beam diagnostics.

INTRODUCTION

Scintillation detectors are used at the GSI/FAIR facility for intensity and micro-spill structure measurements. Ion beams from protons up to uranium with energies in the range of hundreds of MeV/u up to tens of GeV/u have to be characterized. The detectors utilize the interaction of the ion beam with a scintillator which generates photons. A photomultiplier tube (PMT) converts the light into an electrical signal.

The detector produces one pulse for each detected ion. Typical signal width measured from a BC400 or EJ212 plastic scintillator near the PMT location is of an order of 5 ns. The complex slow extraction process from the particle accelerators and the sub Poisson ion particle distribution [1] of the extracted particles lead to a non-negligible percentage of signal pile-ups at counting rates above a few times 10^6 particles per second. Higher counting rates are requested, hence scintillator materials with decay times of the order of nanosecond or shorter are desirable.

* This work was funded by DLR within the ERA.Net RUS Plus Project RUS_ST2017-051.

[†] P.Boutachkov@gsi.de (corresponding author)

The typical dose at which a plastic scintillator has to be exchanged due to radiation damage is of the order of 50-100 kGy. This dose is regularly reached during micro-spill optimization. Therefore we investigated zinc oxide, an inorganic material which can substitute the plastic scintillator.

ZnO(In) RESPONSE TO HEAVY IONS

Fast luminescence from ZnO with indium or gallium doping was discovered in the sixties. A structureless band with a decay constant below a nanosecond located near the optical absorption edge was reported by W. Lehmann in Ref. [2]. The latter property limited the detector applications to cases where a few micrometers of scintillator material provide sufficient light output. In 2012, a breakthrough in ZnO scintillator production was reported by P. A. Rodnyi et al. [3]. Transparent ceramics from ZnO micro- and nano-powders were produced with a diameter of the order of 2 cm and thickness of 0.4 mm. The response of this material was tested at GSI with heavy ions. The results of these tests were reported in Ref. [4]. A photograph of the tested sample and an image with ion beam induced luminescence from 300 MeV/u ^{124}Xe ions is shown in Fig. 1.

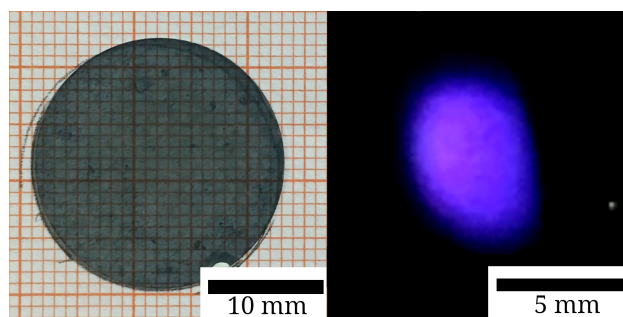


Figure 1: To the left, a ZnO(In) ceramic sample photograph. To the right, a color image of an ion beam induced luminescence by 300 MeV/u ^{124}Xe ions.

An international collaboration was formed under the ERA.Net RUS Plus Project RUS_ST2017-051 with the aim to develop ultra-fast ceramic detectors of ionizing radiation based on zinc oxide. Samples were produced and characterized at the Research Technological Institute of Optical Materials “Vavilov State Optical Institute” and Peter the Great St. Petersburg Polytechnic University. The ceramic microstructure was investigated at the Institute of Solid State Physics of the University of Latvia, while ionoluminescence

TIME-RESOLVED PROTON BEAM DOSIMETRY FOR ULTRA-HIGH DOSE-RATE CANCER THERAPY (FLASH)

P. Casolaro*, G. Dellepiane, A. Gottstein, I. Mateu, P. Scampoli¹, S. Braccini

Albert Einstein Center for Fundamental Physics (AEC), Laboratory for High Energy Physics (LHEP),
University of Bern, Bern, Switzerland

¹also at Department of Physics “Ettore Pancini”, University of Napoli Federico II,
Complesso Universitario di Monte S. Angelo, Napoli, Italy

Abstract

A new radiotherapy modality, known as FLASH, is a potential breakthrough in cancer care as it features a reduced damage to healthy tissues, resulting in the enhancement of the clinical benefit. FLASH irradiations are characterized by ultra-high dose-rates (>40 Gy/s) delivered in fractions of a second. This represents a challenge in terms of beam diagnostics and dosimetry, as detectors used in conventional radiotherapy saturate or they are too slow for the FLASH regime. In view of the FLASH clinical translation, the development of new dosimeters is fundamental. Along this line, a research project is ongoing at the University of Bern aiming at setting-up new beam monitors and dosimeters for FLASH. The proposed detection system features millimeter scintillators coupled to optical fibers, transporting light pulses to a fast photodetector, readout by high bandwidth digitizers. First prototypes were exposed to the 18 MeV proton beam at the Bern medical cyclotron. The new detectors have been found to be linear in the range up to 780 Gy/s, with a maximum time resolution of 100 ns. These characteristics are promising for the development of a new class of detectors for FLASH radiotherapy.

INTRODUCTION

FLASH radiotherapy is a novel radiation delivery modality characterized by very fast irradiations (< 300 ms) and ultra-high dose rates (> 40 Gy/s). By comparison, conventional radiotherapy treatments are performed in a few minutes at dose rates of the order of 0.1 Gy/s. Since the first pioneering work by Favaudon et al. [1], many experiments have shown that FLASH irradiations drastically reduce normal tissue toxicity, while keeping the same effectiveness on the cancer cells as of the conventional radiotherapy [2]. This striking sparing effect on healthy tissue, also termed as FLASH effect, has been observed with more than one radiation type, including electrons, protons, photons, and carbon ions [3]. The dosimetry and beam monitoring of FLASH irradiations are challenging owing to the peculiar characteristics of FLASH beams. Ionization chambers are the gold standard for the dosimetry in conventional radiotherapy; however, these detectors feature relatively slow response and saturation at high dose rates [4]. Consequently they cannot be used for FLASH beams, without corrections. Along this line, a research project is ongoing at the University of

* pierluigi.casolaro@lhep.unibe.ch

Bern aiming at the proof-of-principle of a new detection system for dosimetry and beam monitoring in FLASH radiotherapy. The first dosimeter prototypes, based on plastic scintillators coupled to optical fibers, have been tested at the Bern cyclotron laboratory located at the Bern University Hospital (Inselspital).

MATERIALS AND METHODS

This work reports on two measurements aimed at evaluating the feasibility of the proposed innovative system for ultra-high dose rate beams, namely: 1) the study of the detector response as a function of the average dose rate and 2) the time trend of the proton beam at high time resolution. This section describes the proposed innovative detection system and the specific dosimetry method tested at the Bern medical cyclotron.

The Innovative Detection System

The new detection system for ultra-high dose rate measurements is depicted in the schematic of Fig. 1.

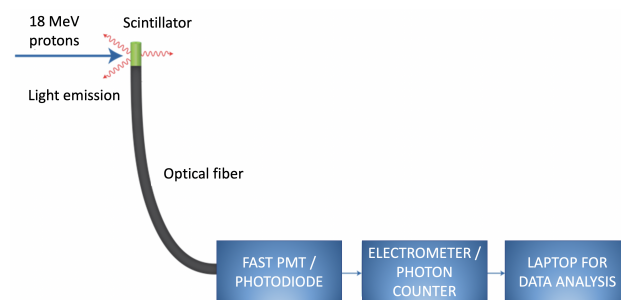


Figure 1: Schematic of the FLASH detection system.

Its main element is a scintillator of millimeter or sub-millimeter size coupled to an optical fiber. The light pulses are delivered to the data acquisition (DAQ) through the optical fiber. In this work, we used a $(0.5 \times 0.5 \times 2)$ mm³ polystyrene scintillator, and two different DAQs, one for the study of the linearity of the dose rate response and another for the beam monitoring at high time resolution. The former comprises a high speed response PhotoMultiplier Tube (PMT) and a Keysight B2985A electrometer; the latter comprises a single-photon detector module based on a silicon avalanche photodiode and a Ortec Multi-Channel Scaler (MCS). The MCS allows for measurements with 65536 chan-

FAST SPILL MONITOR STUDIES FOR THE SPS FIXED TARGET BEAMS

F. Roncarolo*, M. Bergamaschi, D. Belohrad, E. Calvo Giraldo, E. Effinger,
M. Martin Nieto, S. Mazzoni, I. Ortega Ruiz, J. Tan, C. Zamantzas,
P. A. Arrutia Sota, V. Kain, M. A. Fraser, F. M. Velotti, CERN, Geneva, Switzerland

Abstract

At the CERN Super Proton Synchrotron (SPS) the 400 GeV proton beam is supplied to the fixed target experiments in the North Area facility (NA) via a slow extraction process. The monitoring of the spill quality during the extraction, lasting 4.8 seconds with the present SPS setup, is of high interest for minimising beam losses and providing the users with uniform proton-on-target rates. The monitor development challenges include the need for detecting, sampling, processing and publishing the data at rates ranging from few hundred Hz to support the present operation to several hundreds of MHz to serve future experiments proposed within the Physics Beyond Collider (PBC) program. This paper gives an overview of the ongoing studies for optimizing the existing monitors performances and of the R&D dedicated to future developments. Different techniques are being explored, from Secondary Emission Monitors to Optical Transition Radiation (OTR), Gas Scintillation and Cherenkov detectors. Expected ultimate limitations from the various methods will be presented, together with 2022 experimental results, for example with a recently refurbished OTR detector.

SPS SLOW EXTRACTION

The main physics program at the CERN SPS relies on the delivery of 400 GeV protons to the NA fix target experiments. As illustrated in Fig. 1, this is achieved by a 4.8 s third integer slow extraction process [1] at the end of the SPS *fix target beam* cycle, lasting about 10 s from first injection to flat top. Among the parameters for assessing the spill quality,

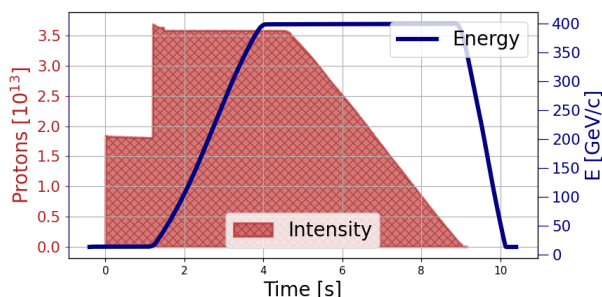


Figure 1: SPS Fix Target beams cycle.

providing the experiments with a constant flux of protons on target during the spill is of paramount importance for the SPS physics program. For this purpose, the SPS 200 MHz RF system is disabled at the end of acceleration with the aim of extracting fully de-bunched beams.

* federico.roncarolo@cern.ch

Table 1: Key Parameters of Interest for the SPS Spill Monitors Requirements

Parameter	Value or Range	Comment
Spill Duration	4.8 s	present operation
	1 s	future, e.g. PBC
Beam Intensity	1 - 400 × 10 ¹¹ p	
Spectrum Harmonics of Interest	50 Hz, 100 Hz	e.g. Noise, PC ripples
	43.86 kHz	SPS 1 st and 2 nd Harmonics*
	476 kHz	PS 1 st Harmonic**
	200 MHz	RF capture
	800 MHz	RF long. blow-up
	10 GHz	Future, e.g. PBC

* the SPS circulating beam structure includes 2×10 μs injections, the *abort gap* for the dump kickers rise

** the slow extracted beam can still contain a time structure from the PS (the SPS injector)

Therefore, measuring the beam current fluctuations at high frequencies during the spill in the transfer line from the SPS ring to the targets is of primary interest. Spill monitors can then provide signals for feed-back or feed-forward systems to equipment, such as RF cavities or magnet power converters, that are typically identified as possible sources of beam intensity fluctuations [2–4]. Table 1 summarises key parameters relevant for the spill monitors functional specifications.

SPS FAST SPILL MONITORS

From the parameters presented in Table 1, one can summarise the main challenges for spill monitoring as follows:

- monitoring beam currents ranging from few nA (1×10^{11} p in 4.8 s) to $\approx 1 \mu\text{A}$ (4×10^{13} p in 1 s)
- by design the particles are un-bunched, standard electromagnetic beam position monitors and current transformers are not suitable
- to support the SPS slow extraction operation and optimisation, the overall monitor bandwidth must cover from very low frequencies to the several hundreds MHz, thus requiring *fast* spill monitors to identify the presence of (unwanted and normally relatively small) residual time structures from the SPS RF.

The SPS is now equipped with three *fast* spill monitors, based on independent measurement techniques and data

SIMULATED BEHAVIOR OF CNT WIRES IRRADIATED IN THE HiRadMat EXPERIMENTAL LINE AT CERN

A. Mariet*, B. Moser, R. Veness, CERN, Geneva, Switzerland
M. Devel, FEMTO-ST institute (UBFC, CNRS), ENSMM, Besançon, France
J.E. Groetz, Chrono Environnement (UFC, CNRS), Besançon, France
A. Mikhalchan, J. J. Vilatela, IMDEA Materials Institute, Madrid, Spain

Abstract

With the planned increase of luminosity at CERN for HL-LHC and FCC, instruments for beam quality control must meet new challenges. The current wires, made up of plain carbon fibers and gold-plated tungsten would be damaged due to their interactions with the higher luminosity beams. We are currently testing a new and innovative material, with improved performance: carbon nanotube fibers (CNTF). The HiRadMat (High Radiation for Material) experimental line at the output of the SPS is a user facility which can irradiate fix targets up to 440 GeV/c. CNTF with various diameters were irradiated in HiRadMat with different intensities, later imaged with a SEM microscope and tested for their mechanical properties. In addition, simulations have been carried out with the FLUKA particle physics Monte-Carlo code [1], in order to better understand the mechanisms and assess the energy deposition from protons at 440 GeV/c in those CNTF wires, depending mainly on their diameters and densities. This could lead to a good estimation of the CNTF temperature during irradiation. In this contribution, we first present the HiRadMat experimental setup and then we discuss the results of our FLUKA simulations.

INTRODUCTION

The search for performance in particle accelerators and in particular the increase in luminosity [2] pushes the engineering of beam instrumentation to be always at the cutting edge of technology. The precision of the quality control of the beams throughout their acceleration is paramount. Transverse profile monitoring is particularly challenging as it is often based on intercepting devices such as wire-scanners and SEM grids. Operational systems at CERN [3] typically use wire made out of carbon fiber and gold-plated tungsten. These materials in the form of wires are subjected to high mechanical and thermal stresses due to the energy deposited by the particles in the material. The physical properties of those materials have reached their limits for very high beam energies / intensities such as those obtained in the CERN Super Proton Synchrotron (SPS) and Large Hadron Collider (LHC). The search for new and innovative materials that could be used in all beam conditions has therefore become a necessity. By their exceptional properties, carbon nanotubes, existing in the form of microscopic fibers, seem to be an ideal candidate. This paper presents, together with energy deposition simulations, the setup of an experiment

performed at the HiRadMat beam line at CERN for the irradiation of carbon nanotube wires (CNT) with high intensity proton beams at 440 GeV/c [4, 5].

WIRE MANUFACTURING

CNT were produced at the IMDEA by floating catalyst chemical vapor deposition (FCCVD) in a reactor tube of mul-lite ceramic (SiO_2) heated to 1570 K with toluene (C_7H_8) and ferrocene ($\text{Fe}(\text{C}_5\text{H}_5)_2$) as carbon and iron source respectively. The carrier gas was hydrogen (H_2). The CNT obtained are mainly double or few multiwalls and some hundreds of μm long. The assembly of individual tubes to form a microscopic fiber (CNTF) occurred in the gas phase during growth. CNT entangle and form a dark aerogel which is drawn through and out of the reactor tube. This aerogel of CNT deposits on the winder to produce a fiber [6, 7] (Fig. 1-a and b). The diameter of the final fiber is controlled by varying the spinning rate of the winder, from 7 m/min for the thick diameters, to 28 m/min for the thin diameters.

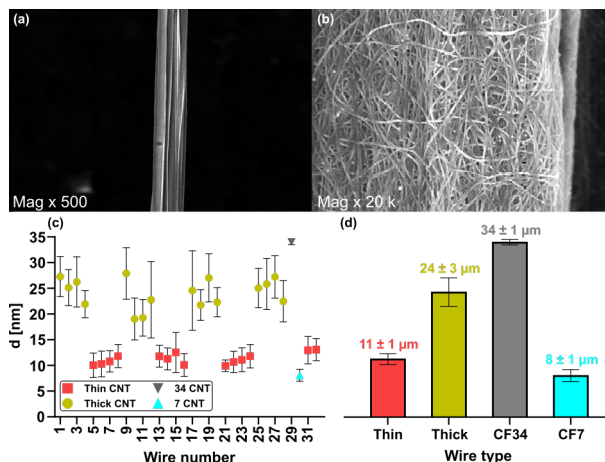


Figure 1: SEM pictures of an as-spun CNTF with a magnification of (a) x500 and (b) x20000; (c) Summary of the average diameters of each sample; (d) mean values in diameter for the thin and thick CNT fibers and average diameter for the 34 and 7 μm carbon fiber. CF stands for Carbon Fiber.

The diameter of the samples was estimated by 30 measurements all along the axis of the wires. Figure 1-d shows the average diameter of the 32 wires with the standard deviation. The red bar represents thin wires and shows an average diameter of 11 μm , the green bar the thick wires with 24 μm diameter and the grey and blue bars the 34 and 7 μm diam-

* alexandre.mariet@cern.ch

FIRST MEASUREMENT OF LONGITUDINAL PROFILE OF HIGH-POWER AND LOW-ENERGY H^- BEAM BY USING BUNCH SHAPE MONITOR WITH GRAPHITE TARGET

R. Kitamura* on behalf of J-PARC linac
 JAEA/J-PARC, Tokai, Naka, Ibaraki, Japan

Abstract

A bunch-shape monitor (BSM) using the highly-oriented pyrolytic graphite (HOPG) target has been developed to measure the high-power and low-energy negative hydrogen ion beam at the front-end. The performance evaluation of the BSM using the HOPG target was conducted. The first measurement of longitudinal beam profiles at the front-end was demonstrated with the BSM. The measurement was consistent with the design simulation of the front-end. As a further application, the BSM using the HOPG target will be an attractive and powerful instrument to study the space-charge effect at the front-end.

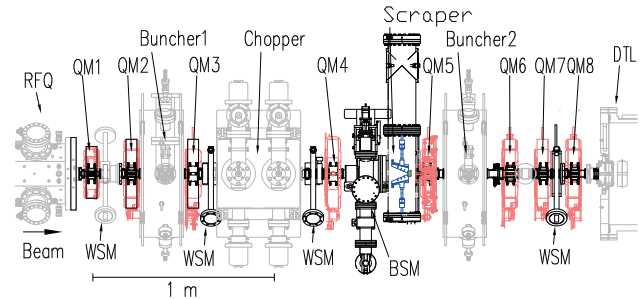


Figure 1: Configuration of the MEBT1.

INTRODUCTION

The Japan proton accelerator research complex (J-PARC) [1] linac supplies the 400-MeV negative hydrogen ion (H^-) beam to subsequent accelerators and experimental facilities. Recently, the user operation with a peak current of 50 mA was stable by the careful maintenance and beam tuning. Detailed beam studies are being conducted to reduce the beam loss towards higher power and the robustness of the stable operation. The medium-energy beam transport 1 (MEBT1) is important for the beam tuning of the linac. Figure 1 shows the configuration of the MEBT1. There are two functions of MEBT1 as follows. One is the beam matching between a 3-MeV radio-frequency quadrupole (RFQ) linac and a subsequent 50-MeV drift-tube linac. The other is the production of the bunch time structure for the injection into the rapid-cycle synchrotron. Since the parameters of the MEBT1 should be tuned to satisfy these requirements, the improvement of the longitudinal tuning in the MEBT1 is an interesting challenge to find a better solution for the high-power beam operation.

The bunch-shape monitor (BSM) [2,3] as the longitudinal beam profile monitor plays the important role to understand and improve the longitudinal beam dynamics in the MEBT1. However, the heat loading from the high-power and low-energy H^- beam in the MEBT1 caused the target failure of the BSM measurement which prevented the stable beam studies. We introduced the new graphite target for the BSM to mitigate the heat loading and successfully measured the longitudinal beam profiles in the MEBT1. In this report, the recent progress of the development of the BSM dedicated to the MEBT1 and its related studies are presented.

NEW TARGETS FOR BSM

The BSM is a standard longitudinal beam profile monitor for the linac. Figure 2 shows the principle of the BSM. Secondary electrons are produced by the interaction between the H^- beam and the BSM target. The negative bias voltage is applied to the target to extract these secondary electrons into the deflector in the BSM. The electrons related to the longitudinal profile of the original H^- beam are modulated by the RF electric field in the deflector.

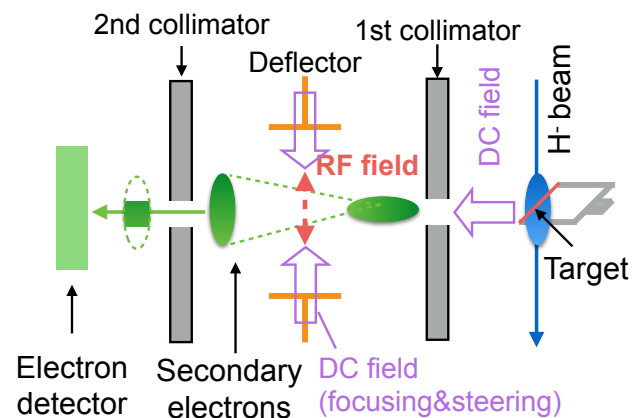


Figure 2: Principle of BSM.

The challenge of the BSM in the MEBT1 is to mitigate the heat loading from the high-power and the low-energy H^- beam. Therefore, we introduced a new strong target material for the BSM. There are three candidates for the BSM target as follows. One is the tungsten wire target, which is used as the standard target material for the usual BSM. However, the wire breaking frequently occurred due to heat loading in the MEBT1. Another candidate is a carbon nanotube (CNT)

* rkita@post.j-parc.jp

SINGLE-SHOT ELECTRO-OPTIC DETECTION OF BUNCH SHAPES AND THZ PULSES: FUNDAMENTAL TEMPORAL RESOLUTION LIMITATIONS AND CURES USING THE DEOS STRATEGY*

Serge Bielawski, Clément Evain, Eléonore Roussel, Christophe Szwaj†

PhLAM, CNRS/Lille University, Lille, France

Christopher Gerth, Bernd Steffen, Deutsches Elektronen-Synchrotron DESY, Hamburg, Germany

Bahram Jalali, UCLA, Los Angeles, CA, USA

Abstract

We review a recent work aiming at improving the resolution of single-shot longitudinal diagnostics, that are based on electro-optic (EO) detection using a chirped laser pulse. This classical technique has indeed been known to present severe limitations in time resolution (and usable bandwidth), especially when long recording windows and/or short bunches are considered. We review recent results on a strategy designed for overcoming this limit, the DEOS technique (Diversity Electro-Optic Sampling). A special experimental design enables to reconstruct numerically the input electric signal with unprecedented temporal resolution. As a result, 200 fs temporal resolution over more than 10 ps recording length could be obtained at European XFEL - a performance that could not be realized using classical spectrally-decoded electro-optic detection. Although DEOS uses a radically novel conceptual approach, its implementation requires few hardware modifications of currently operating chirped pulse electro-optic detection systems.

INTRODUCTION: LIMITATION OF CLASSICAL CHIRPED PULSE ELECTRO-OPTIC DETECTION

Recording electric field evolutions in single-shot and with sub-picosecond resolution is required in electron bunch diagnostics, and THz applications. A popular strategy consists of transferring the unknown electric field onto a chirped laser pulse, which is eventually analyzed [1, 2] (see Fig. 1). The technique has been investigated and/or been used as routine diagnostics at FELIX, DESY, PSI, Eu-XFEL, KARA, SOLEIL, etc. However fundamental time-resolution limitations have been strongly limiting the potential of these methods. This limitation has been generally expressed as the shortest bunch duration τ_R (or THz pulse duration) that can be recorded without deformation [3]:

$$\tau_R = \sqrt{\tau_w \times \tau_L}, \quad (1)$$

where τ_L is the compressed laser pulse duration, and τ_w is the stretched pulse duration, i.e., the duration of the recording window.

* Work supported by: ULTRASYNCR ANR-DFG project, CPER photonics for society, LABEX CEMPI, METEOR CNRS MOMENTUM grant, DESY/Helmholtz, MURI program on Optical Computing Award Number N00014-14-1-0505.

† christophe.szwaj@univ-lille.fr

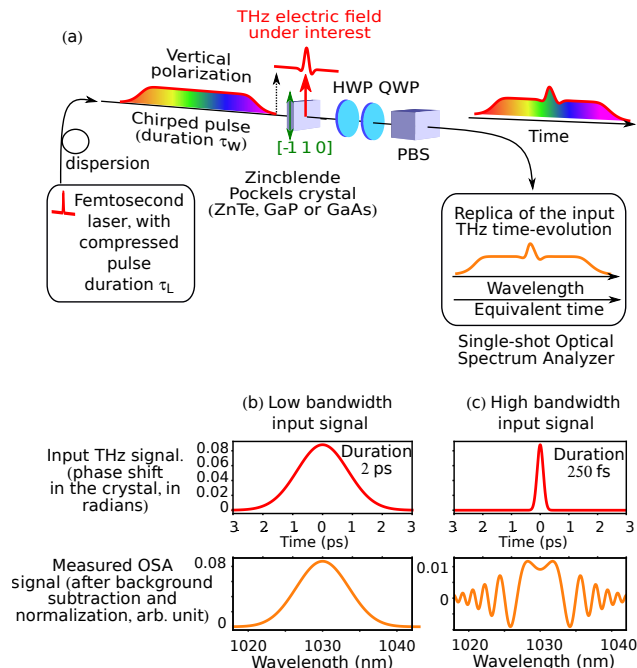


Figure 1: (a) Typical setup and limitations of classical single-output chirped pulse EO detection systems. The THz-bandwidth electric field is typically the Coulomb field created by an electron bunch, or a coherent THz pulse generated by coherent synchrotron radiation, coherent transition radiation, etc. The electric field modulates the intensity of a chirped laser pulse. The readout is performed (also in single-shot) using an optical spectrum analyser, usually composed of a grating and a camera. QWP and HWP: Quarter- and half-wave plates, PBS: Polarizing Beam-Splitter. As a main idea, one can expect the temporal laser modulation to be approximately replicated in the optical spectrum. Actually this works only for relatively low bandwidth THz pulses (b). For short (i.e., large bandwidth) THz pulses, strong deformations are observed (c). The DEOS technique presented here aims at solving this time resolution issue.

TRANSFER FUNCTION APPROACH

A main point of the DEOS approach consists of using the information contained at the two outputs of spectrally decoded EO systems. This involves two steps (see also Fig. 2):

UPGRADED CMS FAST BEAM CONDITION MONITOR FOR LHC RUN 3 ONLINE LUMINOSITY AND BEAM INDUCED BACKGROUND MEASUREMENTS

Joanna Wańczyk^{*,1}

on behalf of CMS Collaboration, CERN, Geneva, Switzerland

¹also at Swiss Federal Institute of Technology Lausanne (EPFL), Lausanne, Switzerland

Abstract

The Fast Beam Condition Monitor (BCM1F) for the CMS experiment at the LHC was upgraded for precision luminosity measurement in the demanding conditions foreseen for LHC Run 3. BCM1F has been rebuilt with new silicon diodes, produced on the CMS Phase 2 outer tracker PS silicon wafers. The mechanical structure was adapted to include a three-dimensional printed titanium circuit for active cooling of the BCM1F sensors. The assembly and qualification of the detector quadrants were followed by the integration with the Pixel Luminosity Telescope (PLT) and Beam Conditions Monitor for Losses (BCML1) on a common carbon fibre carriage. This carriage was installed inside the Compact Muon Solenoid (CMS) behind the CMS pixel detector, at a distance of 1.9 m from the interaction point (IP). BCM1F will provide a real-time luminosity measurement as well as a measurement of the beam-induced background, by exploiting the arrival time information of the hits with a sub-bunch crossing precision. Moreover, regular beam overlap scans at CMS were introduced during Run 2, enabling an independent and nondestructive transverse profile measurement for LHC Operators. These proceedings describe the improved BCM1F detector design, its commissioning, and performance during the beginning of Run 3 operation.

INTRODUCTION

The Fast Beam Condition Monitor (BCM1F) is a dedicated, standalone luminometer, independent from all central CMS services. The sub-bunch crossing (BX) precision, enables the measurement of beam-induced background. The complete detector consists of four C-shapes (see Fig. 1), with a total of 48 channels. Each C-shape pair forms a ring around the beam pipe at an approximate radius of 7 cm, on either side of the interaction point (IP). In Run 2 good per-



Figure 1: Picture of the Run 3 BCM1F C-shape.

* jwanczyk@cern.ch, joannawanczyk@epfl.ch

formance was achieved with mixed sensor types were used (sCVD, pCVD and Silicon). The Silicon sensors had much better signal-noise separation and response linearity [1].

DETECTOR DESCRIPTION

The full system diagram including both the front end and the two parallel back ends is shown in Fig. 2. The detector was completely rebuilt during Long Shutdown 2 (LS2), with radiation hard sensors made of acceptor-doped (p-type) silicon. To provide high performance operation throughout Run 3 period, a three-dimensional (3D) printed titanium active cooling loop was added.

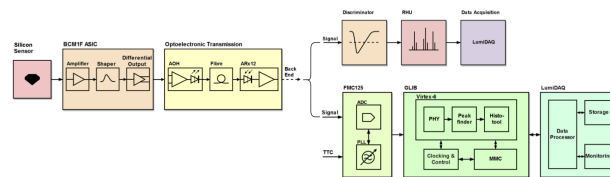


Figure 2: Diagram of the BCM1F detector architecture [2].

Front-End Electronics

Each C-shape is a single flex-rigid printed circuit board, which includes all front-end components: double silicon diodes, ASIC chips, and opto-electronic readout.

The new sensors were produced as a part of the CMS Phase 2 Outer Tracker sensor production [3]. The 300 μm thick wafers were prepared as double silicon sensors, each with dimensions of 1.7 × 1.7 mm². They are A/C-coupled to protect the amplifier from the leakage current, thus providing better signal-to-noise ratio (SNR). The signal is shaped with the fast asynchronous ASIC from the Run 2 design [4], implemented in IBM 130 nm. It provides a short peaking time (<10 ns), narrow pulses, as shown in Fig. 3, and sub-bunch timing resolution. The optical readout is placed at a larger distance from the IP, and uses analog-opto-hybrids (AOH), which convert the current into infrared light at a wavelength of 1310 nm.

The assembly and qualification of the detector quadrants were followed by integration with the Pixel Luminosity Telescope (PLT) and Beam Conditions Monitor for Losses (BCML1). Commissioning was done during the 2021 LHC pilot beam test at the injection energy of 450 GeV.

Back-End Electronics

The optical signal is converted into an 8-bit-equivalent electric signal at the ARx12 optical receiver in the CMS service cavern (USC), shielded from the prompt radiation in the